Lead-free Doped Solder Joint Reliability under Harsh Temperature Cycling Environment to study the Long Term Isothermal Aging Effects of Heat Sinks, Solder Paste Volume, Board Substrate Material, Component Substrate Material and Component Sizes

by

Sivasubramanian Thirugnanasambandam

A dissertation submitted to the Graduate Faculty of
Auburn University
in partial fulfillment of the
requirements for the Degree of
Doctor of Philosophy

Auburn, Alabama
August 4,2018

Keywords: Reliability, Lead-free Solder Doping, Isothermal Aging,
Temperature Cycling, Intermetallic Study, Failure Analysis.

Approved by

John L. Evans, Chair, Charles D. Miller Endowed Chair of Industrial and Systems Engineering
George Flowers, Dean of the Graduate School and Professor of Mechanical Engineering
Jeff Suhling, Department Chair of Mechanical Engineering
Mark Carpenter, Professor of Statistics
Michael Bozack, Professor of Physics
Richard Sesek, Tim Cook Associate Professor of Industrial and Systems Engineering

Abstract

Restriction of Hazardous Substances (RoHS), Waste Electrical and Electronic Equipment Directive (WEEE) organizations have restricted the use of lead in solder materials for consumer electronics. The electronic industry have drifted apart from eutectic 63Sn-37Pb (Tin-Lead) solder to the near eutectic lead-free [Sn-1.0Ag-0.5Cu (SAC105)] and [Sn-3.0Ag-0.5Cu (SAC305)] solder material in past decade. Knowledge about microstructure, mechanical properties, and failure behavior of lead-free solder joints in electronic assemblies are dynamically changing when exposed to isothermal aging and temperature cycling environments. Researchers and scientists in the semiconductor industry and academic world have experimentally demonstrated that the long-term performance of the lead-free solder joint material is dependent on inter metallic composition formed during the reflow of surface mount assembly of electronic packages. The inter metallic composition for the binary eutectic Tin-Lead (63Sn-37Pb) and its degradation properties over long-term isothermal aging are very much different from the Ternary non eutectic Tin-Silver-Copper [Sn-1.0Ag-0.5Cu (SAC105), Sn-3.0Ag-0.5Cu (SAC305)]. However, the initial performance of the ternary Tin-Silver-Copper lead-free solder material is much better than the binary Tin-Lead solder materials reliability. The reliability performance degrade up to 70% for lead-free solder joint materials SAC105 and SAC305 that are exposed to long- term isothermal aging conditions in elevated temperatures (75°C for 24 months).

The major contribution to this degradation in lead-free solder joint material is the accumulation of the low cyclic stress induced on the bulk solder near the intermetallic formation over a long period (>10 months) at elevated temperature(>50°C). This phenomenon observed by many researchers and scientists in the field, demonstrated as the intermetallic composition thickness growth and recrystallization of grain boundaries. There are many investigations targeted to resist this change in material property over time and temperature effects. One such possible investigation is to develop a new solder alloy composition with additional elements in smaller composition as dopants mixed with ternary lead-free (SAC105, SAC305) solder materials. The top materials that qualify for such metallurgical composition are Antimony (Sb), Magnesium (Mg), Nickel (Ni), Cobalt (Co), Indium (In) and Bismuth (Bi). Material researchers and scientists previously evaluated these additives. The results showed finer grain boundaries and reduced the intermetallic formations of the tin with silver or copper during the reflow process of surface mount assembly. The resulting intermetallic formation had a more uniform grain formation in the lead-free bulk solder alloy. This process of adding metallurgical elements in small quantities to the lead-free solder composition is defined “solder doping”. This improves the mechanical properties of the lead-free solder materials initially, but there are limited research results on the effects of the long-term isothermal aging performance of such doped alloys. Lead-free solders have reliability concerns related to elevated process temperatures and the formation of Ag_3Sn intermetallic. Tin-Lead reliability performance compared to that of SAC105, SAC305, and SAC-Bi containing low melting temperature (T_m) alloys show deleterious effects of long-term isothermal aging time and temperature conditions.

Acknowledgments

I would like to express profound gratitude to my advisor, Dr. John L. Evans, for years of support, guidance, and mentorship throughout the challenging parts of my research and graduate study. I would also like to extend my appreciation to my committee members, Dr. George Flowers, Dr. R. Wayne Johnson, Dr. Jeff Suhling, and Dr. Richard Sesek for their valuable time and insight. Particular thanks are due to Dr. Mark Carpenter for his statistical insights during the data analysis related to the publication of several journal papers and reliability predictions. The author particularly thanks Dr. Michael J Bozack for his editorial guidance during the publication of several journal papers and this dissertation, with many useful discussions during the lead-free soldering project. I would also like to thank all my lab-mates, coworkers, and friends: Dr. Sharath Sridhar and Dr. Seth Gordon, Dr. Michael Miller and Mr. John Marcell for their encouragement and friendship. Special thanks go to Dr. Thomas Sanders for his help with the initial LabVIEW program coding and system deployment, and to Dr. Anto Raj for his help in data analysis and Mr. Aditya Bachuwar & Ms. Gayatri Tandel for their help in cross-sectioning and microscopic analysis. Special thanks to my wife Mrs. Bhavanee Gurunathan Sharavanakumaar and my son Mr. Aditya Thirukumaran. Finally, I am, of course, indebted to, my mother Dr. Chitra Subramanian, and my father Dr. Thirugnanasambandam Narayanaswamy who have supported me endlessly although they are so far away.

Table of Contents

List of Tables

List of Figures

List of Equations

List of Abbreviations and Symbols

Ag	Siver
β	Beta (Slope or Shape Parameter)
BGA	Ball Grid Array
Bi	Bismuth
°C	Degree Celcius
CTE	Coefficient of Thermal Expansion
Cu	Copper
e & exp	Exponential Distribution
ENIG	Electroless Nickel Immersion Gold
EDX	Energy-Dispersive X-Ray Spectroscopy
η	ETA (Life Parameter)
FEA	Finite Element Analysis
FR-406	Flame-Retardant-406
γ	Gamma (Location Parameter)
Γ	Gamma Distribution
IEEE	Institute of Electrical and Electronics Engineers
IMC	Intermetallic Compounds
ImAg	Immersion Silver

ImSn	Immersion Tin
iNEMi	International Electronics Manufacturing Initiative
M-6	Megtron-6
OM	Optical Microscopy
OSP	Organic Solderability Preservative
PCB	Printed Circuit Board
Ppm	Parts per Million
PLM	Polarized Light Microscope
QFN	Quad Flat No-lead
RoHS	Restriction of Hazardous Substances
SAC	Tin-Silver-Copper
SEM	Scanning Electron Microscope
SMR	Surface Mount Resistor
SMT	Surface Mount Technology
SMTA	Surface Mount Technology Association
Sn	Tin
T_g	Glass Transition Temperature
T_m	Melting Temperature
THMT	Through-Hole Mount Technology
TTF	Time To Failure
WEEE	Waste Electrical and Electronic Equipment Directive
XRD	X-Ray Diffraction

Chapter 1 Dissertation Context

1.1. Insight to the Electronic Industries

Thales of Miletus has discovered static electricity by rubbing fur on substances such as amber in the 600 B.C.; this is the most ancient well-known record of electricity and electron movement. The inception of consumer electronics began in 1929 with its first public TV broadcast in Germany[1]. Electronics is defined as "The science and technology of the conduction of electricity in a vacuum, a gas, or a semiconductor, and devices based thereon"[2]. The modern electronics industry dates back to the invention of the monolithic semiconductor "integrated circuit," or IC, by Jack Kilby of Texas Instruments in 1958. "In 1965, Gordon Moore made a prediction that would set the pace for our modern digital revolution. From careful observation of an emerging trend, Moore extrapolated that computing would dramatically increase in power, and decrease in relative cost, at an exponential pace"[3]. This phenomenon became the Moore's Law named after Intel cofounder Gordon Moore[3]. Continuing advancements in processing technologies, materials, and designs have enabled seemingly endless increase in the functional density of semiconductor electronics immortalized in the public imagination via Moore's Law in the decades since 1970.

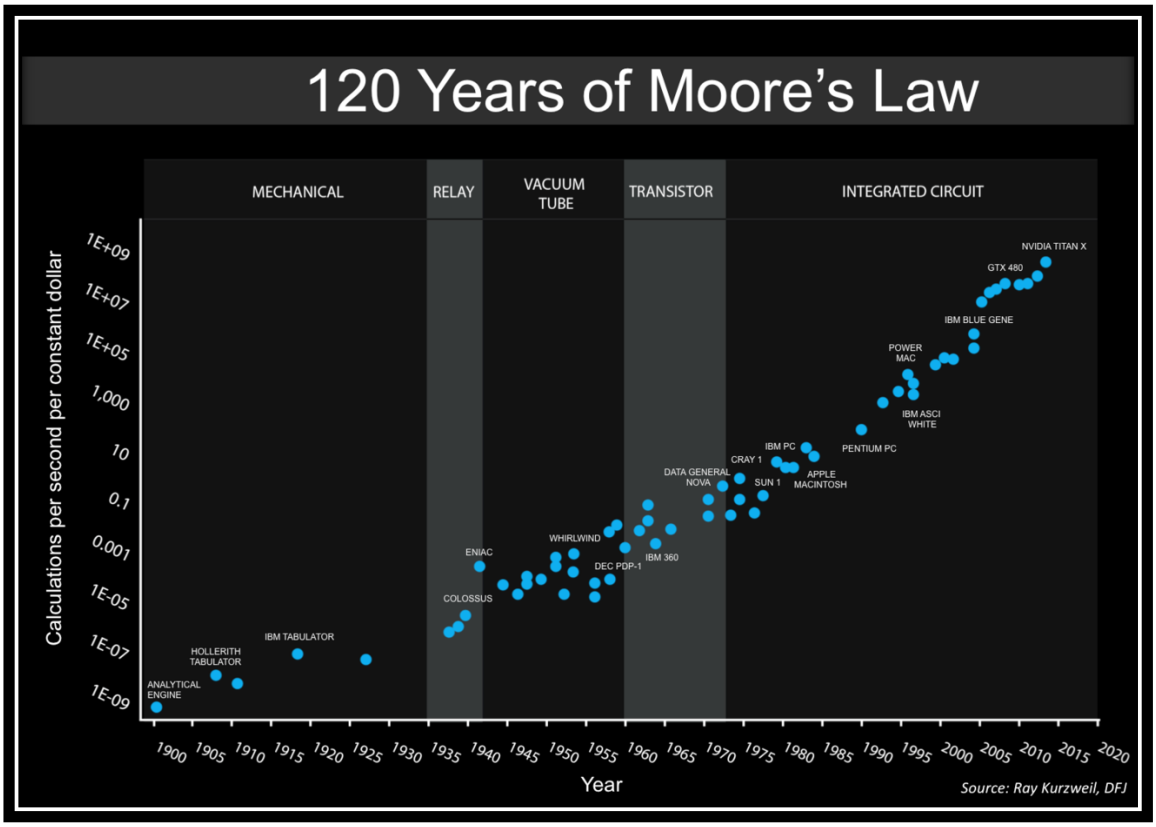

Figure 1 Moore's Law [4]

In 1996, the Electronic Industry surpassed the Automotive Industry to become the largest industry in the world[5]. The modern consumer electronics is still evolving to discover new applications such as virtual augmented realty, and bionic wearables that have transformed and endure to transform the way that people network with each other and incorporate data into their daily activity. Electronics have grown into an indispensable product in the modern digital era of information and globalization. The electronics industry is valued at 4 trillion US dollars and is expected at 5 trillion US dollars by the end of the 2018[5].

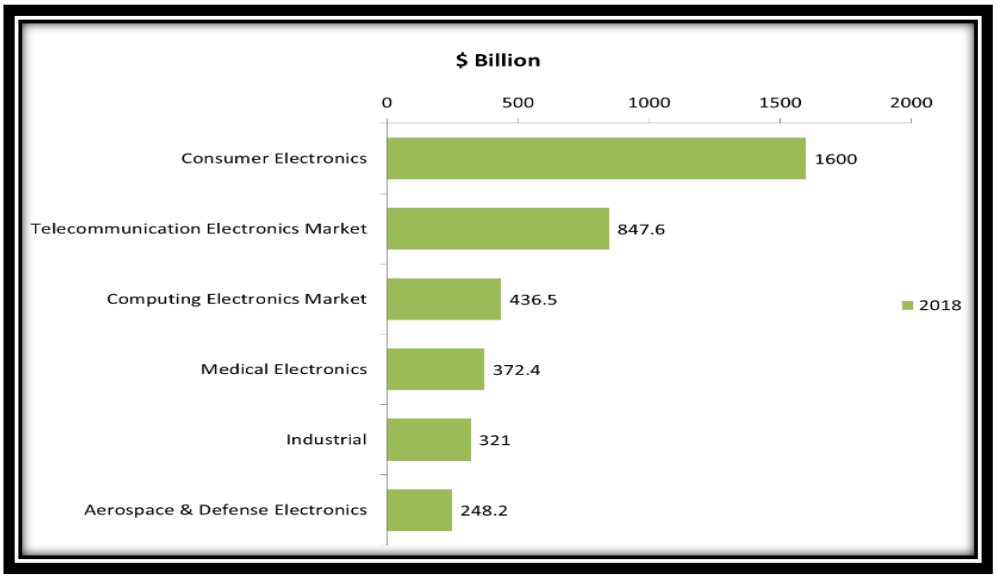

Figure 2 Projected Market Share of Electronics Industry [5]

1.2. Electronic Packaging

Electronic packaging is a multi-disciplinary field, and includes a wide variety of technologies from mechanical, electrical and industrial engineering, chemistry, physics and even marketing and business analytics[6]. The electronic package hierarchy has different levels of interconnections. The electronic system hierarchy starts at level zero (silicon) and continues with Packaging as level one. On level two, the printed wiring board (PWB) manufacturing and board assembly take place. Level three stands for the interconnections between different PWBs, level four for the assembly of the PWB into racks, housings of product etc. Finally, level five represents the connection of several individual products or systems[7]. There are two methods to assemble electronic components onto PCBs: Through-Hole Mount Technology (THMT) and Surface Mount Technology (SMT). Compared to THMT, SMT has many advantages including higher component density, better mechanical performance, higher real-estate rate, and certainly lower cost, so SMT largely replaced THMT in the industry[8].

This dissertation focuses on the solder ball interconnections of the SMT assembly.

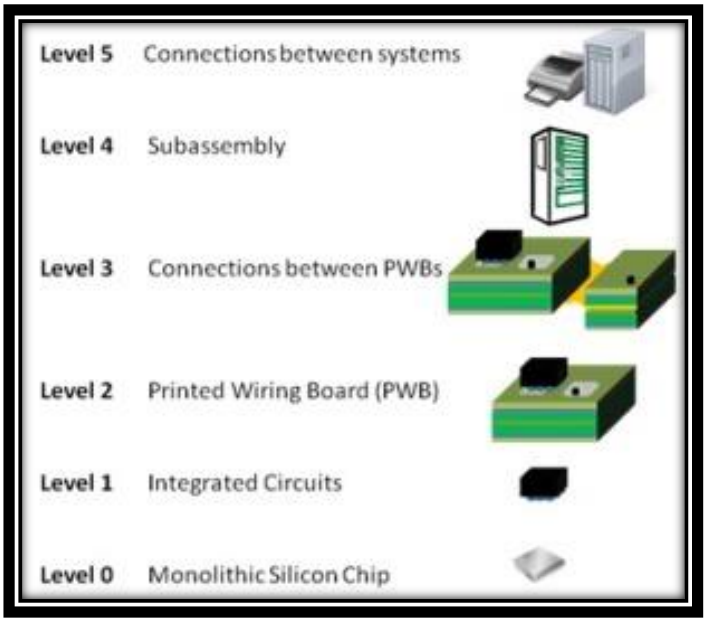

Figure 3 SMT Hierarchy [8]

1.2.1. Silicon Chip

The electronic components have their birth at Silicon "die," or chip, from a single-crystal Silicon Wafer mother. The silicon chip contains many solid-state electronic devices (transistors, resistors, inductors, and capacitors) that have been defined and connected to form functional electrical circuitry[6]. There are many types of carriers with in a silicon chip routed logically to provide movement of electrons with in the circuitry. In this dissertation, the consideration is for chip body size, chip pitch size, laminate material and chip design used.

1.2.2. Body Size

The silicon die needs protection from the outside environment. There is a protective coating called mold compound material. The size of this mold material protecting the silicon chip is the chip body size.

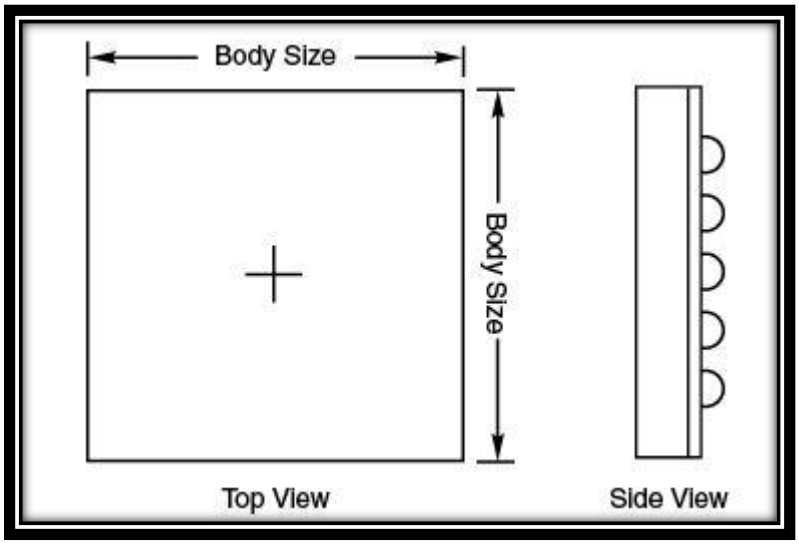

Figure 4 Chip Body Size [9]

1.2.3. Pitch Size

Pitch Size is the distance between the two interconnections within the same silicon chip. The pitch size and chip body size are interdependent on one another. The finer the pitch the smaller the chip body size for any given number of solder balls.

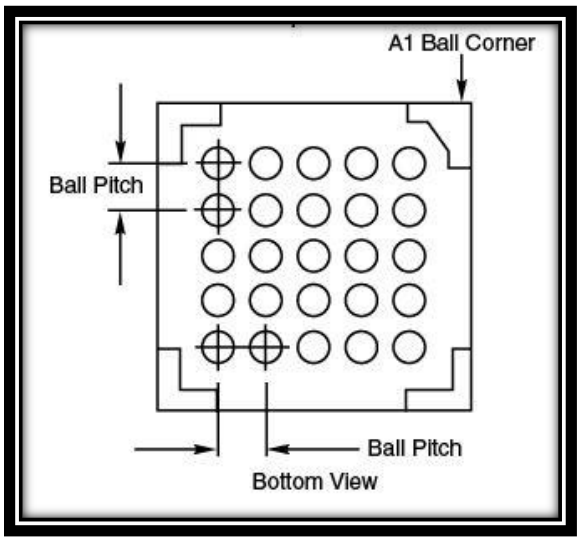

Figure 5 Pitch of Silicon Chip [9]

1.2.4. Laminate Material

Based on the laminate materials used in the flip chip carrier, the classifications are of Ceramic, Tape, Plastic, Dimpled, Metal and Enhanced Plastic types. This dissertation focuses only on the three main classifications namely Ceramic, Plastic and BT-Metal laminates.

Table i Laminate and Material Properties from Practical Components

Package Substrate	Ceramic	Plastic	Metal
Dielectric	Epoxy resin glass reinforced	Ablestik 2300	Polyimide
Wire Type	Copper	Gold	Gold
Encapsulant	Epoxy mold compound	Nitto GE100L	BT (Bismaleimide Triazine)

1.2.5. Chip Design

Based on the design of the chip internal circuitry there are many types of classifications. In this dissertation, the CVBGA97, CVBGA432, CTBGA84, CABGA36, CABGA208 and CABGA256 components are of type one design; PBGA1156 components are of type two design and SBGA304 and SBGA600 are of type three design.

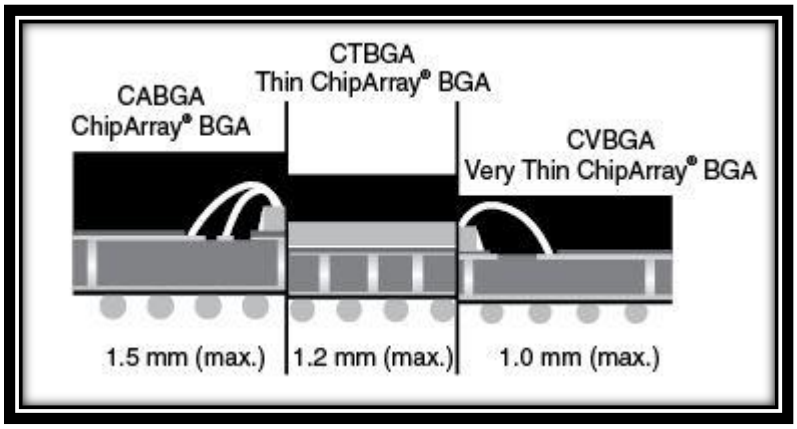

Figure 6 Design Type 1 [9]

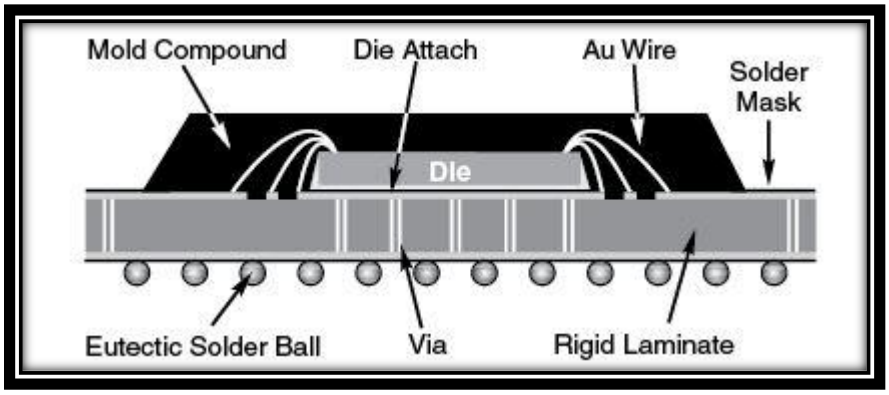

Figure 7 Design Type 2 [9]

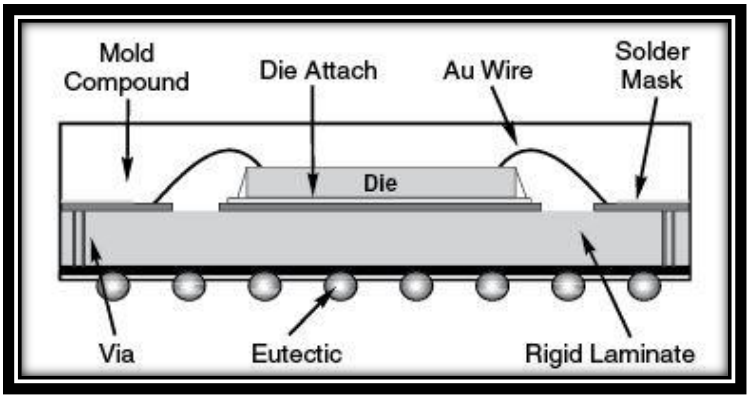

Figure 8 Design Type 3 [9]

1.2.6. Printed Circuit Board (PCB)

A PCB is a non-conductive material (usually called laminate) with logical conductive lines (usually copper) printed or etched on them. Electronic components mounted are on the board and the conductive line traces connect the components together to form a logical working circuit or assembly. The PCB is of single or double side with single or multiple layers of rigid laminate (consisting of a woven-glass-epoxy base material clad) and copper foils. The copper is the conductive trace layer and the rigid laminate is the nonconductive material. In this experiment, Mr. Peter Narbus designed the PCBs and TTM Technologies (Time-To-Market Interconnect Solutions) at Chippewa Falls Division, manufactured the PCBs. The test board dimensions are 173 mm by 254 mm with a board thickness of 5 mm. The printed circuit board (PCB) has eight Copper (Cu) layers and is a double sided test board. Two different printed circuit board materials namely Flame-Retardant-406 and Megtron-6 were tested. The Flame-Retardant-406 board material used in this experiment is a high-temperature multi-functional glass-epoxy Teflon laminate with a glass-transition temperature (T_g) of 170°C, whereas the Megtron-6 board material used in this experiment was a very high-temperature Polyphenylene-Ether blend with a glass- transition temperature (T_g) of 210°C. The glass transition defined as "reversible change in an amorphous polymer or in amorphous regions of a partially crystalline polymer from (or to) a viscous or rubbery condition to (or from) a hard and relatively brittle one"[10]. The glass transition temperature (Tg) defined as "characteristic value of the temperature range over which the glass transition takes place"[10]. The printed circuit board (PCB) incorporates 14,607 pins, 3590 through-holes, and 11017 copper pads. The board also includes 12 tool-holes, each of which has a diameter is 3.8 mm and the distance from the edge of packages/board-features to the center of the holes is at least 7mm. The surface

finish for all boards was Organic Solderability Preservative (OSP).Each printed circuit board has land patterns with local fiducials for the placement of up to 13 components and 30 resistors on top side, while 30 components and 45 resistors on the bottom side. Each component land-pattern is electrically connected to one of the through-holes for monitoring, except for the surface mount resistor (SMR) components, which are electrically daisy-chained together in groups of five (5) for readout through a single channel. All components and SMR components have a common ground channel completing the electrical circuit. The design copper trace pattern used for the top and bottom side of the board are different. Total component and surface mount resistor are 19 channels and 1 ground on the top side of the board. Total component and surface mount resistor are 39 channels on the bottom side with the same-shared ground on the top and bottom side of the board.

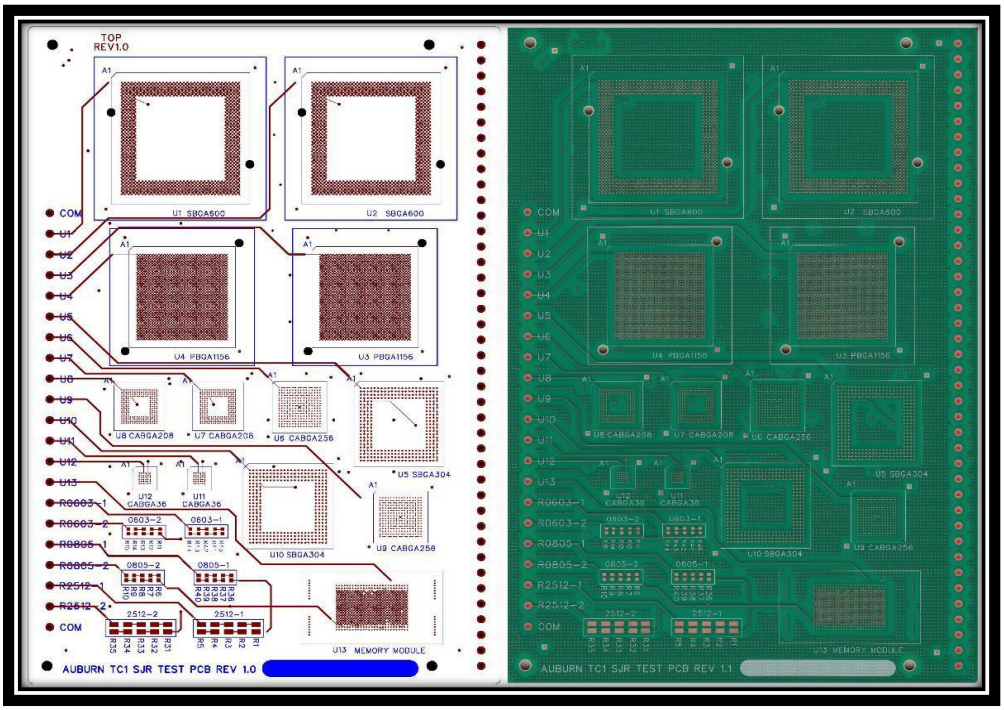

Figure 9 Top Side Board Layout Design and PCB

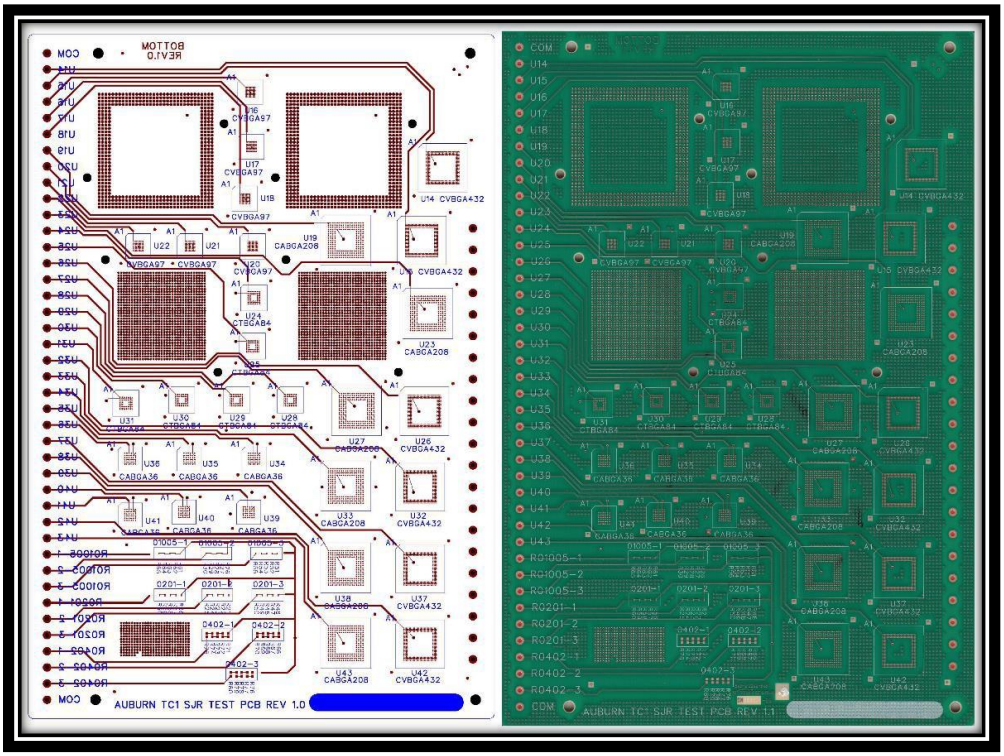

Figure 10 Bottom Side Board Layout Design and PCB

1.2.7. Coefficient of Thermal Expansion (CTE) in PCB

CTE is the dimensional sensitivity in a materials response to a change in temperature[11]. It is representation of percentage change in length per unit temperature. This occurrence is often isotropic, but due to the structure of the laminate in the printed circuit board (PCB), this property becomes anisotropic with two different value of CTE for expansion. First, in the plane of the aligned fibers called “in-plane” and second out of the plane of aligned fibers called “out-of-plane”. These alignment variations are due to the differences in CTE of the glass fiber and the epoxy. The glass fibers have a CTE of approximately 5-6 ppm/°C, while the epoxy typically has a CTE of 35-45 ppm/°C. By applying Schapery Equation the composite board CTEs are calculated, this equation gives a weighted average value for CTE based on the fundamental properties of the individual components of the composite. The following is

Equation 1 Schapery Equation [12]

$$\mathbf{a_c} = \sum_{i=0}^{n} \frac{a_i v_i m_i}{v_i m_i}$$

Where a_c is the composite CTE (expressed in ppm/°C)

a_i is the CTE of the individual components (expressed in ppm/°C)

m_i is the Young’s Modulus of the individual components (expressed as G-Pa)

v_i is the volume of the individual components (expressed in cubic meter)

A tensile testing machine UTM, used to calculate the modulus of elasticity of the boards at room temperature. Samples prepared by cutting the boards in dog-bone shaped as per the ASTM D412 Standards. The length of the dog bone sample was 100mm with the width of 16mm. The length in the middle section was 33mm and the grip section was 30mm. A force per unit length of magnitude

of 2 N/m is applied to the samples. The before surface mount assembly of the Flame-Retardant-406 board and Megtron-6 board properties provided by TTM Technologies are in Table ii.

Table ii Printed Circuit Board Properties from TTM Technologies

Board Type	Coefficient of Thermal Expansion CTE (ppm/°C)			Young's Modulus	Glass Transition Temperature
	x-dir.	y-dir.	z-dir.	E (G-Pa)	(T_g)°C
Megtron-6	15.7	15.7	24.2	27.8	210
Flame-Retardant-406	17.1	17.1	30.5	28.5	170

1.2.8. Surface Mount Assembly

The second level of packaging is the electronic assembly, or Printed Circuit Board Assembly (PCBA). The interconnections of the silicon chip to the printed circuit board is the PCBA.

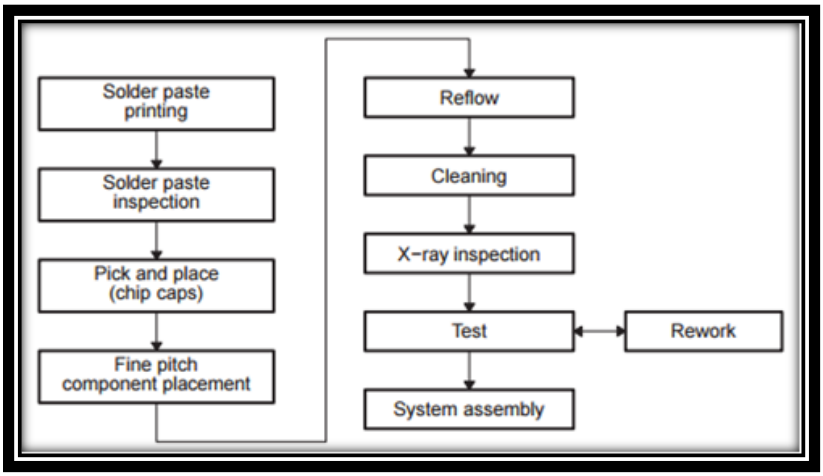

Figure 11 Surface Mount Assembly Process Overview [8]

First step in building an electronic assembly is solder paste printing. Solder paste consists of powder of metal particles suspended in a solder flux. Flux is a thick medium that is a temporary adhesive to hold the components until the solder paste melts during reflow process and makes a metallurgical bond. In this experiment, Kester No clean Flux is used. The prevailing method of solder paste printing to the PCB lands is via a screen or stencil printing process. Stencil aligns over each PCB inside a paste-printing machine and the stencil has apertures through which the solder paste flows onto the PCB land pattern with the help of a squeegee. There are two stencil sizes used in this experiment one for the top sideboard assembly with a 0.127 mm thickness and the bottom sideboard assembly with a 0.0762 mm thickness for finer pitch components. Photo stencils manufactured both the stencils. There are two different solder pastes used in this experiment, SAC305 paste for lead-free solder alloys and a Sn-Pb paste for Tin-Lead solder alloys. Solder paste is printed onto the copper lands of the Printed Circuit Board, with the help of a stencil.

Table iii Solder Paste and Stencil Size

Board Side	Solder Paste			Stencil Thickness
	Kester	Alpha		(mm)
Top	Sn-Pb	SAC305	Innolot	0.127
Bottom	Sn-Pb	SAC305	Innolot	0.0762

Second optional step is by laser measurement on the PCB to check for uniform spread of solder paste volume across the various portions of the PCB. Thirdly, placement machine picks and places components on top of the printed solder paste of the PCBs. Local and global fiducials on the PCB references the placement locations of the component.

Fourthly, components placed on the printed circuit board are photo captured and x-ray processed for any misalignments or misplacements. Once the assembly process passes the visual inspection test. The boards and components are ready for the final step.

Finally, the Surface Mount assembly passes through reflow soldering. Reflow soldering is done by the help of a large convection oven with multiple, independently controlled temperature zones. During solder reflow process, the printed circuit board assembly (PCBA) setup passes through the reflow oven experiencing a specific time temperature profile designed as per the solder paste manufacturer's recommendation. The manufacturers recommended reflow profile helped to create good quality solder joints at all necessary locations on the board while avoiding bridging and other common manufacturing defects. Reflow takes place when the solder alloy exceeds its liquidus temperature.

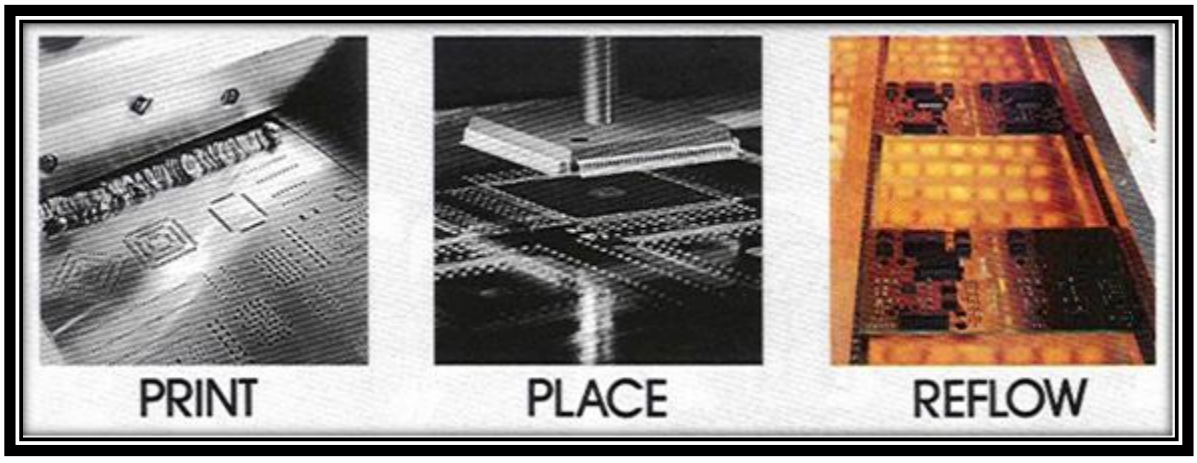

Figure 12 Key Steps in SMT Assembly [9]

There are four different reflow profiles used in this experiment, two for the top side and two for the bottom side.

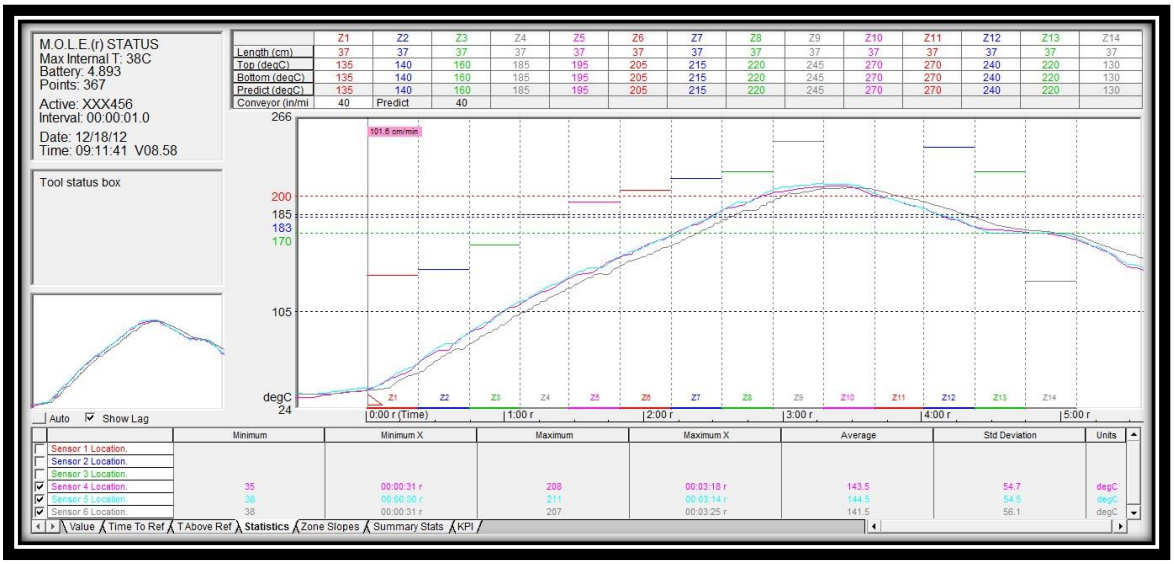

Figure 13 Tin-Lead Reflow Profile Bottom Side Board

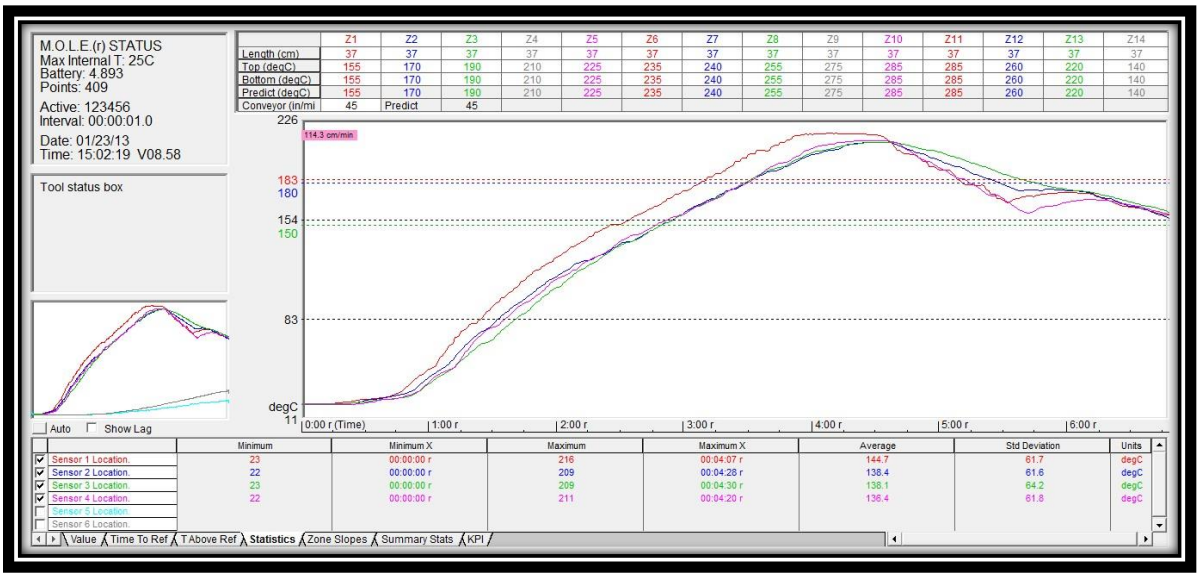

Figure 14 Tin-lead Reflow Profile Top Side Board

The manufacturers recommended preheat stage is to bring the package up to about +125°C (±25°C) the rate of increase from ambient(25°C) to 125 °C should be approximately 2 to 3°C per second. Pre-flow stage is the gradual transition from 125°C to the point of eutectic transformation (+183°C). This stage allows the entire board to achieve an equilibrium near the melting point of the solder.

The rate of temperature change should be between 0.5 to 1 °C per second. Reflow stage is the portion of the profile where the solder changes from a solid to a liquid and the actual flux and flow action occur. Solder will flow to all areas not protected by solder mask. The manufacturer recommends that a rapid rise to a maximum temperature of 235°C with the dwell time above 215°C to be below 30 seconds. The total time above 180°C should be less than 180 seconds. Post dwell above 215°C should transition directly into the package and board cool down ramp. As the package and board drops below the solder liquidus point of +183°C the cool down temperature ramp controls the solder grain size and fatigue resistance. The cool down rate should be approximately 2 to 4°C per second. Do not exceed 5°C per second.

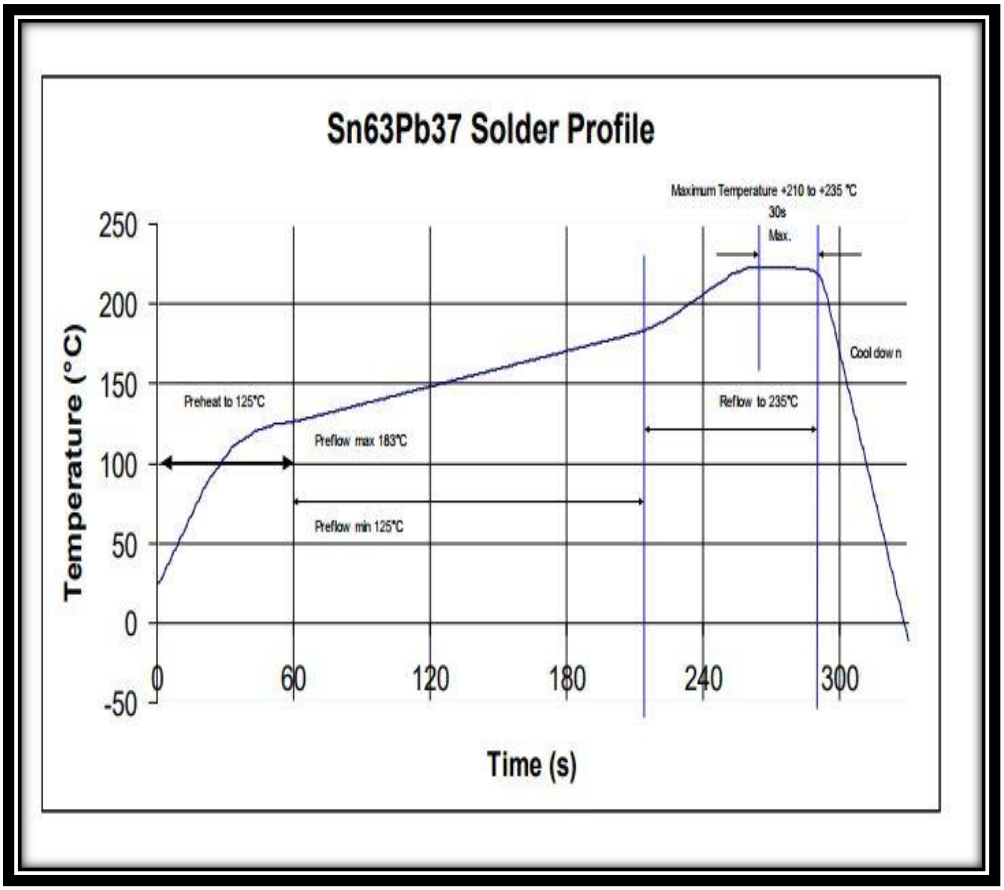

Figure 15 Tin-lead Manufacturer's Recommended Profile [8]

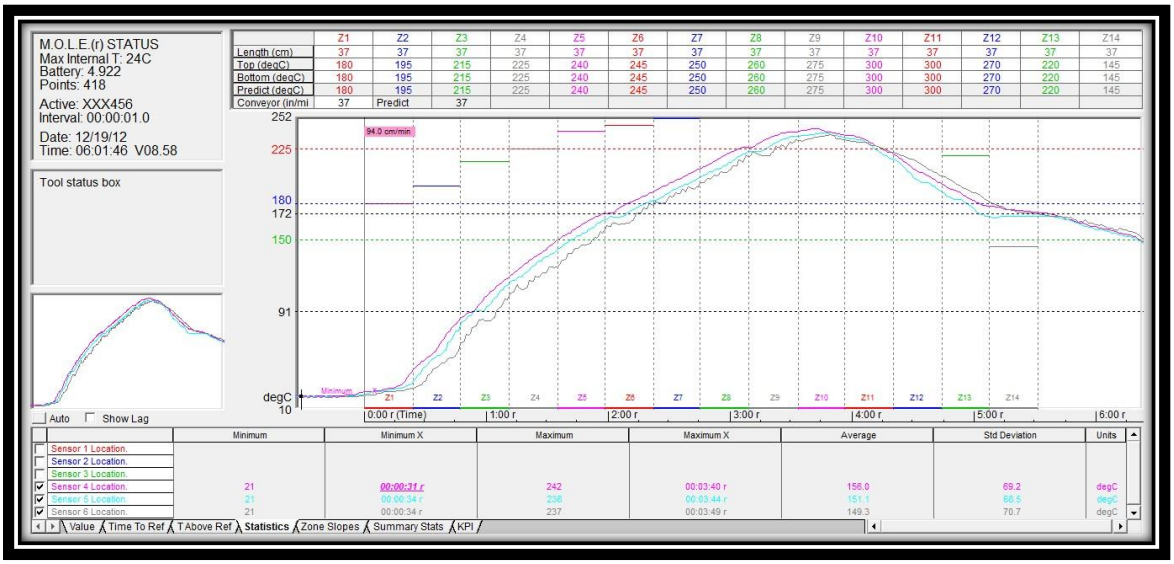

Figure 16 Lead-free Reflow Profile Bottom Side

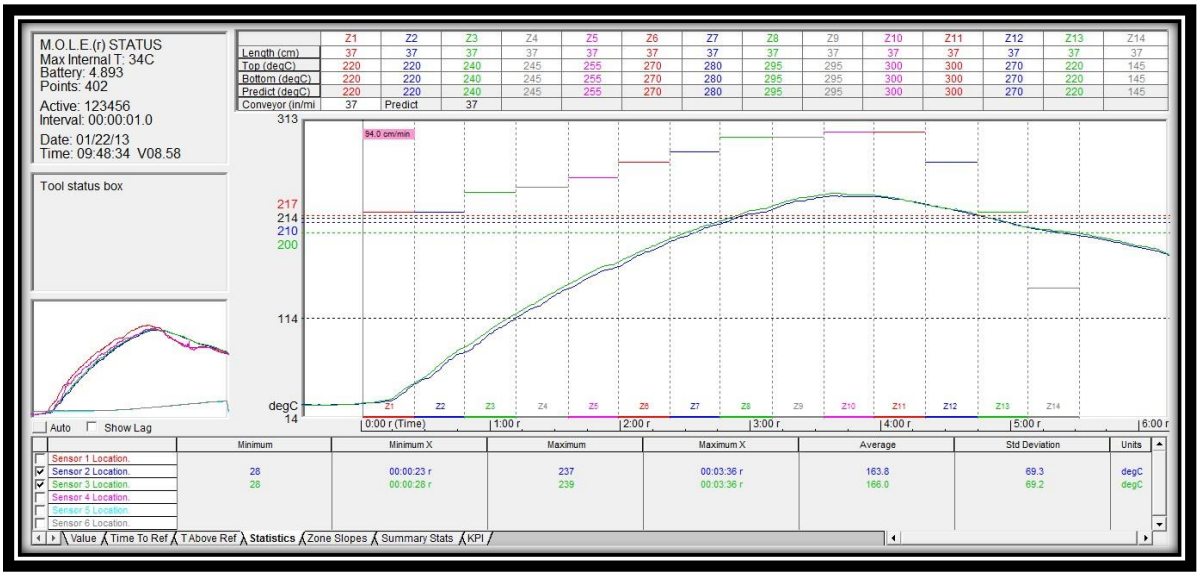

Figure 17 Lead-free Reflow Profile Top Side

The manufacturers recommended preheat stage is to bring the package up to about +170°C (±25°C) the rate of increase from ambient(25°C) to 170 °C should be approximately 2 to 3°C per second. Pre-flow stage is the gradual transition from 170°C to the point of eutectic transformation (+215°C). This stage allows the entire board to achieve an equilibrium near the melting point of the solder.

The rate of temperature change should be between 0.5 to 1 °C per second. The reflow stage portion of the profile where the solder changes from a solid to a liquid and the actual flux and flow action occur. Solder will flow to all areas not protected by solder mask. The manufacturer recommends that a rapid rise to a maximum temperature of 260°C with the dwell time above 250°C to be below 30 seconds. The total time above 217°C should be less than 150 seconds. Post dwell above 217°C should transition directly into the package and board cool down ramp. As the package and board drops below the solder liquidus point of +217°C the cool down temperature ramp controls the solder grain size and fatigue resistance. The cool down rate should be approximately 3 to 5°C per second. Do not exceed 6°C per second.

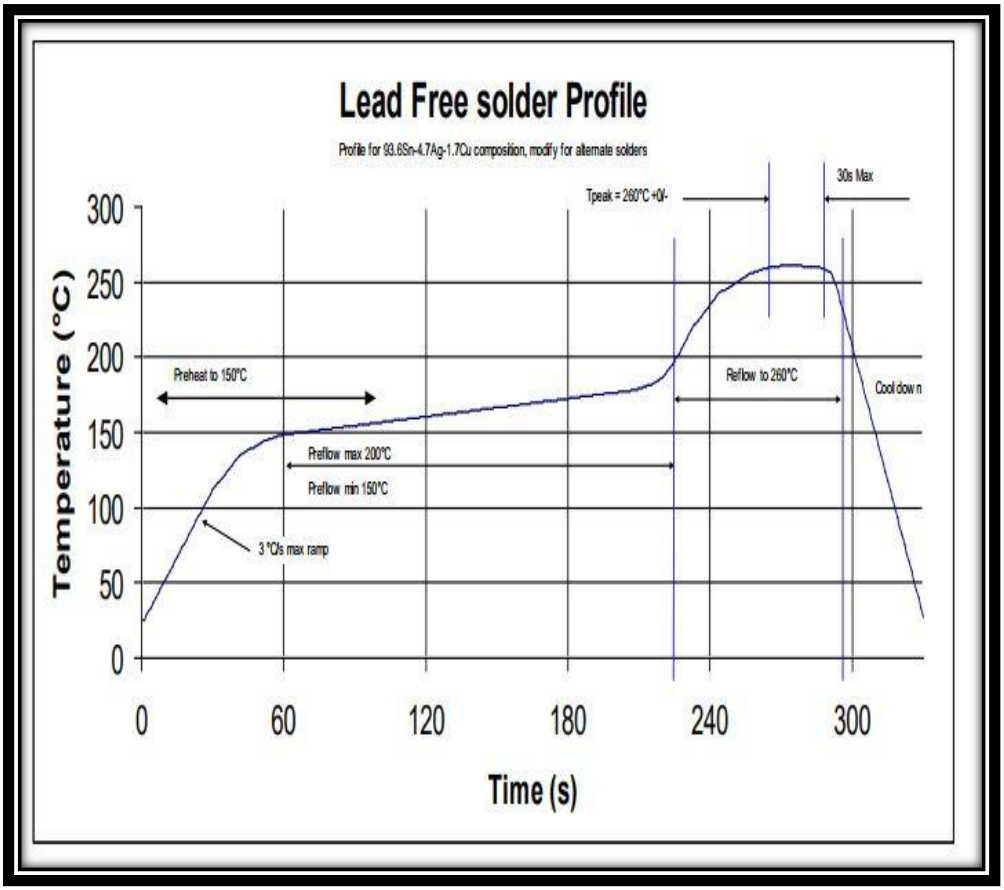

Figure 18 Lead-free Manufacturer's Recommended Profile [8]

1.3. Solder Material

'Solder born from old French, "soudure," meaning fasten together. In English, solder has a noun meaning "a fusible metallic alloy used for uniting less fusible metal surface or parts" dates to 1350 B.C. Lead was first derived as a by-product form silver production. Lead primarily used as a setting agent to fix posts in ground and lock mortised stones. Mesopotamians [3000 B.C.] used lead to join copper pieces'[13]. 'Alloys of lead and tin marked their presence from surviving artifacts and literary source of the Roman Imperial Period. Welded lead strips in stained glass of the five prophet's window in Augsburg Cathedral dating late 11^{th} century is another evidence of material alloys. The 20^{th} Century, modern practices developed with the improvement of extraction techniques which gave raise to exotic metal at affordable cost along with the alloy phase diagrams paving the path for diversity in alloy making today'[14].

1.4. Soldering

'Welding, Brazing, and Soldering of metals are methods for joining separate metalwork pieces by heat treatment. Soldering is a process of heating the two mating surfaces by a molten filler metal with or without the presence of fluxing agent and then cooling them to form a metallurgical bond between the filler metal and the two mating Surfaces. A chemical fluxing agent often used to remove oxides and contamination. Soldering temperature is usually below 450°C or 840°F, or else it is brazing. Thus, Soldering restricts the material selection to low meting elements'[14]. The following Table iv shows the possible materials that qualify for the electronics industry based on their atomic number and melting temperature.

Table iv Materials that qualify for Soldering in Electronic Interconnects

Melting temperature (T_m) (°C)	**Name of element**	**Symbol**	**Atomic number**
30	Gallium	Ga	31
39	Rubidium	Rb	37
44	Phosphorus	P	15
64	Potassium	K	19
98	Sodium	Na	11
113	Sulfur	S	16
114	Iodine	I	53
157	**Indium**	**In**	**49**
180	Lithium	Li	3
217	Selenium	Se	34
232	**Tin**	**Sn**	**50**
254	Polonium	Po	84
271	**Bismuth**	**Bi**	**83**
302	Astatine	At	85
303	Thallium	Tl	81
321	**Cadmium**	**Cd**	**48**
327	**Lead**	**Pb**	**82**
420	**Zinc**	**Zn**	**30**
449	Tellurium	Te	52

1.5. Eutectic Property of Tin-Lead (Sn-Pb)

The term “eutectic” coined from Greek word “eutektos”, meaning ‘Easily Melted’[14]. A eutectic or eutectic mixture is a homogeneous mixture of two or more elements in a ratio that has the lowest melting point, and this melting temperature (T_m)is Eutectic Temperature[15]. Eutectic alloys will have more homogeneous compositions, and provide the lowest possible melting temperature (T_m)for a given alloy mixture. The important point about 63Sn-37Pb Tin-Lead solder is that it is a ‘eutectic’ alloy. Eutectic alloys have a single temperature (183°C) at which the entire alloy melts.

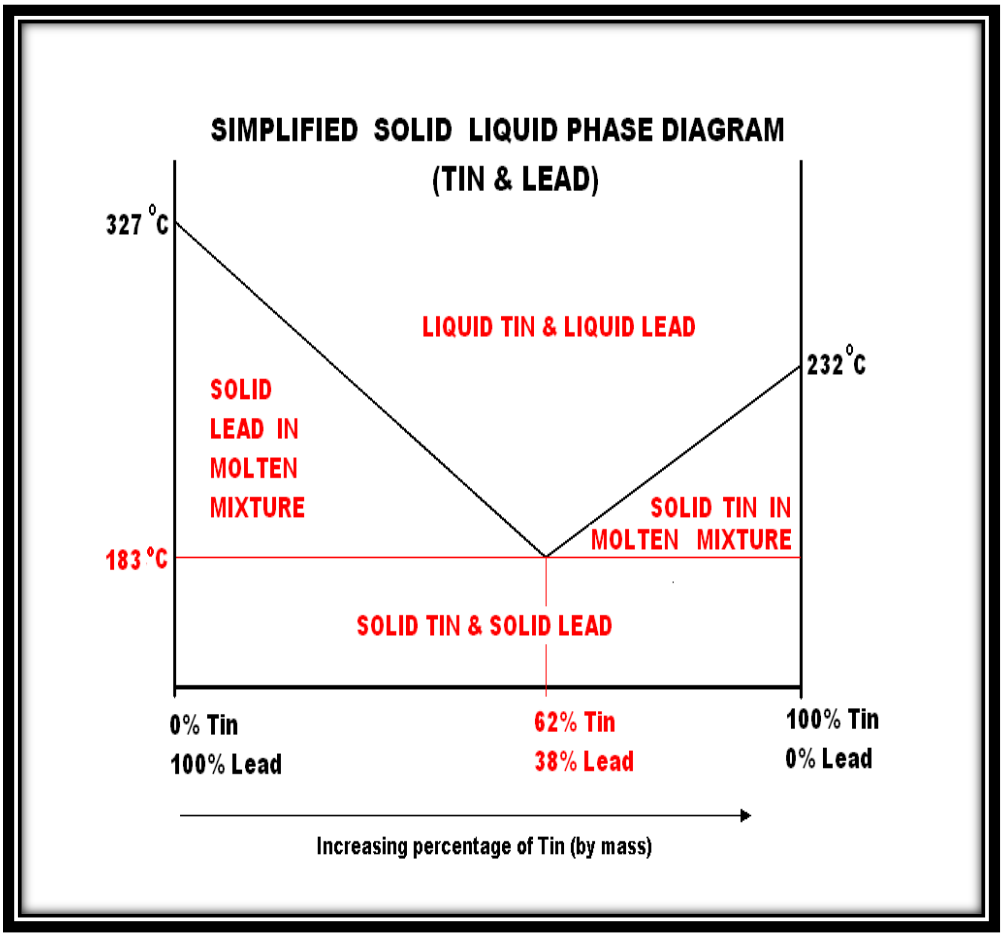

Figure 19 Simple Tin-lead Phase Diagram [16]

For the electronic assembly the 63Sn-37Pb Tin-Lead solder was the most favorite choice of the industry until the lead-free imposition by RoHS and WEEE. Forced upon, the electronic industry had to find new solder materials with eutectic or near eutectic property like that of Tin-Lead.

1.6. Eutectic Property in other Binary Materials

The foremost shot at finding an optimal replacement began with the exploration of binary alloy options. Tin (Sn) was still one of the two binary elements for its low toxicity, relatively low cost, resistance to oxidation and contribution to the melting point or range of an alloy. Much of this analysis performed was by researching the equilibrium phase diagrams of various Sn-based alloys.

Table v Binary Eutectic Alloys of Tin (Sn)

Binary Alloys	**Eutectic**	
	Temperature(°C)	**Composition (wtpercentage)**
Sn-In	120	51
Sn-Bi	139	57
Sn-Cd	177	32.2518
Sn-Pb	183	38.1
Sn-Zn	198.5	9
Sn-Au	217	10
Sn-Ag	**221**	**3.5**
Sn-Cu	**227**	**0.7**

Tin-Zinc (Sn-Zn) and Tin-Cadmium (Sn-Cd) rejected even though having homogeneous eutectic melting temperatures near to that of Tin-Lead (Sn-Pb) are for Zinc oxidation and Cadmium toxicity. Tin-Bismuth (Sn-Bi) rejected even though having lesser homogeneous eutectic melting temperature (T_m)that that of Tin-Lead (Sn-Pb) for its brittle nature and for its low melting temperature. During the transition from lead-free packages, the possibility of Bismuth and 0.1percentage Lead interaction can reduce the melting point by more than thirty degrees, making it difficult to build with other lead frame packages. The eutectic composition of Tin-Silver (Sn-Ag) and Tin-Copper (Sn-Cu) is predominately Tin (Sn) meaning intermetallic compounds are formed within the Sn matrix inhomogeneity into the microstructure. Tin-Silver (Sn-Ag) has a eutectic point at 3.5wtpercentage of silver with a eutectic equilibrium melting temperature (T_m)of 221°C closest to the melting temperature (T_m)of pure tin at 232°C, which is all the more by 40°C than the eutectic Tin-Lead (Sn-Pb) temperature. Silver alloy, is rejected for its economic cost as replacement Lead alloy. Tin-Copper (Sn-Cu) has a eutectic point at 0.7wtpercentage of copper with a eutectic

equilibrium melting temperature (T_m)of 227°C closest to the melting temperature (T_m)of pure tin at 232°C, which is all the more by 44°C than the eutectic Tin-Lead (Sn-Pb) temperature. This Copper alloy is replacement Lead alloy, for its interaction with the copper pad on the Printed Circuit Board.

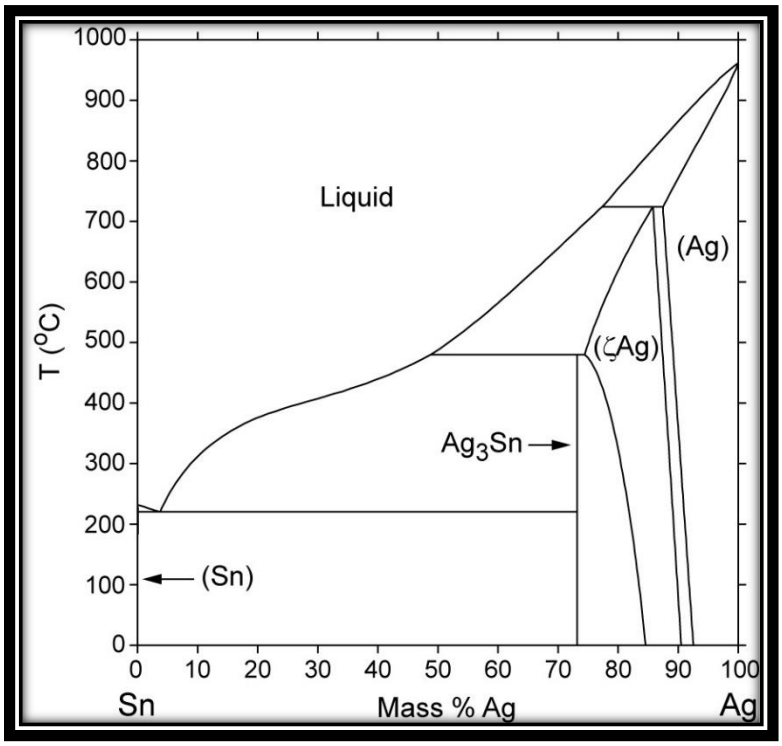

Figure 20 Tin Silver Phase Diagram [17]

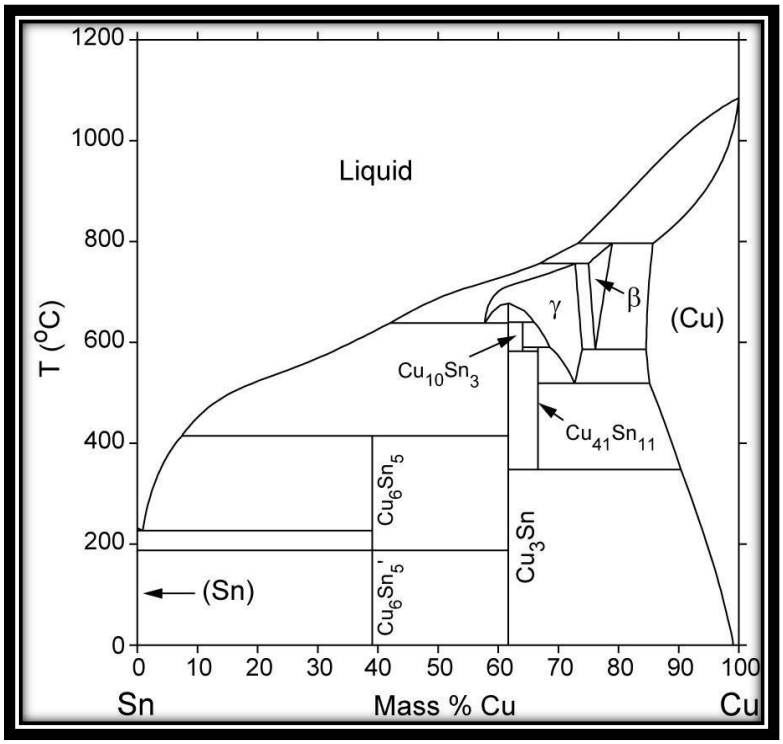

Figure 21 Tin Copper Phase Diagram [17]

1.7. Non-Eutectic Property in other Ternary Materials

The solution to finding a simple binary replacement alloy to Tin-Lead (Sn-Pb) was let go, and a more viable ternary combination of elements came into strategy. The exertion in the ternary alloys is the eutectic equilibrium melting temperature (T_m)range of the alloys. This is much higher than that of the eutectic Tin-Lead (Sn-Pb). To overcome these technical hitches, the industry set some standards to finding the possible replacement ternary alloy.

The criteria as defined in Lead-free Soldering [16] are

- Have melting point as close to Sn-Pb eutectic as possible
- Be eutectic or very close to eutectic
- Contain no more than three elements

- Avoid using existing patents, if possible
- Have the potential for reliability equal to or better than Sn-Pb eutectic.
- Liquidus temperature as close as possible to 183°C
- Solidus temperature as close as possible to liquidus temperature (small pasty range)
- Solidus temperature significantly higher than the solder joints maximum operating temperature.

The original top choices of the electronic industry with ternary alloys were Tin, Silver, Copper, and Bismuth with Sn-Ag-Cu, Sn-Bi-Cu, and Sn-Ag-Bi ternary combinations. But the coagulation of Lead (Pb) and Bismuth (Bi) to form very low intermetallic melting temperatures (Bi-Pb eutectic at 125.9°C, Sn-Pb-Bi ternary eutectic at 98°C), deemed Bi to be phased out.

The Sn-Ag-Cu eutectic ternary alloy is of the composition Sn-3.5Ag-0.9Cu by weight percentage with a eutectic melting temperature (T_m)of 217.4±0.8°C. This bond forms a ternary eutectic made up of faceted Cu_6Sn_5 matrix and non-faceted Ag_3Sn matrix of intermetallic within the predominant Tin(Sn) element[18].

The melting temperature (T_m) of this ternary eutectic is 10°C lower than that of its predecessor binary eutectic Tin (Sn)-Copper (Cu). Near eutectic compounds of Sn-Ag-Cu are the default solder standard in the market today, specifically SAC105, SAC305 and to a lesser extent SAC405. Due to higher Silver cost, (i.e. consumer electronics) the predilection is for a lesser quantity of Silver (Ag).The added benefit is the reduction in the potential formation of undesirable Ag_3Sn platelets[18].

Figure 22 shows the phase diagram of SAC alloys and specifically the Sn-rich region, which highlights the formation of a Sn - Sn+Ag_3Sn-Sn - Cu_6Sn_5 ternary compound.

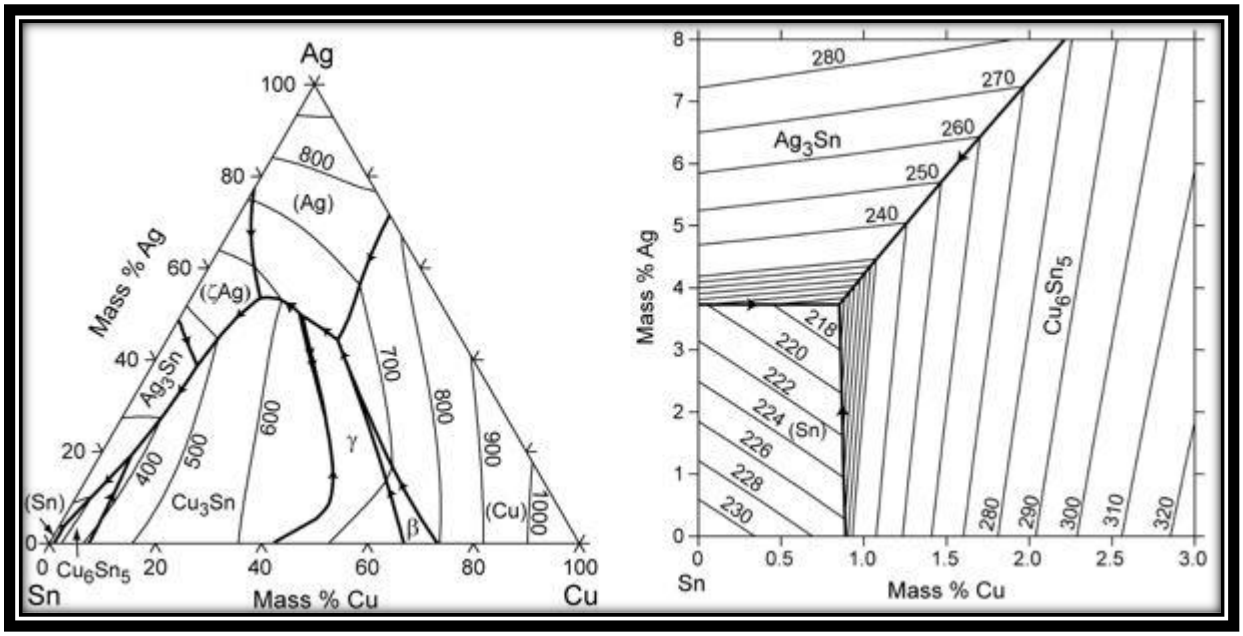

Figure 22 Sn-Ag-Cu Phase Diagram with Tin (Sn)-rich corner of the Phase Diagram [17]

The demand for a replacement alloy for electronic assemblies lead to the current industry standard of tin-silver-copper alloys, (Sn-Ag-Cu or SAC). The most widely used are SAC105 and SAC305, both contain 0.5-weight percentage of Cu and (1-weight percentage and 3-weight percentage) of Silver (Ag) respectively. Although these Sn-based alloys are in wide use, there remain a number of limitations, which necessitate the continued research for a better standard and more reliable alloy. Both Lead-free SAC105 and SAC305 are non-eutectic alloys with melting ranges of 217-225°C and 217-220°C respectively, considerably much higher than the 183°C melting point of eutectic Tin- Lead 63Sn-37Pb.

1.8. Solder Joint

A solder joint is formed when two conductors, one with high melting temperature (T_m) primarily Copper (Cu) (1085°C melting temperature), is fused with another low melting temperature (T_m) secondarily Tin (Sn) (231.9°C melting temperature (T_m)). Tin (Sn) has unique ability to form intermetallic compounds with many different materials. In the case of electronic surface mount, solder joint assembly act as electrical, mechanical and thermal bonds. The solder joint is comprised of two interfaces between the copper and solder called intermetallic as well as the bulk solder (which is filler material between the two interfaces). The interfaces are chemical bonds between the Tin (Sn) from the solder and the Copper (Cu) from the connecting conductors[18].

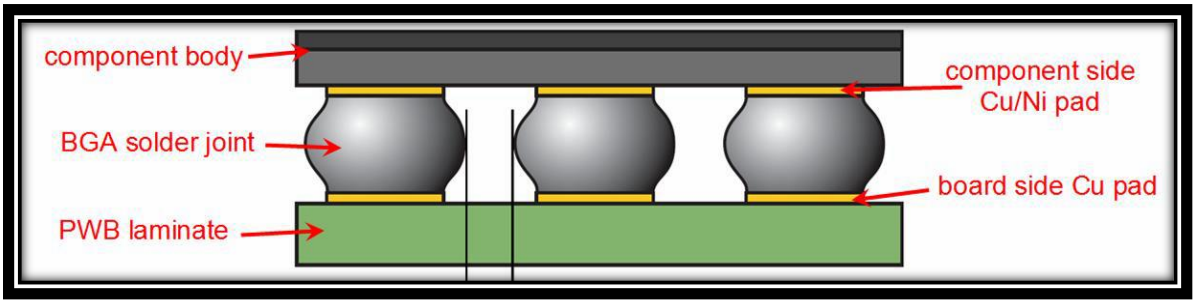

Figure 23 Schematic of a Ball Grid Array Solder Joint [18]

1.9. Quality and Reliability

The solder joint quality and reliability problems have plagued the electronics since its inception. Early electronic designs were fraught with problems such as fundamental design errors, under-estimation of the operating conduction powers, and poor integration into the large system of devices. In fact, the evolution of Reliability Engineering as an independent engineering discipline took place in the Unites States in the 1950s due to the expanding reliance of the military on electronics combined with the ever-increasing complexity of electronic systems.

The semiconductor industry has learned from these problems over the past several decades, and

electronic manufacturers, designers, printed circuit board manufacturers, consultants, and electrical engineers have been working together to improve power consumption, electronic design, fabrication, and operation performances. Over time, these efforts have led to internationally recognized electronic standards (IEEE, IPC, JEDEC, etc.,) for testing and improving electronic reliability.

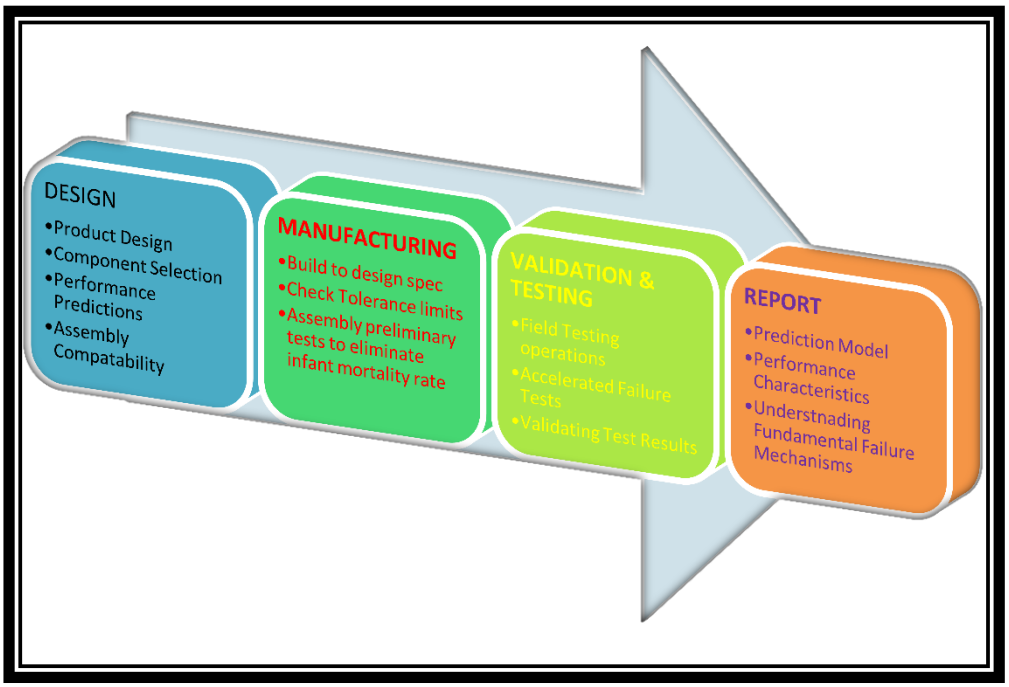

Figure 24 Electronic Systems Testing Life Cycle

The standard electronic product development cycle consists of a number of discrete steps that include activities beyond those normally considered part of the design process. These steps include initial design, computer modeling, component and system testing, model validation, manufacturing, operations and maintenance, and product improvement as shown in Figure 24. Reliability defined as "The probability that an item will perform a required function without failure under stated conditions for a stated period of time" [19]. The reliability of any system depends on the reliability of each individual components of the system.

An assembly is likely to fail due to component failure in the short term and due to solder attach failure in the long-term. Printed Circuit Board (PCB) failure of an electronic component is often traced back to the solder joint failures. Ductile failures are more predictable and are preferable to Brittle type of failures. Two of the common failure modes observed in BGA-type solder joints are failures along the solder near the intermetallic composition boundary regions, and failures through the bulk solder. Depending on the type of failure observed, the data classified are as per their failure modes.

1.10. About this Dissertation

This dissertation assesses the reliability of various combinations of semiconductor packages listed in the Table vi on both Flame-Retardant-406 and Megtron-6 substrate materials. In addition, the effect of heatsinks are studied in the PBGA1156, and SBGA600 components over the two different substrates and the effect of solder paste volume over the two different substrates are studied in the CABGA36 and CABGA208 packages. The surface finish used in the semiconductor electronic package is Organic Solderability Preservative (OSP). In this experiment, the six-element alloy (Sn3.8Ag0.7Cu3Bi1.4Sb0.15Ni) trade name called “Innolot” is one of the many proposed solutions to resist the damage accumulation due to low creep fatigue stress under temperature cycling environment.

Table vi Electronic Packages

Component	Ball Alloy	Paste Material	Pitch	Package Dimension	Package Material
CVBGA97	SAC 305	SAC305	0.4mm	5 sq.mm	Ceramic
	SAC 105				
	SnPb	SnPb			
CVBGA432	SAC 305	SAC305	0.4mm	13 sq.mm	
	SAC 105				
	SnPb	SnPb			
CTBGA84	SAC 305	SAC305	0.5mm	6 sq.mm	
	SAC 105				
	SnPb	SnPb			
CABGA36	SAC 305	SAC305	0.8mm	6 sq.mm	
	SAC 105				
	Innolot				
	SnPb	SnPb			
CABGA208	SAC 305	SAC305	0.8mm	15 sq.mm	
	SAC 105				
	Innolot				
	SnPb	SnPb			
CABGA256	SAC 305	SAC305	1.0mm	17 sq.mm	
	SAC 105				
	SnPb	SnPb			
PBGA1156	SAC 305	SAC305	1.0mm	35 sq.mm	Plastic
	SAC 105				
	SnPb	SnPb			
SBGA304	SAC 305	SAC305	1.27mm	31 sq.mm	BT (Bismaleimide Triazine)
	SAC 105				
	SnPb	SnPb			
SBGA600	SAC 305	SAC305	1.27mm	45 sq.mm	
	SAC 105				
	SnPb	SnPb			

This experiment designed to study the performance of the solder joint materials reliability, is at three different temperature levels and at four different period levels as displayed in Table vii. The performances of the solder materials were determined from the ability of the solder interconnects (solder ball and solder paste combination) to withstand the temperature stresses induced by

alternating temperature extremes.

Table vii Design of Experiment

Time Period	Temperture Storage
0 days	25°C
180 days	25°C
	50°C
	75°C
360 days	25°C
	50°C
	75°C
720 days	25°C
	50°C
	75°C

After the end of each period, the electronic package assemblies were placed in an alternating temperature cycling single zone environmental chamber and then subjected to temperature extremes of (-40°C to +125°C) on a 120-minute temperature profile.

The electrical resistance measurements were continually monitored using a LabVIEW software program, and a Keithley multimeter instrument. The failure as defined by the IPC- 9701 standard is “the interruption of electrical continuity >1000 ohms is a loss in solder interconnection”[20]. Data-logger state machine function of LabVIEW program logs the time stamp, temperature measurement and cycle count. Failure data are stored on a SQL server for further data and Weibull analysis.

The failure data collected from each of the four periods, three different temperatures, two different substrates, and many different packages with three different solder paste materials for various different components as shown from Table vi, Table vii were studied for reliability trends and their mean times to fail are resulted.

The results from this experiment showed various reliability trends as a function of the following factors

- Type of Component Substrate Material
- Size of the Component
- Type of Board Substrate Material
- Type of Solder Alloy Material
- Type of Solder Paste Material
- Volume of Solder Paste Material (Available only for CABGA36 and CABGA208)
- Effect of Heat Sinks (Available only for PBGA1156 and SBGA600)

The conclusive final trend from all of the above-mentioned factors is that as aging time-period increases, reliability of solder joint materials decreases and, as aging temperature of the storage increases, reliability of solder joint materials decreases. There is also a direct correlation of aging time and aging temperature to that of the intermetallic composition growth. The degradation of reliability trends calculated are from the experimental failure data using proportional hazards and survival/reliability Weibull analysis methods, for the above-mentioned factors at different aging time-periods and aging temperatures.

After the intermetallic and microstructural grain orientation studies that cause physics of such failure modes, the reliability trends of the solder material degradation are better understood. Lead-free solder alloy materials with good thermal performance generally tend to have either high Ag content (>3.0%), or high Bi content (>3.0%), or high Sb content (>1.5%). Failure analysis of solder joints show continuous increase in the thickness of Intermetallic Compounds (IMC) at solder joint-copper pad interface and within the solder bulk as time and temperature progresses.

For solder alloys that contain high Ag content (>3.0%), large plate-like Ag_3Sn growth observed within the bulk solders of Sn matrix. Inter-metallic-composition (IMC) observed near the copper pad are of Cu_6Sn_5 lumps. IMC thickness analysis shows that during temperature aging and cycling, the IMC layer in both the component and board side interfaces coarsen significantly and evident from the optical microscopy measurements.

Thus, the material from the copper pads and solder joints diffused into the IMC to form recrystallization observed through polarized optical microscopy. Solder alloys with high bismuth (>3%) and silver (>3%), can help limit the growth of the IMC layer thickness, as well as prevent copper diffusion from the PCB copper pad into solder joint, hence help stabilize and strengthen the interfacial IMC layer and improve reliability performance. Most observed crack propagation is either on the component-side or on the board-side, near interfacial regions. For a few instances, cracks observed are through the bulk solder.

1.11. Dissertation Outline

This dissertation contains the following chapters:

- Chapter 1: Dissertation Context
- Chapter 2: High Accelerated Life Testing for Solder Joint Reliability in Temperature Cycling Test
- Chapter 3: Description of Experimental Setup and Data Acquisition System.
- Chapter 4: Reliability Data Analysis using 3-parameter Weibull Distribution plots
- Chapter 5: Failure analysis
- Chapter 6: Statistical Prediction Models for System Level Reliability
- Chapter 7: Results and Conclusion

Chapter 2 High Accelerated Life Testing for Solder Joint Reliability in Temperature Cycling Test

2.1. Accelerated Life Testing

Reliability is "Times-To-Failure (TTF) data obtained under normal operating conditions of a product in order to quantify the life characteristics of a product, system or component". The exertion in this method of data collection is the long service life times of modern consumer electronics, versus the available time to test the product between design and release. To overcome this difficulty and to evaluate the products by their failure modes and life characteristics, a new engineering test method called "Accelerated Life Testing (ALT)" to accelerate failures more swiftly than normal use conditions is needed. Accelerated Life Testing is a "set of methods that attempts to replicate and predict the quantitative effect on product life by subjecting it to conditions (Temperature, Stress, Strain, Vibration, etc.,) higher than that of actual service parameters"[21]. Accelerated life testing approach gives information quicker on product life distribution. First, a model is fit for accelerated failure data. Second, by model extrapolation an estimate of product life distribution under normal use condition is derived [22]. The accelerated life testing is of two types Qualitative and Quantitative. The qualitative tests yield information on failure modes only, (HALT, HAST, torture tests, shake and bake tests) and quantitative accelerated life tests which yield information on life characteristics of the product, component or system under normal use conditions, and thereby provide reliability information[21].

Electronic products, components or systems, expected to perform their functions successfully for long periods (often years). The time required to obtain times-to-failure data must be considerably less than the expected life of the product. For high-accelerated life tests (HALT), time-to-failure information in harsh environments for the product is collected. There are two methods of acceleration, usage rate acceleration and overstress acceleration, that help obtain times-to-failure data at an accelerated pace. Accelerated life test stress levels are to be chosen such that they only accelerate the failure modes under consideration but do not introduce new failure modes that would never occur under use conditions[21].

2.2. Accelerated Life Data Analysis

In an accelerated test, data collection is an important step. Failure data are classified as many types depending on the nature and design of the experiment.

Complete Data

It is the easiest and most accurate data to work with; complete data means that the time to failure value for each sample unit in the experiment is available. For example, if we tested five units and they all failed (and their times-to-failure were recorded), we would then have complete information as to the time of each failure in the sample.

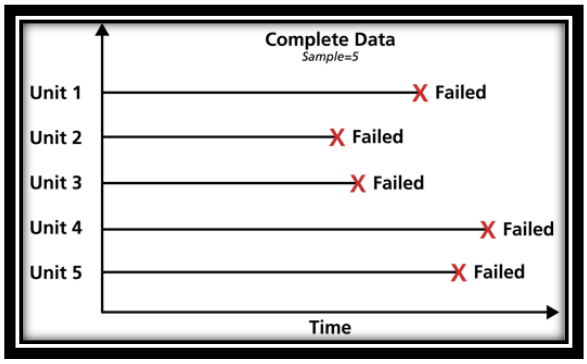

Figure 25 Complete Life Data

Censored Data

In real world experiments, all of the units in the experiment would not have failed i.e., the exact times-to-failure of all the units is not available. This type of data is censored data. There are three types of possible censoring schemes, right censored (suspended data), interval censored and left censored.

Right Censored (Suspension) Data

The most common type of censoring is right censored data, or suspended data. In this case, the life data contains units that did not fail during the accelerated life testing. For example, if we tested five units and only three had failed by the end of the test, we would have right censored data (or suspension data) for the two units that did not failed.

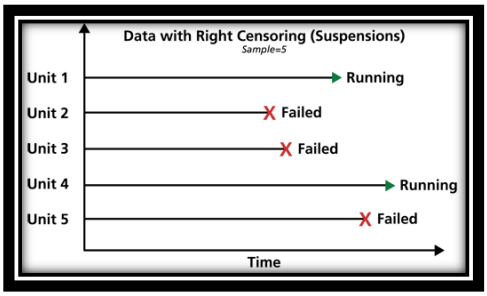

Figure 26 Right Censored (Suspended) Data

Interval Censored Data

The second common type of censoring is interval-censored data. Interval censored data reflects uncertainty to the exact time of unit failure, but the last good known data and post failure data are available within an interval. For example, if we are running a test on five units and inspecting them every 100 hours, we only know that a unit failed or did not fail between inspections. Specifically, if we inspect a certain unit at 100 hours and find it operating, and then perform another inspection at 200 hours to find that the unit is no longer operating, then the only information we have is that the unit failed at some point in the interval between 100 and 200 hours.

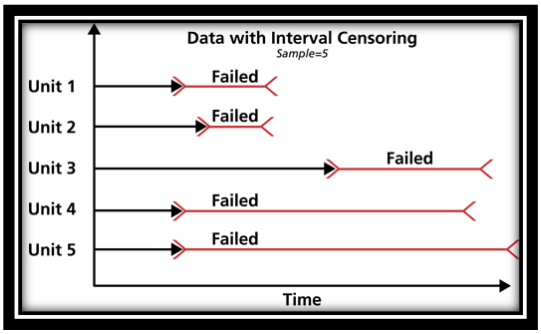

Figure 27 Interval Censoring Data

Left Censored Data

The uncommon type of censoring is the left censored data. In left censored data, the exact failure time of unit is unknown but the post failure data is available. For instance, we may know that a certain unit failed sometime before 100 hours but not exactly when. In other words, it could have failed any time between 0 and 100 hours.

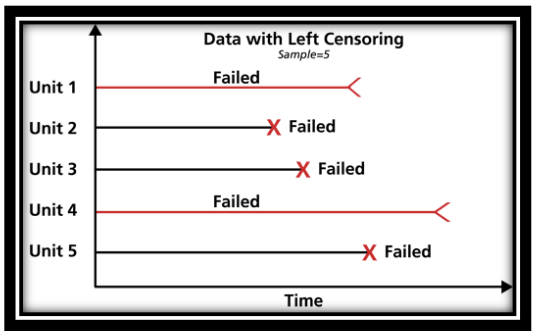

Figure 28 Left Censored Data

2.3. Accelerated Life Data Distributions

To extrapolate the information from accelerated life test data to use level conditions, the times-to-failure data are fit for an underlying life distribution. A pdf of the times-to-failure of the product gives the meaningful information of the product at accelerated test level conditions.

This pdf, used to make predictions and estimates of life measures of interest at that particular test conditions. The objective in an accelerated life test, however, is not to obtain predictions and estimates at the particular elevated test conditions at which the units were tested, but to obtain these measures at another state, the usage condition. To accomplish this objective, we must devise a method to traverse the path from the accelerated test level pdf to extrapolate a use level information.

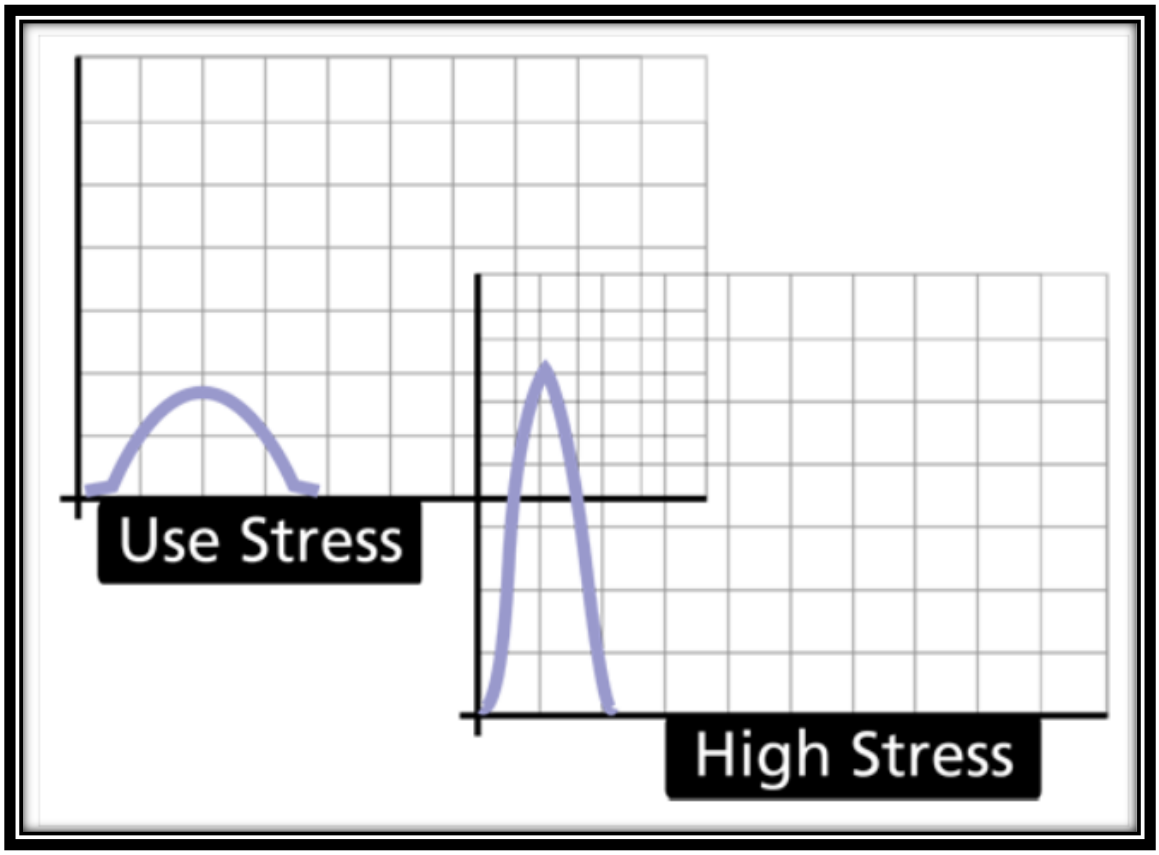

Figure 29 Accelerated Life Pdf versus Use Life Pdf [21]

There are three lifetime distributions commonly used in accelerated life test analysis, namely the exponential, the lognormal and the Weibull distributions.

Exponential Distribution

Most common reliability prediction is exponential distribution. The exponential distribution can only model the behavior of units that have a constant failure rate (or units that do not degrade with time or wear out). Therefore, this is inappropriate to consider for accelerated life tests that have time dependent failures. This distribution though fits the accelerated life data collected, is not used[21].

Lognormal Distribution

Lognormal distribution is used in general reliability prediction analysis (i.e., cycles-to-failure in fatigue, material strengths and loading variables in probabilistic design). When the natural logarithms of the times-to-failure are normally distributed, then one can say that the data follow the lognormal distribution[21]. This distribution will not fit the need for determining the higher temperature induced effects. Therefore, this is inappropriate to consider for accelerated life tests that have temperature dependent failures.

Weibull Distribution

The Weibull distribution is a general reliability distribution used to model material strength, times-to-failure of electronic and mechanical components, equipment or systems[22]. In its most general case, the 3-parameter Weibull pdf is given by

Equation 2 Pdf 3-parameter Weibull

$$f(t) = \frac{\beta}{\eta}\left(\frac{t-\gamma}{\eta}\right)^{\beta-1} e^{-\left(\frac{t-\gamma}{\eta}\right)^{\beta}}$$

If the location parameter, γ, assumed zero, then the distribution becomes the 2-parameter Weibull

Equation 3 Pdf 2-parameter Weibull

$$f(t) = \frac{\beta}{\eta}\left(\frac{t}{\eta}\right)^{\beta-1} e^{-\left(\frac{t}{\eta}\right)^{\beta}}$$

Where

β = Shape Parameter (or slope)

η = Scale Parameter

γ = Location Parameter (or failure free life)[22]

Mean-Time-To-Failure (MTTF)

The Mean-Time-To-Failure $\bar{T}$ is the length of time that a system is in its operation between failures[23]. This is the average "time to failure" for that system. Mathematically, it is

Equation 4 Mean-Time-To- Failure [22]

$$\bar{T} = \gamma + \eta.\Gamma\left(\frac{1}{\beta} + 1\right)$$

Note that some practitioners erroneously assume that η is equal to the MTTF ($\overline{T}$). This is only true for the case of β =1 since [Γ (1+1) = (2-1)! =1] [22]

Median

The median is the value separating the higher half of a probability distribution from the lower half. For a data set, it is the "middle" value[24]. Mathematically, the median $\breve{T}$ of the distribution is

Equation 5 Median 3-parameter Weibull [22]

$$\breve{T} = \gamma + \eta.[ln(2)]^{\frac{1}{\beta}}$$

Mode

The mode of a dataset is the element that occurs most often in the collection[25]. Mathematically, the mode $\tilde{T}$ of the distribution is

Equation 6 Mode 3-parameter Weibull [22]

$$\tilde{T} = \gamma + \eta.\left(1 - \frac{1}{\beta}\right)^{\frac{1}{\beta}}$$

Standard Deviation

In statistics, the standard deviation is a measure, used to quantify the amount of variation or dispersion of a set of data values[26]. The standard deviation σ_T of the distribution is

Equation 7 Standard Deviation 3-parameter Weibull [22]

$$\sigma_T = \eta.\sqrt{\left(\Gamma\left(\frac{2}{\beta}+1\right)-\Gamma\left(\frac{1}{\beta}+1\right)^2\right)}$$

Reliability Function

The reliability function R (t) is

Equation 8 Reliability Function 3-parameter Weibull [22]

$$R(t) = e^{-\left(\frac{t-\gamma}{\eta}\right)^{\beta}}$$

Cumulative Distribution Function

The cumulative distribution function F (t) is

Equation 9 Cumulative Distribution Function F (t) 3-parameter Weibull [22]

$$F(t) = 1 - e^{-\left(\frac{t-\gamma}{\eta}\right)^{\beta}}$$

Characteristic Life

The characteristic Life and mean life are not the same values for the weibull distribution.

For a 3-parameter weibull distribution, characteristic life is determined by equating t = η in

Equation 9 thereby reducing it to

Equation 10 Characteristic Life Equation for 3-parameter [22]

$$F(\eta) = 1 - e^{-\left(1-\frac{\gamma}{\eta}\right)^{\beta}}$$

For the 2-parameter case this is further simplified to $F(\eta) = 0.632$ since γ =zero. Therefore, η, the characteristic life, in the case of 2-parameter weibull is the time at which 63.2% of the units

will fail.

2.4.Survival Analysis and Hazards Rate Function

In reliability engineering, the most commonly accepted norms of the failure function is hazard rate function. In addition to the earlier probability density functions of Weibull parameters, the failure rate or hazard rate functions h (t) are often used to understand the defect modes from accelerated failure testing. The following graph shows the hazard rate comparison of measures of central tendency in a reliability bathtub curve[27].

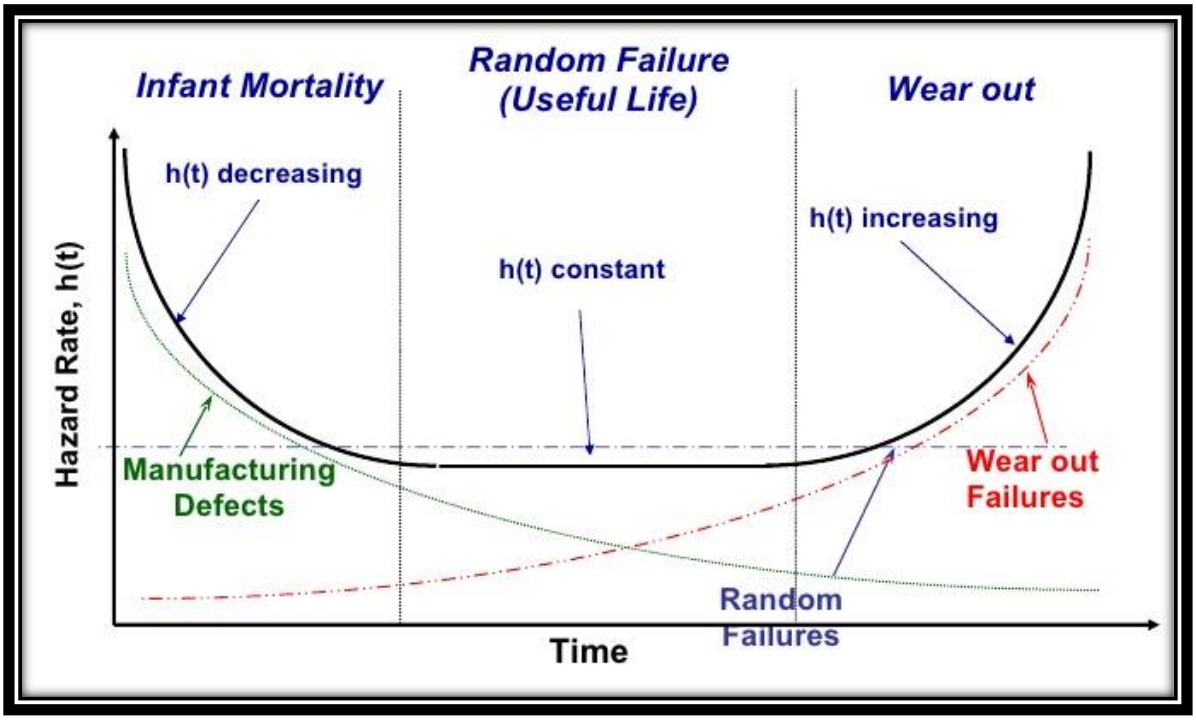

Figure 30 Hazard Rate Bathtub Curve [28]

First, it is important to understand the quantities necessary for survival analysis. Consider T to be the time until failure. The Reliability or Survival function, R (t) is the probability of an entity surviving beyond time t[29].

Equation 11 Survival function [30]

$$\boldsymbol{R(t) = P(T > t)}$$

Where R (t) is a monotone non-increasing function, when T is a continuous random variable with probability density function f (t), the Cumulative Distribution Function is given by [31]

$$\boldsymbol{F(t) = P(T \leq t)}$$

Then the reliability function [32]

$$\boldsymbol{R(t) = \int_{t=0}^{\infty} f(t)dt = 1 - F(t)}$$

$$\boldsymbol{f(t) = -\frac{dR(t)}{dt}}$$

The probability density function, f (t) following Weibull distribution is [33]

$$\boldsymbol{f(t) = \frac{\beta}{\eta}\left(\frac{t-\gamma}{\eta}\right)^{\beta-1} e^{-\left(\frac{t-\gamma}{\eta}\right)^{\beta}}}$$

Moreover, the reliability function R (t) is[34],

$$\boldsymbol{R(t) = e^{-\left(\frac{t-\gamma}{\eta}\right)^{\beta}}, t > 0}$$

Where the shape$\beta > 0$; failure lifetime, $\eta > 0$ and location, $\gamma > 0$ are the unknown parameters. The characteristic lifetime is number of cycles at which $F(\eta) = 1 - e^{-\left(1-\frac{\gamma}{\eta}\right)^{\beta}}$ of the population is expected to fail. Hazard function is the conditional failure rate in reliability or instantaneous rate of failure [35],

Equation 12 Hazard function

$$\mathbf{h(t) = \lim_{\Delta t \to 0} \frac{P[t \leq T < t + \Delta t | T \geq t]}{\Delta t}}$$

From the above Equation 12, Δt is the approximate probability that an entity at time t experiencing an event in [t, t+Δt). The restriction on hazard function is that it is non-negative (h (t) ≥ 0). The hazard function relates to the survival function and pdf in the following way,

$$\boldsymbol{h(t) = \frac{f(t)}{R(t)}}.$$

In Weibull 3-Parameter case [36],

$$\boldsymbol{h(t) = \frac{\beta}{\eta}\left(\frac{t-\gamma}{\eta}\right)^{\beta-1}, t > 0}.$$

Let h (t | Z) be the hazard rate for an entity with risk vector Z at time t. The proportional hazard rate model proposed by Cox is

$$h(t|Z) = h_o(t)\exp(\beta^T Z) = h_o(t)\exp(\sum_k \beta_k Z_K)$$

Where $h_o(t)$ is arbitrary baseline hazard rate, β is the vector of p parameters and the exponential term is a known function. This is the semiparametric model because the parametric form assumed is only for covariate effect. Cox model which is also known as proportional hazard model for two entities with covariate values Z and Z^*, because the ratio of their hazard rates is [29]

$$\frac{h(t|Z)}{h(t|Z^*)} = \frac{h_o(t)\exp(\sum_{k=1}^{p}\beta_k Z_k)}{h_o(t)\exp(\sum_{k=1}^{p}\beta_k Z_k^*)} = \exp[\sum_{k=1}^{p}\beta_k(Z_k - Z_k^*)]$$

Which is a constant. Hence**,** hazard rates are proportional. This equation is called Hazard ratio of an entity with risk factor Z experiencing the event as compared to an entity with risk factor Z^*. This experiment consists of five categorical variables such as Paste combination, Paste Volume, Component Size, Effect of Heat Sink and Aging Time. The censor indicator used in this experiment is delta. The Time to Failure measured in cycles is the response variable.

2.5.Accelerated Factor Coffin Mason Equation

Accelerated life testing for components exposed to temperature variations is through accelerated Temperature Cycling Tests. The temperature variations from the field use of the components are due to repetitions (i.e., turn on and off conditions), or due to the result of cyclic environmental changes (i.e., temperature variations from day to night as satellites orbit the earth, etc.). These repeated temperature changes can result in temperature fatigue and lead to accumulated low fatigue failure after many temperature cycles. Accelerated temperature cycling test is cycling the components to alternating high and low temperatures that exceed its normal use temperatures but within their destruct specifications. Temperature Cycling according to MIL-STD-883 is air-to-air testing. This dissertation deals with testing performed using an air-to-air temperature cycling in a single zone environmental chamber. This produces an accelerated rate of temperature change called ramp rate. The acceleration factor resulting from the temperature cycle test is the ratio of the component life at normal operating conditions to the life at accelerated test conditions and is given by [37] Equation 13 Coffin-Manson equation [38]

$$AF = \left(\frac{\Delta T_{Test\ Cycle}}{\Delta T_{Field\ Cycle}}\right)^{m}$$

Where

AF = Acceleration Factor

$\Delta T_{\text{Test Cycle}}$ = Test temperature difference (°C)

$\Delta T_{\text{Field Cycle}}$ = Field temperature difference (°C)

m = Fatigue or Coffin-Manson exponent

The fatigue or Coffin-Manson exponent is important, as small changes in this exponent can have

larger changes in the acceleration factor. Exponents for many materials are available readily, and it is experimentally possible to determine the fatigue exponent by performing multiple test values of ΔT[39]. Norris and Landzberg proposed the "plastic strain range is proportional to the thermal range of the cyclic loading (ΔT)". They modified the Coffin-Manson equation to account for effects of thermal cycling frequency (f) and the maximum temperature (T). The equation is given by [40] Equation 14 Norris Landzberg modified Coffin Manson equation [41]

$$AF = \frac{N_{Field}}{N_{Test}} = \left(\frac{f_{Field}}{f_{Test}}\right)^{-m} \left(\frac{\Delta T_{Field\ Cycle}}{\Delta T_{Test\ Cycle}}\right)^{-n} \left(e^{\frac{E_a}{k}\left(\frac{1}{T_{Field\ max}} - \frac{1}{T_{Test\ max}}\right)}\right)$$

Where, field and test for use of field and test conditions respectively.

AF	=	Acceleration Factor
N	=	Cycles to Failure
f	=	Frequency of cycles in a day (24 hours)
ΔT_{Test}	=	Test temperature difference (Kelvin)
ΔT_{Field}	=	Field temperature difference (Kelvin)
E_a	=	Activation Energy of the failure mode electron-volts [42]
k	=	Boltzmann's constant (8.6173303 x 10-5 eV/°K) [43][42]
E_a/k	=	1414 for Tin-Lead; 2185 for Sn-Ag-Cu [43] [42]
m	=	1/3 for Tin-Lead; 0.136 for Sn-Ag-Cu [43][42]
n	=	1.9 for Tin-Lead; 2.65 for Sn-Ag-Cu [43][42]

This model is used to estimate the field lifetime duration of accelerated test data. This model still not perfected over the years, is the most relevant model currently available in the industry to estimate the time to failure distribution for solder joint fatigue[44].

Chapter 3 Description of Experimental Setup and Data Acquisition System

3.1. Printed Circuit Board Assembly

The printed circuit board assembly components included in this dissertation are only Ball Grid Arrays of various size and type, ranging in size dimension from 5mm x 5mm to 45mm x 45mm. Practical Components supplied all the dummy-die components (die is non-functioning). Each of the component is daisy chained i.e. an electrical signal applied to the component's data channel will pass through each solder joint of the component in series. This design type called "daisy chain" is standard in solder joint testing as it allows a single electrical test to check for connectivity of all the solder joints in the component. The test printed circuit board incorporates land patterns for 5 mm, 6mm, 13mm, 15mm, 17mm, 31mm, 35mm and 45 mm Ball Grid Array (BGA) packages with solder ball pitch ranging from 0.4 mm to 1.27 mm. The Memory Module and the SMRs in the test are No Lead packages, which is present in the test to study the effect of paste composition for passive components. The paste volumes are different in the Top with 0.127mm and Bottom with 0.076 mm of the test printed circuit board and only two components appear on both sides of the board the CABGA 36 (6mm ceramic BGA) and the CABGA 208 (15mm ceramic BGA). All the test printed circuit boards are assembled only on one side (i.e., the components present are only on either the Top or Bottom side of the board).In total, 921 test boards were assembled. The full test matrix of the printed circuit boards shown in Table viii.

Table viii Printed Circuit Board Assembly

Solder Paste	Board Type	Solder Paste Volume	0 day	180 Days			360 Days			720 Days			Total
			25° C	25° C	50° C	75° C	25° C	50° C	75° C	25° C	50° C	75° C	
Tin-lead	Flame-Retardant-406	Top (0.127 mm)	14	14	14	14	14	14	14	14	14	14	**140**
		Bottom (0.076 mm)	5	5	5	5	5	5	5	5	5	5	**50**
	Megtron-6	Top (0.127 mm)	15	0	0	15	0	0	15	0	0	15	**60**
		Bottom (0.076 mm)	5	0	0	4	0	0	5	0	0	5	**19**
Sn-Ag-Cu 305	Flame-Retardant-406	Top (0.127 mm)	30	30	30	30	30	30	30	30	30	30	**300**
		Bottom (0.076 mm)	10	10	10	10	10	10	10	10	10	10	**100**
	Megtron-6	Top (0.127 mm)	15	x	x	15	x	x	15	x	x	15	**60**
		Bottom (0.076 mm)	5	x	x	5	x	x	5	x	x	5	**20**
Innolot	Flame-Retardant-406	Top (0.127 mm)	30	x	x	30	x	x	x	x	x	30	**90**
		Bottom (0.076 mm)	10	x	x	10	x	x	x	x	x	10	**30**
	Megtron-6	Top (0.127 mm)	9	x	x	9	x	x	9	x	x	9	**36**
		Bottom (0.076 mm)	4	x	x	4	x	x	4	x	x	4	**16**
Total			**152**	**59**	**59**	**131**	**59**	**59**	**132**	**59**	**59**	**152**	**921**

STI Electronics Inc. assembled the test printed circuit boards. The screen-printing machine used was a Speed line Technologies MPM Momentum. Two pick-and-place machines used were the Juki KE- 2080L and Juki FX3.

Solder reflow was done using a Heller 1913 MKIII reflow oven. Optical inspection and transmission X-ray tomography analysis determined the assembled test printed circuit boards and typical solder joint quality following reflow.

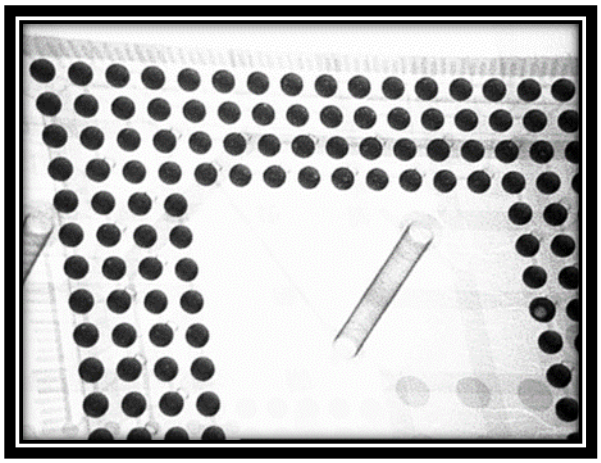

Figure 31 Voiding Analysis by XRD [9]

Two components required post-assembly attachment. The Memory Module consists of a Land Grid Array (LGA) socket attached during the PCBA process, but the paired Pin Grid Array (PGA) component were manually placed into the LGA socket once the circuit board assemblies had been received at Auburn University. Similarly, the heat sinks for the SBGA 600 (45 sq.mm) and PBGA 1156 (35 sq.mm) components.

3.2. Testing Standard

In this dissertation, to study the accelerated life testing on solder joint reliability under temperature cycling test conditions, a temperature cycling harsh environment test in accordance to the JEDEC test standard JESD22-A104E (Revision of JESD22-A104D, March 2009) is used. The standard applies to single zone environmental chamber temperature cycling, covers component, and solder interconnection testing. The load placed is in a stationary chamber and is heated or cooled by introducing hot or cold air into the chamber[45].

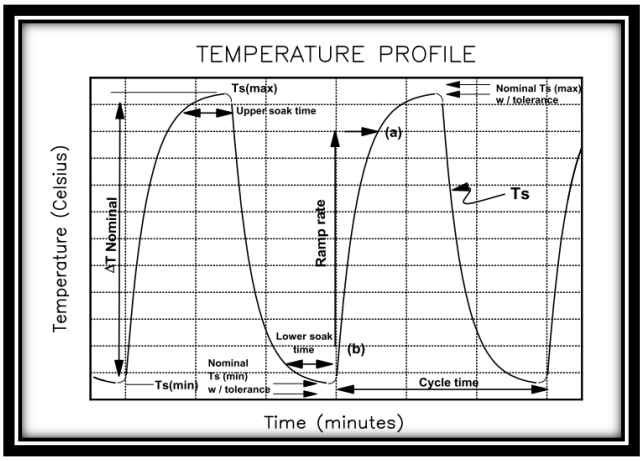

Figure 32 JEDEC JESD22-A104E Temperature Cycle Testing Profile [45]

The JEDEC JESD22-A104E standard followed in this experiment is profile G with soak temperatures of (-40°C) and +125°C. The test standard allows for modifications of the standard profile requirements on ramp rates to account for thermal mass of larger test.

3.3. Experimental Setup

Inside the single zone temperature cycling environment chamber, all test boards are vertically placed one on top of another. Each daisy-chained component is wired, out to a data acquisition system. The test boards are spaced using a Fancort Industries spacing racks for uniform heat absorption and dissipation. The data acquisition system consists of a Keithley 7002 switch scanning multiplexer coupled with a high accuracy Keithley 2001 digital multi-meter, which allows for continuous monitoring of resistance change in each component.

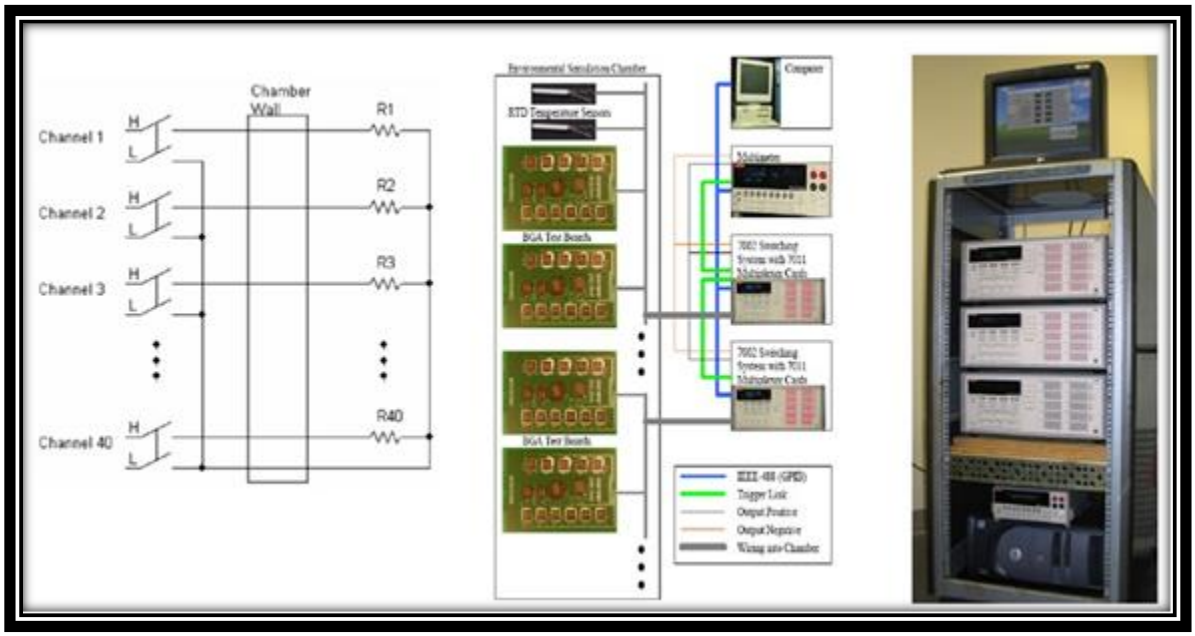

Figure 33 Schema of Monitoring Setup [8]

3.4. Software Monitoring Protocol

Due to the magnitude of the test and the limited availability of equipment to monitor the test, a modified IPC-9701 monitoring standard is used. The IPC-9701 standard dictates that each of the test components to be continuously recorded. The failure criterion defined as "the interruption of electrical continuity that is greater than 1000 Ω". In this dissertation, however the failure criterion is disruption of electrical continuity greater than 1000 Ω; but each of the test components resistance measurement recorded is not continuous. Thereby an interval based censored failure is used statistically to understand the failure of the components. In this dissertation, the protocol used for monitoring the test components consisted of two measurements a positive and a ground. The resistance between them is cyclically recorded (intervals) in a database. Though this sounds simple enough theoretically the magnitude of the problem is far higher to achieve in practice. This protocol developed by Dr. John Evans and various members of CAVE^3 is widely accepted at Auburn University as an alternative to the IPC-9701 standard[46].

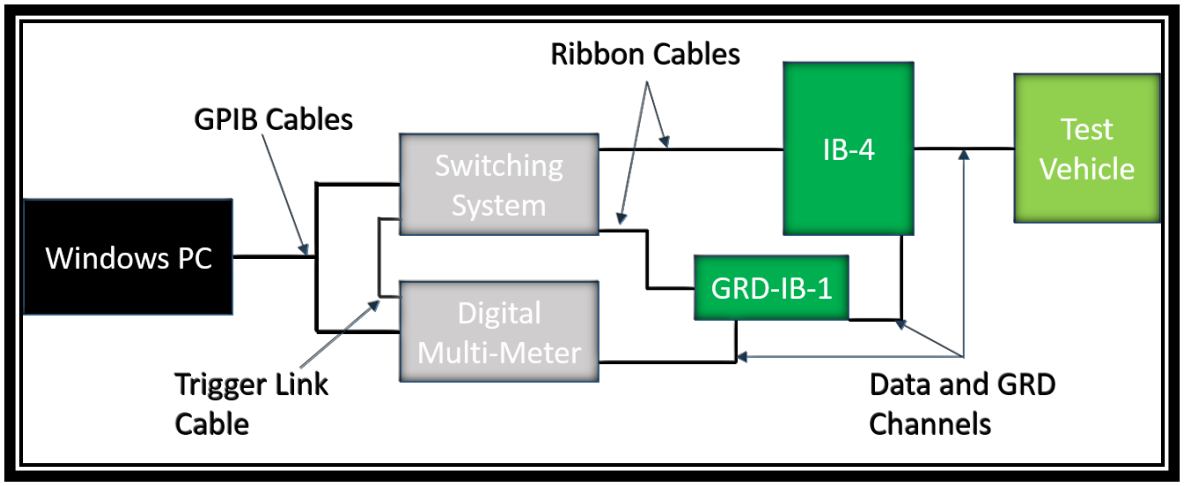

Figure 34 Software Program Protocol [9]

The test boards physical setup and connections to the software monitoring, displayed in the Figure 35. The software monitoring system stores the information of the temperature, cycle count, component unique identity, board unique identity, failure count and also the time to failure onto an excel sheet. This has an independent state machine system that writes the data to the excel sheets without any data loss. The data are then loaded onto a MS SQL Server manually and stored for future data analysis.

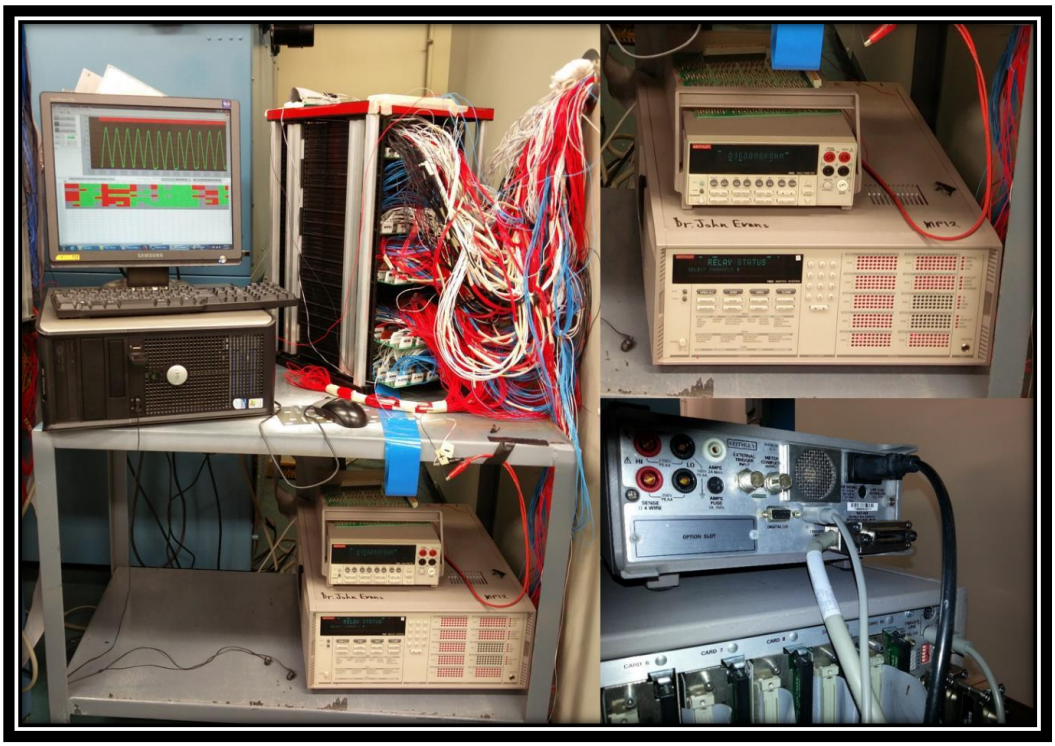

Figure 35 Physical Interface Connections to the Software Monitoring Protocol[9]

3.5. Board Storage and Aging Temperatures

The test boards are stored in an isothermal aging condition for a period of 720 days in various environmental chambers. The storage temperatures chosen are to be at 25°C, 50°Cand 75°C. The test boards subjected are to temperature cycling JEDEC JESD22-A104E standard testing at time intervals of 0 days, 180 days, 360 days and 720 days. The following

Figure 36 displays isothermal condition for 75°C stored up to 720 days.

Figure 36 Test Board Storage inside an Environmental Chamber [9]

Chapter 4 Reliability Data Analysis using 3-parameter Weibull Distribution plots

The reliability data from the test components have an interval censoring as the new protocol do not continuously record the resistance data. The data analyzed is by Reliasoft's Weibull++ software and the method used in this analysis is interval censoring with suspensions. The distribution used for computing the Mean-Time-To-Failure is the 3-parameter Weibull with Shape, Scale and Location parameters as shown in the Equation 4. In order to understand the various effects of this experiment, the total test subdivided are into various smaller study groups.

The test result discussed in this dissertation and calculation to derive these results are shown in the Appendix B with Weibull Charts and Statistical Analysis. In this dissertation, the label format used consists of three X-axis labels, the first line represents the solder alloy material and the second line represents the solder paste material, the third line represents the board substrate material.

4.1. Reliability Study on the effect of Heat sinks

The effects of heat sinks can only be experimented in the PBGA 1156 and SBGA 600 components. These components have special heat sink placement locations on the test boards to attach the heatsinks. In both the components, the results showed a significant difference in the performance of the solder joints by the presence of heatsinks. This difference is significant across all the different solder paste materials, substrate materials, at different aging time temperatures.

4.1.1. Mean-Time-To-Failure of PBGA 1156 Components

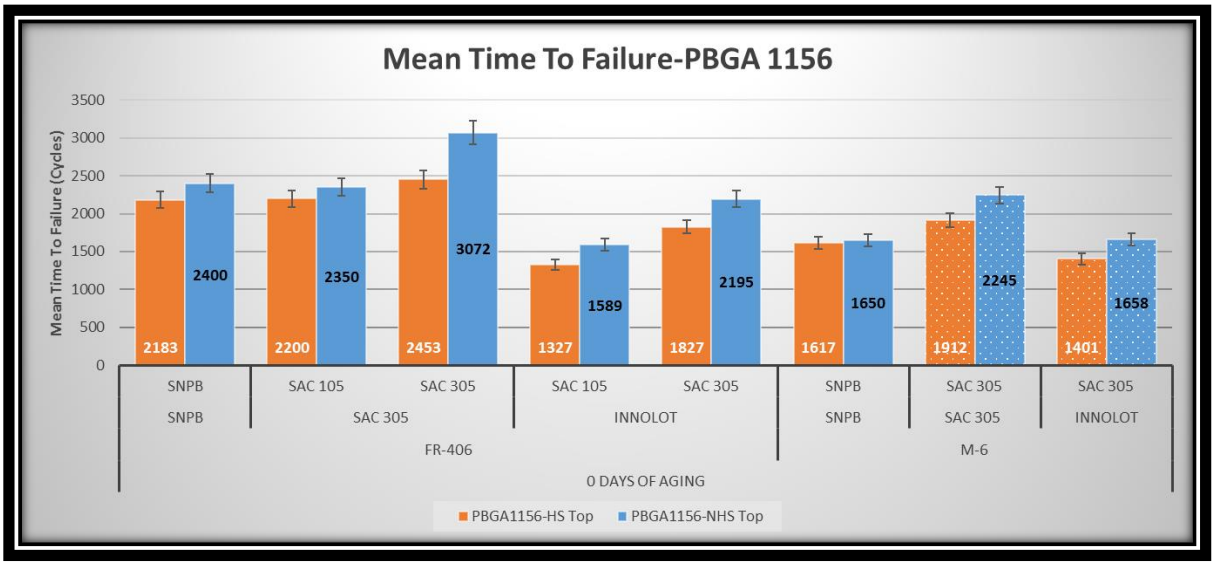

Figure 37 Mean-Time-To-Failure for PBGA 1156 Components Tested @ 0 days of Aging

The test results show a clear difference in the performance of the PBGA 1156 components due to the presence of heatsinks. The Mean-Time-To-Failures of the components with the Heat Sink are lesser than that of the components without the heat sinks. Across all the various physical properties of the board substrate materials and solder materials, the effect seen is to be the same. Therefore, the initial test conclusion is that the heat sinks are not improving the overall reliable life of the components. For the FR-406 board substrate, Tin-Lead solder materials with the heat sinks reduced the reliable life by 217 temperature cycles and SAC305 solder materials by 619 temperature cycles. For the Megtron-6 board substrate, Tin-Lead solder materials with the heat sinks reduced the reliable life by 33 temperature cycles and SAC305 solder materials by 333 temperature cycles. In both the substrates, the Tin-Lead solder materials showed no significant differences in the presence of heatsinks whereas the SAC305 solder materials have a negative effect on the reliable life of the component due to the presence of heat sinks[46].

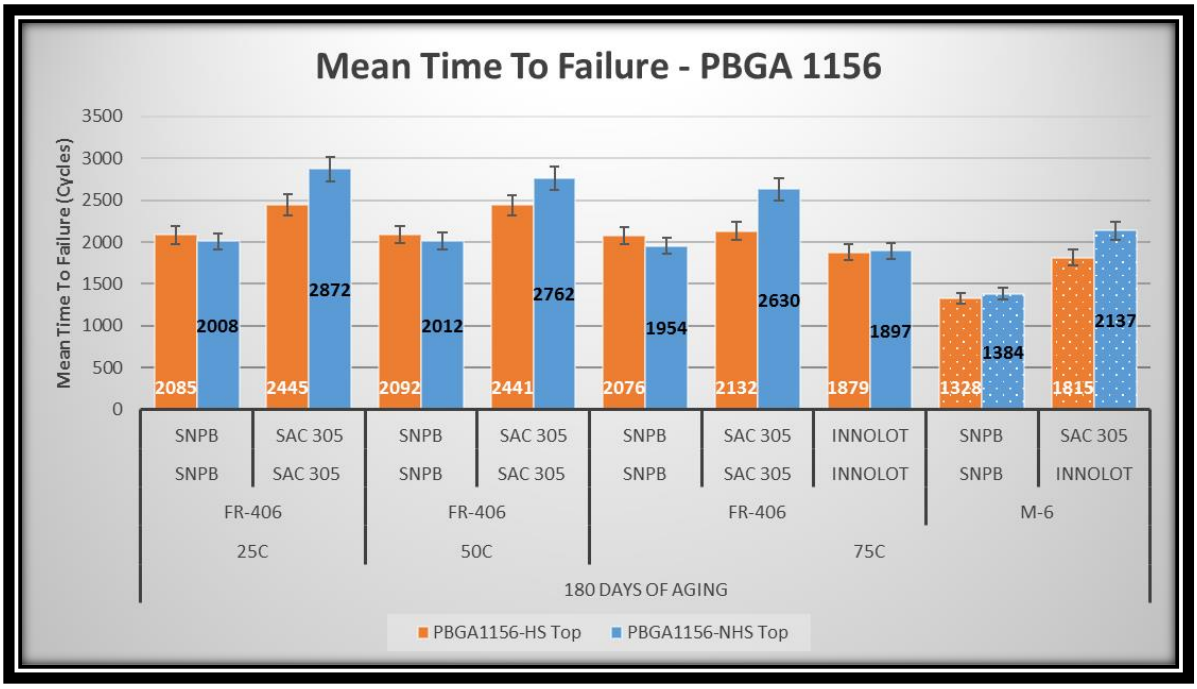

Figure 38 Mean-Time-To-Failure for PBGA 1156 Components Tested @ 180 days of Aging

The test results from aging the test boards to 180 days show a difference in the performance of the PBGA 1156 components due to the presence of heatsinks in the SAC305 solder materials. The overall Mean-Time-To-Failures of the components with Heat Sinks are lesser than that of the components without the heat sinks in SAC305 solder materials. For the Megtron-6 substrate, SAC305 paste and alloy combinations were not present so the comparison is between Innolot paste and SAC305 alloys. In both the substrates, the Tin-Lead solder materials showed no significant differences in the presence of heatsinks whereas the SAC305 solder materials have a negative effect on the reliable life of the component due to the presence of heat sinks. Also in the FR-406 substrate, the negative effect of the presence of heat sinks is increasing as the aging temperature increases. The reason for such adverse effects are due to the CTE mismatch of the board substrate

and the plastic mold compound materials. The CTE is directly related to the T_g of the materials. The T_g of FR-406 substrate is 170°C; Megtron-6 substrate is 210°C and the PBGA 1156 component mold material is 196°C [47].

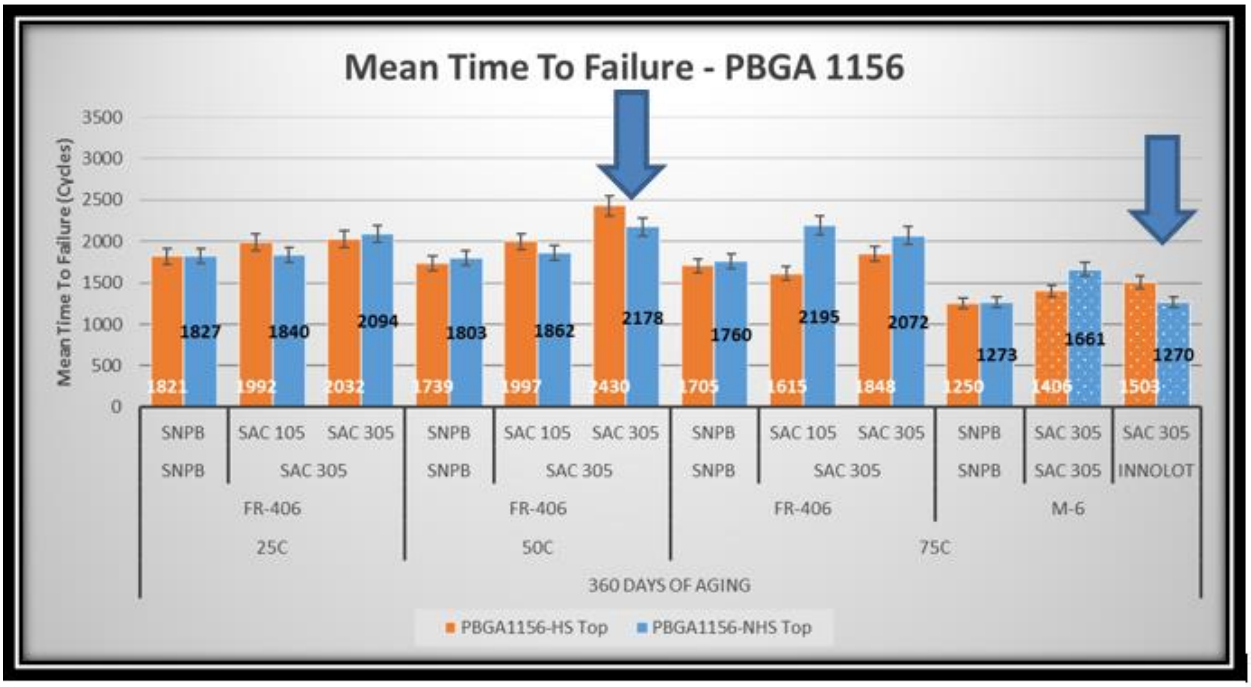

Figure 39 Mean-Time-To-Failure for PBGA 1156 Components Tested @ 360 days of Aging

The test results from aging the test boards to 360 days show a weird pattern in the performance of the PBGA 1156 components due to the presence of heatsinks in SAC305 materials. The Mean-Time-To-Failures of the components with the Heat Sink are dependent on a variety of factors in this experiment the solder ball alloy, aging temperature and board substrates. The Tin-Lead material is not significantly different with the presence of heatsinks across all the three isothermal aging temperatures whereas the Lead-free materials do not perform well with the presence of the heatsinks at 25°C and 75°C aging temperatures. The Innolot Solder paste and SAC305 solder alloy was present only on the Megtron-6 substrate at 75°C aging temperature and seems to have a

positive effect when the heat sinks are present. In both the substrates, the Tin-Lead solder materials showed no significant differences in the presence of heatsinks whereas the SAC305 solder materials have a negative effect on the reliable life of the component due to the presence of heat sinks. Also in the FR-406 substrate, the negative effect of the presence of heat sinks is seen only at the 25°C and 75°C aging temperatures and this turned positive at 50°C aging temperature[48].

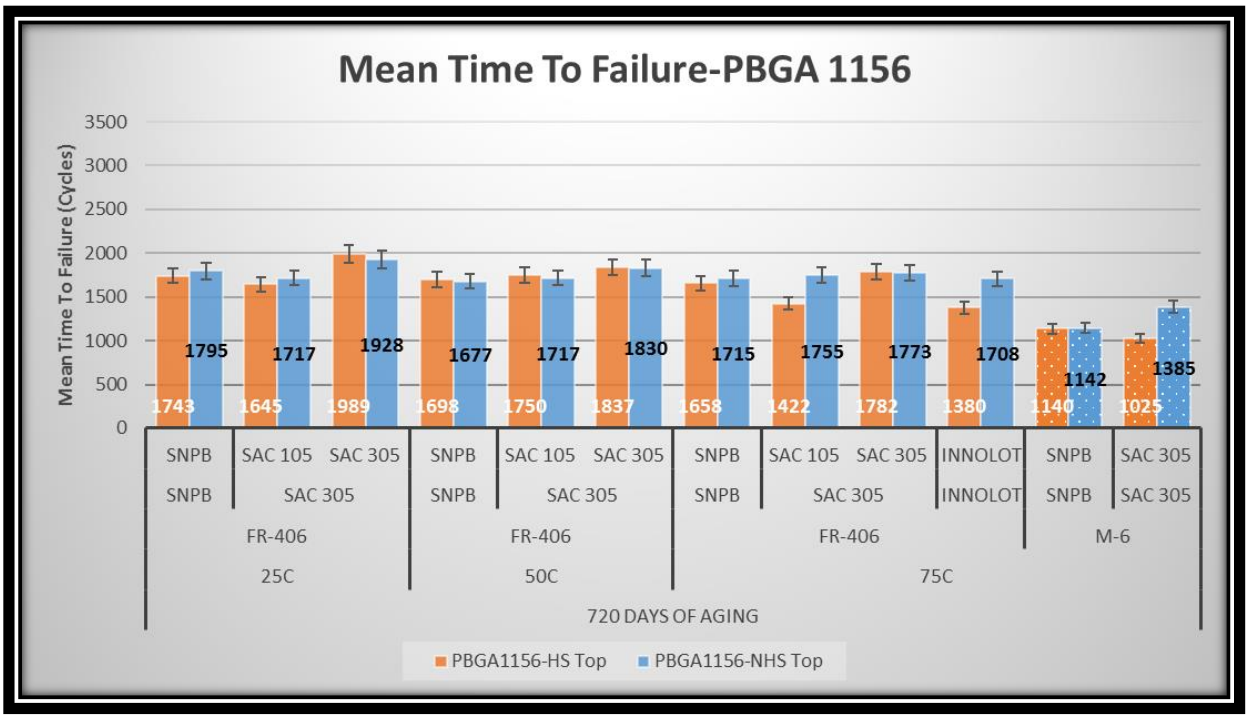

Figure 40 Mean-Time-To-Failure for PBGA 1156 Components Tested @ 720 days of Aging

The test results from aging the test boards to 720 days show similar trend in the performance of the PBGA 1156 components due to the presence of heatsinks. The Mean-Time-To-Failures of the components with Heat Sink are dependent on a variety of factors in this experiment the solder ball alloy, aging temperature and board substrates. The Tin-Lead material show no significant difference in the presence of heatsinks across all the isothermal aging temperatures and board substrate materials whereas the Lead-free materials do not perform well with the presence of the

heatsinks at higher aging temperature of 75°C. This effect is similar in both the board substrates. The Innolot Solder paste and SAC305 solder alloy present on the Megtron-6 substrate is still under testing and no significant failures are available as of now to make a meaningful conclusion. Hence discarded in this chart. Dr. Anto Raj is currently leading the research for future conclusive testing results on this portion[49].

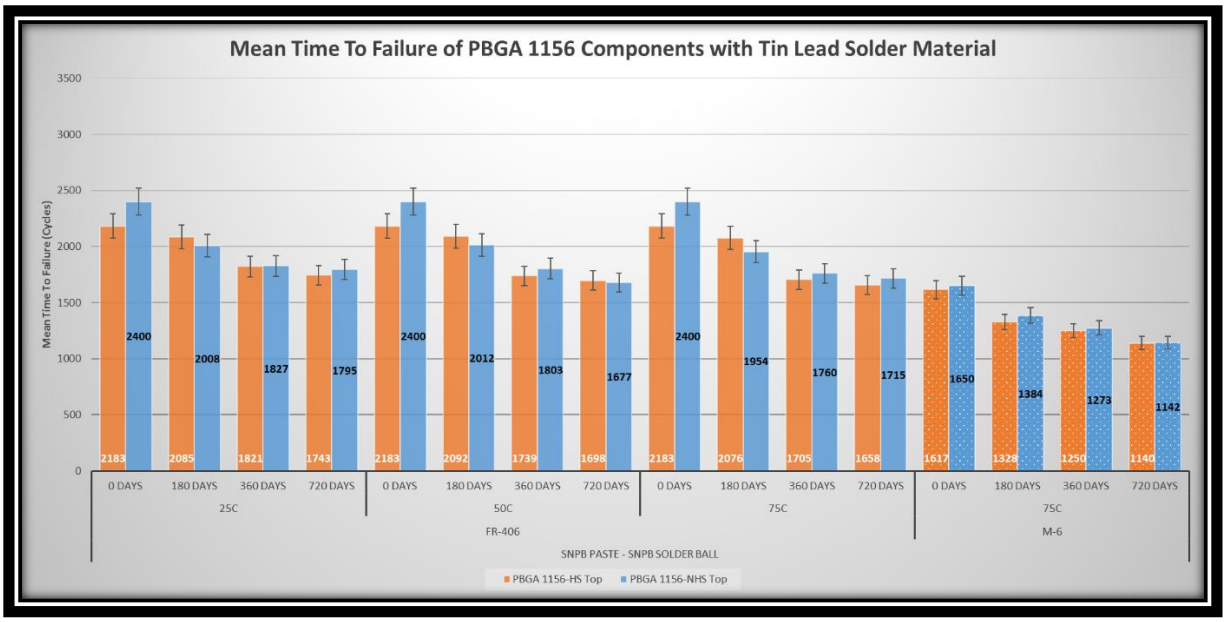

Figure 41 Mean-Time-To-Failure for PBGA 1156 Components Tested with Tin-lead Solders

The test results from the Tin-lead Solder Paste and Alloy combination show that the presence of heat sink is marginally adverse to the performance of the solder joints. The Mean-Time-To-Failures of the components with Heat Sink and without heat sinks show that there are no significant difference in their performances for the PBGA 1156 components. However, the aging time and aging temperature have been the major contributor in the degradation of their reliability. This effect observed is in both the FR-406 and Megtron-6 substrates. However, the FR-406 substrate is far

superior in performance compared to the Megtron-6 substrate. Another interesting observation from the results are that the degradation effect of aging time seems to become lesser after 180 days of aging, this observation holds true across all the three aging temperatures and also between the two different substrates. The damage accumulated from the solder joints behave in a fashion that they approach to a constant after 180 days of aging in this thermal cycling test environment[50].

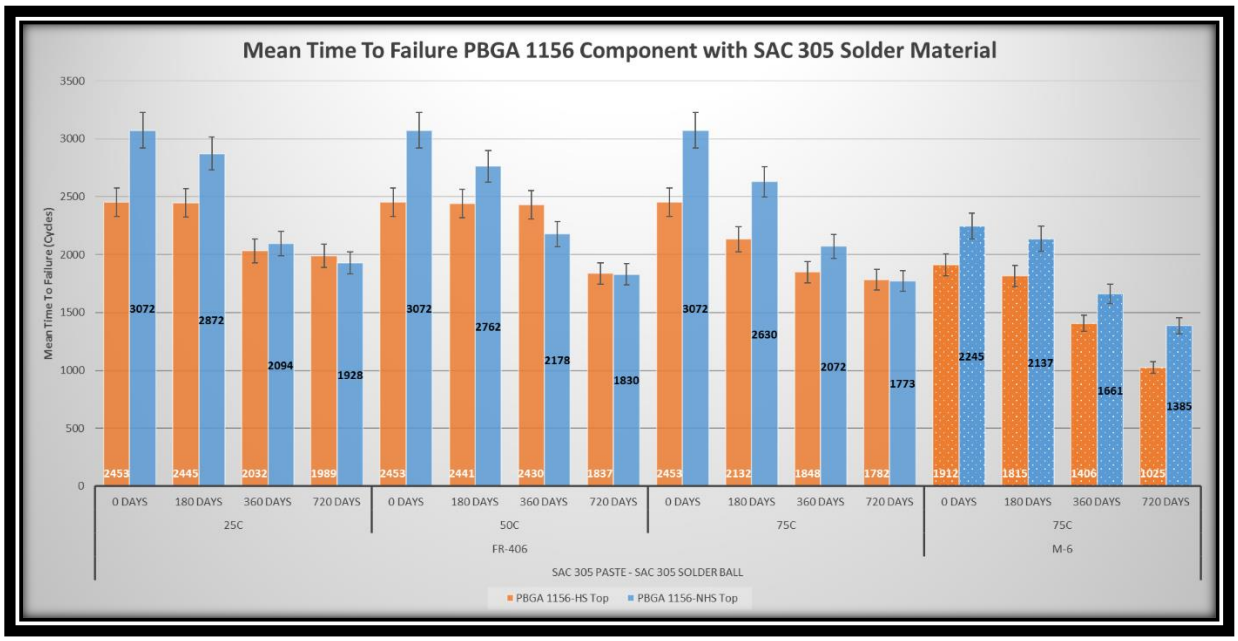

Figure 42 Mean-Time-To-Failure for PBGA 1156 Components Tested with SAC305 Solders

The test results from the SAC305 Solder Paste and Alloy combination show that the presence of heat sink is extremely adverse to the performance of the solder joints. The Mean-Time-To-Failures of the components with Heat Sink and without heat sinks show that there is a significant difference in their performances for the PBGA 1156 components. However, the aging time and aging temperature have been major contributor in the degradation of their reliability. This effect observed is in both the FR-406 and Megtron-6 substrates. However, the FR-406 substrate is far superior in performance compared to the Megtron-6 substrate. Another interesting observation from the

results are that the degradation effect of aging time seems to become lesser after 180 days of aging, this observation holds true across all the three aging temperatures and not between the two different substrates. The damage accumulated from the solder joints behave in a fashion that they approach to a constant after 180 days of aging in this thermal cycling test environment for the FR-406 substrate but not with the Megtron-6 substrate. This is due to the differences in the T_g of the board substrate materials and also due to the time above liquidus for the reflow profile of the SAC.

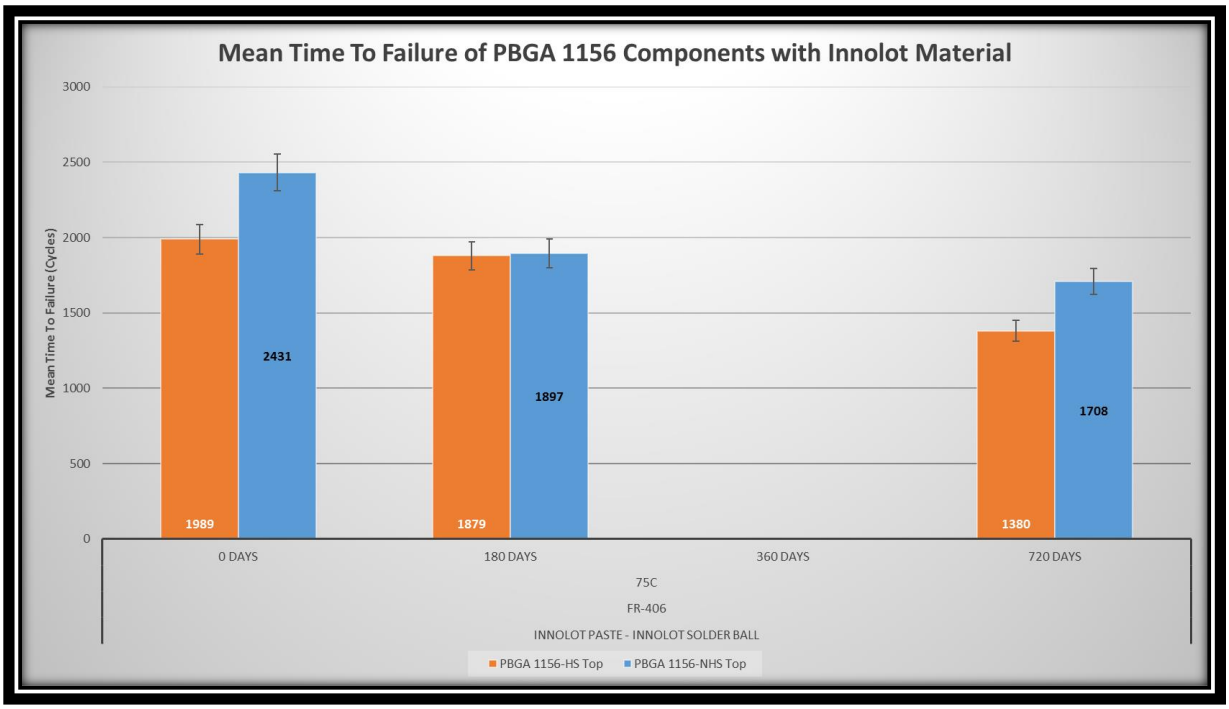

Figure 43 Mean-Time-To-Failure for PBGA 1156 Components Tested with Innolot Solders

Due to the limited availability of the resources in Innolot solder paste and alloys at the time of board build. The test data is available only for the FR-406 at 0 days, 180 days and 720 days of aging. The test results from the Innolot Solder Paste and Alloy combination show that the presence of heat sink is extremely adverse to the performance of the solder joints. The Mean-Time-To-Failures of the components with Heat Sink and without heat sinks show that there is a significant

difference in their performances for the PBGA 1156 components. However, the aging time and aging temperature have been major contributor in the degradation of their reliability. However, for the Innolot materials, unlike Tin-Lead and SAC305 materials the degradation effect of aging time do not approach a constant after 180 days of aging and after 720 days of aging in this temperature cycling test environment. Limited research is available on the creep properties of the Innolot material after aging. Dr. Anto Raj is currently investigating the behavior of Innolot material after aging in his dissertation.

4.1.2. Mean-Time-To-Failure of SBGA 600 Components

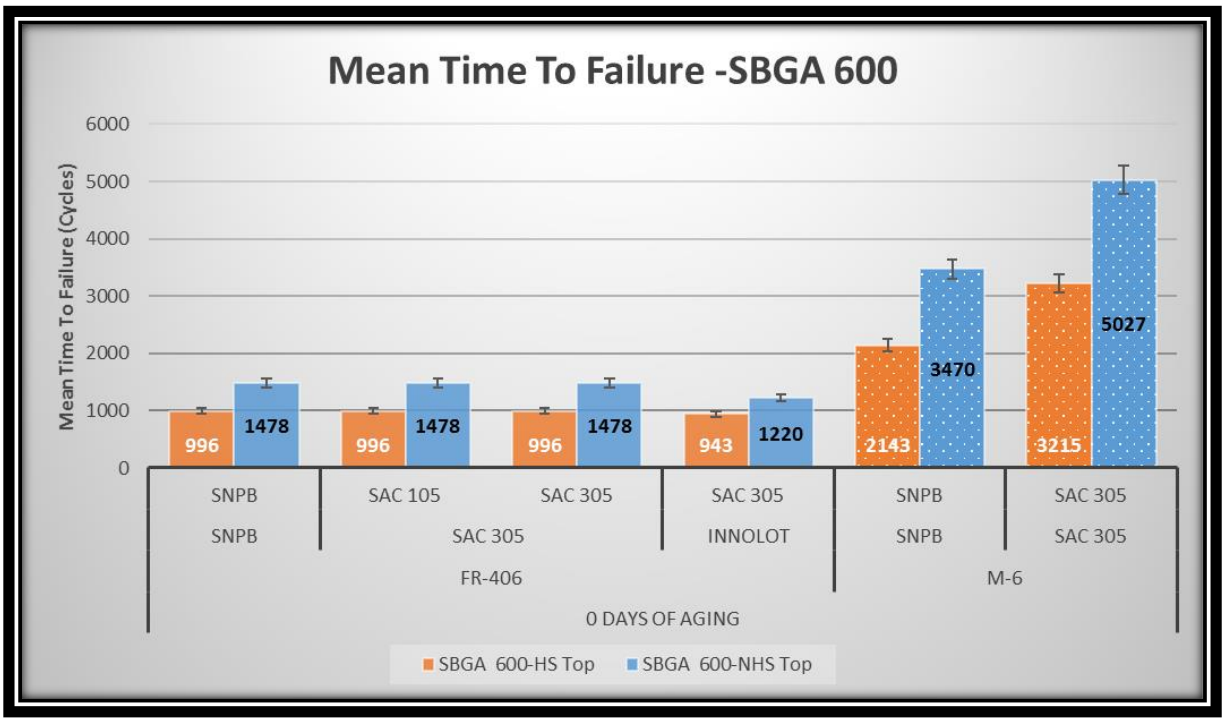

Figure 44 Mean-Time-To-Failure for SBGA 600 Components Tested @ 0 days of Aging

The test results show a clear difference in the performance of the SBGA 600 components due to the presence of heatsinks and is dependent on the board substrate material. The Mean-Time-To-Failures of the components with the Heat Sink are lesser than that of the components without the

heat sinks. Across all the various physical properties of the solder materials, the effect seen is to be the same. Therefore, the initial test conclusion is that the heat sinks are not improving the reliability of the SBGA 600 components but the Megtron-6 substrate is having a significant effect on the components performance.

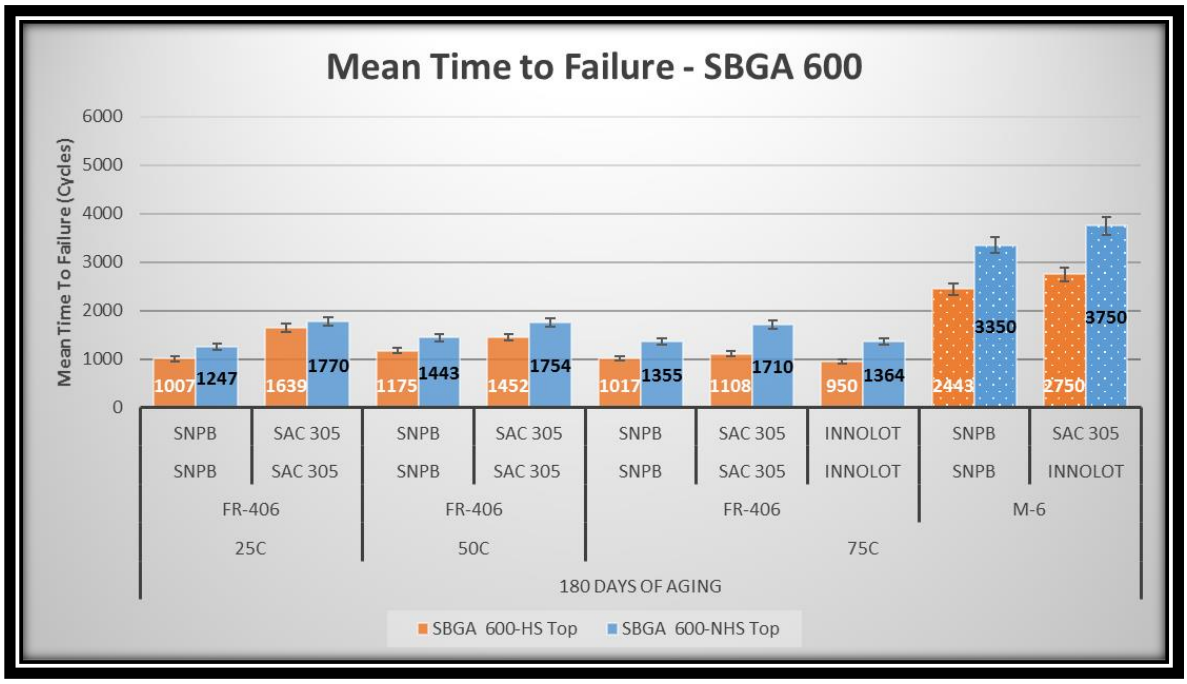

Figure 45 Mean-Time-To-Failure for SBGA 600 Components Tested @ 180 days of Aging

The test results from aging the test boards to 180 days show a clear difference in the performance of the SBGA 600 components due to the presence of heatsinks. The overall Mean-Time-To-Failures of the components with Heat Sinks are lesser than that of the components without the heat sinks but with one exception. Here, the board substrate materials have made a difference in the performance of the SBGA 600 components. Both the Tin-Lead material and Lead-free materials do not perform well with the presence of the heatsinks. This effect is similar in both the board substrates.

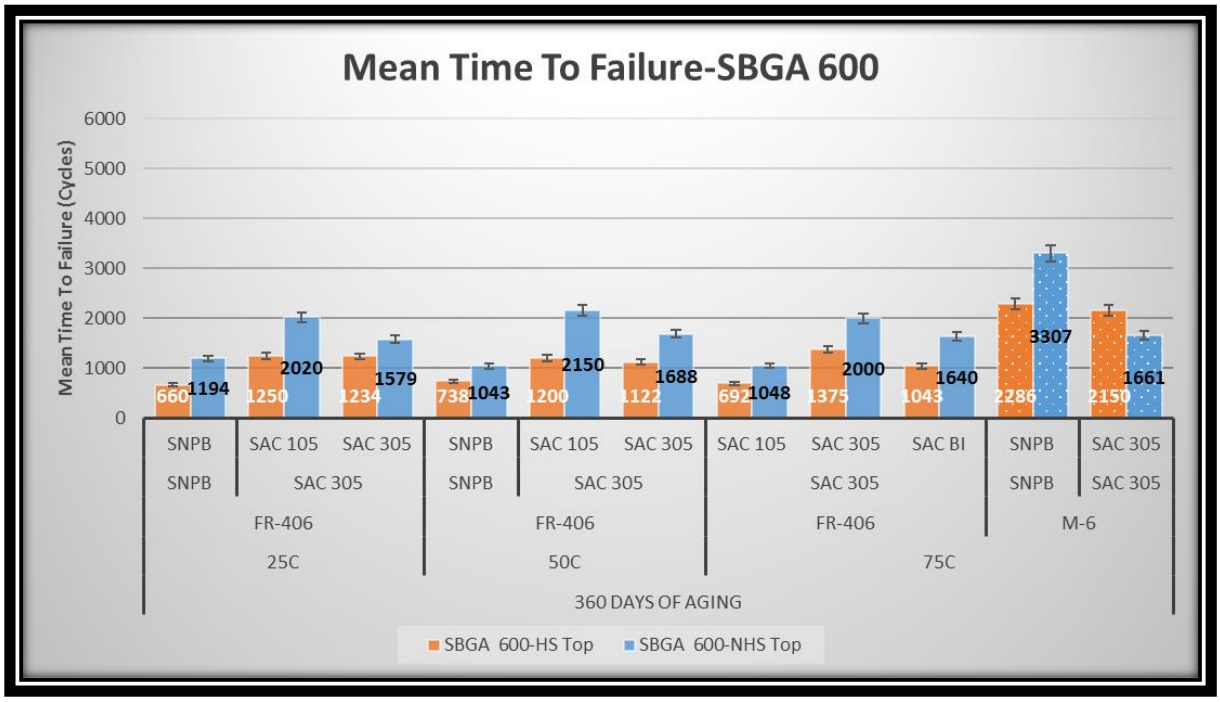

Figure 46 Mean-Time-To-Failure for SBGA 600 Components Tested @ 360 days of Aging

The test results from aging the test boards to 360 days show a difference in the performance of the SBGA 600 components due to the presence of heatsinks and board substrates. The overall Mean-Time-To-Failures of the components with Heat Sinks are lesser than that of the components without the heat sinks. Here, the board substrate materials have made a difference in the performance of the SBGA 600 components. Both the Tin-Lead material and Lead-free materials do not perform well with the presence of the heatsinks. This effect is similar in both the board substrates. The Megtron-6 substrate is having a significant improvement effect on the Tin-Lead materials components performance with heat sinks. However, lead-free materials with Megtron-6 substrate show deleterious effects in the presence of heatsinks. This warrants for detailed materials analysis and creep properties of the SAC305 material in Megtron-6 substrates. Further explanation for this phenomenon is in the Chapter 5.

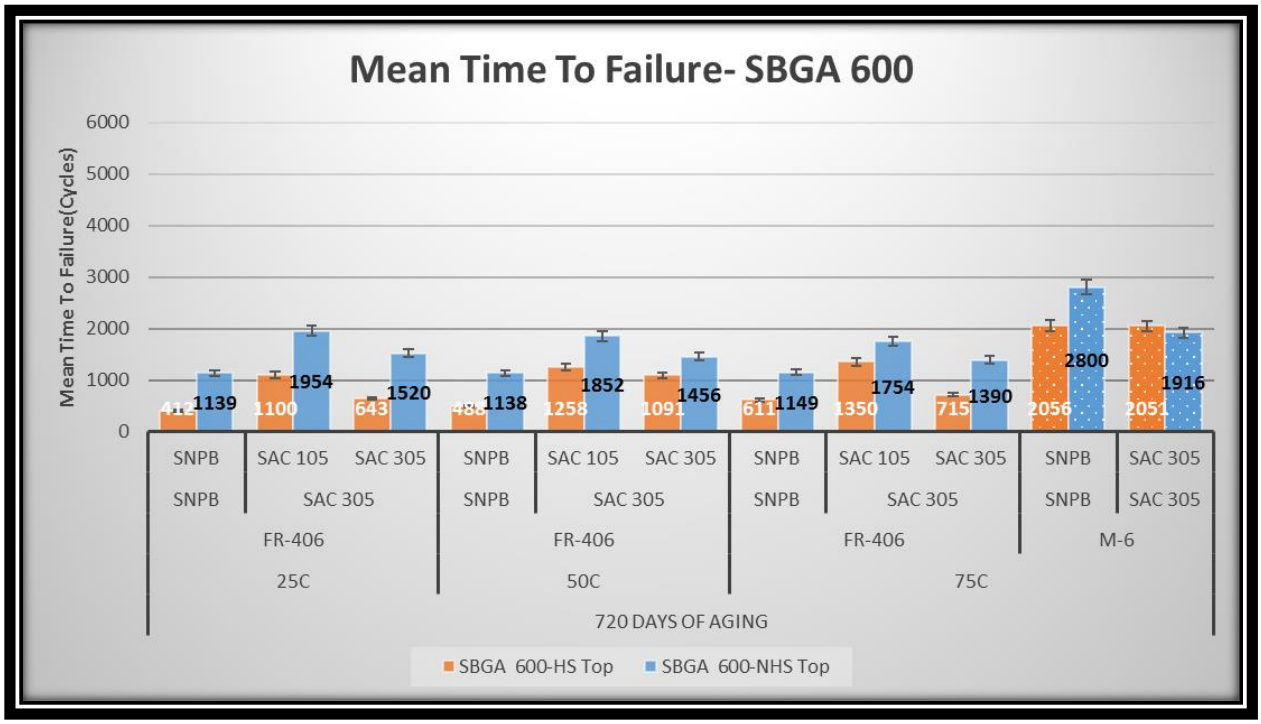

Figure 47 Mean-Time-To-Failure for SBGA 600 Components Tested @ 720 days of Aging

The test results from aging the test boards to 720 days show a clear difference in the performance of the SBGA 600 components due to the presence of heatsinks. The overall Mean-Time-To-Failures of the components with Heat Sinks are lesser than that of the components without the heat sinks but with one exception. Here, the Megtron-6 board substrate material with SAC305 material have made a reversal in the trend of the SBGA 600 components i.e., the components with the heat sinks have performed better than that of the components without heat sinks. Both the Tin-Lead material and Lead-free materials do not perform well with the presence of the heatsinks for the FR-406 substrate. However, the Megtron-6 substrate performs better than the FR-406 substrate at 720 days of aging at 75°C.

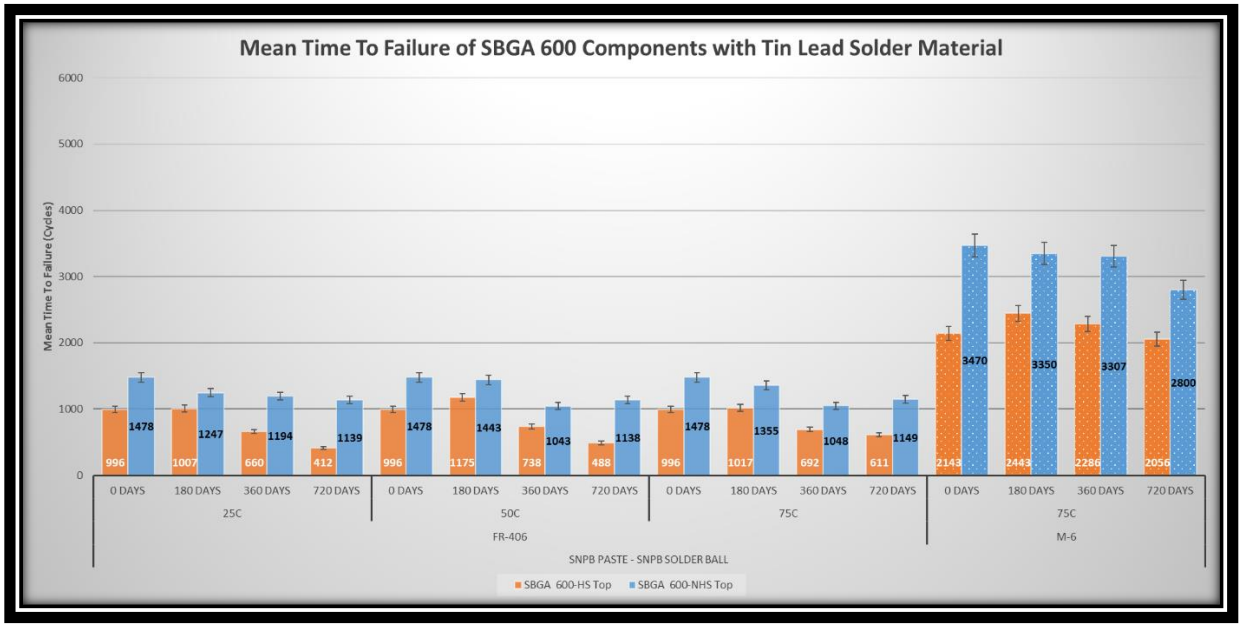

Figure 48 Mean-Time-To-Failure for SBGA 600 Components Tested with Tin-lead Solders

The test results from the Tin-lead Solder Paste and Alloy combination show that the presence of heat sink is adverse to the performance of the solder joints. The Mean-Time-To-Failures of the components with Heat Sink and without heat sinks show that there is a significant difference in their performances for the SBGA 600 components. However, the aging time and aging temperature have been the major contributor in the degradation of their reliability. This effect observed is in both the FR-406 and Megtron-6 substrates. However, the Megtron-6 substrate is far superior in performance compared to the FR-406 substrate. Another observation from the results are that the degradation effect of aging time seems to be dominant even after 180 days of aging, this observation holds true across all the three aging temperatures and also between the two different substrates. The damage accumulated from the solder joints do not seem to approach to a constant

after 180 days of aging in this thermal cycling test environment unlike the PBGA 1156 components. Here, the main difference between the components are the package mold material.

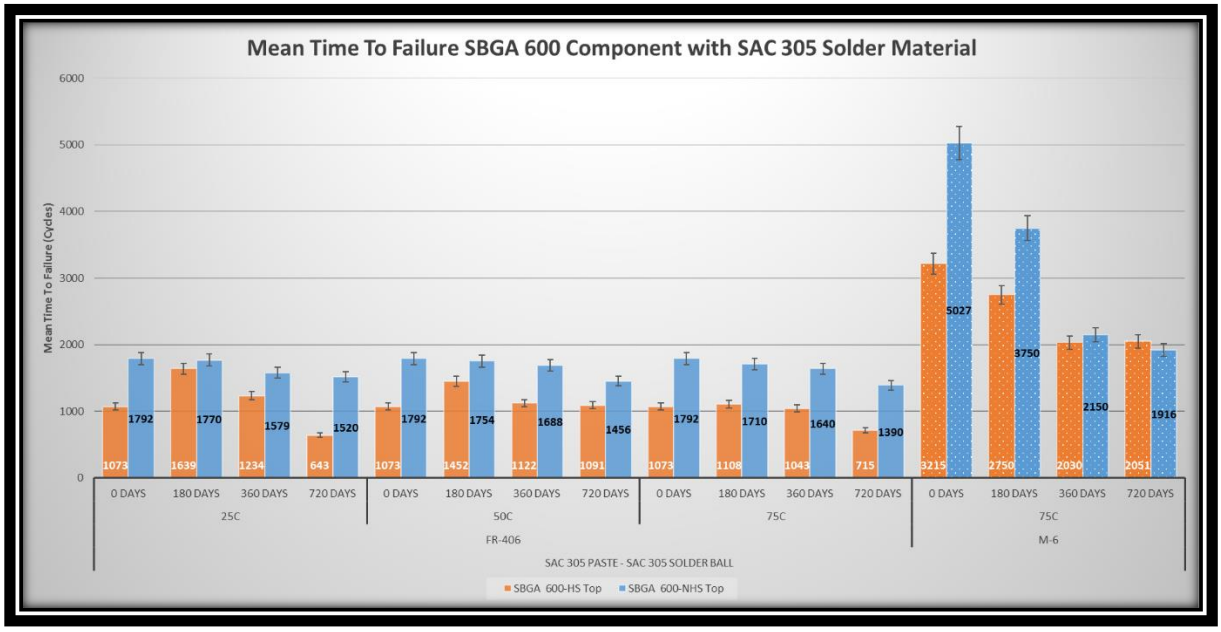

Figure 49 Mean-Time-To-Failure for SBGA 600 Components Tested with Lead-free SAC-305

The test results from the Lead-free SAC305 Solder Paste and Alloy combination show that the presence of heat sink is extremely adverse to the performance of the solder joints. The Mean-Time-To-Failures of the components with Heat Sink and without heat sinks show that there is a significant difference in their performances for the SBGA 600 components. However, the aging time and aging temperature have been major contributor in the degradation of their reliability. This effect observed is in both the FR-406 and Megtron-6 substrates. However, the Megtron-6 substrate is far superior in performance compared to the FR-406 substrate. Another important observation from the test results are that the Megtron-6 substrate after aging for 720 days components with heat sinks performed better than that without the heatsinks. The degradation effect of aging time seems to become lesser after 360 days of aging, this observation holds true across all the three

aging temperatures and between the two board substrates. The damage accumulated from the solder joints behave in a fashion that they approach to a constant after 360 days of aging in this thermal cycling test environment.

4.1.3. Effects of Heat Sinks

- In PBGA 1156 components, the effect of heat sink is adverse for the Tin-lead and Lead-free solder materials (both SAC305 and Innolot). The Tin-lead solder materials seems to approach a degradation constant but not so in the case of Lead-free materials.
- In SBGA 600 components, the effect of heat sink is adverse for the Tin-lead and Lead-free solder materials (SAC305). The Tin-lead solder materials showed adverse effects with both the FR-406 substrate and Megtron-6 substrate but the Lead-free (SAC305) material after aging to 720 days showed that the components with the heat sinks performed better than that of the components without heat sinks.

Summarizing the effects of heat sinks for isothermal aging conditions, the components with the heat sinks have an adverse effect on the solder joint performance. This conclusion is true for Tin-lead and Lead-free materials, in both the substrates across all the aging temperatures and between the PBGA 1156 and SBGA 600 components. However when the Megtron-6 substrate when aged to 720 days with SAC305 lead-free solder material the SBGA 600 components performed better with the heat sinks.

4.2. Reliability Study on the effect of Volume of the Solder Paste

The effects of solder paste volume can only be experimented in the CABGA 36 and CABGA 208 components. These are the only components that are present in two different solder volumes. However, the CABGA 36 components had very few failures to estimate a meaningful conclusion.

In CABGA 208 components, the results showed a significant difference in the performance of the solder joints due to the variations in solder paste volume for the doped SAC-Bi alloy. This difference is significant across all three different aging temperatures and aging times.

4.2.1. Mean-Time-To-Failure of CABGA208 Components

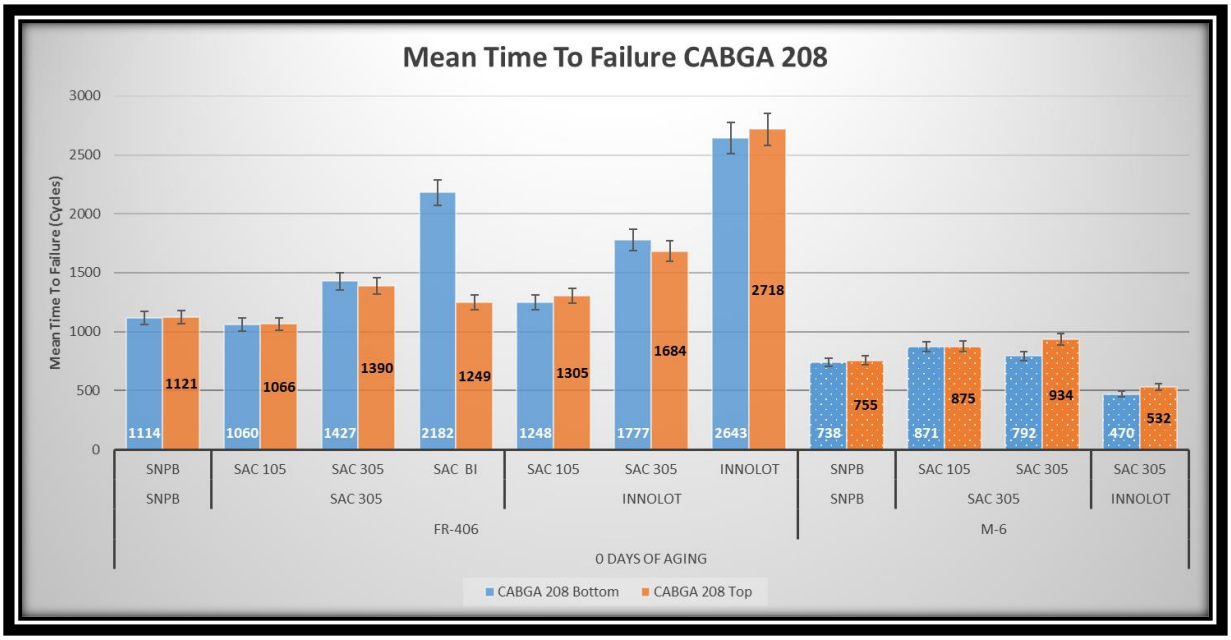

Figure 50 Mean-Time-To-Failure for CABGA 208 Components Tested @ 0 days of Aging

The test boards built in two batches the Top side with 0.127 mm and the Bottom side with 0.076 mm. The test results show no difference in the performance of the CABGA 208 components due to the higher paste volume but there seems to be an effect of the solder paste volume on the board substrate material. The Mean-Time-To-Failures of the CABGA 208 components with the higher paste volume are lesser than that of the components with lower paste volumes for the FR-406 substrate. However, for the Megtron-6 substrate the higher paste volume components performed better than that of the lower paste volume components. Therefore, the initial test conclusion is that the solder paste volume correlated is to that of the board substrate material and not dependent on

the component solder materials. The lead-free Innolot material with the FR-406 substrate is the clear best performer for the CABGA 208 components. The next best material that performed well are the Bismuth doped solder alloys on the SAC305 paste with FR-406 substrate with less solder paste i.e., the dopant of Bi have improved the performance of the components.

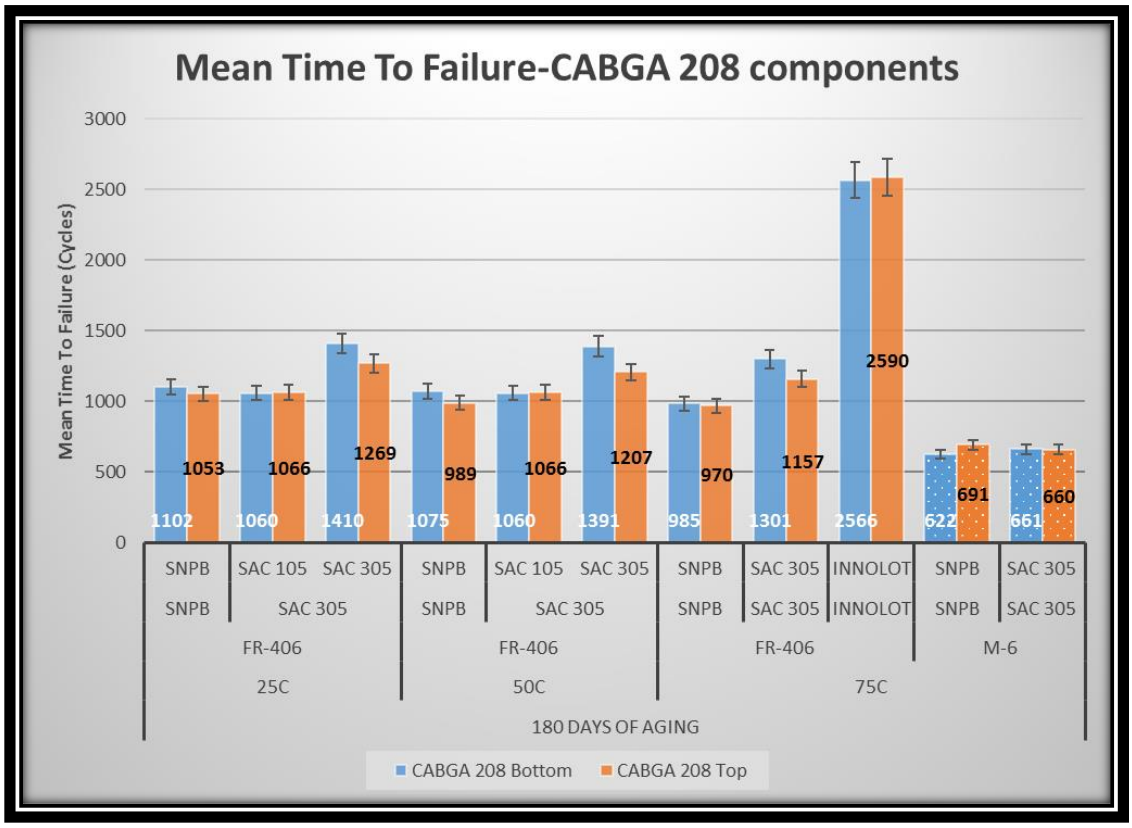

Figure 51 Mean-Time-To-Failure for CABGA 208 Components Tested @ 180 days of Aging

The test results from aging the test boards to 180 days show a difference in the performance of the CABGA 208 components due to the higher paste volume but there seems to be an effect of the solder paste volume on the board substrate material. The Mean-Time-To-Failures of the CABGA 208 components with the higher paste volume are lesser than that of the components with lower paste volumes for the FR-406 substrate. However, for the Megtron-6 substrate the higher paste

volume components performed better than that of the lower paste volume components. Both the Tin-Lead material and Lead-free materials show the same trend with respective to their board substrate material. This effect is similar across all aging temperatures. The lead-free Innolot material with the FR-406 substrate is the clear best performer for the CABGA 208 components.

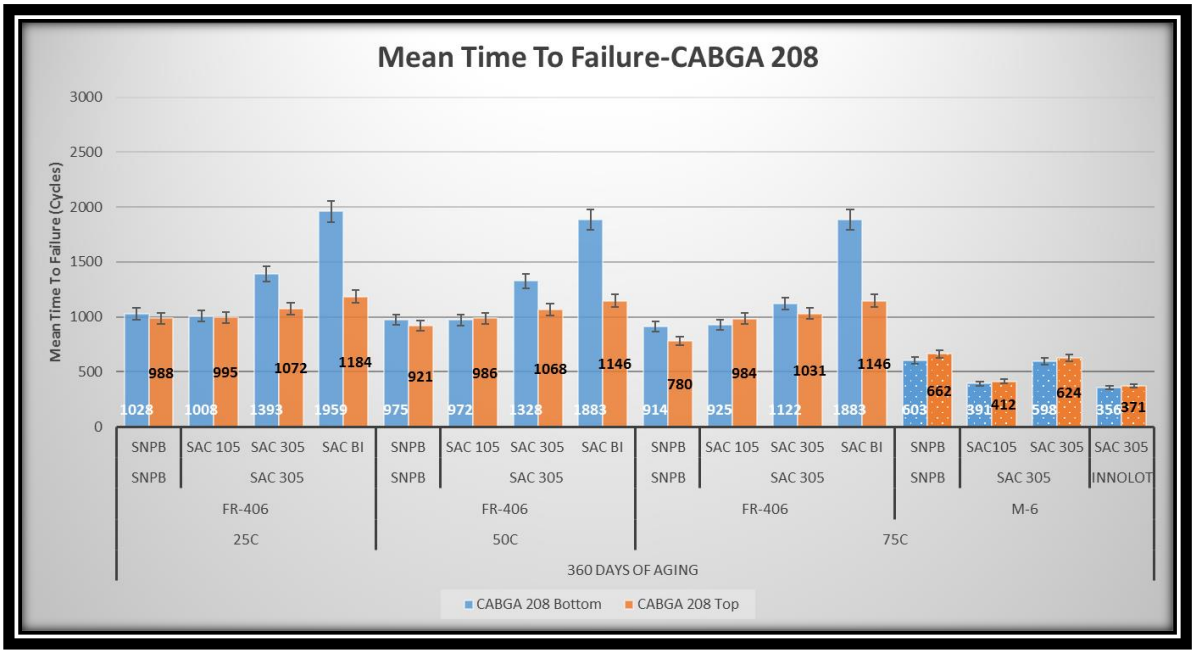

Figure 52 Mean-Time-To-Failure for CABGA 208 Components Tested @ 360 days of Aging

The test results from aging the test boards to 360 days show a difference in the performance of the CABGA 208 components due to the higher paste volume but there seems to be an effect of the solder paste volume on the board substrate material. The Mean-Time-To-Failures of the CABGA 208 components with the higher paste volume are lesser than that of the components with lower paste volumes for the FR-406 substrate. However, for the Megtron-6 substrate the higher paste volume components performed better than that of the lower paste volume components. Both the Tin-Lead material and Lead-free materials show the same trend with respective to their board substrate material. This effect is similar across all aging temperatures. The lead-free Bismuth

doped alloy with SAC305 solder paste in the FR-406 substrate is the clear best performer for the CABGA 208 components. The lead-free Innolot material is not available in this subset, as they were not available in the test design after aging them to 360 days; therefore, we lack the performance of Bi doped alloys against the Innolot materials.

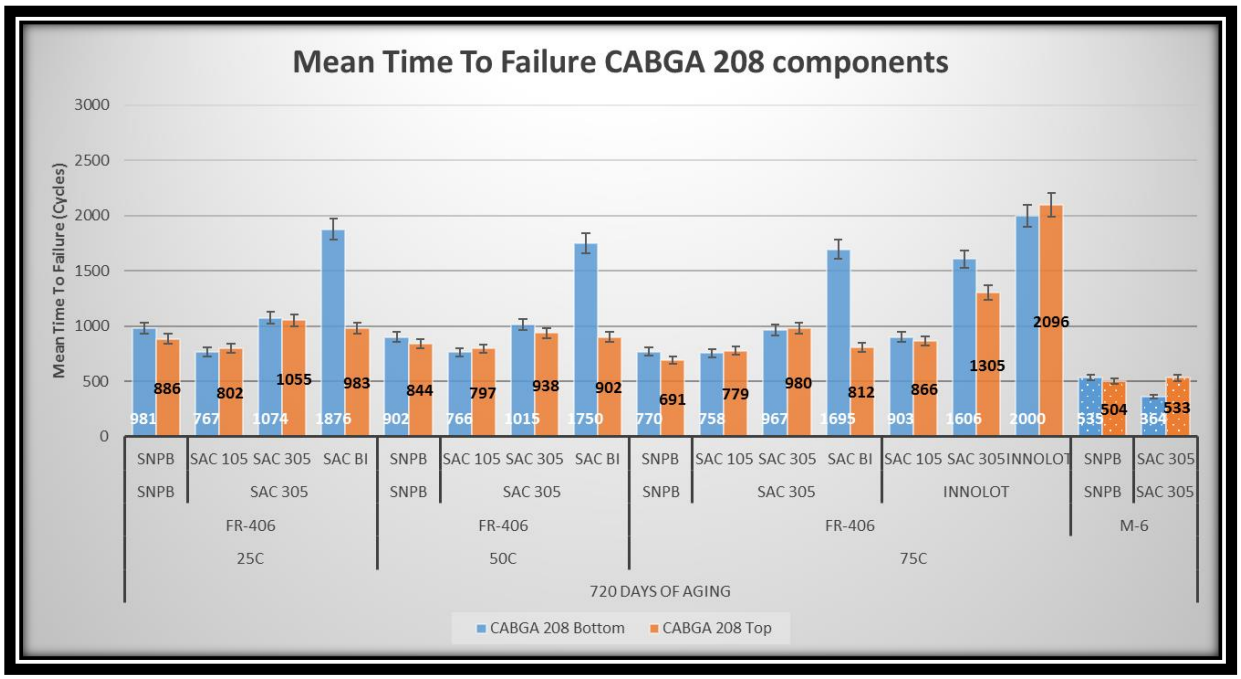

Figure 53 Mean-Time-To-Failure for CABGA 208 Components Tested @ 720 days of Aging

The test results from aging the test boards to 720 days show a difference in the performance of the CABGA 208 components due to the higher paste volume but there seems to be an effect of the solder paste volume on the board substrate material. The Mean-Time-To-Failures of the CABGA 208 components with the higher paste volume are lesser than that of the components with lower paste volumes for the FR-406 substrate. However, for the Megtron-6 substrate the higher paste volume components performed better than that of the lower paste volume components. Both the

Tin-Lead material and Lead-free materials show the same trend with respective to their board substrate material. This effect is similar across all aging temperatures. The lead-free Innolot material in the FR-406 substrate is the clear best performer for the CABGA 208 components.

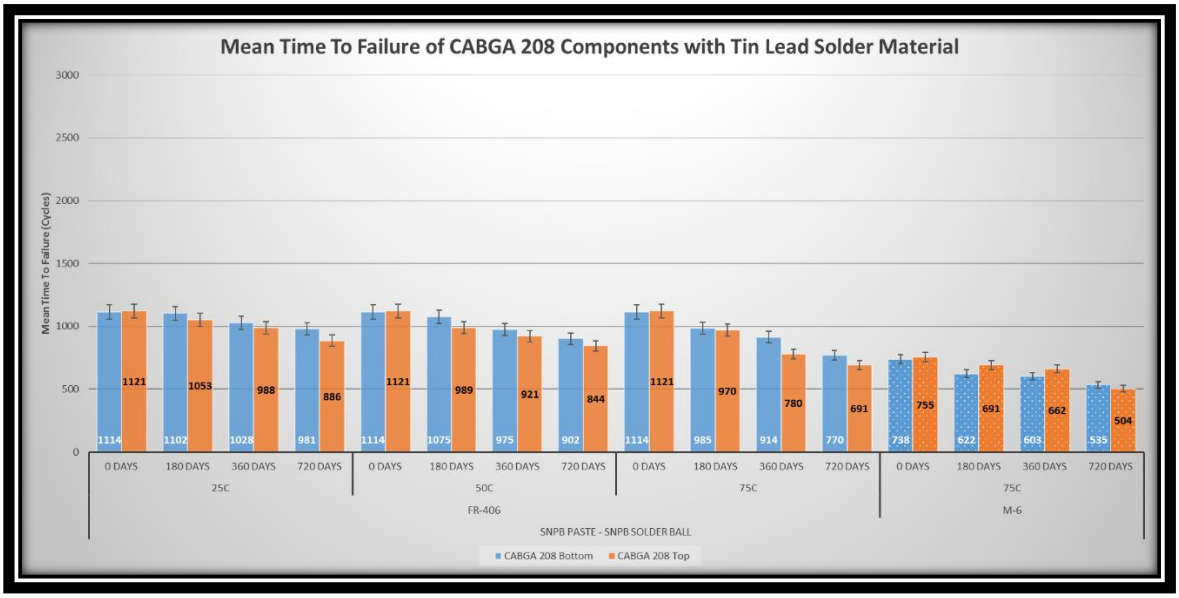

Figure 54 Mean-Time-To-Failure for CABGA 208 Components Tested with Tin-lead Solders

The test results from the Tin-lead Solder Paste and Alloy combination show that the lesser the solder paste volume is used the better the performance of the solder joints for the FR-406 board substrate across all aging time and temperatures. However, this is vice versa the case for the Megtron-6 substrate. The aging time and aging temperature have been the major contributor in the degradation of the reliability of the solder joints. This effect observed is in both the FR-406 and Megtron-6 substrates. The FR-406 substrate is far superior in performance compared to the Megtron-6 substrate. Another observation from the results are that the degradation effect of aging time seems to be less dominant after 180 days of aging, this observation holds true across all the

three aging temperatures and also between the two different substrates. The damage accumulated from the solder joints seem to approach to a constant after 180 days of aging in this thermal cycling test environment.

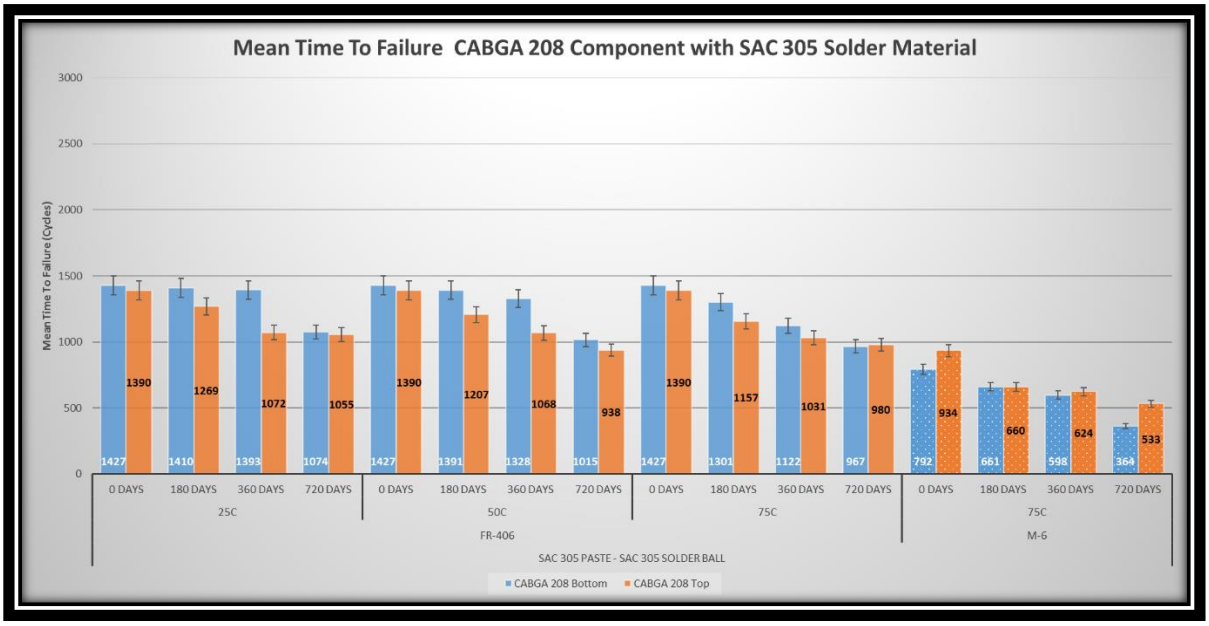

Figure 55 Mean-Time-To-Failure for CABGA 208 Components Tested with SAC305 Solders

The test results from the SAC305 Solder Paste and Alloy combination show that the lesser the solder paste volume is used the better the performance of the solder joints for the FR-406 board substrate across all aging time and temperatures. However, this is vice versa the case for the Megtron-6 substrate. The aging time and aging temperature have been the major contributor in the degradation of the reliability of the solder joints. This effect observed is in both the FR-406 and Megtron-6 substrates. The FR-406 substrate is far superior in performance compared to the Megtron-6 substrate. Another observation from the results are that the degradation effect of aging time seems to be less dominant after 180 days of aging, this observation holds true across all the

three aging temperatures and also between the two different substrates. The damage accumulated from the solder joints seem to approach to a constant after 180 days of aging in this thermal cycling test environment.

4.2.2. Effects of Solder Paste Volume

- In FR-406 board substrate material, the CABGA 208 components performed better with the lesser solder paste volume. Both Tin-lead and Lead-free solder materials (both SAC305 and Innolot) showed the same trend in their Mean-Time-To-Failures.
- In Megtron-6 board substrate material, the CABGA 208 components performed better with higher solder paste volume. Both Tin-lead and Lead-free solder materials (both SAC305 and Innolot) showed the same trend in their Mean-Time-To-Failures.

4.3. Reliability Study on the effect of Board Substrate Material

The effect of board substrates are experimented for Tin-lead and Lead-free SAC305 materials, aged for 0 days, 360 days and 720 days at 75°C. All the components in the test matrix have experienced failures in this experiment except the CVBGA 97 component, which had far fewer numbers of failures to make a meaningful comparison. In both the substrates, the results showed a significant difference in the performance of the solder joints based on the solder materials physical properties. This difference is significant across all the different components, aging time and temperatures. In this reliability study, only 75°C one of the three aging temperature is chosen, since Megtron-6 substrate was aged only at that temperature.

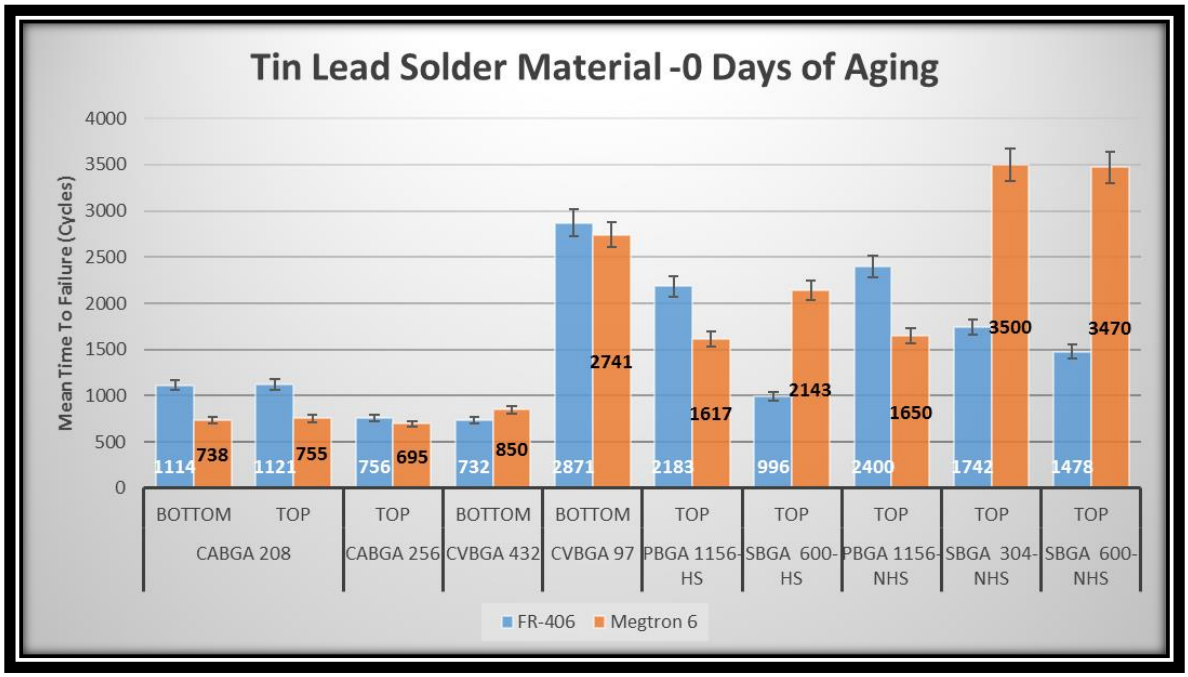

Figure 56 Mean-Time-To-Failure of various Tin-lead components aged 0 days @75°C

The test results show a significant difference in the performance of the SBGA and PBGA components due to the variance in the board substrate materials. The Mean-Time-To-Failures of the ceramic and plastic mold materials are better with FR-406 substrate and that of the BT materials are better with Megtron-6 substrates. Therefore, the initial test conclusion is that the board substrate material and package mold-compound materials are dependent on each other.

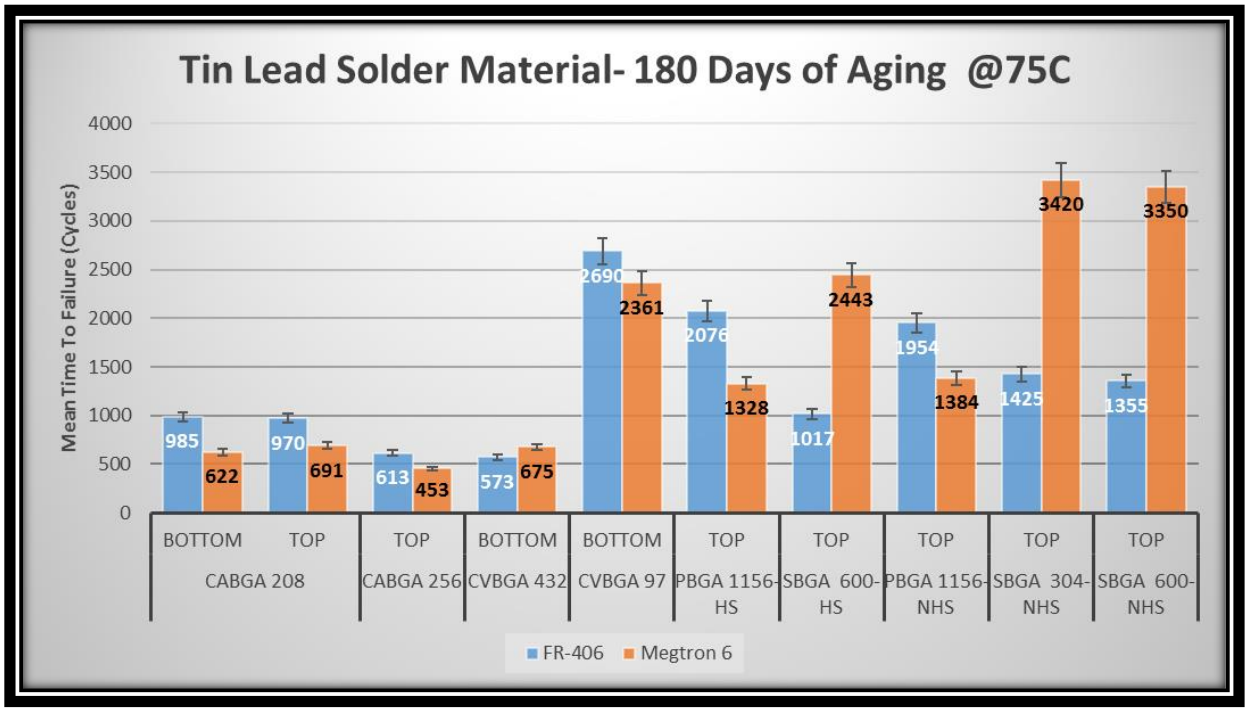

Figure 57 Mean-Time-To-Failure of various Tin-lead components aged 180 days @75°C

The test results show a significant difference in the performance of the SBGA and PBGA components due to the variance in the board substrate materials. The Mean-Time-To-Failures of the ceramic and plastic mold materials are better with FR-406 substrate and that of the BT materials are better with Megtron-6 substrates. Therefore, the initial test conclusion that the board substrate material and package mold-compound materials are dependent on each other is still true after aging for 180 days @ 75°C.

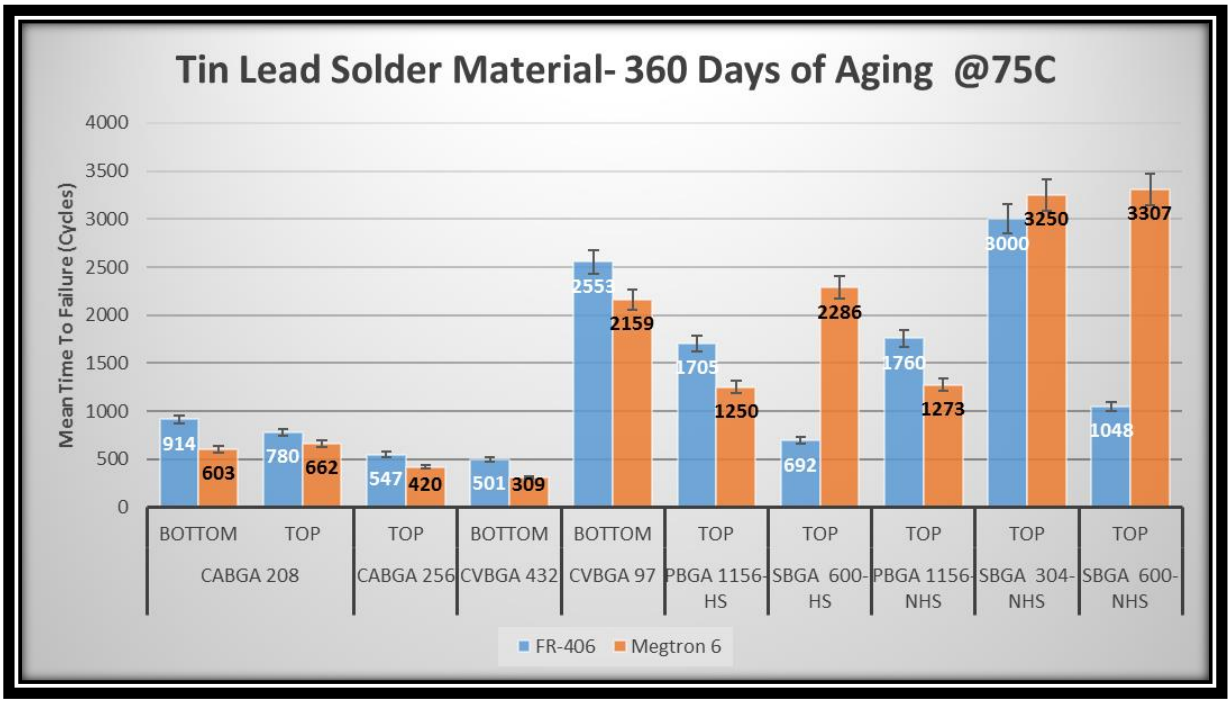

Figure 58 Mean-Time-To-Failure of various Tin-lead components aged 360 days @75°C

The test results show a significant difference in the performance of the SBGA and PBGA components due to the variance in the board substrate materials. The Mean-Time-To-Failures of the ceramic and plastic mold materials are better with FR-406 substrate and that of the BT materials are better with Megtron-6 substrates. Therefore, the initial test conclusion and 180 days aged @ 75°C conclusion that the board substrate material and package mold-compound materials are dependent on each other is still true after aging for 360 days @ 75°C. A very important observation on the SBGA 600 component is that the reliability of the component dropped by more than 50% in the case of the FR-406 substrate but not such a significant drop experienced in the case of the Megtron-6 substrate.

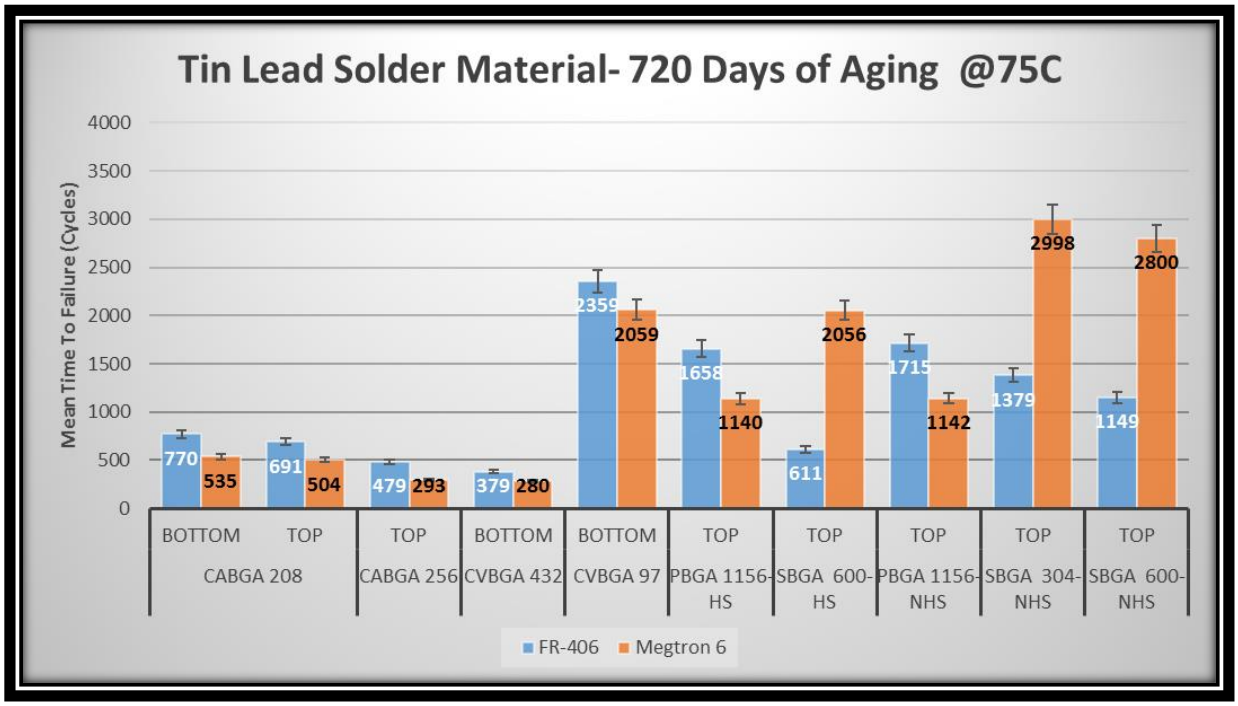

Figure 59 Mean-Time-To-Failure of various Tin-lead components aged 720 days @75°C

The test results show a significant difference in the performance of the SBGA and PBGA components due to the variance in the board substrate materials. The Mean-Time-To-Failures of the ceramic and plastic mold materials are better with FR-406 substrate and that of the BT materials are better with Megtron-6 substrates. Therefore, the initial test conclusion, 180 days aged @ 75°C conclusion, and 360 days aged @ 75°C conclusion that the board substrate material and package mold-compound materials are dependent on each other is still true after aging for 720 days @ 75°C. A very important observation on the SBGA 600 component is that the reliability of the component remained similar to that of the 360 days aging @ 75°C.

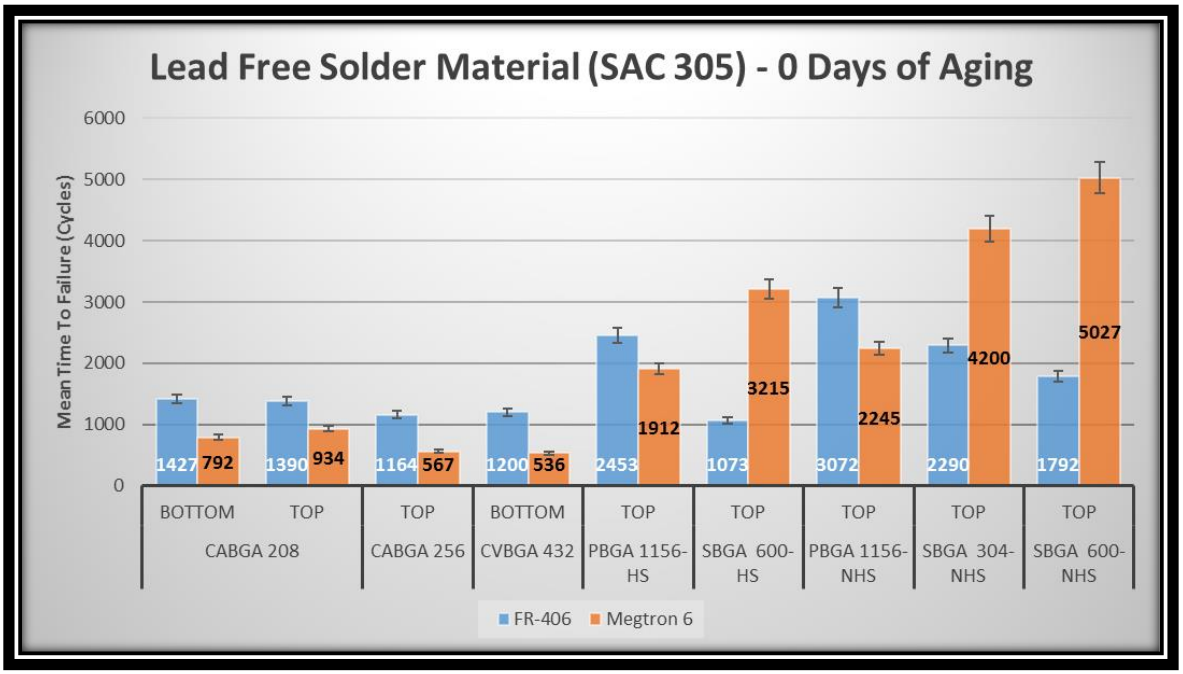

Figure 60 Mean-Time-To-Failure of various Lead-free components aged 0 days @75°C

The test results show a significant difference in the performance of the SBGA and PBGA components due to the variance in the board substrate materials. The Mean-Time-To-Failures of the ceramic and plastic mold materials are better with FR-406 substrate and that of the BT materials are better with Megtron-6 substrates. Therefore, the initial test conclusion is that the board substrate material and package mold-compound materials are dependent on each other. An important point on the SBGA 600 component and SBGA 304 component is that the Mean-Time-To-Failure are estimated using the Weibull distribution[51].

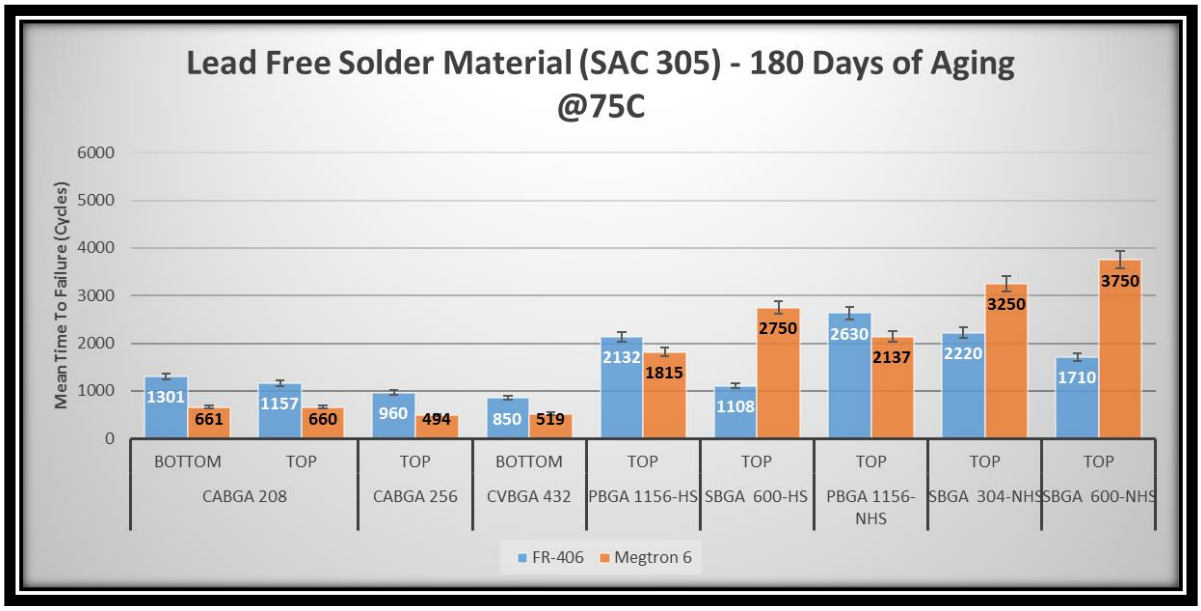

Figure 61 Mean-Time-To-Failure of various Lead-free components aged 180 days @75°C

The test results show a significant difference in the performance of the SBGA and PBGA components due to the variance in the board substrate materials. The Mean-Time-To-Failures of the ceramic and plastic mold materials are better with FR-406 substrate and that of the BT materials are better with Megtron-6 substrates. Therefore, the initial test conclusion that the board substrate material and package mold-compound materials are dependent on each other is still true after aging for 180 days @ 75°C.

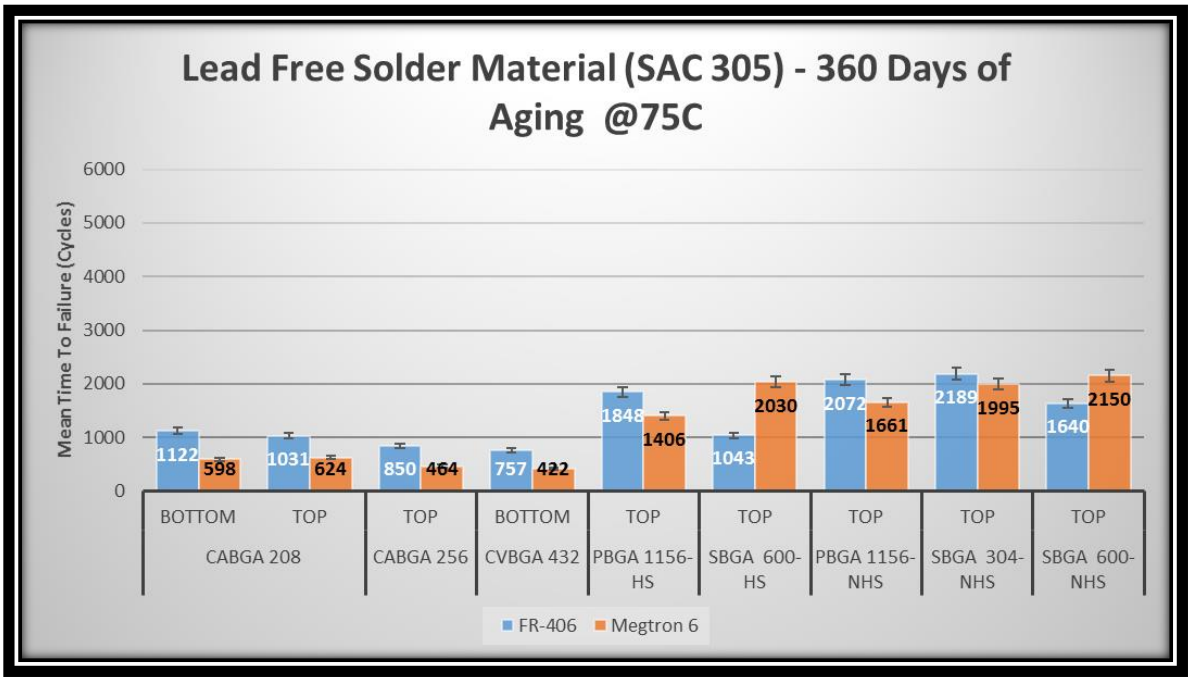

Figure 62 Mean-Time-To-Failure of various Lead-free components aged 360 days @75°C

The test results show a significant difference in the performance of the SBGA and PBGA components due to the variance in the board substrate materials. The Mean-Time-To-Failures of the ceramic and plastic mold materials are better with FR-406 substrate and that of the BT materials are better with Megtron-6 substrates. Therefore, the initial test conclusion and 180 days aged @ 75°C conclusion that the board substrate material and package mold-compound materials are dependent on each other is still true after aging for 360 days @ 75°C.

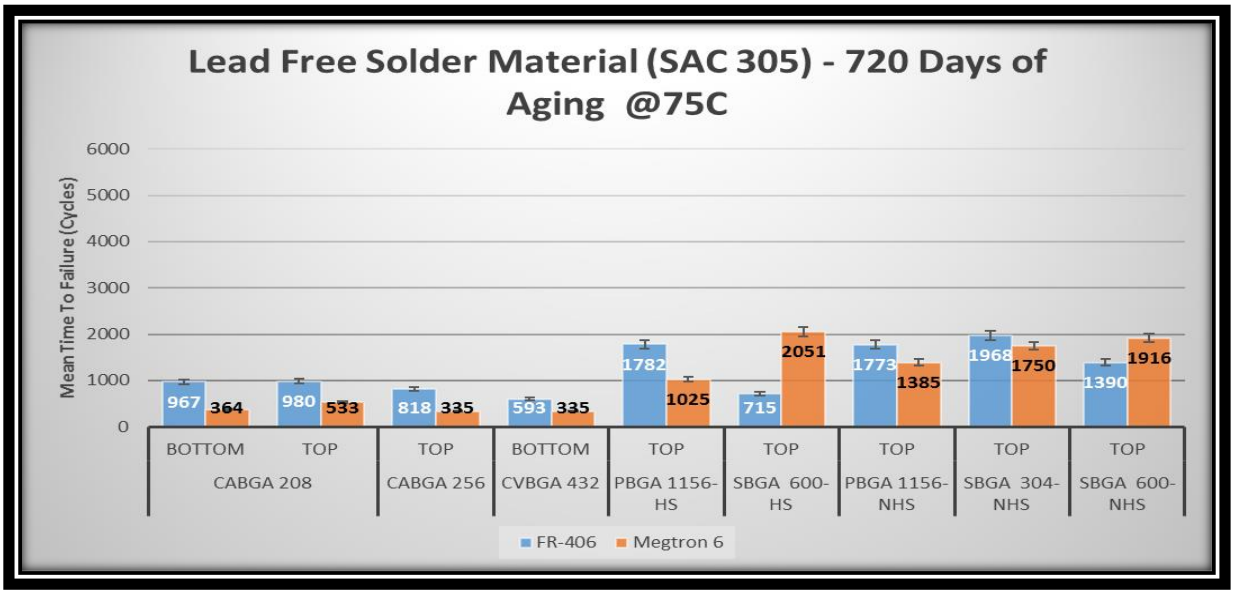

Figure 63 Mean-Time-To-Failure of various Lead-free components aged 720 days @75°C

The test results show a significant difference in the performance of the SBGA and PBGA components due to the variance in the board substrate materials. The Mean-Time-To-Failures of the ceramic and plastic mold materials are better with FR-406 substrate and that of the BT materials are better with Megtron-6 substrates. Therefore, the initial test conclusion and 180 days aged @ 75°C conclusion that the board substrate material and package mold-compound materials are dependent on each other is still true after aging for 720 days @ 75°C.

4.4. Reliability study on the effect of Aging Time Temperatures

The test results show a degradation in the performance of all of the test components after aging through time and temperatures. The Mean-Time-To-Failures of the CABGA 256 component compared with Tin-lead and Lead-free (SAC305 material) solders between the FR-406 substrate and Megtron-6 substrates shown in the

Figure 64. There is a direct correlation of the degradation to aging time and temperatures.

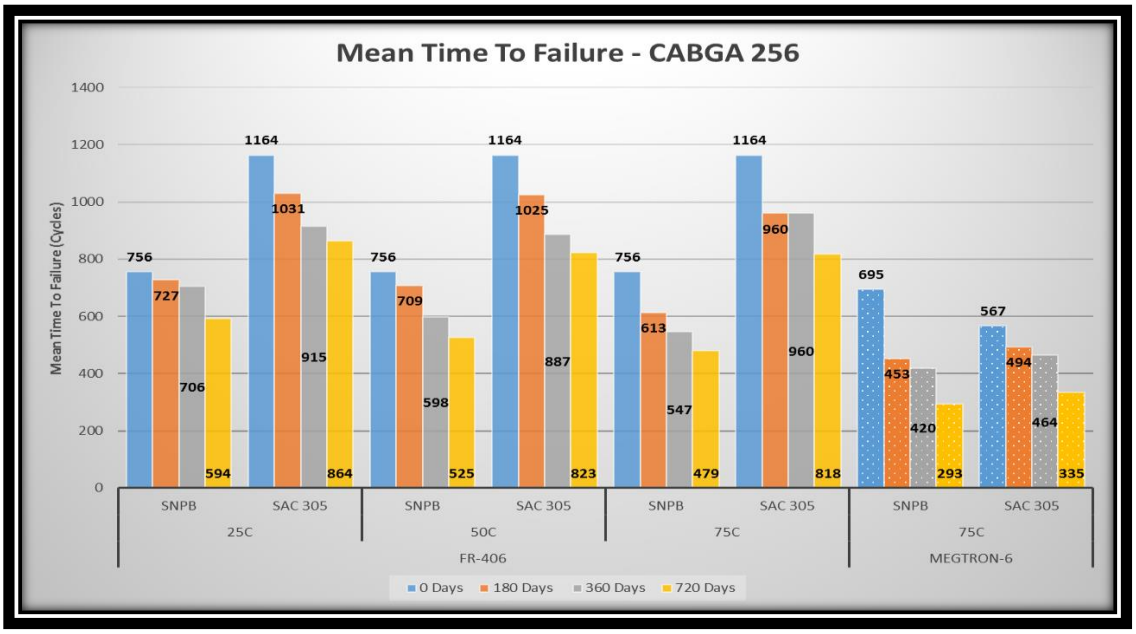

Figure 64 Mean-Time-To-Failure of CABGA 256 Components in all aging time temperatures

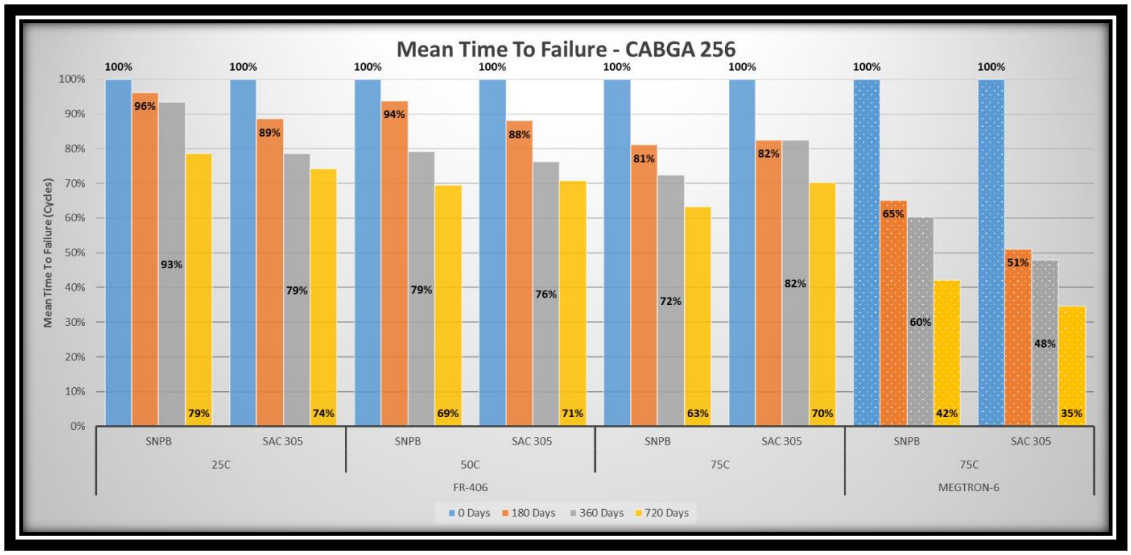

Figure 65 Degradation Chart on Mean-Time-To-Failure for CABGA 256 Component with Tin lead and Lead-free (SAC305) Material

Figure 64 and Figure 65 show the materials degradation due to effect of aging time and temperature. As, the aging time and temperature increases the materials degradation accelerates.

Tin-lead materials degradation percentages were better than lead-free SAC305 after aging time and temperatures for both the substrates. However, for the 75 °C with FR-406 substrate the lead-free SAC305 materials had lesser degradation effect compared with tin-lead materials. Important understanding of these charts are that the degradation percentages compared are with respect to their no aging baseline mean times to fail. The lead-free SAC305 materials even after aging still have higher mean life than that of their tin-lead counter parts in FR-406 substrate. Another important observation is that the effect of degradation of tin-lead material is more, compared to that of the lead-free SAC305 material in the Megtron-6 substrate. This is explained by the glass transition temperature (T_g) differences in both the substrates and the CTE mismatch is higher with tin-lead materials. This is a new information available in this test and not reported in any of the predecessors research work from our research group. The general overall trend seen in all the materials in both the substrate is that the aging time and temperatures are detrimental to the solder joint performance. This negative effect correlated to other packages in the test, also correlated to similar research papers and dissertations in the academic and industrial communities.

Chapter 5 Sample Preparation and Failure Analysis

Solder joint are subjected to temperature cycling in actual application and in accelerated life testing. CTE mismatch of solder joint materials cause them to undergo cyclic temperature stresses. This cyclic loading leads to thermo-mechanical fatigue damage, which involves damage accumulation, crack initiation, crack propagation, and failure. In addition, the microstructure, mechanical response, and failure behavior of lead free solder joints in electronic assemblies are constantly evolving when exposed to isothermal aging and thermal cycling environments. Isothermal aging leads to both grain and phase coarsening, and causes recrystallization at Sn grain boundaries. These changes in the microstructure cause the cracks and lead to failure of the solder joints[52]. In this chapter, the author discusses the specimen preparations and optical microscopic study on grain structures.

5.1. Summary of Sample Preparation Procedure

Sectioning: In order to work with a specimen of reasonable size, small samples are cut out of larger test pieces. This also provides a cross-section of the sample, which may provide a more representative picture of the bulk microstructure than the surface.

Mounting: Cold Mount the component using the thermoset epoxy system, using appropriate labels. Once set, release the specimen as carefully as possible to minimize possible cracking of the epoxy.

Grinding and Polishing:

The grinding and polishing procedure used in this dissertation explained in Table ix.

Table ix Polishing Procedure

Abrasive Paper	Lubrication	Piston Force (Psi)	Speed (rpm)	Polishing Time
Buehler P120 Grit SiC Paper (0.12 μ)	Water	100	200	Reach the Outer Layer of Solder Joints
Buehler P400 Grit SiC Paper (0.4 μ)		100	200	Until the Solder Joints are free from Scratches
Buehler P1200 Grit SiC Paper (1.2 μ)		100	200	Until the Center of the Solder Joints are reached
Buehler P1500 Grit SiC Paper (1.5 μ)		50	100	10 minutes
Buehler P2500 Grit SiC Paper (2.5 μ)		60	100	8 minutes
Micro cloth with Polycrystalline Diamond Suspension (3 μ)	Polycrystalline Diamond Suspension	50	100	4 minutes
Micro cloth with Polycrystalline Diamond Suspension (1 μ)	Polycrystalline Diamond Suspension	60	100	7 minutes
Micro Cloth Polycrystalline Diamond Suspension (0.05 μ)	Nanometer Colloidal Alumina	60	100	5 minutes

5.2. Failure Analysis

The common destructive failure analysis used in assessing electronic solder joints is cross sectioning and studying for microstructural growth. This technique is an adaptation of metallurgical analysis method. The basic steps in metallurgical sample preparation are 1) Sectioning, 2) Mounting, Grinding, Polishing, and Etching [53].In this dissertation, the specimens have been prepared without etching process and examined using EDS, optical & electron microscopy. Intermetallic Growth Measurements on representative solder materials shown are using SEM (Scanning Electron Microscope), BSE (Back-scattered Electron) Images, EDS (Energy Dispersive Spectrometry) Points-of-Interest and Maps, IMC (Intermetallic Compound) thickness measurements from Optical Cross Polarized Microscopy.

The Scanning Electron Microscopy is available only for very limited set of samples due to the cost of Microscopy and Carbon coating of the samples needed on the SEM. The optical microscopy images are available for almost all the samples in the test that have failures. The intermetallic measurements from the optical microscopy show a significant growth of Tin Silver precipitates within the bulk solder material. The copper-tin intermetallic elements formed between the copper pads and tin silver solder joints near the board side are studied. The crack initiation and growth of the crack propagation are visible in the optical 50X and 100X zoom lenses.

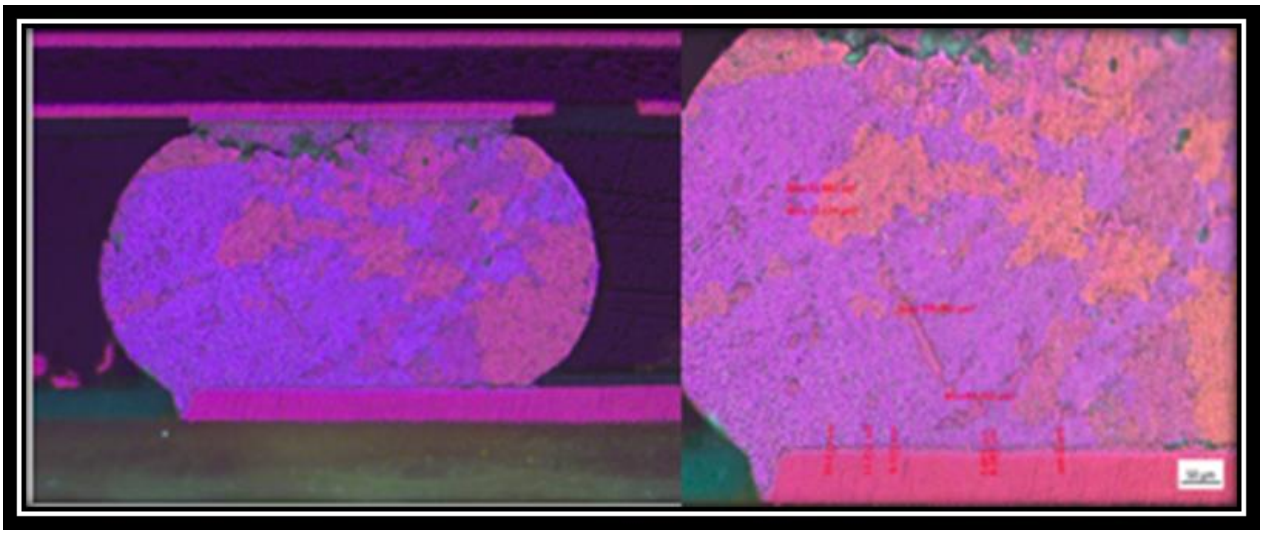

Figure 66 SBGA 600 Component with SAC305 Material with Heat Sink

The above Figure 66 shows the optical microscopy image of the SBGA600 component with SAC305 alloy on SAC305 paste, which is isothermally aged @180 days for 25°C. The average intermetallic thickness at the board copper side is 8.797 microns. The plate like elements seen in the Tin (Sn) matrix are the Silver Tin precipitates (Ag_3Sn). The area of the precipitate is approximately 305.4545 squared microns. The temperature cycle count for the above sample is 1366. The above sample shows that the crack propagated on the chip side and board side. Both the crack propagations are perpendicular in growth along the intermetallic occurring within the bulk solder material. This is a common characteristic failure mechanism in the temperature cycling tests. The major reason behind this type of crack initiation and growth are the CTE mismatch of the board FR-406 substrate and the components metallic mold materials. The polarized image also reveals the various intermetallic grain orientations formed on the solder joints[54][55][56].

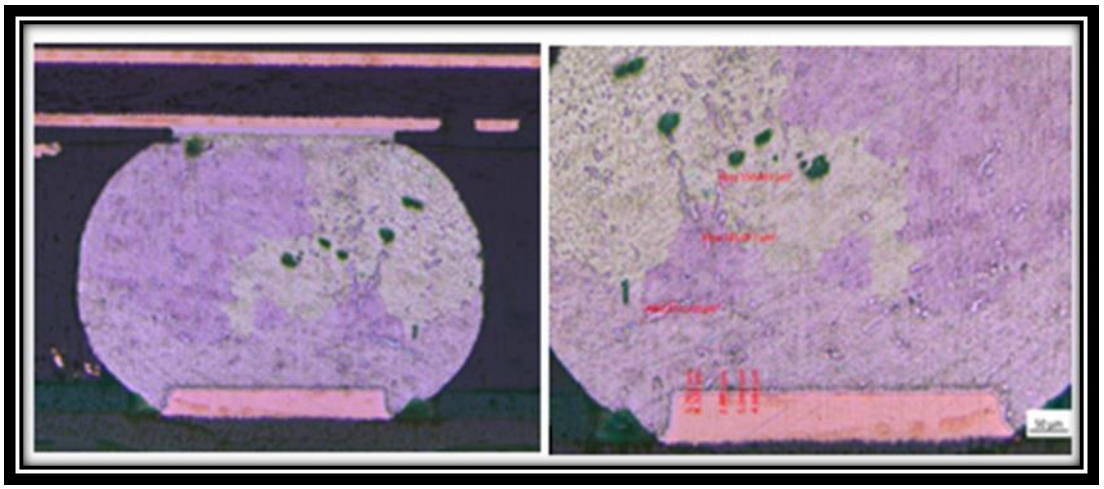

Figure 67 CABGA 208 Component with SAC305 Material

The above Figure 67 shows the optical microscopy image of the CABGA208 component with SAC305 alloy on SAC305 paste, which is isothermally aged @180 days for 75°C. The average intermetallic thickness at the board copper side is 4.5496 microns. The plate like elements seen in the Tin (Sn) matrix are the Silver Tin precipitates (Ag3Sn). The area of the precipitate is approximately 242.931 squared microns. The temperature cycle count for the above sample is 1120. The above sample shows that the crack propagated on the chip side and board side. The crack propagation is perpendicular to the sample near the intermetallic formed with in the Copper-tin bulk solder. The ceramic compound on the mold materials and the Megtron-6 board substrate materials have a wide difference in their CTE. This accumulation of stresses over large number of thermal cycles initiates the granular structural growth of the intermetallic. The grains coarsen and harden along the intermetallic layer forming additional CTE mismatch on the bulk solder joints. Eventually resulting in the crack initiation and growth of the cracks along the intermetallic layer with in the copper tin matrix. The polarized image also reveals the various intermetallic grain orientations formed on the solder joints[57][58][59].

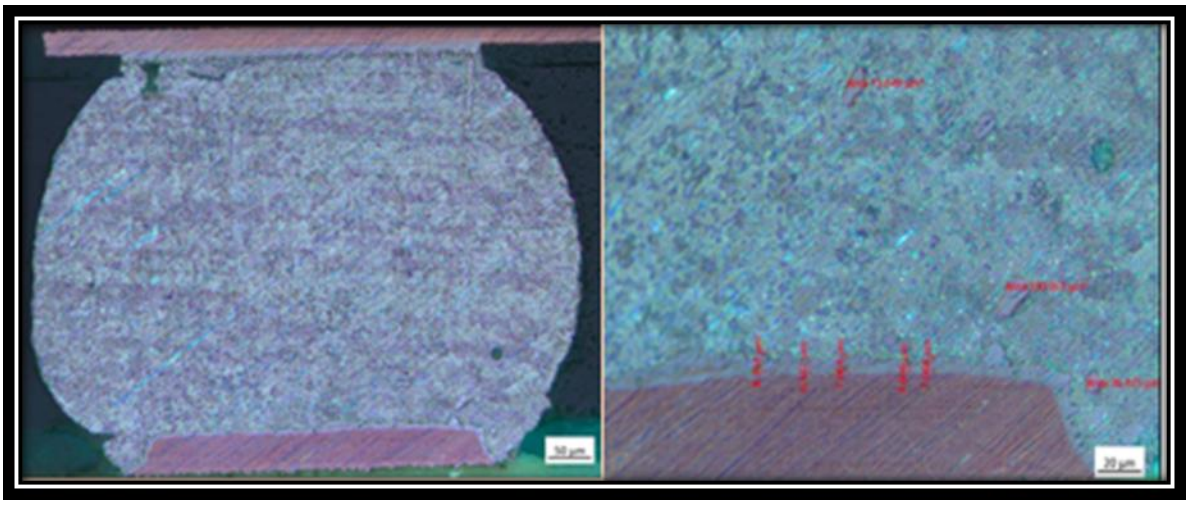

Figure 68 PBGA 1156 Component with SAC305 Material

The above Figure 68 shows the optical microscopy image of the PBGA 1156 component with SAC305 alloy on SAC305 paste, which is isothermally aged @180 days for 75°C. The average intermetallic thickness at the board copper side is 6.488 microns. The plate like elements seen in the Tin (Sn) matrix are the Silver Tin precipitates (Ag_3Sn). The area of the precipitate is approximately 70.054 squared microns. The temperature cycle count for the above sample is 1500. The above sample shows that the crack propagated on the chip side. In this solder joint, the plastic mold compound materials restrict the copper tin bulk solder from any lateral flexures. The FR-406 substrate materials are more closely associated to similar CTE values of the solder joints. No cracks originated on the bottom of the solder joints for this reason. The solder joints are more ductile near the bottom board substrate, whereas brittle near the Ni coated plastic compounds on the top chip side. Crack introduced are only on the component side of the solder joints along the intermetallic layer and grows perpendicular to the solder joints until complete failure occurs. This is due to the damage accumulation of low cyclic temperature stress of harder Ni based intermetallic layer[59][60][61].

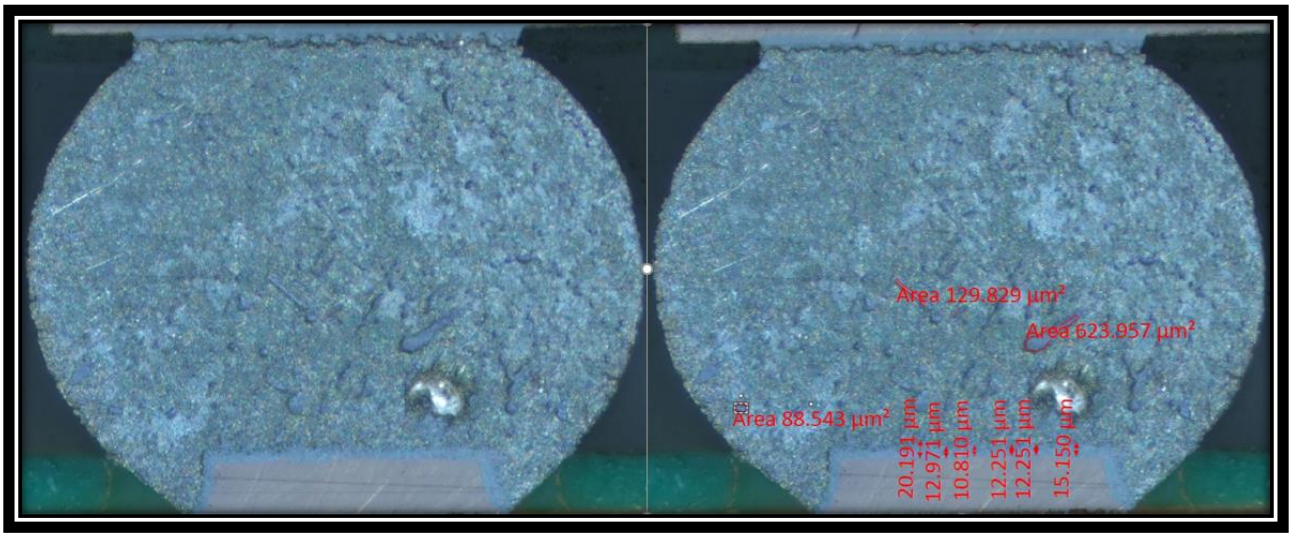

Figure 69 PBGA 1156 Component with Innolot Material

The above Figure 69 shows the optical microscopy image of the PBGA 1156 component with SAC105 alloy on Innolot paste, which is isothermally aged @180 days for 75°C. The average intermetallic thickness at the board copper side is 13.9373 microns. The plate like elements seen in the Tin (Sn) matrix are the Silver Tin precipitates (Ag_3Sn). The area of the precipitate is approximately 280.7763 squared microns. The temperature cycle count for the above sample is 1500. The above sample shows that the crack propagated on the chip side. There are different failure modes observed with in the FR-406 substrate Innolot samples. Namely, the joints fail fully across the top (component-side), with secondary cracks appearing at the bottom (board-side) of the joint. The board-side cracks, however, do not fully compromise the joint. In some joints, the component-side cracks are close to the IMC (intermetallic compound) layers while in other cases they move through areas of the "bulk" solder in a form that may indicate dynamic recrystallization driven failures[62]–[64]. There are numerous other solder joints shown in the Appendix C.

Chapter 6 Statistical Predictions of the Reliability of System and Accelerated Factor

In this chapter overall board level mean times to fail are, predicted from their individual component mean times to fail using Reliability Block Diagrams. Most real world applications of electronics demand series type connection. Only a few systems have both parallel and series type connections depending on their specific applications. In this chapter, only series type connection for top side to predict the board level reliability[65][66].

6.1. Top Side Test Board Level Reliability Predictions based on Series Connection

The Top Side has SBGA 600 and PBGA 1156component with two options with or without heat sinks, CABGA 208, CABGA 256. The two solder materials compared (Tin-lead, Lead-free SAC305) and two different board substrates (FR-406, Megtron-6) predicted in this experiment.

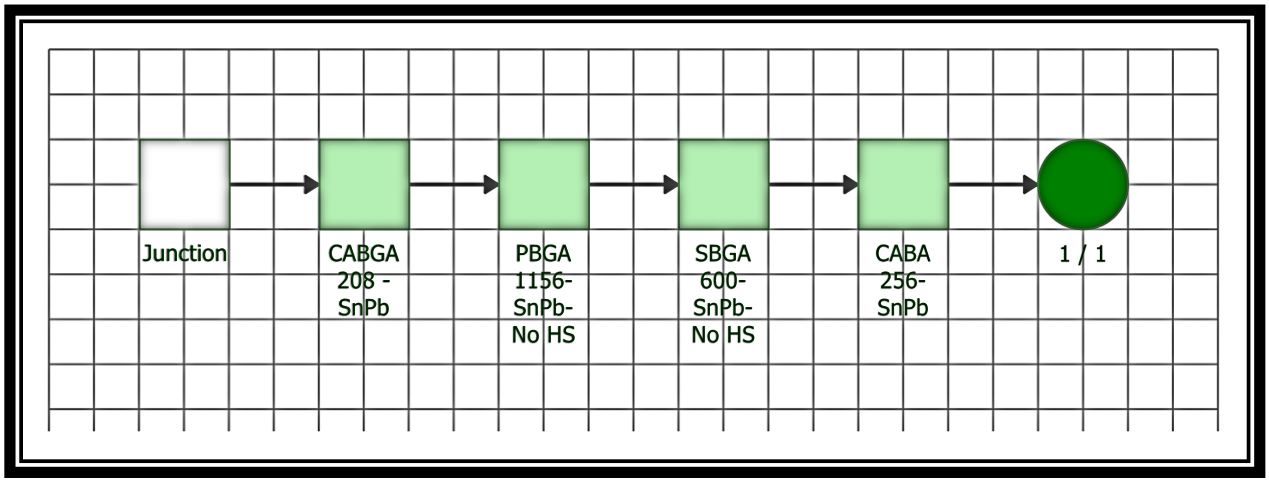

Figure 70 Reliability Block Diagram to predict the Series Connection of the components with Heat Sinks on Tin-lead Solder Material in FR-406 substrate

Similar RBD, series connection considered is for the components without heat sinks and for other factors such as the solder material, aging time temperatures and board substrates.

The Mean-Time-To-Failures for the overall system reliability of the test boards computed at 0 Days of Aging and shown in the Figure 71 . For the FR-406 substrate, the heat sinks are not improving the overall reliability of the package but with Megtron-6 substrate, the heat sinks are improving the reliability of the overall package in both the lead-free and tin-lead materials.

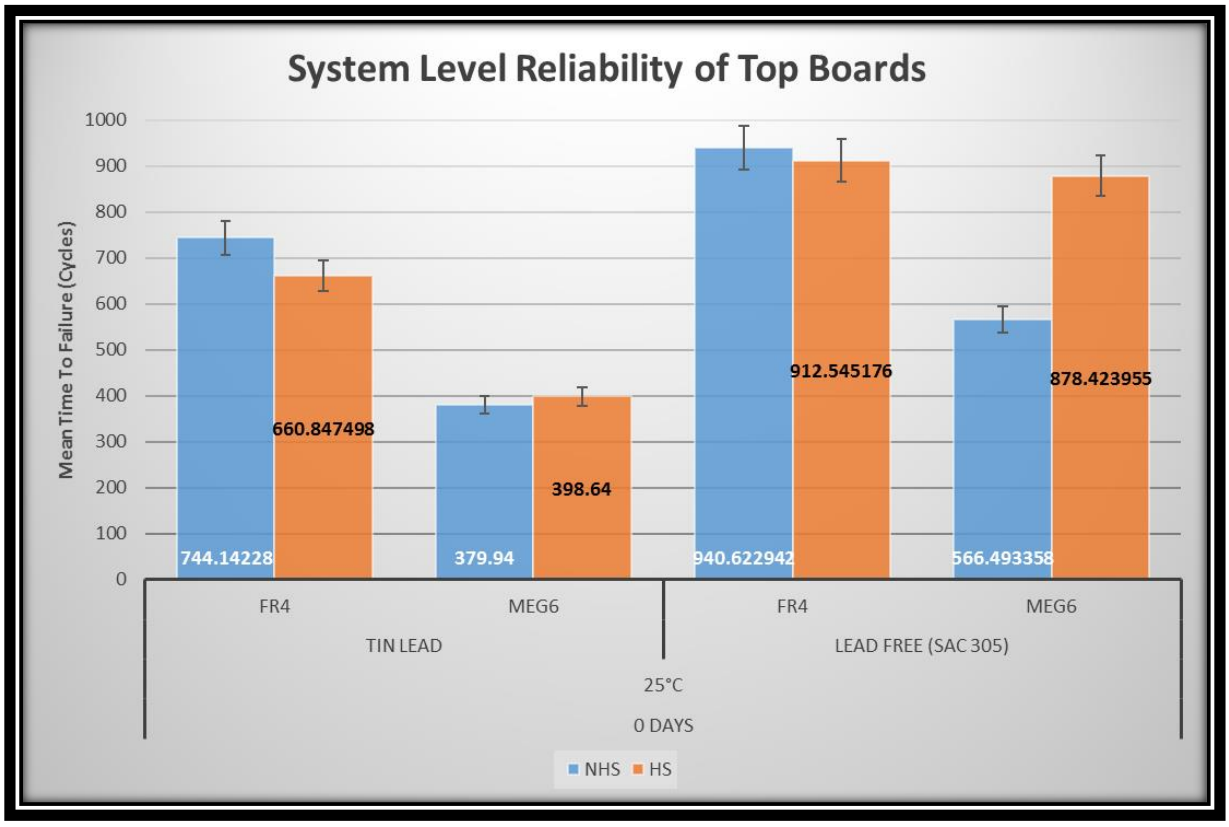

Figure 71 Effect of Heat Sinks System Level Predicted Reliability of Top Boards with Tin-lead and Lead-free (SAC305) Solder Materials

6.2. Accelerated Factors for prediction of Field Reliability

In this section, the accelerated are computed for the Top sideboards for Tin-Lead and Lead-Free SAC305 materials with and without the heatsinks for the FR-406 substrate and Megtron-6 substrates.

Assumption for Field Usage

ΔT_{Field} = Average Computer temperature range = 40 (Kelvin) [67]

f_{Field} = Frequency of cycles in a day (24 hours) = 10 cycles (assumption)

Experimental Data

k = Boltzmann's constant (8.6173303 x 10-5 eV/°K) [43][42]

E_a/k = 1414 for Tin-Lead; 2185 for Sn-Ag-Cu [43] [42]

m = 1/3 for Tin-Lead; 0.136 for Sn-Ag-Cu [43][42]

n = 1.9 for Tin-Lead; 2.65 for Sn-Ag-Cu [43][42]

ΔT_{Test} = 398.15-228.15 = 170 kelvin

f_{Test} = Frequency of cycles in a day (24 hours) = 20 cycles

Applying the above known and assumed values to the Equation 14 Norris Landzberg modified Coffin Manson equation [41] , the acceleration factor for the tin-lead and lead-free materials are estimated as

$AF_{Tin\text{-}Lead}$ = 2.3

AF_{SAC305} = 2.5

Based on these numerical data, the actual service life in years of the top side assembled boards for the Tin-Lead materials and Lead-Free SAC305 materials is calculated.

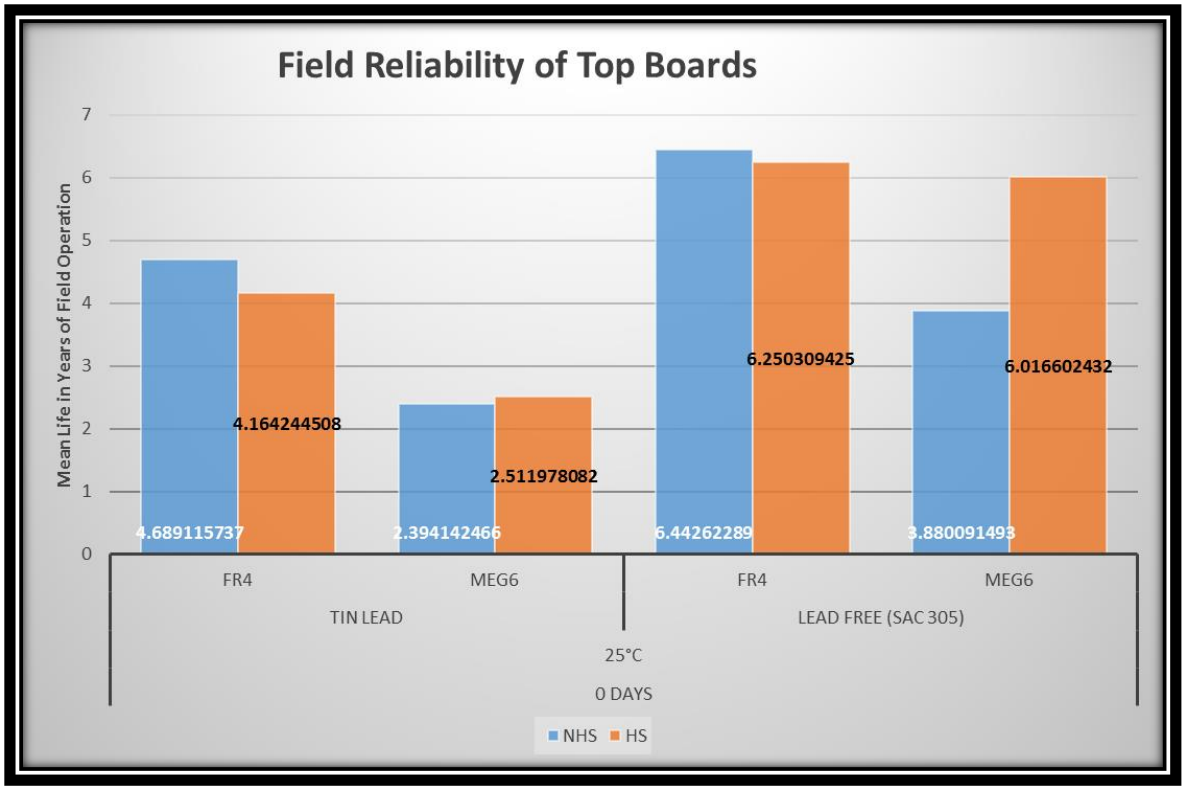

Figure 72 Predicted Field Reliability on the effect of Heat Sinks in Top Boards with Tin-lead and Lead-free (SAC305) Solder Materials

From the initial predicted field reliability of the test boards assembled on the top side has a significant difference between Tin-Lead and Lead-Free materials[68]. The field performance of the high temperature aged test boards require a more detailed acceleration factor with more mechanical properties of the test board substrates and component yield stresses. This information of models are currently being researched using ANSYS software, by Dr.Suhling's research group.

Chapter 7 Summary and Future Work

In this temperature cycle accelerated life test, reliability of individual solder materials and their rate of degradation with respect to a variety of factors is studied.

- Degradation Effect of Solder Material between two substrate materials FR4-06 & Megtron-6
- Degradation Effects of various solder alloys Tin-lead, Lead-free (SAC105, SAC305, SAC-Bi material and the six-element alloy Innolot (Sn3.8Ag0.7Cu3Bi1.4Sb0.15Ni)).
- Degradation Effects of Solder Materials with respect to Time and Temperatures.
- Effect of Heat Sinks on the solder joints
- Effect of Solder Volume and
- Prediction of the System Level Package using Statistical Analysis.

The degradation effect of the Tin-lead and Lead-free Solder materials are directly proportional to the aging time temperatures and are independent of the Substrate Materials. The degradation of Lead-free materials (SAC305 and Innolot) are much higher than that of the Tin-lead material.

The effect of heat sinks is dependent on the substrate materials used. The FR-406 material is better without the presence of heat sinks on all the solder materials whereas the Megtron-6 substrate material performs better with the presence of the heatsinks. The solder volume studied in the CABGA 208 component showed that there are no significant change in the effect of the solder paste volume. The prediction of the systems level package reliability showed that the FR-406 and Megtron-6 substrate materials have a wide difference in overall package level reliability with FR-406 doing much better than the Megtron-6 substrates.

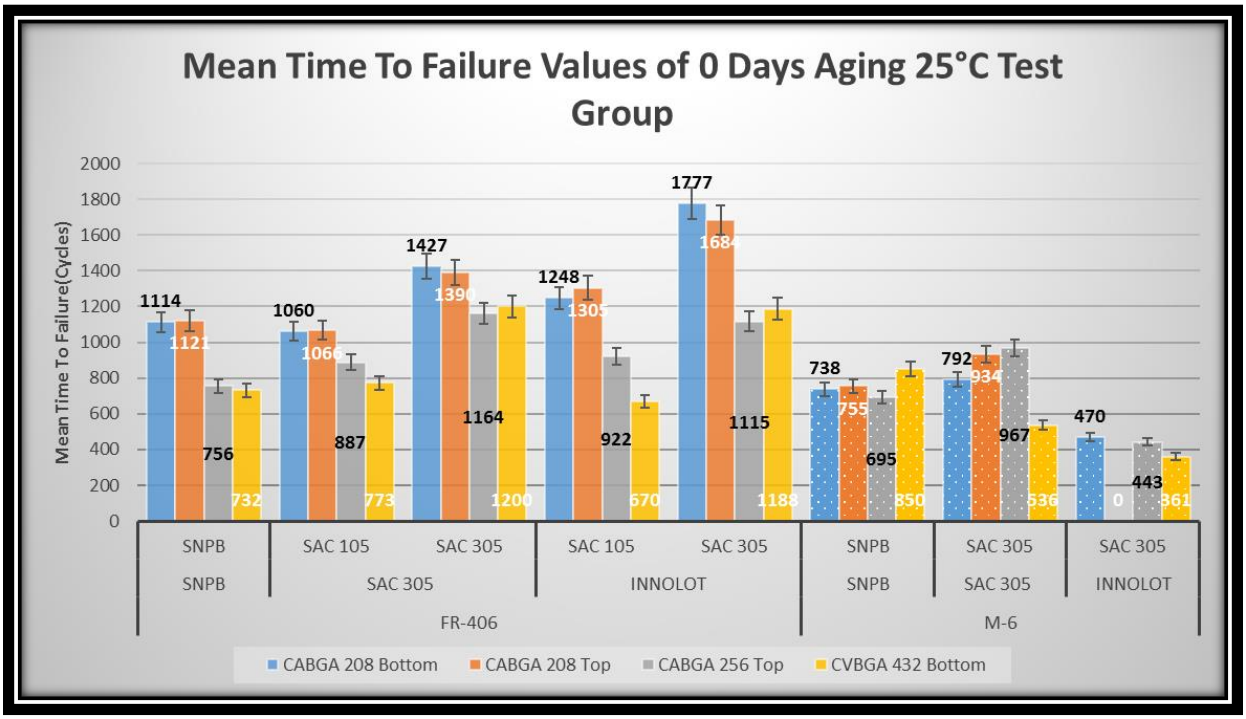

Figure 73 Summary of the Test Results for Smaller Pitch BGA Components @ 0 Days of Aging 25°C

Similar summary test charts shown are through the reliability results chapter and reliability trends were studied the IMC growth measurements and crack initiation and propagation through the bulk solders showed the mode of failure in these components.

Summarizing the results of this dissertation

- Lead-free materials degrade at a higher rate than the Tin-lead solder materials; this rate of degradation is also dependent directly on the temperature of operating conditions.
- There is improvement in reliability of component by attachment of heat sinks for the Megtron-6 substrate test boards.
- The higher the doping level of Bismuth the higher is its performance in the test.

7.1. Current Project Work

Current project status for the Thermal Cycling (TC) test is as follows: 0 days, 180 days, 360 days and 720 days aging test groups have completed 3000 temperature cycles. Failures have mostly concluded for the medium-size plastic ball grid array (BGA) packages (13mm-19mm), with failures continuing for the smaller (5mm-6mm) and larger (31mm-45mm) packages. Data analysis continues, and new statistical approaches clarify points from the current knowledgebase.

In terms of the Failure Analysis effort, a very large number of samples have been cross-sectioned and being investigated to determine the overall characteristic failure modes. An extensive and lengthy investigation requiring many resources is in application to elucidate how the failure mechanics relate to the experimental variables. A move to a lower cost scanning electron microscope solution has been in the works for the last year and had allowed for faster and easier FA work. Additional microscopy work will continue to proceed on this basis, both on additional no aging samples and on more samples from subsequent aging groups. A large number of samples is available from the existing test vehicles, including a subset that has been stored at low temperature to control ongoing microstructural evolution.

In additional to the conclusion of the 720 days aging of thermal cycling test and further Failure Analysis, another key aspect of ongoing efforts needs to be the addition of FEA (Finite Element Analysis) modeling. Although such models are not necessarily accurate for predicting failures, they are generally effective for understanding the significance of different test parameters and understanding critical factors in the mechanics of failure. Our research group has partnered with

Dr. J.C. Suhling's group (Auburn University, Mechanical Engineering Dept.) in order to produce FEA models for the project. These models should help to shed light on some of the most interesting results, such as the substrate effects noted and, hopefully, why micro-alloying appears to be effective for some packages but not for others[9].

7.2. Future Work in Progress and Related Testing

"Solder Doping" (micro-alloying) strategy appears to be an encouraging approach for improving the reliability of printed circuit assemblies at a relatively low cost. New doped solder materials, currently in a series of follow-on experiments to high-stress environments. Some of this follow- on studies have concluded, some are currently in progress[9].

The "Downselect" Test: This test was a "crash and burn" test involving 14 different solders designed for high-temperature thermal cycling reliability. Ten (10) different solder manufacturers supplied fourteen (14) different solder materials for testing. Some materials were available in both solder paste and solder spheres (which were used to ball BGA packages), while others were available in only paste or spheres. Two smaller test vehicles used: 1) Mechanical Test Vehicle Design, and 2) Thermal Test Vehicle Design. There were two test groups: 0 days and 180 days aging at 125°C. Three (3) accelerated testing method employed: 1) liquid-to-liquid thermal shock, 2) Vibration, and 3) Drop Testing. The goal of the test was to determine the top five (5) materials for further testing on the Phase II test vehicle under thermal cycle testing. The test was successful in selecting five materials that exhibit liquid-to-liquid thermal shock reliability far in excess of that of SAC305. The dopants from the solder materials include Antimony (Sb), Zinc (Zn) and Bismuth (Bi).The "TV9" Test: A thermal cycling test involving several of the higher performing materials from the down select test. The thermal test vehicle design from down select test was selected as this

board is closer to commercial applications in its thickness and material (FR-406). This test is ongoing at close to 2400 thermal cycles.The Phase II Test: Using the same test vehicle from this project and using only Megtron-6 board substrate material, the new test will evaluate the thermal cycling reliability of the five (5) “high-temperature reliability” solder materials identified in the Downselect test. Only paste doping will be tested. There are four test groups: 0 days, 180 days, 360 datys and 720 days of aging at 75°C.The assembly for this experiment has concluded, and the 0 days,180 days and 360 days aging test group has completed approximately 3000 cycles. The 720 days aging group will soon begin testing in Jan 2018.

The “Failure Analysis” is currently in progress for the Phase I, Down select, TV9 and Phase II projects. In total about 5000 samples have been prepared for failure analysis. There were about 200 samples were carbon coated and SEM analyzed, for micro alloying and micro cracking. The other samples were prepared only to study the failure modes in a low cost optical microscopy. This project has about 200 samples remaining for analysis, to study intermetallic and failure modes in optical microscopy. Dr. Anto Raj is currently following up on this project work with Mr. Aditya Bachuwar and Ms. Gayatri Tandel.

“Statistical Proportional Hazards Model” is currently in progress for the entire test data collected. Dr. Carpenter has guided extensively in modeling the data using SAS and helped better analyze the hazards ratio for various censoring groups.

“Simulation Modeling” is currently in progress for the Phase I project with Dr.Suhling’s research group from Mechanical engineering department.

“Journal Papers”, 2 each from the down select and Phase I project have been submitted pending acceptance from IEEE transactions for publications.

Appendix A Additional Inspection and Voiding Images

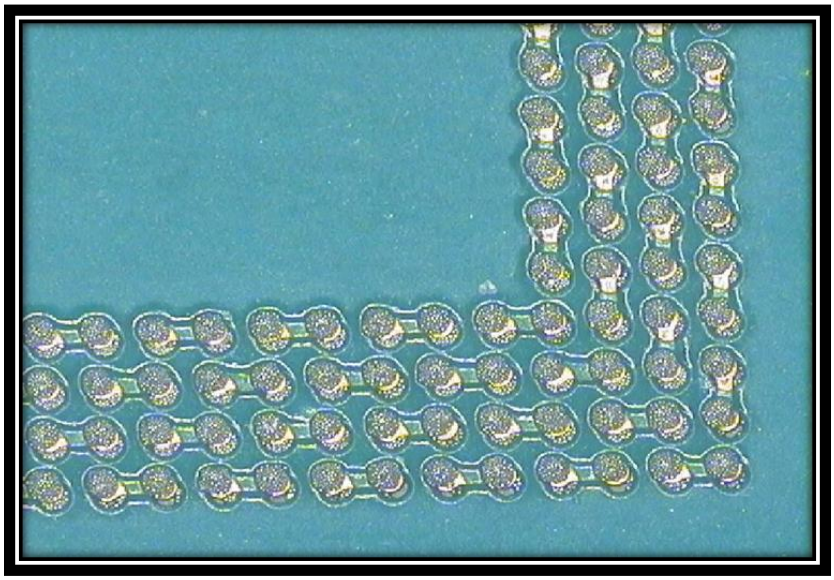

Figure 74 Misaligned Solder Paste Print prior to X-Y Realignment

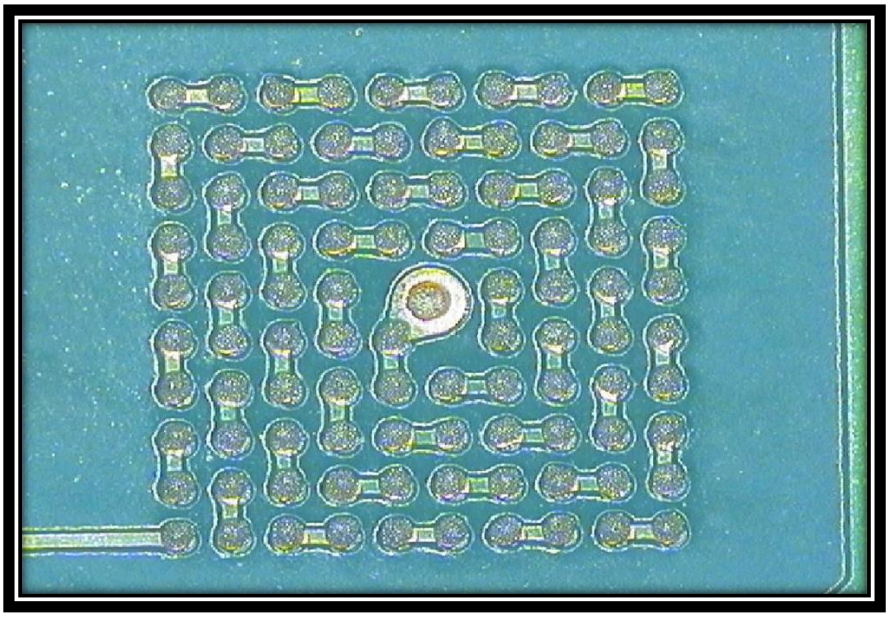

Figure 75 Misaligned Solder Paste Print prior to X-Y Realignment

Figure 74 and Figure 75 show misaligned paste prints prior to x-y realignment. Boards were reprinted, and machine variables adjusted, until proper alignment was produced.

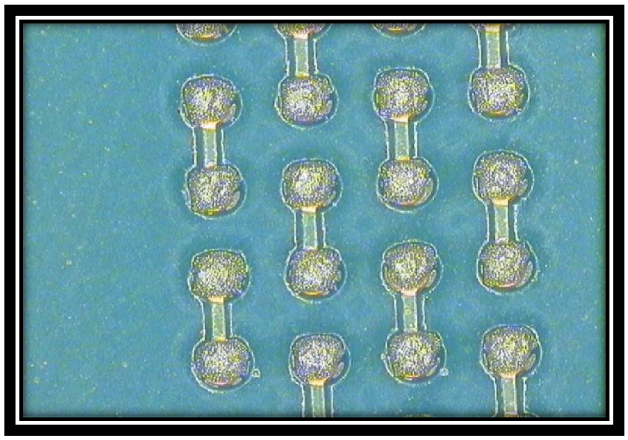

Figure 76 Corrected Alignment Solder Paste Print after X-Y Realignment

Figure 76 shows a properly aligned paste prints following x-y realignment. Setup boards were reprinted, and machine variables adjusted, until proper alignment was produced.

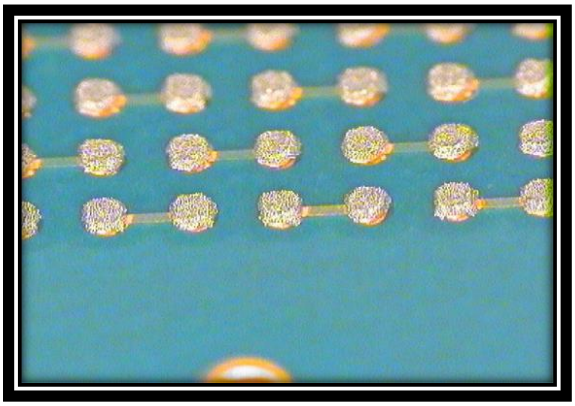

Figure 77 Solder Paste Height, Volume and Slump in Side View

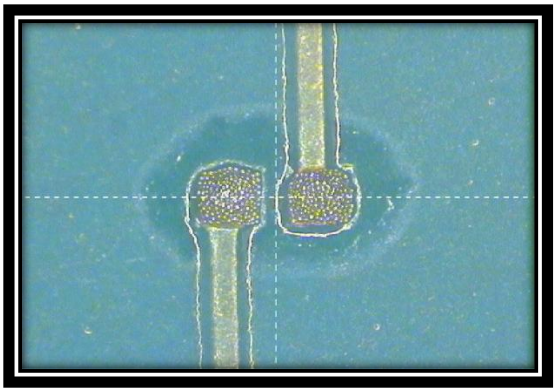

Figure 78 Solder Paste Coverage and Slump

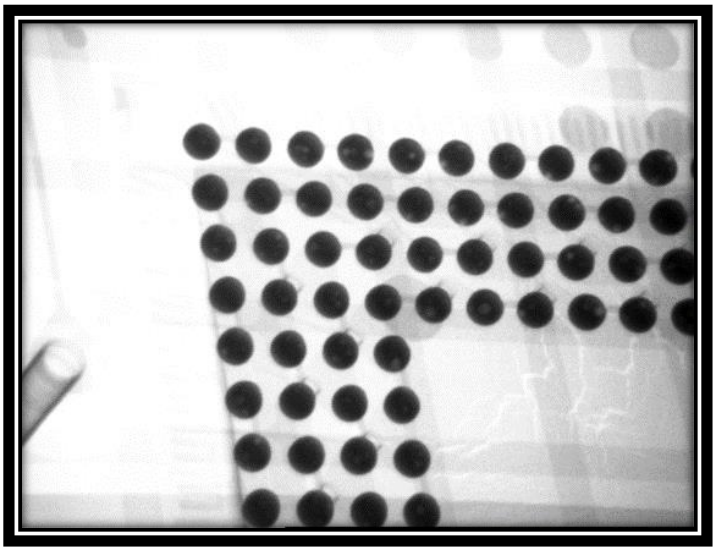

Figure 79 X-Ray Voiding Image

Figure 79 shows the transmission x-ray micrograph of a CVBGA 432 component on Megtron-6 substrate with Tin-lead solder material. Voiding is within the acceptable limits for eutectic Sn-Pb solder.

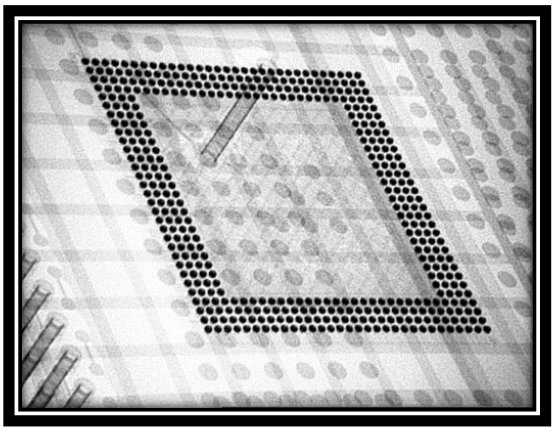

Figure 80 X-Ray Voiding Image

Figure 80 shows the transmission x-ray micrograph of a CVBGA 432 component on FR-406 substrate with Tin-lead solder material. Voiding is within the acceptable limits for eutectic Sn-Pb solder.

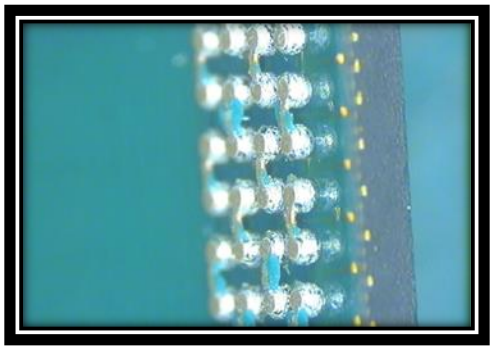

Figure 81 Pry Test Result

Figure 81 shows a CABGA 208 component (side view) following a pry test. The solder joints are intact and copper traces found ripped out of the substrate. This indicates excellent solder joint strength. Similar analysis of the voiding x-ray inspection, solder paste volume measurement, and pry test results analyzed for all of the test materials. Inspection for quality of the built test boards with components performed.

Appendix B Statistical Analysis

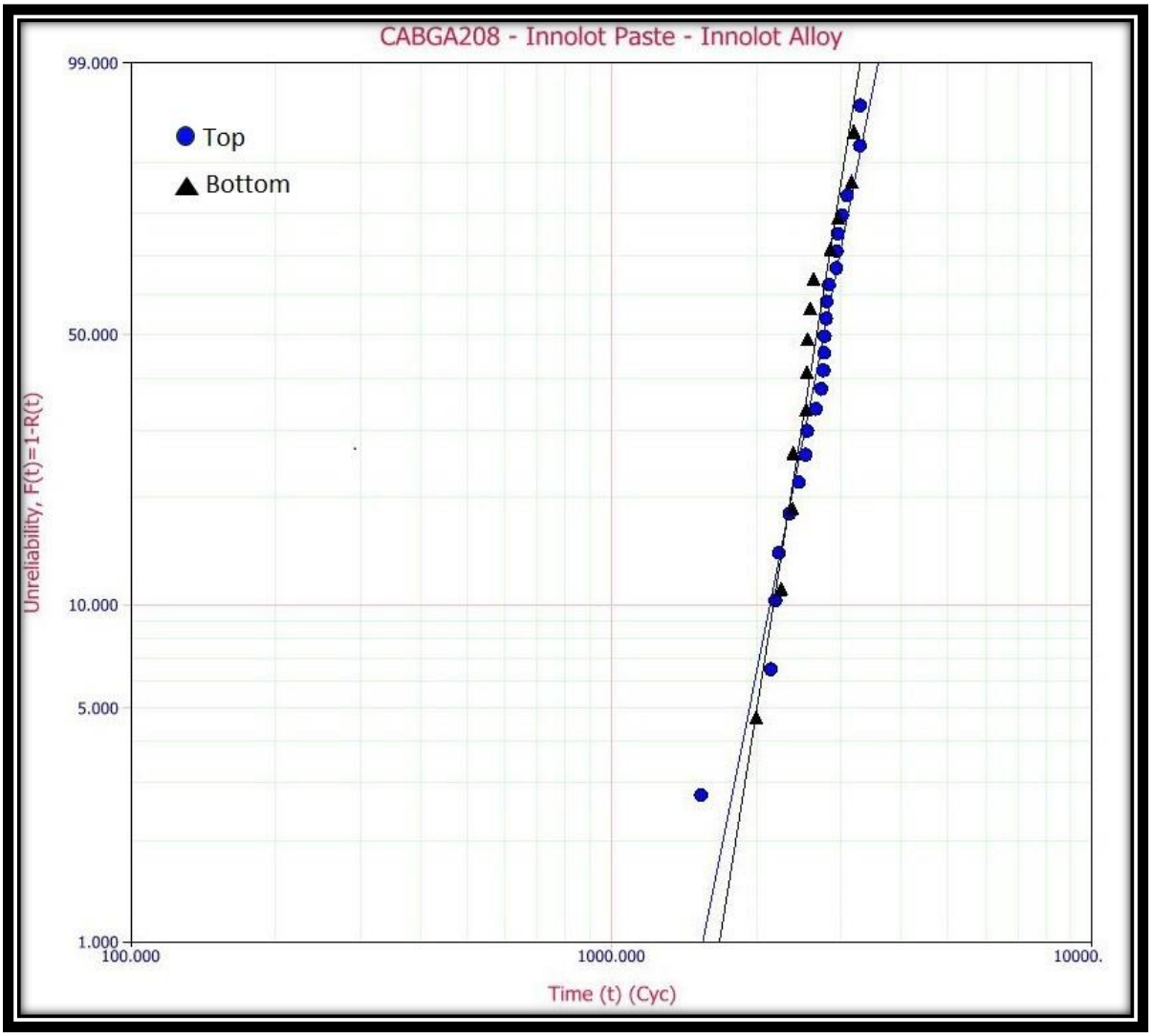

Figure 82 CABGA 208 component with FR-406 substrate with Innolot Material @ 0 Days of Aging using 2-Parameter Weibull Analysis

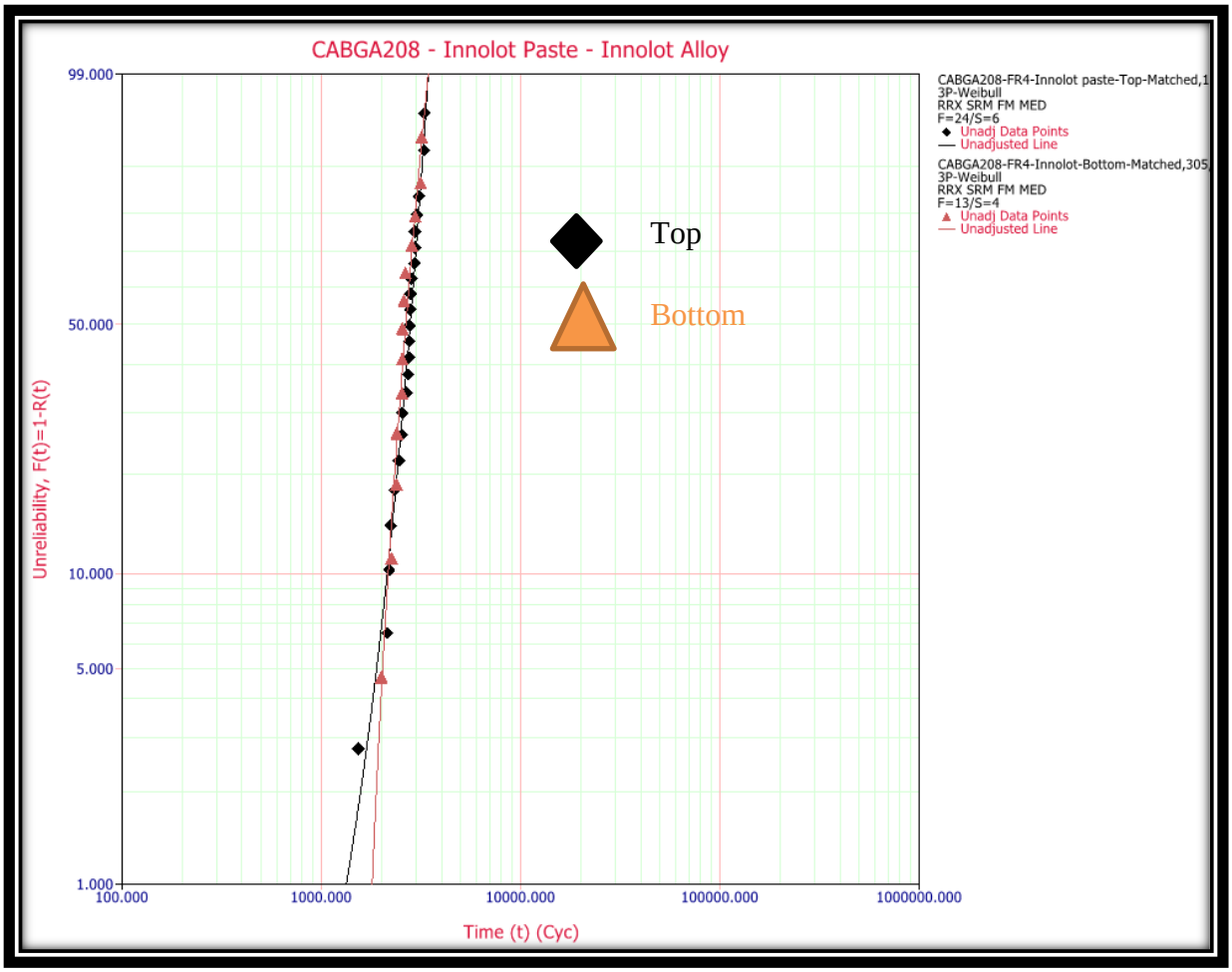

Figure 83 CABGA 208 component with FR-406 substrate with Innolot Material @ 0 Days of Aging using 3-Parameter Weibull Analysis

The above graphs Figure 82 and Figure 83 shows the CABGA 208 Innolot paste and alloy combination on FR-406 substrate with the Top and Bottom sideboards. The top side has outperformed the bottom side in the 0 Days test group. The top side data group have 24 failure data points and 6 success components in them and both the bottom side test groups have 13 failure data points and 4 success data points in them. The failure distribution is very much similar on the top and bottom side of the test boards.

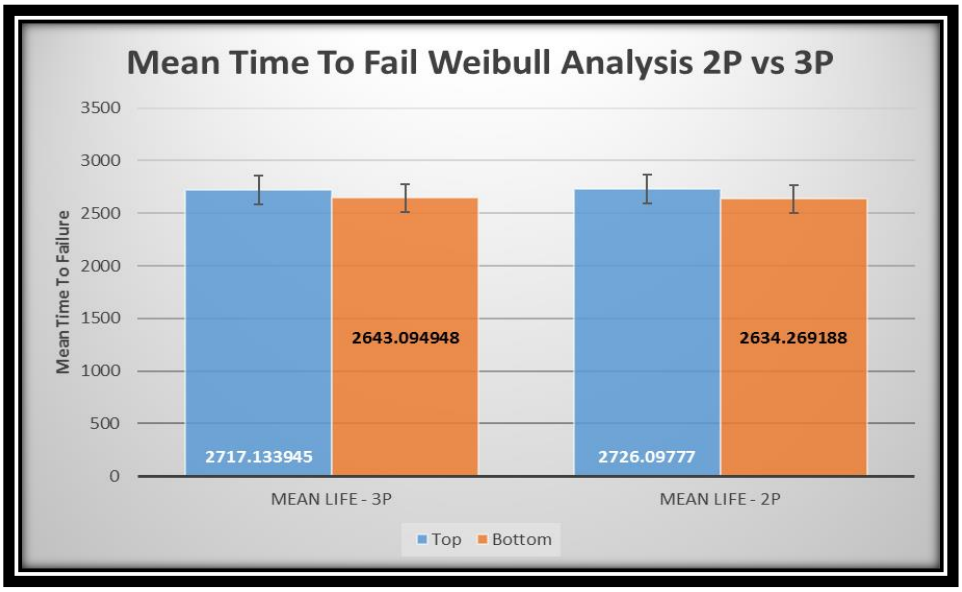

Figure 84 Mean –Time- To- Failure for CABGA 208 component with FR-406 substrate with Innolot Material @ 0 Days of Aging using 2- Parameter and 3-Parameter Weibull Analysis

Table x Weibull Analysis Results for the CABGA 208 component with FR-406 substrate with Innolot Material at 0 Days of Aging using 2- Parameters and 3- Parameters

	Top	Bottom	Top	Bottom
Distribution:	Weibull-3P	Weibull-3P	Weibull-2P	Weibull-2P
Analysis:	NLRR	NLRR	RRX	RRX
CB Method:	FM	FM	FM	FM
Ranking:	MED	MED	MED	MED
Beta	1024.166298	4.082881	7.300135	9.0975
Eta (Cyc)	353160.7984	1447.073749	2907.964198	2780.454299
Gamma (Cyc)	-350243.89	1329.93125	0	0
Mean Life (Cyc)	2717.133945	2643.094948	2627.09777	2634.269188
Rho (Fitness)	97.7874%	98.2584%	96.9312%	97.0892%

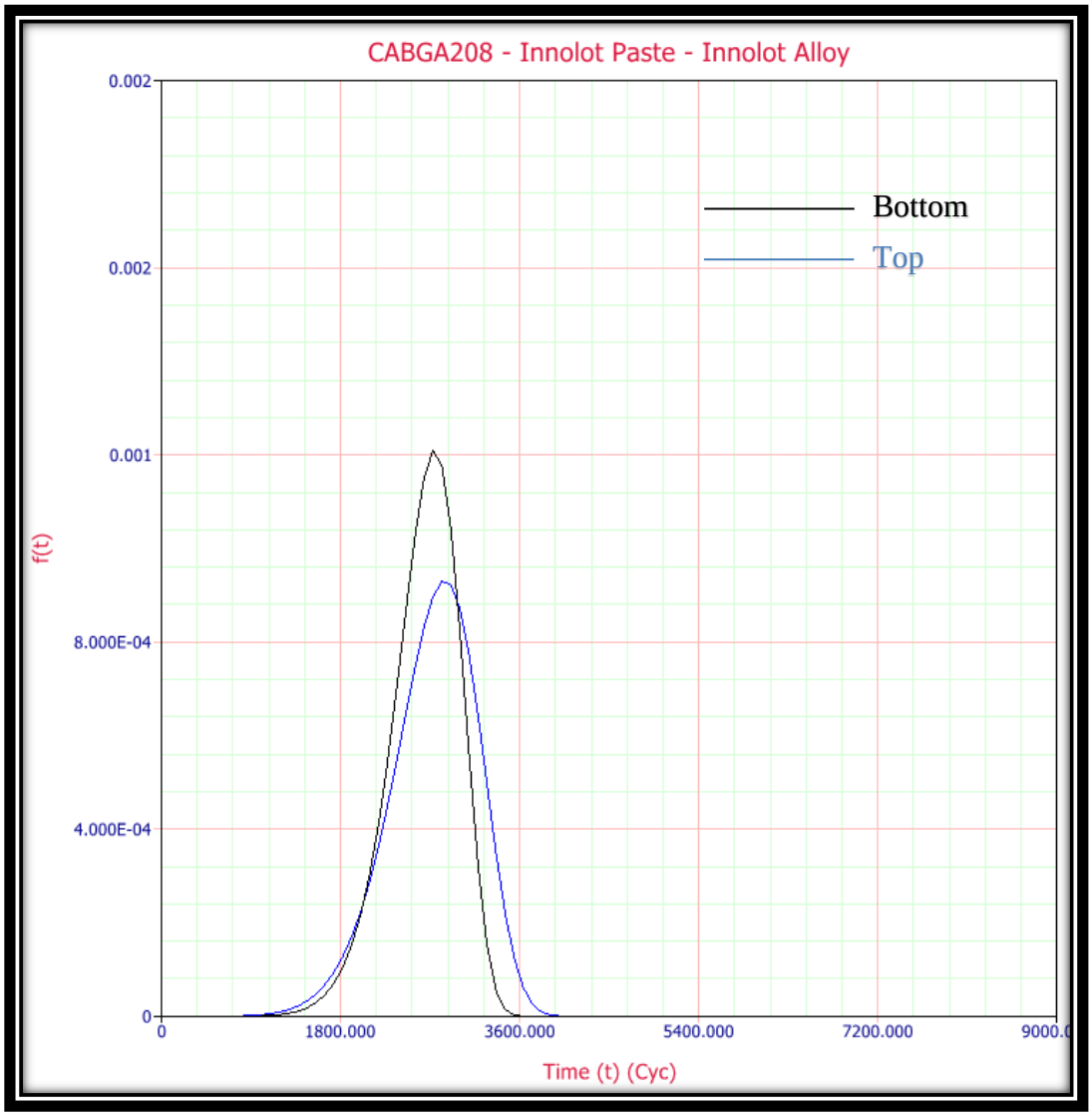

Figure 85 Pdf plot of CABGA 208 component with FR-406 substrate with Innolot Material at 0 Days of Aging using 2-Parameter Weibull Analysis

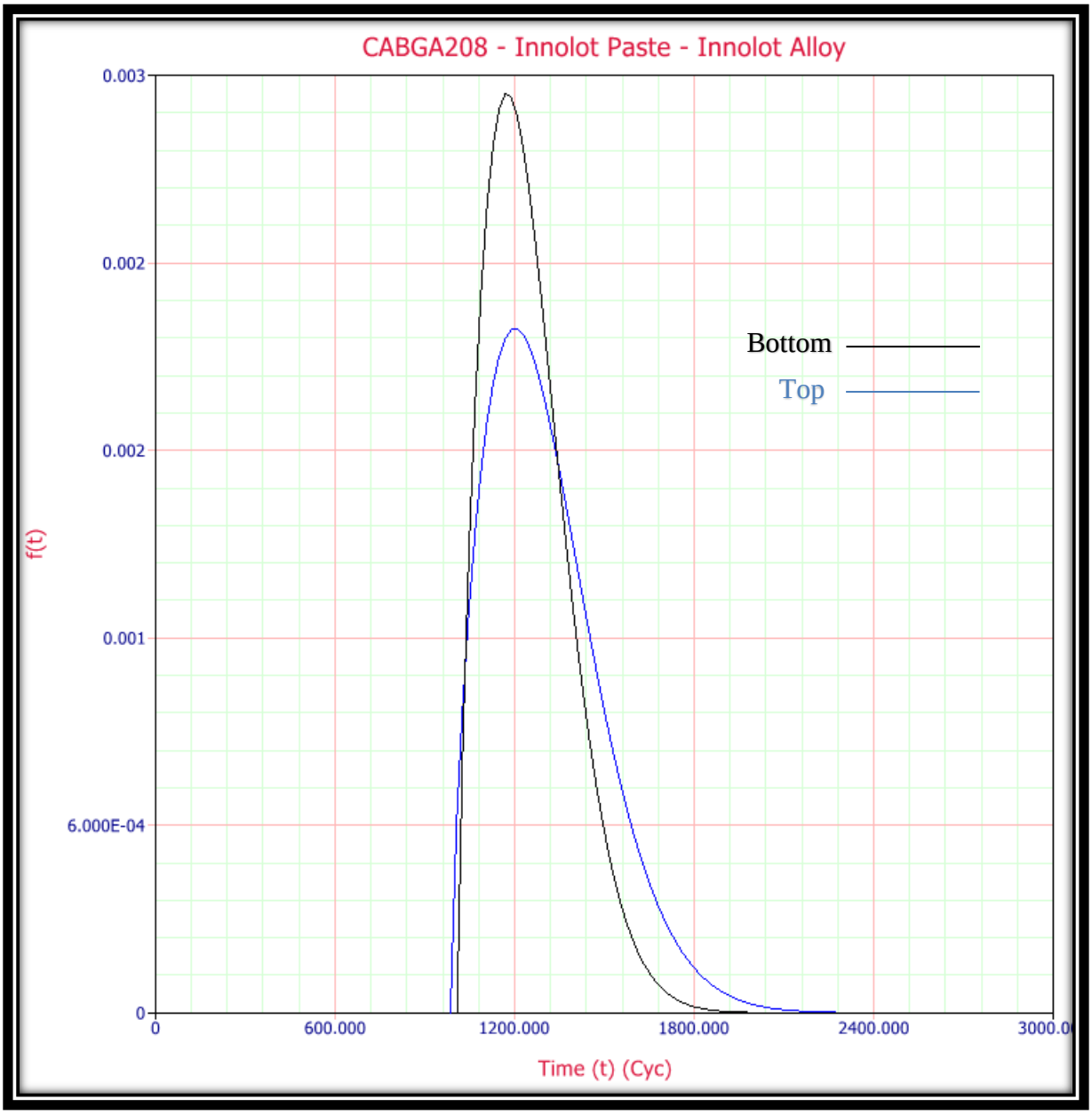

Figure 86 Pdf plot of CABGA 208 component with FR-406 substrate with Innolot Material at 0 Days of Aging using 3-Parameter Weibull Analysis

In this dissertation, all of the Mean Life reported are as per the 3- Parameter approach. The reason for the 3-Parameter approach is that it accounts for the Location Parameter.

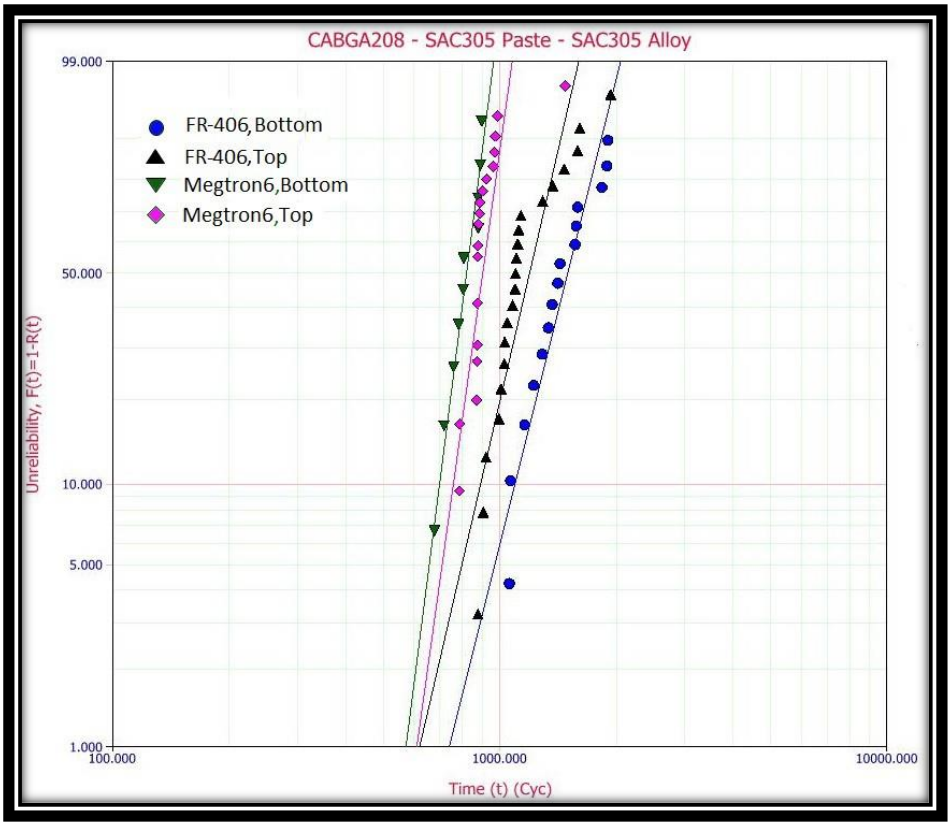

Figure 87 CABGA 208-0 Days-SAC305 Solder

The CABGA 208 component is available in both the Top and Bottom side of the boards. The above graph shows the data for the SAC305 alloy used in SAC305 paste. The components are built on FR-406 substrate. The graph displays the comparison of the Top vs Bottom side components test data for the No Aged group, with the bottom side having higher reliability than that of the top side. The FR-406 top side data group have 21 failure data points and no success components in them and its bottom side test groups have 15 failure data points and 1 success data points in them. The Megtron-6 top side data group have 28 failure data points and no success components in them and its bottom side test groups have 10 failure data points and no success data points in them. The failure distribution is very much similar on the top and bottom side of the test boards[68].

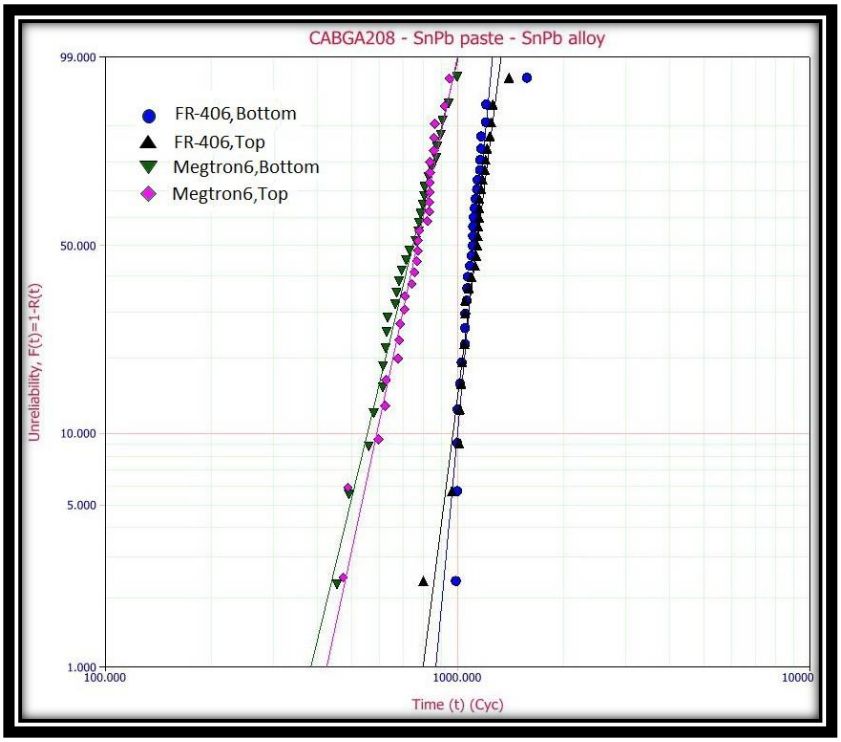

Figure 88 CABGA 208-0 Days-Tin-lead Solder

The CABGA 208 component is available in both the Top and Bottom side of the boards. The above graph shows the data for the Sn-Pb alloy used in SAC305 paste. The components are built on FR-406 substrate. The graph displays the comparison of the Top vs Bottom side components test data for the No Aged group, with the FR-406 having higher reliability than that of the Megtron-6. The FR-406 top side data group have 29 failure data points and no success components in them and its bottom side test groups have 29 failure data points and no success data points in them. The failure distribution is very much similar on the top and bottom side of the FR-406 test boards. The Megtron-6 top side data group have 28 failure data points and no success components in them and its bottom side test groups have 30 failure data points and no success data points in them. The failure distribution is very much similar on the top and bottom side of the Megtron-6 test boards.

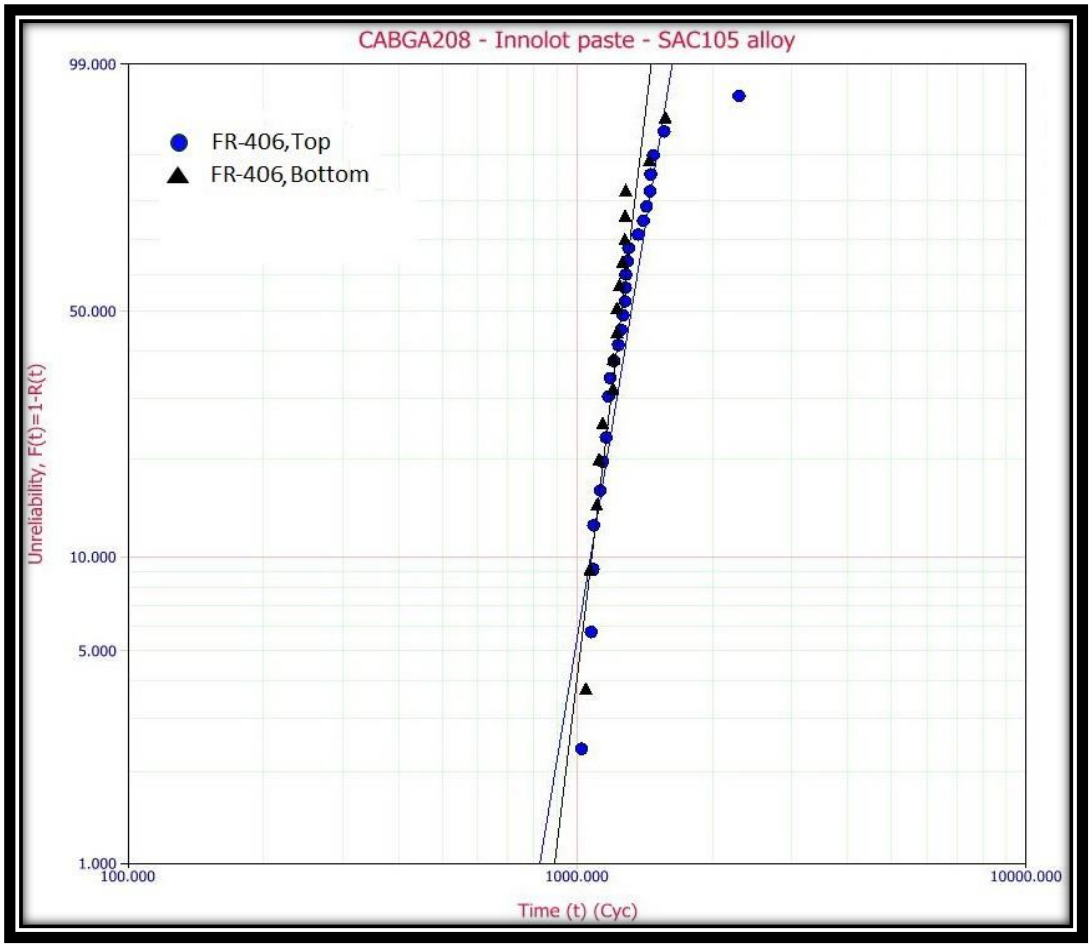

Figure 89 CABGA 208-0 Days -INNOLOT PASTE AND SAC105 ALLOY

The CABGA 208 component is available in both the Top and Bottom side of the boards. The above graph shows the data for the SAC105 alloy used in Innolot paste. The components are built on FR-406 substrate. The graph displays the comparison of the Top vs Bottom side components test data for the No Aged group, with the Top having higher reliability than that of the Bottom. The FR-406 top side data group have 27 failure data points and 3 success components in them and its bottom side test groups have 16 failure data points and 2 success data points in them. The failure distribution is almost similar on the top and bottom side of the FR-406 test boards.

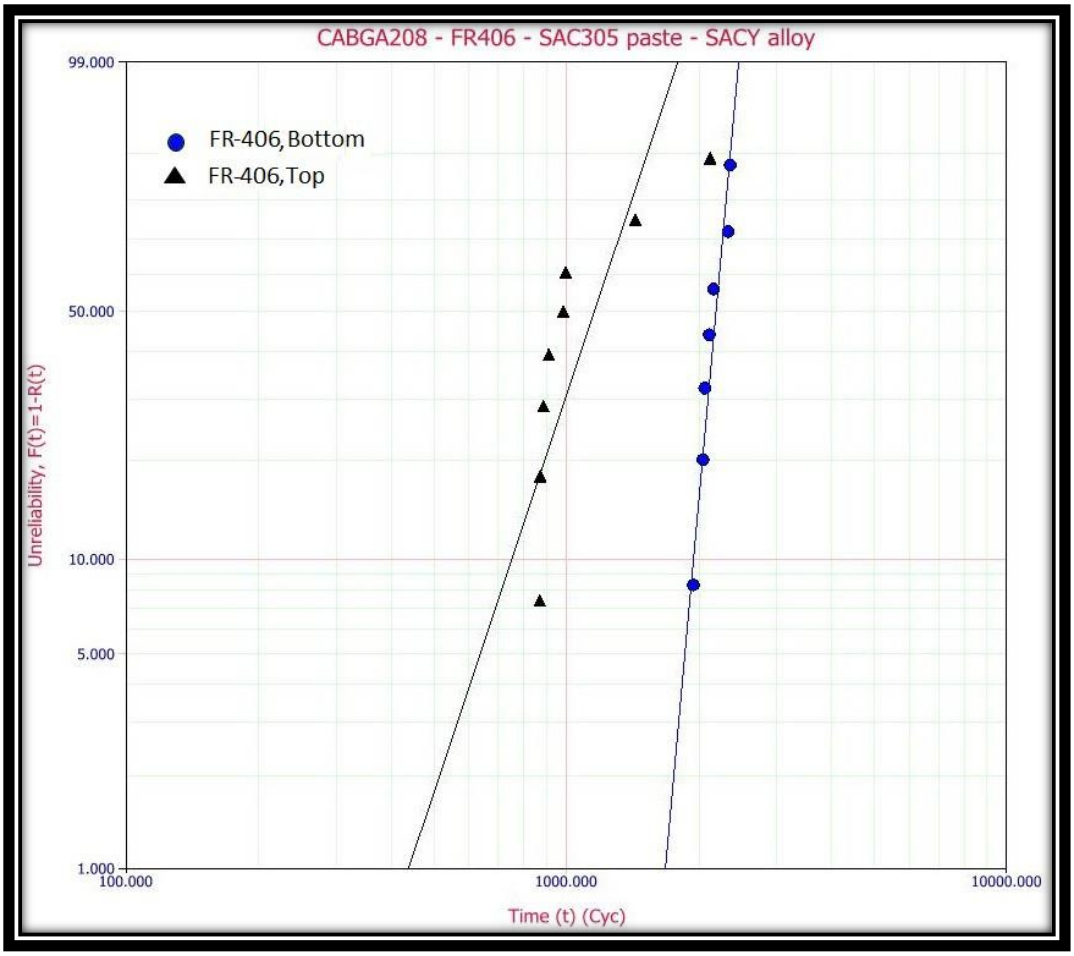

Figure 90 CABGA 208-0Days-SAC305 PASTE AND SAC-Bi ALLOY

The CABGA 208 component is available in both the Top and Bottom side of the boards. The above graph shows the data for the SACY alloy used in SAC305 paste. The components are built on FR-406 substrate. The graph displays the comparison of the Top vs Bottom side components test data for the No Aged group, with the Bottom having higher reliability than that of the Top. The FR-406 top side data group have 8 failure data points and 1 success components in them and its bottom side test groups have 7 failure data points and 1 success data points in them. The failure distribution is almost similar on the top and bottom side of the FR-406 test boards.

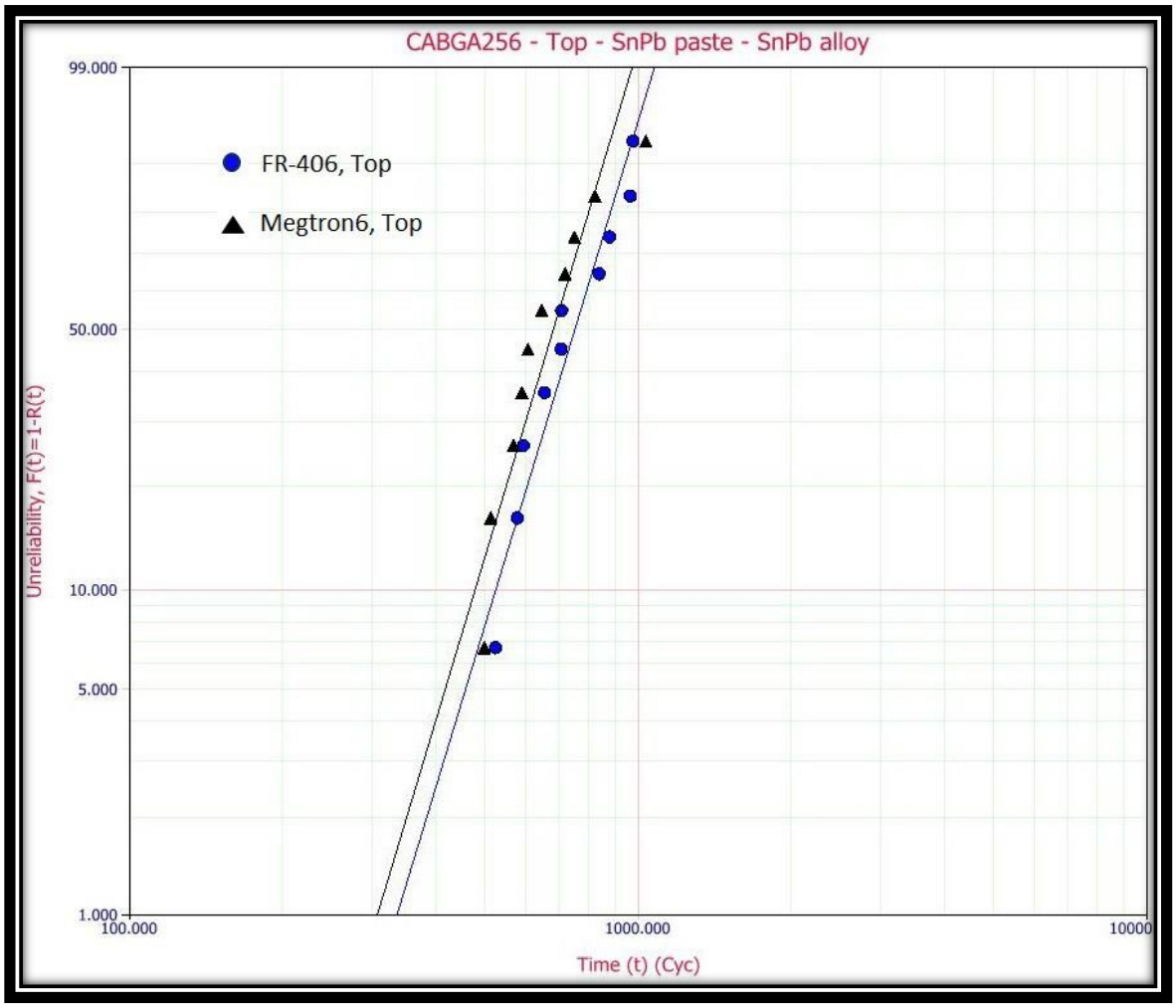

Figure 91 CABGA 256-0Days-SN-PB PASTE AND ALLOY –FR-406 VS MEGTRON-6

The CABGA 256 component is found on both the top and bottom but significant failures are found only from the top side of the boards. For the Sn-Pb paste and alloy combination of the CABGA 256 FR-406 and Megtron-6 substrates behave fairly similar with FR-406 slightly better than that of the Megtron-6 boards. Both the series have 10 failure data points.

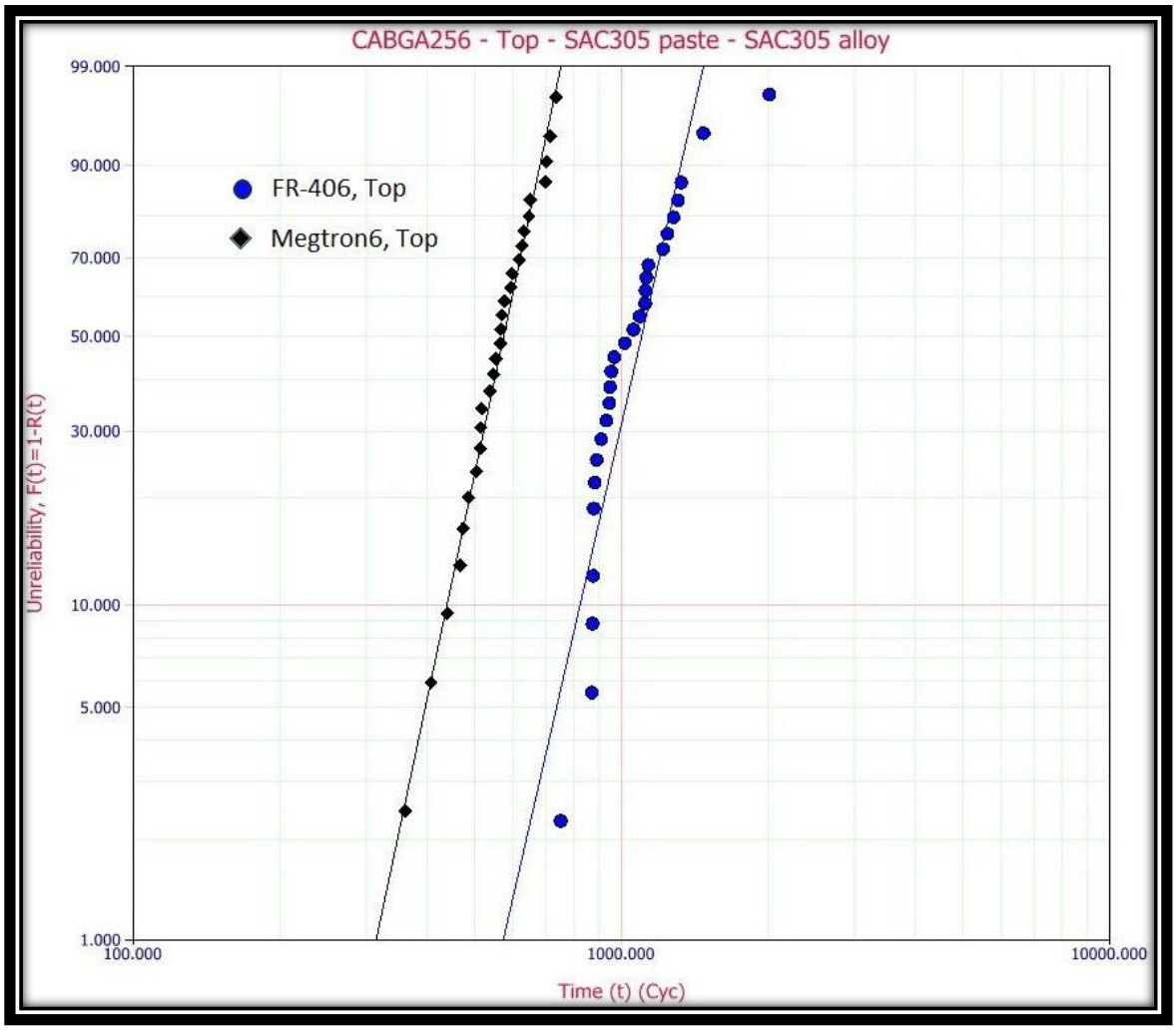

Figure 92 CABGA 256-0Days-SAC305 PASTE AND ALLOY –FR-406 VS MEGTRON-6

The CABGA 256 component is found on top side of the boards. For the SAC305 paste and alloy combination of the CABGA 256, FR-406 and Megtron-6 substrates behave fairly similar with FR-406 having better reliability than that of the Megtron-6 boards. Both the series have 30 data points. The FR-406 has 29 failure data points and 1 success data point. The Megtron-6 has 28 failure data points and no censored data point.

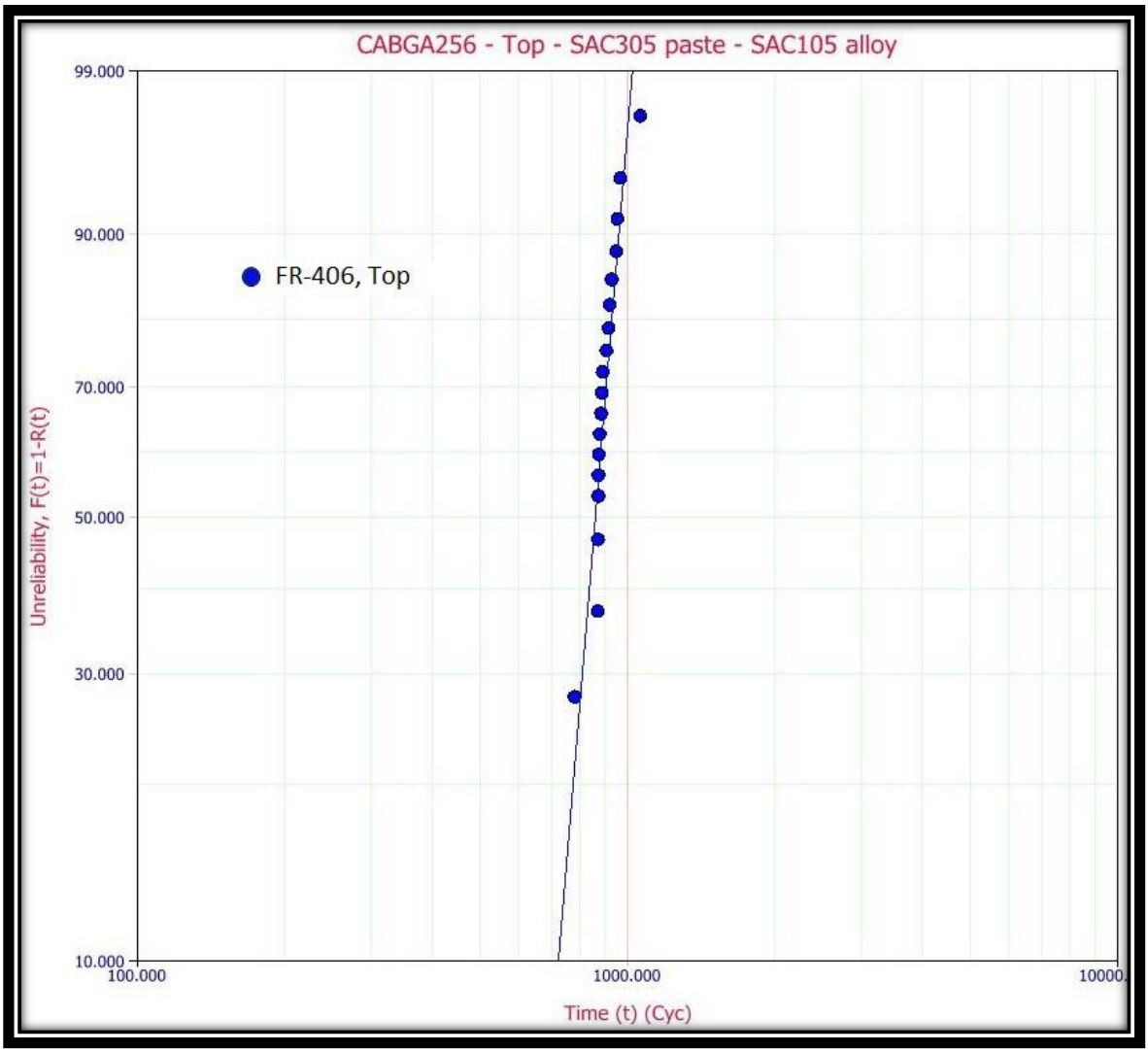

Figure 93 CABGA 256-0Days-SAC305 PASTE AND SAC105 ALLOY –FR-406

The CABGA 256 component is available in the Top side of the boards. The above graph shows the data for the SAC105 alloy used in SAC305 paste. The components are built on FR-406 substrate. The graph displays test data for the No Aged group. The FR-406 substrate has 31 failure data points and no success data point.

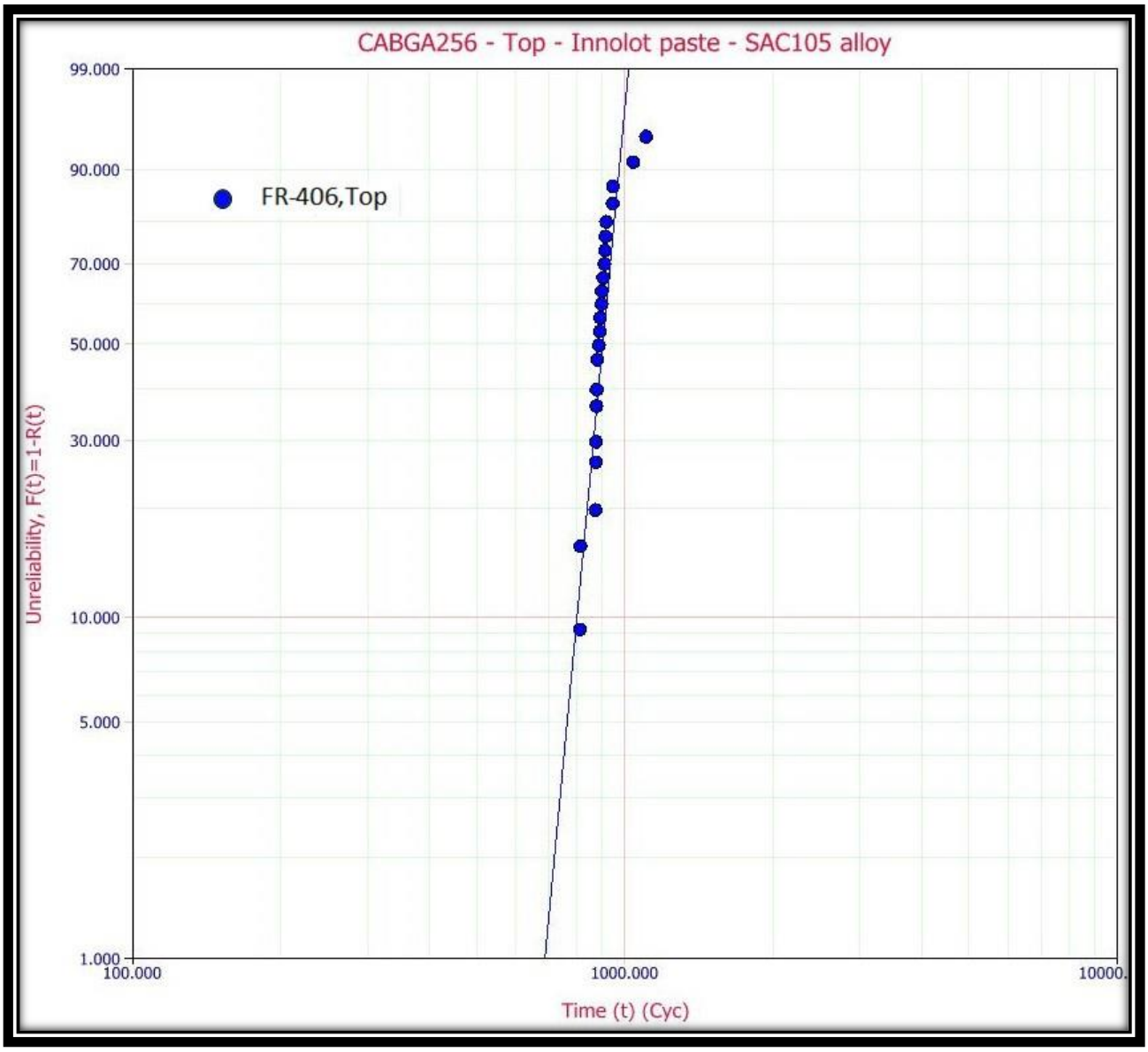

Figure 94 CABGA 256-0 Days-INNOLOT PASTE AND SAC105 ALLOY –FR-406

The CABGA 256 component is available in the Top side of the boards. The above graph shows the data for the SAC105 alloy used in Innolot paste. The components are built on FR-406 substrate. The graph displays test data for the No Aged group. The FR-406 substrate has 28 failure data points and 2 success data points[69].

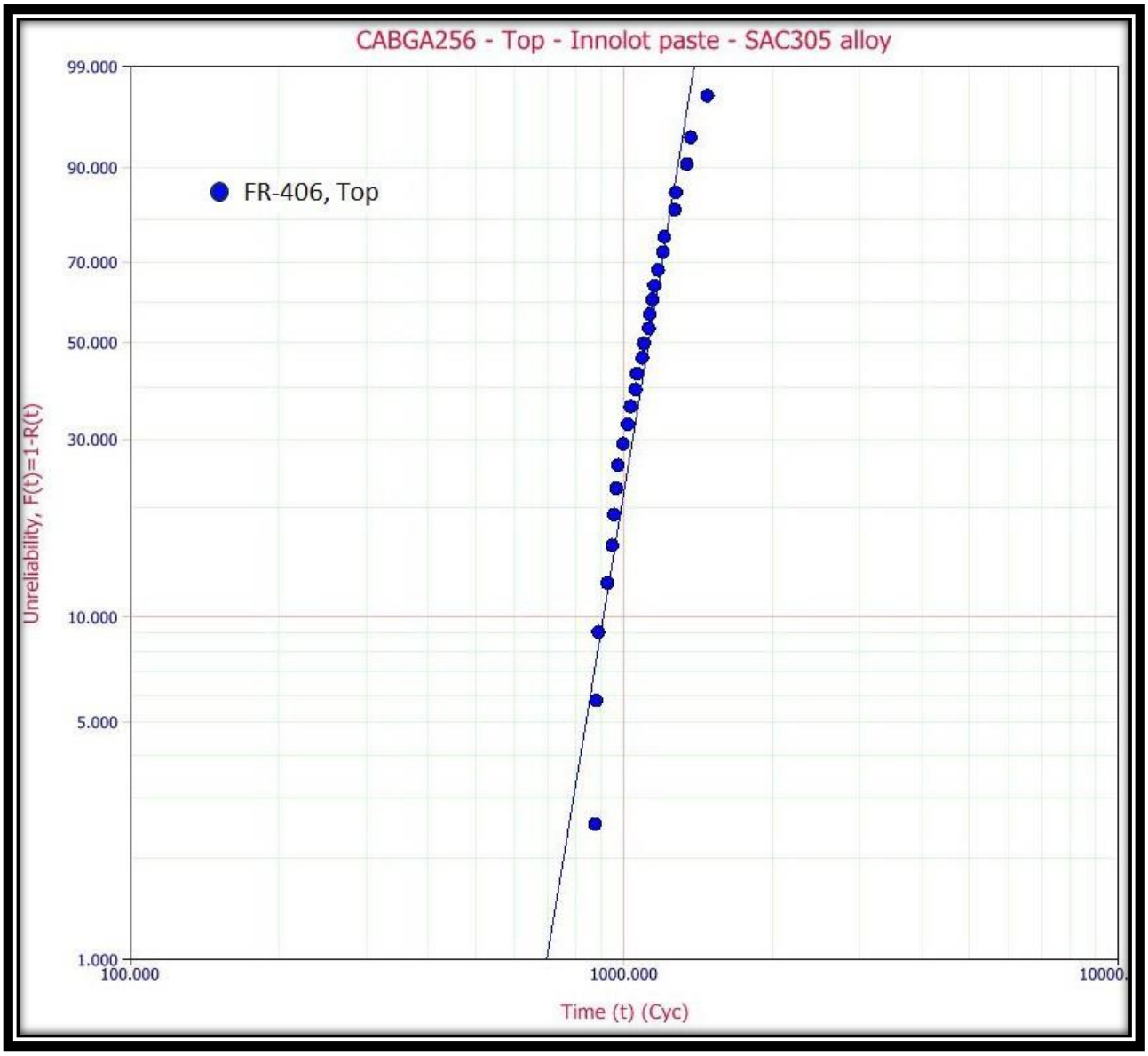

Figure 95 CABGA 256-0Days-INNOLOT PASTE AND SAC305 ALLOY –FR-406

The CABGA 256 component is available in the Top side of the boards. The above graph shows the data for the SAC305 alloy used in Innolot paste. The components are built on FR-406 substrate. The graph displays test data for the No Aged group. The FR-406 substrate has 27 failure data points and 3 success data points[70].

Appendix C Journal Papers

Short Term Isothermally Aged Doped Lead Free Solder Reliability subjected to Mechanical Testing with Semiparametric Estimation

ABSTRACT

This paper discusses a statistical methodology for evaluating doped lead-free solder alloy performance for high reliability products using survival reliability analysis and provides a detailed application of the technique for mechanical testing. The vibration and drop test experimental failure results are from 15 mm CABGA 208 components. In this experiment, SAC105 and SAC 305 solder balls with Bi, Ni and Sb doped solder pastes are studied. This test result gives an indication of material combinations that are a potential solution to the traditional material degradation problem of SAC 305 solder alloys. The materials that have the highest and lowest characteristic life compared to the SAC 305 solders are SAC 405 and SAC105 respectively. The results discuss the effects of different paste dopant materials and dopant volumes, and their impact on reliability of surface mount components. The test components consists of two different solder volumes one on 0.1524 mm (6mil) stencil thickness and another on a 0.1016 mm (4mil) stencil thickness to study the differences in doping volume effects of the new alloys. The test vehicles have a thickness of 1.016 mm, made up of FR4 substrate with a glass transition temperature of 170°C. This experiment investigates the performance of solder joints in mechanical testing before and after 6 months of aging at 125°C. In drop test, each test vehicle is dropped 300 times (1500G, 0.5 ms) or until failure. In vibration test, each test vehicle underwent 20 hours of $4.6G_{rms}$ vibration in a constant stress profile. The tests were, performed independently to each other. The performance of the solder materials were determined from the ability of the components and solder

interconnects to withstand the mechanical stresses induced by vibration and drop extremes. It is understood that solder materials have significant impact on the Time to Failure. The experimental variables include solder paste materials, solder sphere materials, and solder volume. The response variable used in this test is Time to Failure (in hours for vibration test and drop counts for drop test). The effect of experimental variables on Time to Failure are at 5% level of significance using Cox Proportional Hazard Model.

KEYWORDS: BGA, PCB, Lead-free, Reliability, Isothermal Aging, Flip Chip, Doping, Weibull Analysis.

NOMENCLATURE

AIC	Akaike Information Criterion
ASTM	American Society for Testing & Materials
BGA	Ball Grid Array
CABGA	Chip Array Ball Grid Array
FR	Flame Retardant
IPC	Association Connecting Electronics Industries
JEDEC	Joint Electron Device Engineering Council
KM	Kaplan-Meier
OSP	Organic Solderability Preservative
PCB	Printed Circuit Board
PH	Proportional Hazard
QFN	Quad Flat No-Lead package
RoHS	Restriction of Hazardous Substances

SAE	Society of Automotive Engineers
SAS	Statistical Analysis Software
SBC	Schwarz Bayesian Criterion
SEM	Scanning Electron Microscopy
TV	Test Vehicle

Symbols

Ag	Silver
Bi	Bismuth
Cu	Copper

Innolot

Ni	Nickel
Pb	Lead
Sb	Antimony
Sn	Tin
SAC105	98.5%Sn – 1.0%Ag – 0.5%Cu
SAC305	96.5%Sn – 3.0%Ag – 0.5%Cu
SAC405	95.5%Sn – 4.0%Ag – 0.5%Cu

Greek Symbols

β	Slope
η	Characteristic Life
ρ	Probability plot
λ	Hazard rate

INTRODUCTION

Aerospace and automotive companies are being restricted to provide RoHS compliant solders. Their products require new innovative solders that withstand the higher vibration, drop/shock performance, and combined-environment reliability compared to the conventional SAC305 alloys. The NASA-DoD Lead-Free Electronics Project confirmed that pad cratering is one of the dominant failure modes that occur in various board level reliability tests, especially under dynamic loading[1]. The mechanical properties (and related failure behavior) of lead free solder joints change based on elevated temperatures and aging durations. Previous results by the Center for Advanced Vehicle and Extreme Environment Electronics ($CAVE^3$) at Auburn University have shown a rapid deterioration in the material behavior of SAC105, SAC305 and Innolot solder joints[2].

Ternary eutectic SAC 305 solders known for their low cost, low melting point, good wetting and mechanical properties have always been the industrial standard for the electronic packages, but their thermo-mechanical performance deteriorates when subjected to harsh environments. At lower reflow process temperatures, the long-term deterioration of thermo-mechanical properties of material are observed to be less significant. So a potential solution to this delinquent is using one of the several of ternary and quaternary alloy compositions that melt about 10°C lower than that of the SAC305 alloys.[1]. From an initial selection list of 25 solder paste materials studied for metallurgical performance, a final list of 8 lead free solder paste materials were chosen for experimental setup to predict their behavior on mechanical harsh environmental test. The results demonstrated a significant degradation of the performance of the solder joints after aging for 6 months at 125°C. The degradation of solder materials is studied through the reliability survival

analysis methodology and by means of 2-parameter Weibull analysis (0 months data), 3-parameter Weibull analysis (6 months data). The experimental results showed a possible solution for replacement solder material to the SAC 305 alloys for automotive and aerospace industries.

Test Vehicle

The test vehicle (TV) printed circuit board is a standard 4-layer FR4 material composed of copper via's, glass epoxy covered by a thin solder mask on both sides and an overlaid silkscreen for labeling. The test boards had 16 BGA's, 20 Resistors and 6 QFN's respectively. The plating material used for the test vehicles is Organic Solder-ability Preservative (OSP). CABGA 208 from Amkor were the primary components chosen for the study. The test vehicle are designed, with the capability to house multiple packages of CABGA 208 to provide an opportunity to investigate the effect of material alloy, reflow profile and solder paste of components combined with solder paste volume.

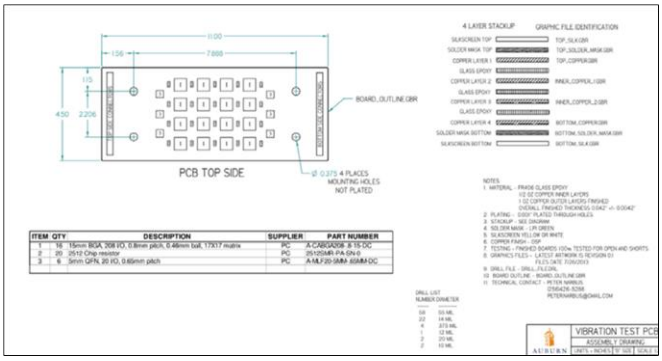

Fig. 96 Test Vehicle Design

The BGA alloys used in this test consists of SAC105, SAC305 alloys with doped paste material. Since the SAC 305 alloy is the most widely used industrial standard, the test designed as 75% SAC 305 alloys and 25% of SAC 105. The SAC 305 paste material is set as the baseline for comparison.

The test board is grouped into 4 different zones as the stress levels from the experiments are different across the different locations of the test boards. The zone and special alloy locations are highlighted in the following diagram.[3]

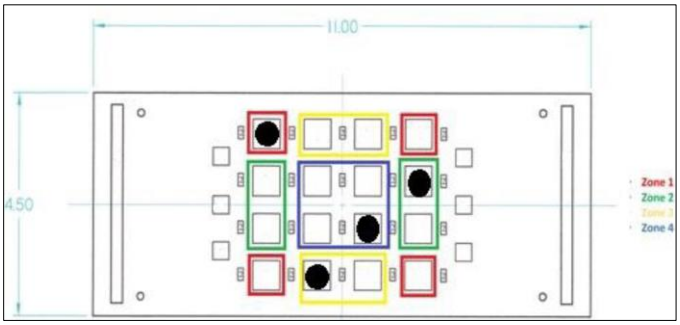

Fig. 97 Test Vehicle Zonal Mapping[2]

For evaluating the performance of various doped solders alloys used with the BGA components, we chose the 15 mm CABGA 208 package. It consisted of 208 interconnections with a 0.8mm lead pitch. The solder balls were 0.46mm diameter in 17X17 matrix with standard daisy chain wiring scheme. Figure 3 gives a detailed description of the same.

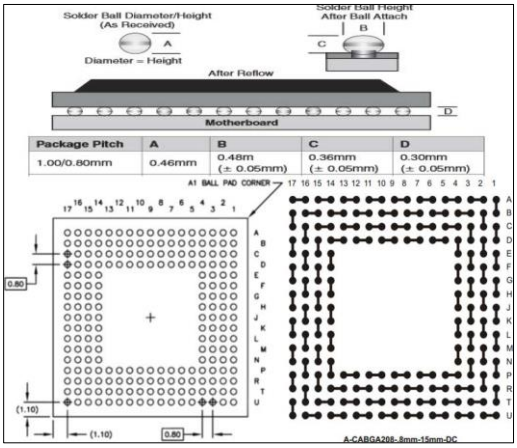

Fig. 98 CABGA 208 Component Design[3]

The other components in the board design are the 2512 resistors as it is the most common and the largest size used in the electronics industry, and an Amkor Micro-Lead-Frame QFN, it contained 20 leads at 0.65 mm pitch with total size $5mm^2$.[3]

After the placement of components, the test boards are reflowed in the Vitronics SMR-800 reflow oven. The paste manufacturers recommended reflow profile settings were followed to set temperatures in different zones and conveyor speeds. The thermal profiling equipment used to monitor the board temperature here is KIC 2000. Two different stencil volumes were

After reflow process, all the samples were electrically tested.

All the components reflowed had 100% electrical yield. The built components were tested, for residual voids.

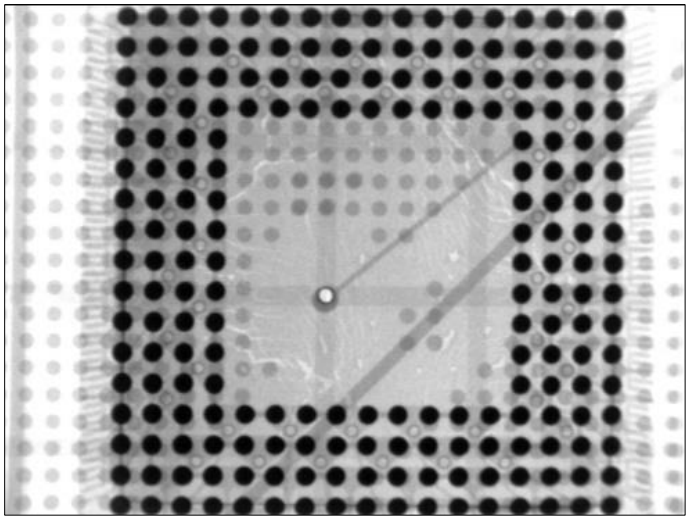

Figure 99 X ray Voiding

The test build matrix and solder composition for paste and alloys are listed in the Table 3.

Table 11. Test Build Matrix

Solder paste	Stencil	Solder Alloy	Reflow Profile
SAC305	6mil	SAC305	Best
	6mil	SAC105	Best
Sn-3.8Ag-0.7Cu-3Bi-1.5Sb-0.02Ni	4mil	SAC305	Best
	4mil	SAC105	Best
	6mil	SAC305	High
	6mil	SAC105	High
	6mil	SAC305	Low
	6mil	SAC105	Low
SAC Doped Sb	4mil	SAC305	Best
	4mil	SAC105	Best
	6mil	SAC305	High
	6mil	SAC105	High
	6mil	SAC305	Low
	6mil	SAC105	Low
Sn-3.8Ag-0.7Cu-1.4Sb-0.15Ni-3Bi	4mil	SAC305	Best
	4mil	SAC105	Best
	6mil	SAC305	High
	6mil	SAC105	High
	6mil	SAC305	Low
	6mil	SAC105	Low
SAC405-Dopants	6mil	SAC305	Best
	6mil	SAC105	Best
SACX	6mil	SAC305	Best
	6mil	SAC105	Best

EXPERIMENTAL SETUP

Vibration Test Setup

In order to vibrate the test vehicles, a fixture system had to be designed that would be capable of holding the boards perpendicular to the electro-dynamic shaker table along the X and Y-axes while vibrating in the Z-direction. Each test vehicle was affixed to one side of the aluminum fixture using a set of four screws, four washers, and four either large or small spacers. To determine the natural frequency of the fixtures and test vehicles, a laser source and an oscilloscope is used upon the boards to measure the natural frequencies of the test assembly. In this setup, the laser source records the frequencies induced with the highest distortions. Only the first natural frequency that induces more damage to the components is measured in this test. The setup test assemblies were mounted on an LDS LV217 electro-dynamic shaker table and subject to a 4.6 G_{rms} constant stress vibration profile. According to the results, one major natural frequency appears at between 350 to 400 HZ. The magnitudes are very consistent with close peak magnitudes.[4][2]

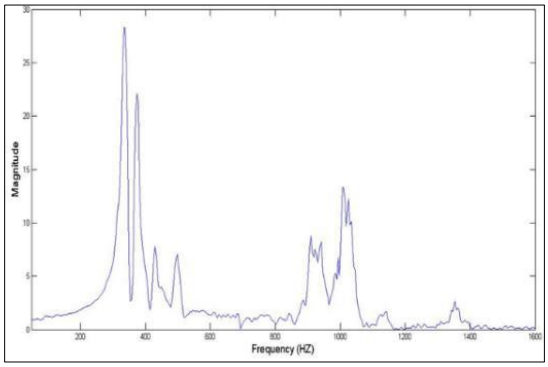

Fig. 100 Aluminum Fixture Bode Plot

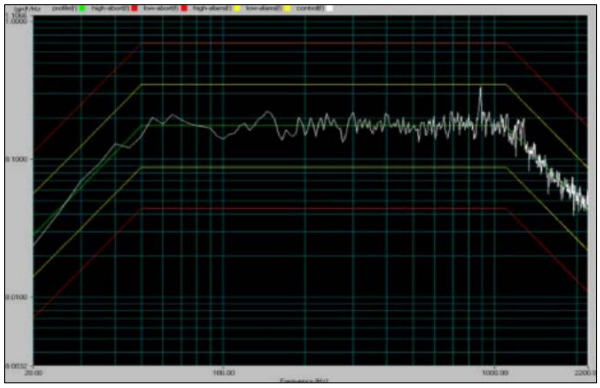
Fig. 101 Vibration Stress Profile 4.6 G_{rms}

The test component resistance was hand probed with a hand-held ohmmeter for electrical continuity once every 60 minutes.

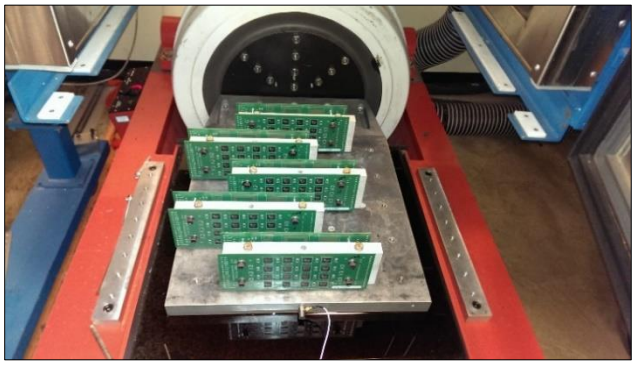
Fig. 102 Vibration Test Setup

Drop Test Setup

Lansmont M23 shock test drop tower was used to conduct the drop test experiment. SAE F5/ASTM 26Rl standard felt was used to absorb the generated shock in this experiment. JEDEC BS 111 test standard was followed, the maximum peak acceleration of 1500G and half-sine impact pulse duration of 0.5 milliseconds was maintained throughout the experiment. Test vehicles were dropped to a maximum of 300 times. The test component resistance were hand probed with a hand held ohmmeter for electrical continuity once every 20 drops.[5]

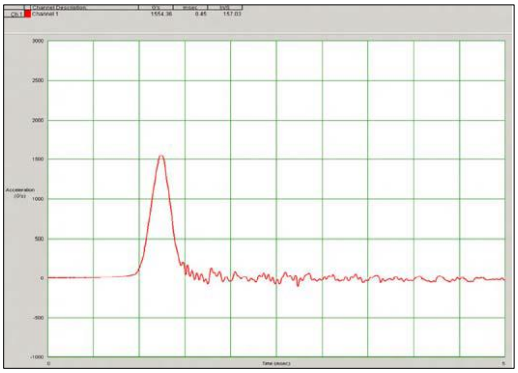

Fig. 103 Drop Test Profile 1500G, 0.5ms

Failures were recorded as per the IPC-SM785 standard, i.e., the solder joint failure can be defined as an interruption of electrical continuity greater than 1000 ohms.

STATISTICAL ANALYSIS OF TEST RESULTS

Vibration Test

First, it is important to understand the quantities necessary for survival/reliability analysis. Consider T to be the time until certain event. The survival function S(t), also known as the reliability function, is described as the probability of an entity surviving beyond time t. Survival function is given by

$$\mathbf{S(t) = P(T > t)} \qquad (1)$$

S(t) is a monotone non-increasing function. When T is a continuous random variable with probability density function f(t), the Cumulative Distribution Function is given by

$$\mathbf{F(t) = P(T \leq t)} \qquad (2)$$

The survival function can be found by

$$\mathbf{S(t) = \int_t^{\infty} f(u)du = 1 - F(t)} \qquad (3)$$

$$\mathbf{f(t) = -\frac{dS(t)}{dt}} \qquad (4)$$

For example, the probability density function of T following Weibull distribution is

$$\boldsymbol{f(t) = \frac{\beta}{\eta}\left(\frac{t}{\eta}\right)^{\beta-1} e^{-(t/\eta)^{\beta}}}$$

And the reliability function S(t) is,

$$\boldsymbol{S(t) = e^{-\left(\frac{t}{\eta}\right)^{\beta}},\ t > 0}$$

Where the slope, $\boldsymbol{\beta > 0}$ and characteristic lifetime, $\eta > \mathbf{0}$ are the parameters. Another quantity known as Hazard function is denoted as the conditional failure rate in reliability or instantaneous rate of failure,

$$\mathbf{h(t)} = \lim_{\mathbf{\Delta t \to 0}} \frac{\mathbf{P[t \le T < t+\Delta t | T \ge t]}}{\mathbf{\Delta t}} \qquad (5)$$

From the above equation, h(t)Δt is the approximate probability that an entity at time t experiencing an event in [t, t+Δt). The restriction on hazard function, h(t) is that it is nonnegative, h(t) ≥ 0 [23]. The hazard function relates to the survival function and pdf in the following way, $\boldsymbol{h(t) = \frac{f(t)}{S(t)}}$. In Weibull case,

$$\boldsymbol{h(t) = \frac{\beta}{\gamma}\left(\frac{t}{\gamma}\right)^{\beta-1}, t > 0.}$$

Cumulative Hazard Function is probability of event up to time t.

$$\mathbf{H(x) = \int_0^x h(u)\, du} \qquad (6)$$

In the Weibull case,

$$H(x) = x^{\beta}, x > 0, \beta > 0.$$

Consider the data of sample size n consists of triple $\{(T_j, \delta_j, Z_j(t)), j = 1 \text{ to } n\}$ where T_j is the time on study for the j^{th} subjects, δ_j is an event indicator for j^{th} individual ($\delta_j = 1$ if the event occurred and $\delta_j = 0$ if censored) and $Z_j(t)$ is the vector of p covariates, which may depend on time. Let h (t | Z) be the hazard rate for an entity with risk vector Z at time t. The proportional hazard rate model proposed by Cox [11] is given below.

$$h(t|Z) = h_o(t)\exp(\beta^T Z) = h_o(t)\exp(\textstyle\sum_k \beta_k Z_K) \qquad (7)$$

where $h_o(t)$ is an arbitrary baseline hazard rate, β is the vector of p parameters. This is known as Semiparametric model because the parametric form is assumed only for covariate effect. Cox model which is also known as proportional hazard model for two entities with covariate values Z and Z^*, because the ratio of their hazard rates is

$$\frac{h(t|Z)}{h(t|Z^*)} = \frac{h_o(t)\exp(\sum_{k=1}^{p}\beta_k Z_k)}{h_o(t)\exp(\sum_{k=1}^{p}\beta_k Z_k^*)} = \exp[\sum_{k=1}^{p}\beta_k(Z_k - Z_k^*)] \quad (8)$$

which is a constant. Hence hazard rates are proportional. Equation (8) is called Hazard ratio of an entity with risk factor Z experiencing the event as compared to an entity with risk factor Z^* [23].

This experiment, presented in this paper, consists of five categorical variables such as Paste combination, Stencil thickness, Profile and Aging Time. The censor indicator used in this experiment is delta. The Time to Failure measured in hours is considered as response variable.

Table 4. Data description

Variables	**Description**
Paste Combination	Solder paste with Solder alloy combination
Reflow Profile	Reflow Profile – Low, High and Best
Aging Time	Aging Time – 0months and 6months
Delta	Status at endpoint (1=Failed, 0=Censored)
Failure	Time to Failure (Hours)

The proportional hazard model has been used to fit the above data. The model is implemented using SAS®. Initially the global hypothesis is tested such that all coefficients are 0. The data set also consisted of tied observations. The Breslow method is used to calculate the log likelihood

with tied observations [23]. Let $t_1 < t_2 < \ldots < t_D$ be the distinct and ordered event times. Let d_i be the number of failures at t_i. D_i is set of all individuals which fails at t_i. Let s_i be the sum of vectors Z_j over all individuals which fails at t_i where $s_i = \sum_{j \in D_i} Z_j$. The set of all individuals at risk prior to t_i is R_i.

$$L(\beta) = \prod_{i=1}^{D} \frac{\exp(\beta^t s_i)}{\left[\sum_{j \epsilon R_i} \exp(\beta^t Z_j)\right]^{d_i}} \qquad (9)$$

The log likelihood is calculated by taking logarithm of above equation and multiplying by -2. The criterion -2logL is obtained using above method. Akaike Information Criterion (AIC) shown in Table 4 examines likelihood and number of parameters included in model.

$$\text{AIC} = -2\text{logL} + 2\text{k} \qquad (10)$$

Where k is number of covariates. Here the smaller the AIC, the better the data fits into model. Schwartz Bayesian Criterion (SBC) gives more penalization for additional covariates, where SBC is found using Equation (11).

$$\text{SBC} = -2\text{logL} + \text{klogn} \qquad (11)$$

Table 5. Model Fit Statistics

Model Fit Statistics		
Criterion	**Without covariates**	**With covariates**
-2 LOG L	19803.456	19256.336
AIC	19803.456	19350.336
SBC	19803.456	19597.382

The hypothesis is tested to check whether all the coefficients (β_i's) are 0. The likelihood ratio statistics is calculated by finding the difference between -2logL with covariates and without covariates as shown in Table 5. The Likelihood ratio statistics is shown to be 547.1201. The null

hypothesis is rejected indicating at least one of the coefficient is not 0.

Table 6. Test of Global Hypothesis

Testing Global Null Hypothesis: BETA=0			
Test	**Chi-Square**	**DF**	**Pr > ChiSq**
Likelihood Ratio	547.1201	47	<.0001
Score	557.1691	47	<.0001
Wald	471.7449	47	<.0001

The Table 5 shows the effect of covariates and its interaction which contribute to distribution of time to failure response. It is shown that there is significant difference in time to failure among each levels of Paste combination and Aging time at 5% level of significance. Also, variation is observed among each level of Reflow profile and Aging time. The effect of Aging is also significant. In this paper, it is important to understand the effect of aging for each solder material combination. In terms of interaction, there is difference in time to failure for interaction between Paste combination, Reflow profile and Aging with Wald Chi-Square as 26.9532 and p-value 0.0026.

Table 7. Overall Test of variables

Joint Tests			
Effect	**DF**	**Wald Chi-Square**	**Pr > ChiSq**
Paste combination	11	86.5909	<.0001
Reflow Profile	2	29.369	<.0001
Paste combination*Reflow Profile	10	19.1439	0.0385
Aging Time	1	6.2669	0.0123
Paste combination*Aging Time	11	114.6917	<.0001
Reflow Profile*Aging Time	2	32.7945	<.0001
Paste combination*Reflow Profile*Aging Time	10	26.9532	0.0026

The effect of interaction in terms of Reflow profile, paste combination and Aging are calculated using Semiparametric estimates based on Maximum Likelihood Estimate.

Table 8. Analysis of Maximum Likelihood Estimates for 15mm BGA package

Analysis of Maximum Likelihood Estimates								
Stencil	Profile	Paste	DF	Parameter Estimate	Standard Error	Chi-Square	Pr > ChiSq	Hazard Ratio
6mil	Best	SAC305 + SAC305	1	-0.69076	0.28019	6.0781	0.0137	0.501
		SAC305 + SAC105	1	-1.08727	0.28329	14.7302	0.0001	0.337
		SAC405-Dopants + SAC305	1	-0.00559	0.19832	0.0008	0.9775	0.994
		SAC405-Dopants + SAC105	1	1.22956	0.37597	10.6954	0.0011	3.42
		SACX + SAC305	1	0.02549	0.224	0.013	0.9094	1.026
		SACX + SAC105	1	1.25535	0.37097	11.4515	0.0007	3.509
6mil	High	Sn-3.8Ag-0.7Cu-1.4Sb-0.15Ni-3Bi + SAC305	1	1.34114	0.25793	27.0366	<.0001	3.823
		Sn-3.8Ag-0.7Cu-1.4Sb-0.15Ni-3Bi + SAC105	1	1.79179	0.49227	13.2484	0.0003	6
		Sn-3.8Ag-0.7Cu-3Bi-1.5Sb-0.02Ni + SAC305	1	1.03316	0.31203	10.9632	0.0009	2.81
		Sn-3.8Ag-0.7Cu-3Bi-1.5Sb-0.02Ni + SAC105	1	2.59425	1.05015	6.1027	0.0135	13.387
		SAC doped Sb + SAC305	1	1.45228	0.24808	34.2691	<.0001	4.273
		SAC doped Sb + SAC105	1	2.47542	0.63784	15.0619	0.0001	11.887
6mil	Low	Sn-3.8Ag-0.7Cu-1.4Sb-0.15Ni-3Bi + SAC305	1	1.12947	0.23077	23.9538	<.0001	3.094
		Sn-3.8Ag-0.7Cu-1.4Sb-0.15Ni-3Bi + SAC105	1	1.59629	0.44945	12.6144	0.0004	4.935
		Sn-3.8Ag-0.7Cu-3Bi-1.5Sb-0.02Ni + SAC305	1	0.70745	0.20511	11.8964	0.0006	2.029
		Sn-3.8Ag-0.7Cu-3Bi-1.5Sb-0.02Ni + SAC105	1	1.38389	0.42937	10.3881	0.0013	3.99
		SAC doped Sb + SAC305	1	-0.05173	0.20812	0.0618	0.8037	0.95
		SAC doped Sb + SAC105	1	0.61037	0.41224	2.1922	0.1387	1.841
4mil	Best	Sn-3.8Ag-0.7Cu-1.4Sb-0.15Ni-3Bi + SAC305	1	1.74061	0.26809	42.1551	<.0001	5.701
		Sn-3.8Ag-0.7Cu-1.4Sb-0.15Ni-3Bi + SAC105	1	1.91784	0.48692	15.5138	<.0001	6.806
		Sn-3.8Ag-0.7Cu-3Bi-1.5Sb-0.02Ni + SAC305	1	1.97576	0.26929	53.8312	<.0001	7.212
		Sn-3.8Ag-0.7Cu-3Bi-1.5Sb-0.02Ni + SAC105	1	1.39756	0.485	8.3036	0.004	4.045
		SAC doped Sb + SAC305	1	0.10939	0.21779	0.2523	0.6155	1.116
		SAC doped Sb + SAC105	1	0.93246	0.47098	3.9196	0.0477	2.541

Table 8 shows the calculation of estimates for 15mm BGA package. It is found that the Baseline SAC305 follows proportional hazard assumption and its p-value is 0.0137. The parameter estimates for the Baseline SAC305 is -0.69076. The Hazard ratio is derived by taking the exponential of the parameter estimates. The hazard ratio or relative risk is defined as the ratio of hazard rate in treatment group versus control group. In this case, for the baseline SAC305, after taking the exponential of parameter estimate we get 0.501. It means the relative risk for the SAC305 material with SAC305 solder alloy after 6months of isothermal aging at 125°C will increase the failure by 0.501 times compared with after assembled material.

From the Table 8, it is shown that all the solder pastes except SAC405-Dopants+SAC305, SACX+SAC305, SAC Doped Sb+SAC105 (6mil Low profile) and SAC Doped Sb+SAC305 (6mil Low profile and 4mil Best profile) follow proportional hazard assumption.

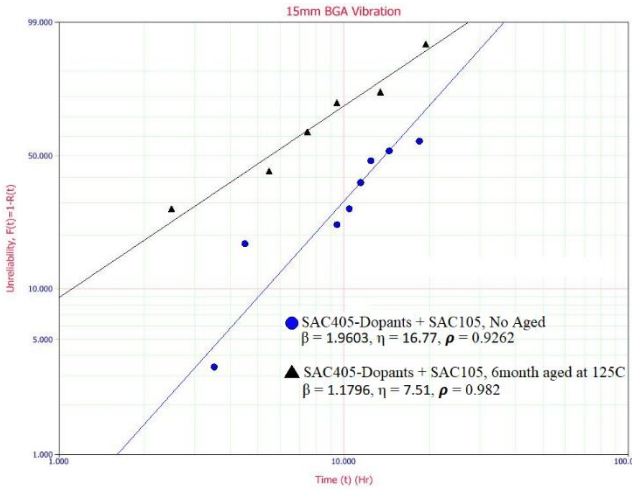

Fig. 8 Weibull graph for vibration reliability of SAC405-Dopants paste with SAC105 solder alloy

The lower relative risk is seen in Baseline SAC305 with SAC305 and SAC105 solder alloy. The relative risk is higher for Sn-3.8Ag-0.7Cu-3Bi-1.5Sb-0.02Ni and SAC doped Sb+SAC105 after aging.

The vibration reliability for SAC405-Dopants paste with SAC105 solder alloy between No Aged and Aged is shown in Figure 8. This graph is converted into Product limit estimator as shown in Figure 9.

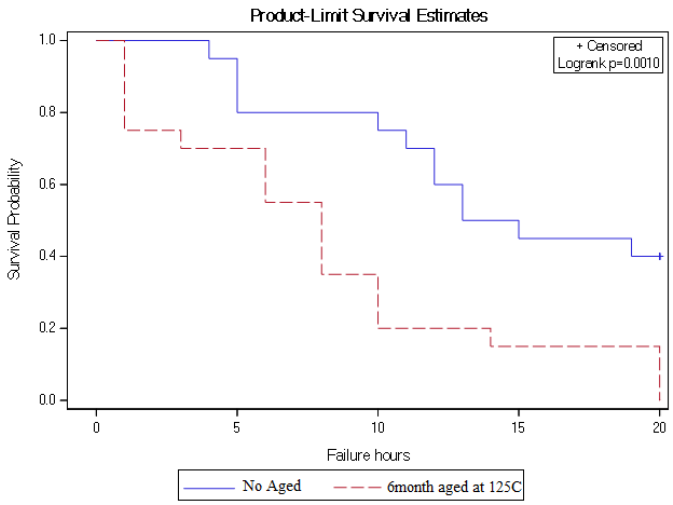

Fig. 9 Kaplan Meier Survival curve comparison for SAC405-Dopants paste with SAC105 solder alloy

The nonparametric estimation of survival function is performed using Kaplan Meier method which is commonly known as Product Limit estimator [24]. The hypothesis is tested to determine whether the survivor function, $S_1(t)= S_2(t)=\ldots=S_K(t)$ for all t, are the same for all paste materials. It is defined such that for all values of t in the range where there is data:

$$\hat{S}(t) = \begin{cases} 1 & \text{if } t < t_1 \\ \prod_{t_i \le t}\left[1 - \frac{d_i}{Y_i}\right] & \text{if } t_1 \le t \end{cases} \qquad (12)$$

Where d_i is the number of events and Yi is the number at risk. The survival probability is calculated at each event. The Product Limit Estimator is a step function with jumps at the observed event times. The size of these jumps depends not only on number of events observed at each event time ti, but also on pattern of censored observations prior to ti. The log-rank test is used to compare the survivor function between groups. It is well known and widely used to test the difference in survivor function [23]. For the two group comparison, the log-rank test is capable of comparing survivor function of the form $S_1(t) = [S_2(t)]^{\gamma}$ (13)

Where γ is a positive number other than 1. In this paper, the Product Limit survival curves are compared to test the hypothesis that there is a difference in survival function among each solder pastes using log-rank test.

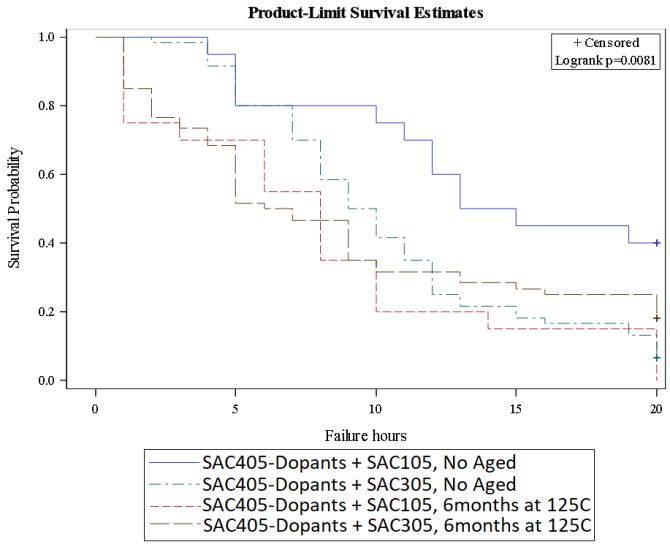

Fig. 10 Kaplan Meier Survival curve comparison for SAC405-Dopants paste with SAC105 and SAC305 solder alloy

Figure 10 shows the comparison for 15mm BGA package using SAC405-Dopants with SAC105 and SAC305 solder alloys. After assembly, it is seen that SAC105 solder alloy performed better than SAC305 alloy under vibration condition. Looking into 6month aged performance there is a crossover between two alloys at 8 hours. After 8 hours of testing, SAC305 alloy did better than SAC105 alloy. There is a difference in survivor function among the pastes with different alloys.

The Product Limit survival curve for Sn-3.8Ag-0.7Cu-3Bi-1.4Sb-0.15Ni paste with SAC105 and SAC305 is shown in Figure 11. The survival curve for No aged alloy is substantially higher compared with its aged. The solder paste Sn-3.8Ag-0.7Cu-3Bi-1.4Sb-0.15Ni with SAC105 solder alloy outperformed SAC305 after assembly. But after 6months of aging, Sn-3.8Ag-0.7Cu-3Bi-

1.4Sb-0.15Ni with SAC305 solder alloy did better than SAC105 solder alloy. There is a strong evidence that survivor functions are different for at least one of the solder pastes after assembly and post aging.

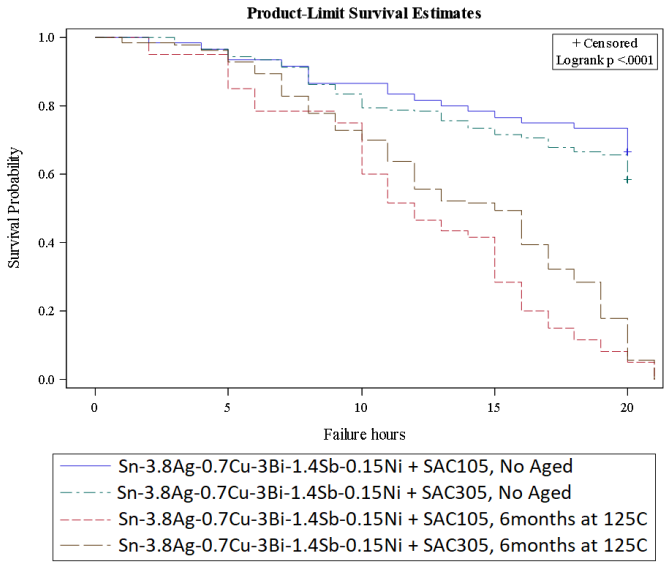

Fig. 11 Kaplan Meier Survival curve comparison for Sn-3.8Ag-0.7Cu-3Bi-1.4Sb-0.15Ni paste with SAC105 and SAC305 solder alloy

The vibration performance of 15mm BGA with SAC Doped Sb paste is shown in Figure 12. The SAC105 solder alloy is significantly better than SAC305 solder alloy at No aged. The survival curves for aged materials is close to each other which is opposite to what appeared in after assembly performance. The p-value is less than 0.0001 suggesting that there is difference in survival function.

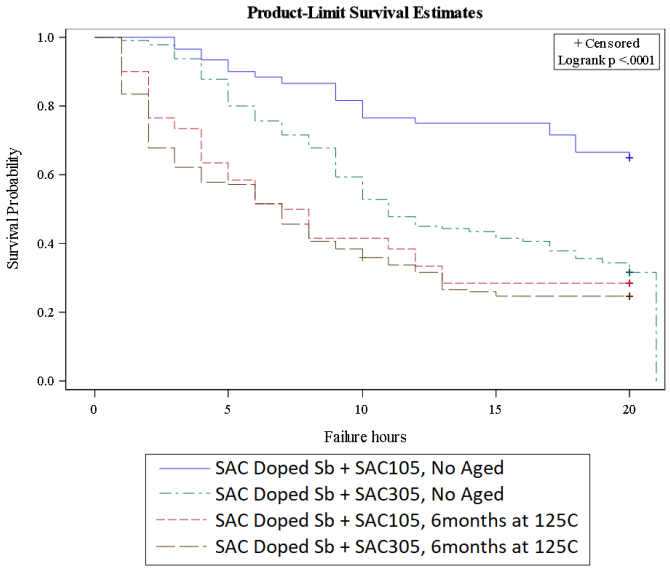

Fig. 12 Kaplan Meier Survival curve comparison for SAC Doped Sb paste with SAC105 and SAC305 solder alloy

Figure 13 shows the comparison for 15mm BGA package using SACX with SAC105 and SAC305 solder alloys. After assembly, it is seen that SAC105 solder alloy performed better than SAC305 alloy under vibration condition. Looking into 6month aged performance, SAC305 alloy did better than SAC105 alloy. There is a difference in survivor function among the pastes with different alloys.

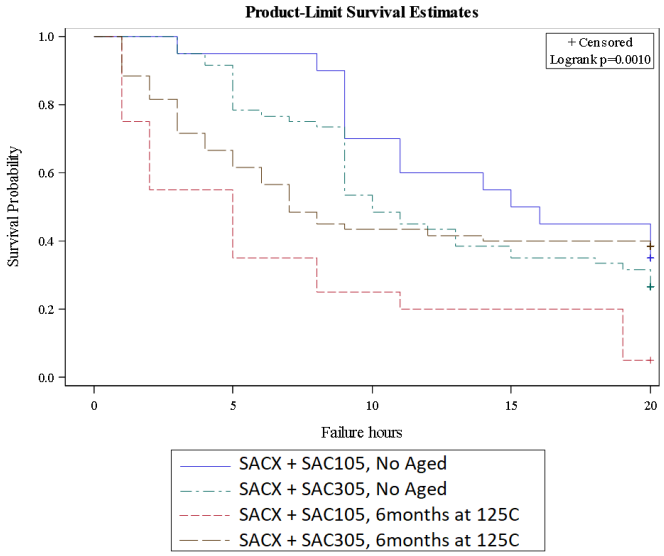

Fig. 13 Kaplan Meier Survival curve comparison for SACX paste with SAC105 and SAC305 solder alloy

After assembly, it is seen that Sn-3.8Ag-0.7Cu-3Bi-1.5Sb-0.02Ni solder with SAC105 solder alloy is more reliable than SAC305 under vibration testing. After aging, it appears that SAC305 performed well until 7 hours and later SAC105 did better than SAC305 solder alloy. With p-value<0.0001, hypothesis testing indicates there is a difference in survival function among at least one of the solder mixes.

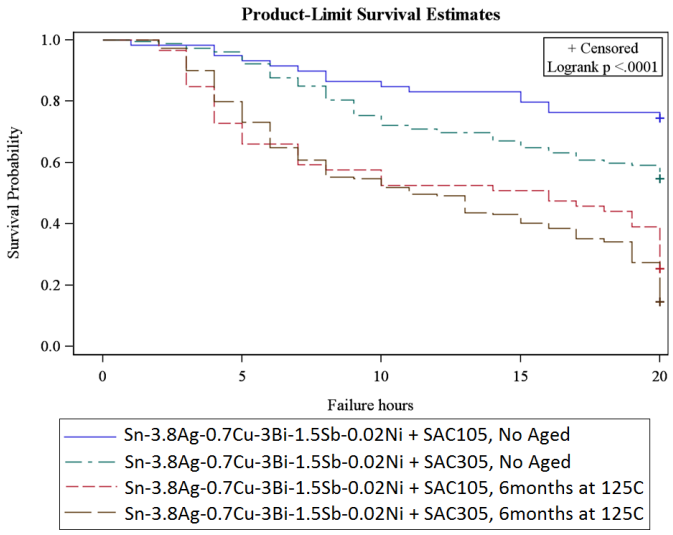

Fig. 14 Kaplan Meier Survival curve comparison for Sn-3.8Ag-0.7Cu-3Bi-1.5Sb-0.02Ni paste with SAC105 and SAC305 solder alloy

The results shown above indicates a significant difference in survivor function in at least one of solder pastes among all combinations. The graphs compare between each solder pastes. It is important to find the difference in survivor function between SAC305 solder paste and all the other pastes. Also, it is necessary to analyze the significant variation between pastes after assembly and after aging.

Pairwise comparison is being done between pastes and p-values are calculated for each comparison. Table 9 shows the p-value for each solder pastes compared with the baseline SAC305 solder paste with SAC305 solder alloy among No aged and 6month aged group as seen in 5^{th} and 6^{th} column of Table 9.

Table 9. Pairwise comparison of solder pastes compared with SAC305 solder paste (SAC305 solder alloy) and after aging

Solder paste	Stencil	Solder Alloy	Profile	p-value in comparison with SAC305		p-value in comparison with Aged
				0m	6m	
SAC305	6mil	SAC305	Best	N/A	N/A	0.0119
	6mil	SAC105	Best	0.6546	0.4793	<.0001
Sn-3.8Ag-0.7Cu-1.4Sb-0.15Ni-3Bi	4mil	SAC305	Best	0.0171	<.0001	<.0001
	4mil	SAC105	Best	0.0508	<.0001	<.0001
	6mil	SAC105	High	0.0005	<.0001	0.0036
	6mil	SAC305	High	0.0144	<.0001	<.0001
	6mil	SAC305	Low	0.9109	0.0016	0.0002
	6mil	SAC105	Low	0.7551	<.0001	0.0002
Sn-3.8Ag-0.7Cu-3Bi-1.5Sb-0.02Ni	4mil	SAC305	Best	0.0654	<.0001	<.0001
	4mil	SAC105	Best	0.0645	<.0001	0.002
	6mil	SAC105	High	<.0001	<.0001	0.0014
	6mil	SAC305	High	<.0001	0.0605	0.0005
	6mil	SAC305	Low	0.0131	<.0001	0.0018
	6mil	SAC105	Low	0.6206	<.0001	0.0009
SAC Doped Sb	4mil	SAC305	Best	0.0228	<.0001	0.0711
	4mil	SAC105	Best	0.106	<.0001	0.0408
	6mil	SAC105	High	<.0001	<.0001	<.0001
	6mil	SAC305	High	0.0474	<.0001	<.0001
	6mil	SAC305	Low	<.0001	<.0001	0.79
	6mil	SAC105	Low	0.3125	<.0001	0.0303
SAC405-Dopants	6mil	SAC305	Best	<.0001	<.0001	0.9973
	6mil	SAC105	Best	0.056	<.0001	0.001
SACX	6mil	SAC305	Best	0.0063	0.0004	0.8575
	6mil	SAC105	Best	0.0474	<.0001	0.0005

For example, the table shows there is significant difference between vibration performance of Sn-3.8Ag-0.7Cu-1.4Sb-0.15Ni-3Bi+SAC305 solder alloy (4mil stencil thickness) and SAC305 after assembly and after aging with p-values 0.0171 and less than 0.0001. The last column in the above table indicates the significance test for survival curves for each solder paste post-aging compared with its own after assembly. For instance, there is a strong evidence in difference in survival curve between No aged and 6month aged for all paste except SAC Doped Sb+SAC305 (4mil Best profile, 6mil Low profile), SAC405-Dopants+SAC305 solder alloy and SACX+SAC305 solder alloy.

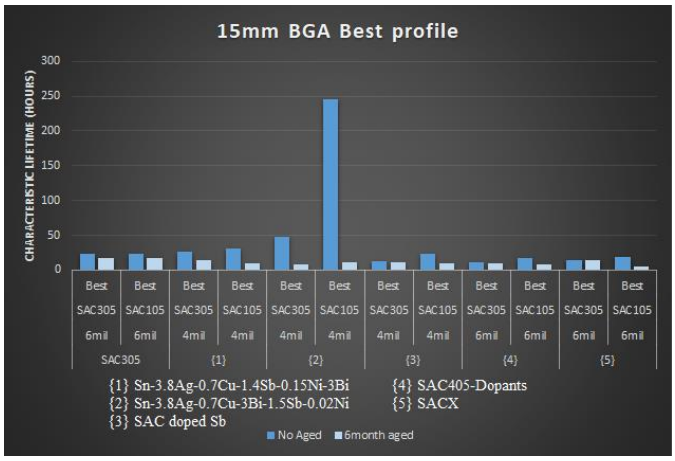

Fig. 15 Characteristic lifetime comparison for 15mm BGA Best profile

The Characteristic lifetime summary of 15mm BGA package built with Best profile is shown in Figure 15. From that summary, Sn-3.8Ag-0.7Cu-3Bi-1.5Sb-0.02Ni solder paste is most reliable after assembly compared with all other solder paste built using Best profile. But they did not perform well after aging and SAC305 paste outperformed other solder pastes after 6 months of isothermal aging at 75C.

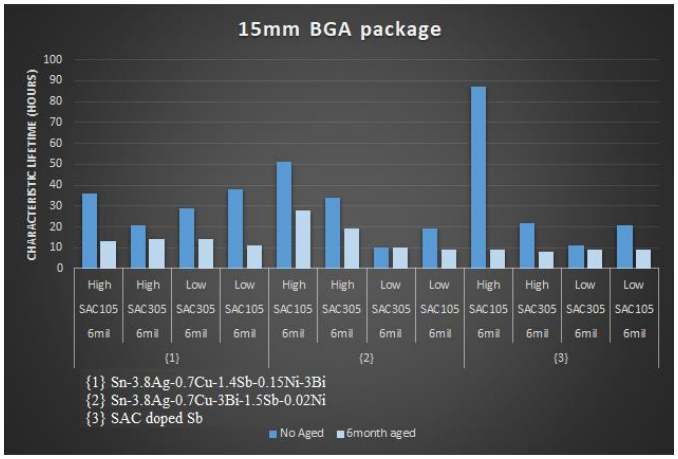

Fig. 16 Characteristic lifetime comparison for 15mm BGA High and Low profile

SAC doped Sb with SAC105 solder alloy did well after assembly compared with other paste as

seen in Figure 16 but have shown severe deterioration after aging. Also, it is shown that Sn-3.8Ag-0.7Cu-3Bi-1.5Sb-0.02Ni solder paste is reliable for both no aged and aged.

Drop Test

Similar analysis is done using Product-Limit estimator approach. Solder materials using SAC305 solder alloy and Best profile after assembly are compared in Figure 17. SAC305 solder paste with SAC305 solder alloy outperformed other solder alloys. There is significant difference in survival curve for at least one of the solder paste with p-value less than 5%.

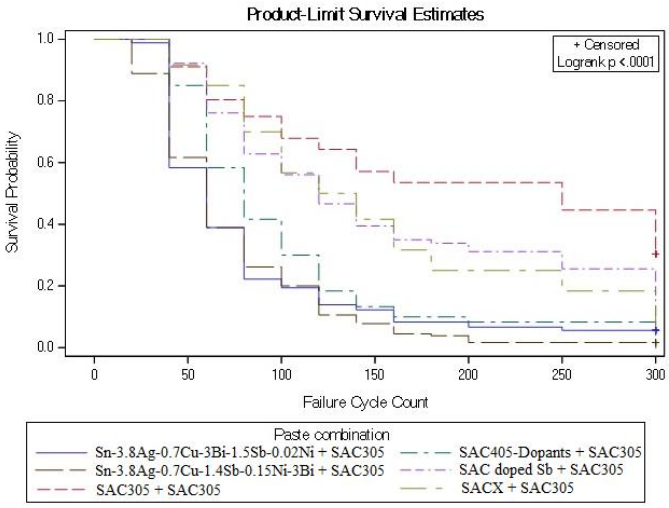

Fig. 17 Survival curve comparison for 15mm BGA package with SAC305 solder alloy subjected to drop shock after assembly

In terms of materials built using SAC105 solder alloy, SAC doped Sb have better performance than the other solder pastes as seen in Figure 18. There appears to be variation in survival function between solder pastes with SAC105 solder alloy with p-value less than 0.0001 as shown in Figure 18.

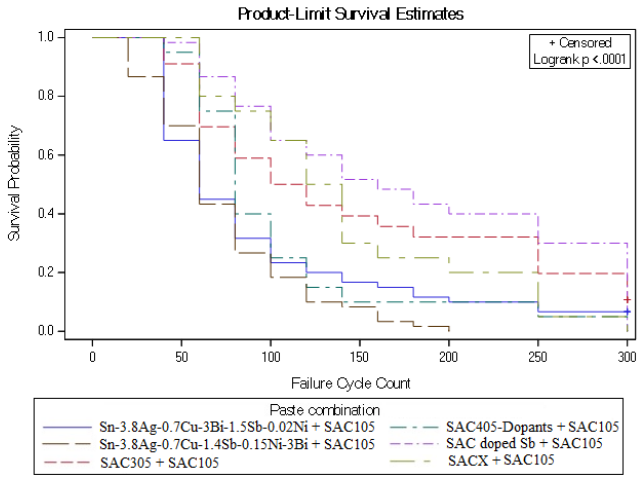

Fig. 18 Survival curve comparison for 15mm BGA package with SAC105 solder alloy subjected to drop shock after assembly

Figure 17 and 18 have shown the comparison of solder paste with SAC305 and SAC105 after assembly. Figure 19 shows the drop test survival curves for pastes with SAC305 solder alloy shown in Figure 20 after aging. With SAC305 solder alloy, Sn-3.8Ag-0.7Cu-1.4Sb-0.15Ni-3Bi solder is highly reliable after 6months of aging as seen in Figure 19. SAC305 solder paste is better after Sn-3.8Ag-0.7Cu-1.4Sb-0.15Ni-3Bi solder paste. The test of hypothesis that survival function of the solder pastes is the same is rejected at 5% level of significance.

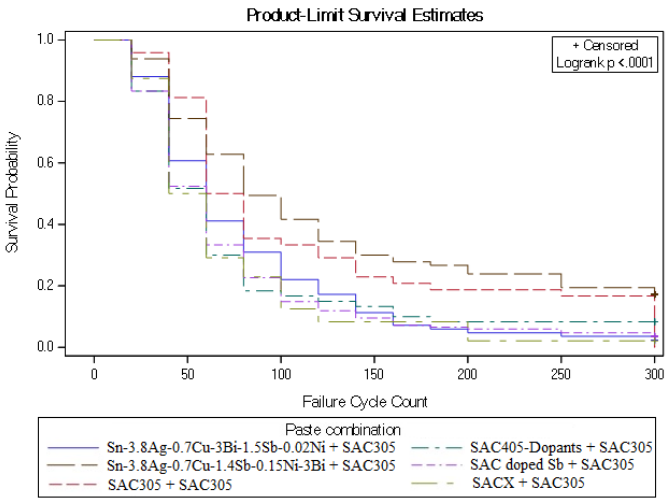

Fig. 19 Survival curve comparison for 15mm BGA package with SAC305 solder alloy subjected to drop shock after

aging

For the materials built using SAC105 solder alloy, SAC305 solder paste have better drop test performance along with 3.8Ag-0.7Cu-1.4Sb-0.15Ni-3Bi. SAC doped Sb with SAC105 solder alloy used to be reliable after assembly but the same paste with SAC105 solder alloy did not do well after 6months of aging as seen in Figure 20. The survival curve trend is significantly different from each other having p-value less than 0.0001.

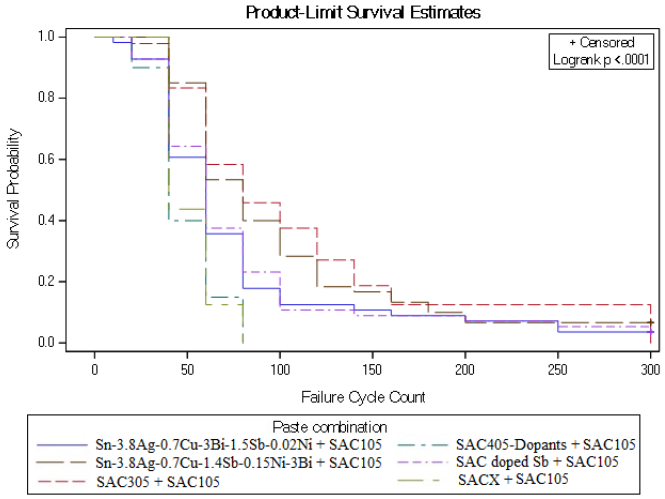

Fig. 20 Survival curve comparison for 15mm BGA package with SAC105 solder alloy subjected to drop shock after aging

The Lifetime summary is provided in Figure 21 for all solder pastes with SAC105 and SAC305. SAC305 with SAC305 solder alloy have shown higher lifetime after assembly but severe degradation is seen after aging. For SAC105 solder alloy, SAC Doped Sb is highest for No aged.

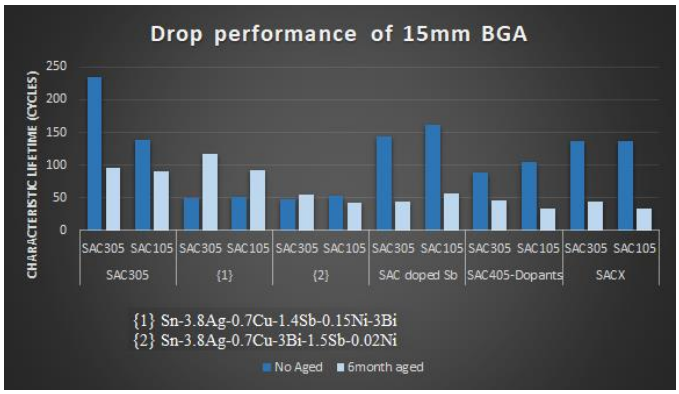

Fig. 21 Characteristic lifetime comparison for 15mm BGA package subjected to Drop test

The interesting trend to note is that there is significant improvement in drop test after aging for 3.8Ag-0.7Cu-1.4Sb-0.15Ni-3Bi especially. There is slight improvement for SAC305 solder alloy with 3.8Ag-0.7Cu-1.5Sb-0.02Ni-3Bi solder paste after aging. After aging, it can be seen that 3.8Ag-0.7Cu-1.4Sb-0.15Ni-3Bi showed better reliability.

Summary

The characteristic life of the 15mm BGA with different mix of material compositions in terms of 6mil, 4mil stencil thickness and different profiles are compared. Sn-3.8Ag-0.7Cu-1.4Sb-0.15Ni-3Bi and Sn-3.8Ag-0.7Cu-3Bi-1.5Sb-0.02Ni material showed better reliability for 4mil stencil thickness and Best profile. For Low profile, SAC doped Sb is reliable. On comparing the best materials in SAC105 solder spheres, Sn-3.8Ag-0.7Cu-1.4Sb-0.15Ni-3Bi paste showed better performance in High profile. Cox PH model has been developed to determine Hazard rates for each covariates. All the experimental variables showed significant impact on Time to Failure. The survival curve shows that Sn-3.8Ag-0.7Cu-1.4Sb-0.15Ni-3Bi, Sn-3.8Ag-0.7Cu-3Bi-1.5Sb-0.02Ni and SAC doped Sb showed better survival probability. The Failure Analysis and Intermetallic thickness measurement needs to be done in order to investigate crack propagation.

Short Term Isothermally Aged Doped Lead Free Solder Reliability subjected to Thermal Shock with Semiparametric Estimation

ABSTRACT

This paper discusses a statistical methodology for evaluating Pb-free solder alloy performance for high reliability products using reliability analysis and provides a detailed application of the technique for liquid to liquid thermal shock testing. The temperature shock test experimental failure results are from 15 mm CABGA208 component. In this experiment, SAC305 solder balls with In, Mn, Bi, Ni and Sb doped solder pastes are studied. This test result gives an indication of material combinations that are a potential solution to the traditional material degradation of SAC305 solder alloys. The materials that have the highest and lowest characteristic life compared to SAC305 solder pastes are Sn-3.4Ag-0.7Cu-3.2Bi-3Sb-Ni-Co and Sn-0.5Ag-1Cu-0.03Mn solder pastes respectively. The results discuss the effect of solder paste dopant material and their impact on reliability of surface mount components. The test components consists of two different time periods. The initial baseline time period is 10 days@25°C and accelerated lifetime period is 180 days @125°C. The substrate material for printed circuit board is FR-4 with glass transition temperature of 170°C and thickness of 0.5237mm. In this test, each test board is temperature cycled 3000 times (-40 to 125C) or until failure. The test were performed to determine the solder interconnect strength. The performance of solder interconnect is determined from the ability of solder materials to withstand high alternating temperature extremes. The results discuss the effects of isothermal aging at 125°C, for different paste materials with SAC305 and matched solder alloy. The test vehicles were subjected to high temperature accelerated life test (HALT) in liquid to liquid shock (LLTS) testing. Each test vehicle underwent 3000 thermal cycles with peak temperatures of

-40°C to +125°C on a 15-minute thermal profile (5 minutes dwell time and 2.5 minutes transition time). The hot and cold bath were filled with Galden® PFPE D02TS with an application range from -97 °C to +165 °C. Reliability of the test packages were determined from the ability of the components and solder interconnects to withstand the thermal stresses induced by alternating high and low temperature extremes. The effect of solder doping combination and aging on Time to Failure were assessed at 5% level of significance using Proportional Hazard Model. It is found that both solder doping combination, aging effect and its interaction have significant impact on the Time to Failure. The hazard ratio are calculated for each solder paste material. The lowest and highest failure rates are highlighted in this paper, compared to baseline SAC305 and it is correlated with the experimental data.

KEYWORDS: BGA, PCB, Lead-free, Reliability, Isothermal Aging, Doping, Weibull Analysis.

NOMENCLATURE

AIC	Akaike Information Criterion
BGA	Ball Grid Array
CABGA	Chip Array Ball Grid Array
FR	Flame Retardant
IPC	Association Connecting Electronics Industries
JEDEC	Joint Electron Device Engineering Council
KM	Kaplan-Meier
OSP	Organic Solderability Preservative
PCB	Printed Circuit Board
PH	Proportional Hazard

RoHS	Restriction of Hazardous Substances
SAE	Society of Automotive Engineers
SAS	Statistical Analysis Software
SBC	Schwarz Bayesian Criterion
SEM	Scanning Electron Microscopy
TV	Test Vehicle

Symbols

Ag	Silver
Bi	Bismuth
Cu	Copper

Innolot

Ni	Nickel
Pb	Lead
Sb	Antimony
Sn	Tin
SAC105	98.5%Sn – 1.0%Ag – 0.5%Cu
SAC305	96.5%Sn – 3.0%Ag – 0.5%Cu

Greek Symbols

β	Slope
η	Characteristic Life

ρ Probability plot

$\boldsymbol{\lambda}$ Hazard rate

INTRODUCTION

Among the various factors influencing the life of the electronic components, the performance of solder joint materials has an important role to determine the whole package life.[1] The effect of process-induced characteristic life on the durability of lead-free solder interconnects in electronic components need more detailed investigation. Voids influence the mechanical properties of joints and decrease the strength, ductility, creep, and fatigue life of the joints. This phenomenon results in the formation of cracks, which reduce the reliability. [2] The mechanical properties (and related failure behavior) of lead-free solder joints vary for different materials in electronic assemblies. Prior work by the Center for Advanced Vehicle and Extreme Environment Electronics ($CAVE^3$) at Auburn University has shown rapid deterioration in the reliability of SAC105, SAC305 and Innolot solder joints under elevated temperature conditions [3].

Several, recent ternary and quaternary solder alloys that melt about 10°C lower than SAC305 have been found to have superior mechanical and thermal mechanical reliability [4].

From an initial list of 200 alloys examined for metallurgical performance, a total of 13 lead-free solder alloys and paste combinations were chosen for experiments on mechanical and thermo-mechanical harsh environment test. The results demonstrated a significant degradation of the performance of the solder joints after aging for 6 months at 125°C.

Test Vehicle

The test vehicle (TV) is a standard 6-layer FR4 printed circuit board composed of Cu vias, glass epoxy covered by a thin solder mask on both sides, and an overlaid silkscreen for labeling. The test board (Fig. 1) had three 15mm BGA's (CABGA208), two 31mm BGA's (SBGA304), one 35mm BGA (PBGA1156), six 2512 resistors and six QFN's. The plating material was OSP. The 15mm BGA (CABGA 208) from Amkor were the primary components chosen for the study. The test vehicle was designed to accommodate different BGA packages to investigate the effects of solder paste and solder alloy.

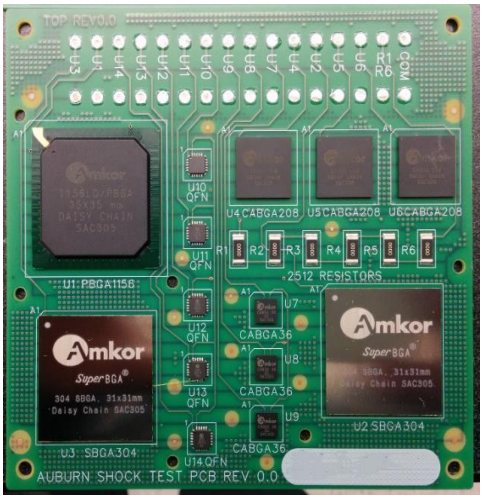

Fig. 104 Test Vehicle Design

The BGA alloys used were SAC305 and doped alloys. After the components were assembled, the test boards were placed in a Vitronics SMR-800 reflow oven. After reflow process, all the samples were electrically tested. All the components reflowed had 100% electrical yield. The test build matrix and solder composition for paste and alloys are listed in the Table 12.

Table 12. Build Matrix

Solder paste	**Solder Alloy**
Sn-3Ag-0.5Cu	Sn-3Ag-0.5Cu
	Sn-0.92Cu-2.46Bi
Sn-2.5Ag-0.5Cu-2In	Sn-3Ag-0.5Cu
	Sn-2.5Ag-0.5Cu-2In
Sn-3.8Ag-0.8Cu-3Bi-x1-x2	Sn-3Ag-0.5Cu
	Sn-3.8Ag-0.8Cu-3Bi-x1-x2
Sn-3.8Ag-0.7Cu-3Bi-1.5Sb-0.02Ni	Sn-3Ag-0.5Cu
Sn-3.4Ag-0.7Cu-3.2Bi-3Sb-Ni-Co	Sn-3Ag-0.5Cu
	Sn-3Ag-3Bi-0.8Cu-Ni
	Sn-2Ag-Cu-Ni
Sn-0.5Ag-1Cu-0.03Mn	Sn-3Ag-0.5Cu
SAC Doped Sb	Sn-3Ag-0.5Cu

EXPERIMENTAL SETUP

All boards assembled with different solder materials are subjected to thermal shock test with temperatures being -40°C to +125°C in Thermal Shock Chamber. Fifty boards were tested at a time in the chamber. The thermal shock cycle consists of dwell time with 5 minutes at each temperature extreme and transition time of 2.5 minutes. The test was subjected to standard high and low temperature test in a thermal liquid shock environmental chamber with perfluorocarbon liquid (Galden D02TS fluid) to assess the solder joint performance. Galden D02TS fluid is filled on both hot and cold bath. The basket transfer mechanism is controlled by Watlow F4 controller. The Time to Failure (Cycles) for each component was measured after every 50 cycles.

EXPERIMENTAL RESULTS

The 3-parameter Weibull (β, η, g) have used for analyzing the reliability data for 15mm BGA package. The characteristic lifetime (η) is number of cycles at which 63.2% of the population is expected to fail. The CABGA 208

has a dimension of 15x15mm with 0.8mm pitch size. It is found in all boards. The Weibull plot for 15mm BGA with various solder pastes in terms of 4mil stencil thickness and Best profile is shown in Figure 2.

STATISTICAL METHODS

First, it is important to understand the quantities necessary for survival analysis. Consider T to be the time until certain event. The Reliability function, R (t) is described as the probability of an entity surviving beyond time t. Survival function is given by

$$\mathbf{R(t) = P(T > t)} \qquad (1)$$

R(t) is a monotone non-increasing function. When T is a continuous random variable with probability density function f(t), the Cumulative Distribution Function is given by

$$\mathbf{F(t) = P(T \leq t)} \qquad (2)$$

The reliability function can be found by

$$\mathbf{R(t) = \int_t^{\infty} f(u)du = 1 - F(t)} \qquad (3)$$

$$\mathbf{f(t) = -\frac{dR(t)}{dt}} \qquad (4)$$

The probability density function, f (t) following Weibull distribution is

$$\mathbf{f(t) = \frac{\beta}{\eta}\left(\frac{t-\gamma}{\eta}\right)^{\beta-1} e^{-\left(\frac{t-\gamma}{\eta}\right)^{\beta}}} \qquad (5)$$

And the reliability function R(t) is,

$$\mathbf{R(t) = e^{-\left(\frac{t-\gamma}{\eta}\right)^{\beta}}, t > 0} \qquad (6)$$

Where the shape,$\boldsymbol{\beta > 0}$, scale $\eta > \mathbf{0}$ and location g > 0 are the parameters. The characteristic lifetime (η) is number of cycles at which 63.2% of the population is expected to fail. Another quantity known as Hazard function is denoted as the conditional failure rate in reliability or instantaneous rate of failure,

$$\mathbf{h(t) = \lim_{\Delta t \to 0} \frac{P[t \le T < t+\Delta t | T \ge t]}{\Delta t}} \qquad (7)$$

From the above equation, h(t)Δt is the approximate probability that an entity at time t experiencing an event in [t, t+Δt). The restriction on hazard function, h(t) is that it is nonnegative, h(t) ≥ 0 [23]. The hazard function relates to the survival function and probability density function in the following way, $\boldsymbol{h(t) = \frac{f(t)}{R(t)}}$. In Weibull case,

$$\mathbf{h(t) = \frac{\beta}{\eta}\left(\frac{t-\gamma}{\eta}\right)^{\beta-1}, t > 0.} \qquad (8)$$

Consider the data of sample size n consists of triple {(T_j, δ_j, Z_j (t)), j = 1 to n} where T_j is the time on study for the j^{th} subjects, δ_j is an event indicator for j^{th} individual (δ_j = 1 if the event occurred and δ_j = 0 if censored) and Z_j(t) is the vector of p covariates, which may depend on time. Let h (t | Z) be the hazard rate for an entity with risk vector Z at time t. The proportional hazard rate model proposed by Cox [1] is given below.

$$h(t|Z) = h_o(t)\exp(\beta^T Z) = h_o(t)\exp(\sum_k \beta_k Z_K) \qquad (9)$$

where $h_o(t)$ is an arbitrary baseline hazard rate, β is the vector of p parameters and the exponential term is a known function. This is known as Semiparametric model because the parametric form is assumed only for covariate effect. Cox model which is also known as proportional hazard model for two entities with covariate values Z and Z^*, because the ratio of their hazard rates is

$$\frac{h(t|Z)}{h(t|Z^*)} = \frac{h_o(t)\exp(\sum_{k=1}^{p} \beta_k Z_k)}{h_o(t)\exp(\sum_{k=1}^{p} \beta_k Z_k^*)} = \exp[\sum_{k=1}^{p} \beta_k (Z_k - Z_k^*)] \quad (10)$$

which is a constant. Hence hazard rates are proportional. Equation (8) is called Hazard ratio of an entity with risk factor Z experiencing the event as compared to an entity with risk factor Z^* [2-4]. This experiment consists of five categorical variables such as Paste combination, Stencil thickness, Profile and Aging Time. The censor indicator used in this experiment is delta. The Time to Failure measured in cycles is considered as response variable.

Table 3. Data description

Variables	**Description**
Paste Combination	Solder paste with Solder alloy combination
Aging Time	Aging Time – 0months and 6months
Delta	Status at endpoint (1=Failed, 0=Censored)
Failure	Time to Failure (Cycles)

The proportional hazard model has been used to fit the above data. The model is implemented using SAS®. Initially the global hypothesis is tested such that all coefficients are 0. The data set also consisted of tied observations. The Efron method is used to calculate the log likelihood with tied observations [23]. Let $t_1 < t_2 < \ldots < t_D$ be the distinct and ordered event times. Let d_i be the

number of failures at t_i. D_i is set of all individuals which fails at t_i. Let s_i be the sum of vectors Z_j over all individuals which fails at t_i where $s_i=\sum_{j\epsilon D_i} Z_j$. The set of all individuals at risk prior to t_i is R_i.

$$L(\beta) = \prod_{i=1}^{D} \frac{\exp(\beta^t s_i)}{\prod_{j=1}^{d_i}\left[\sum_{k\epsilon R_i}\exp(\beta^t Z_k) - \frac{j-1}{d_i}\sum_{k\epsilon D_i}\exp(\beta^t Z_k)\right]} \qquad (11)$$

The log likelihood is calculated by taking logarithm of above equation and multiplying by -2. The criterion -2logL is obtained using above method. Akaike Information Criterion (AIC) shown in Table 4 examines likelihood and number of parameters included in model.

$$\text{AIC} = -2\text{logL} + 2\text{k} \qquad (12)$$

Where k is number of covariates. It is equivalent to R^2 in ordinary least squares regression methods. Here the smaller the AIC, the better the data fits into model. Schwartz Bayesian Criterion (SBC) gives more penalization for additional covariates, where SBC is found using Equation (13).

$$\text{SBC} = -2\text{logL} + \text{klogn} \qquad (13)$$

Table 4. Model Fit Statistics

Model Fit Statistics		
Criterion	**Without Covariates**	**With Covariates**
-2LOG L	4426.36	4044.105
AIC	4426.36	4090.105
SBC	4426.36	4181.503

The hypothesis is tested to check whether all the coefficients (β_i's) are 0. The likelihood ratio statistics is calculated by finding the difference between -2logL with covariates and without covariates as shown in Table 4. The Likelihood ratio statistics is shown to be 382.2565. The null hypothesis is rejected indicating at least one of the coefficient is not 0.

Table 5. Test of Global Hypothesis

Testing Global Null Hypothesis			
Test	**Chi-Square**	**DF**	**p-value**
Likelihood Ratio	382.257	23	<.0001
Score	519.421	23	<.0001
Wald test	344.946	23	<.0001

The Table 6 shows the effect of covariates and its interaction which contribute to distribution of time to failure response. It is shown that there is significant difference in time to failure among each levels of Paste combination and Aging temperature at 5% level of significance. The effect of Aging is also significant. In this paper, it is important to understand the effect of aging for each solder material combination with respect to package. In terms of interaction, there is difference in time to failure for interaction between Paste combination and Aging with Wald Chi-Square as 64.6662 and p-value less than 0.0001.

Table 6. Overall Test of variables

Effect	**DF**	**Wald Chi-Square**	**p-value**
Paste Combination	11	87.1715	<.0001
Aging Temperature	1	14.8294	0.0001
Aging Temperature*Paste Combination	11	64.6662	<.0001

The effect of interaction in terms of paste combination and Aging are calculated using semiparametric estimates based on Maximum Likelihood Estimate. Table 7 shows the calculation of estimates for 15mm BGA package. It is found that the Baseline SAC305 follows proportional hazard assumption and its p-value is <0.001. The parameter estimates for the Baseline SAC305 is 1.85228. The Hazard ratio is derived by taking the exponential of the parameter estimates. The

hazard ratio or relative risk is defined as the ratio of hazard rate in treatment group versus control group. In this case, for the baseline SAC305, after taking the exponential of parameter estimate we get 6.374. It means the relative risk for the SAC305 material with SAC305 solder alloy after 6months of isothermal aging at 125°C will increase the failure by 6.374 times compared with after assembled material.

Table 7. Analysis of Maximum Likelihood Estimates for 15mm BGA package

Solder paste	Solder Alloy	DF	Parameter Estimate	Standard Error	Chi-Square	p-value	Hazard Ratio
Sn-3Ag-0.5Cu	Sn-3Ag-0.5Cu	1	1.85228	0.40441	2.0978	<0.0001	6.37434
	Sn-0.92Cu-2.46Bi	1	0.71505	0.43734	2.6733	0.102	2.04429
Sn-2.5Ag-0.5Cu-2In	Sn-3Ag-0.5Cu	1	1.18451	0.26912	19.373	<.0001	3.26908
	Sn-2.5Ag-0.5Cu-2In	1	0.84277	0.44653	3.5613	0.0591	2.32279
Sn-3.8Ag-0.8Cu-3Bi-x1-x2	Sn-3Ag-0.5Cu	1	3.43926	1.05417	1.0644	0.0011	31.1639
	Sn-3.8Ag-0.8Cu-3Bi-x1-x2	1	0.82114	0.47297	3.0141	0.0825	2.27309
Sn-3.8Ag-0.7Cu-3Bi-1.5Sb-0.02Ni	Sn-3Ag-0.5Cu	1	0.06074	0.3863	0.0247	0.8751	1.06262
Sn-3.4Ag-0.7Cu-3.2Bi-3Sb-Ni-x	Sn-3Ag-0.5Cu	1	0.26324	0.33681	0.6108	0.4345	1.30114
	Sn-3Ag-3Bi-0.8Cu-Ni	1	3.48163	1.04806	1.1036	0.0009	32.5127
	Sn-2Ag-Cu-Ni	1	1.09369	0.61575	3.1548	0.0757	2.98527
Sn-0.5Ag-1Cu-0.03Mn	Sn-3Ag-0.5Cu	1	2.63529	0.35222	55.9811	<.0001	13.9474
SAC Doped Sb	Sn-3Ag-0.5Cu	1	1.53896	1.11911	1.8911	0.1691	4.65974

From the Table 7, it is shown that Sn-3.4Ag-0.7Cu-3.2Bi-3Sb-Ni doped with Sn-3Ag-3Bi-0.8Cu-Ni, Sn-0.5Ag-1Cu-0.03Mn paste with SAC305 solder alloy and Sn-3.8Ag-0.8Cu-3Bi-x1-x2 with SAC305 have shown higher relative risk compared with the Baseline SAC305. The lower relative risk of aging is seen in Sn-3.8Ag-0.7Cu-3Bi-1.5Sb-0.02Ni and Sn-3.4Ag-0.7Cu-3.2Bi-3Sb-Ni-x material from the table. The Weibull graph is shown comparing after assembled and 6month aged thermal shock reliability of the baseline SAC305 paste with SAC305 alloy in Figure 20.

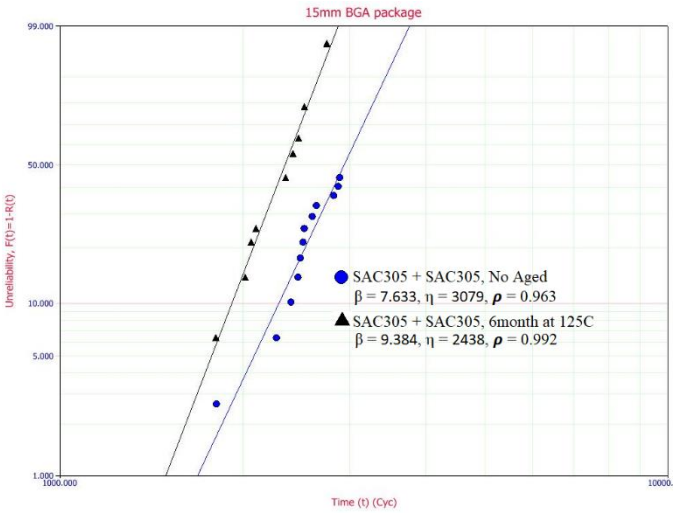

Fig. 21 Thermal Shock Reliability of 15mm BGA package built using SAC305 paste with SAC305 solder alloy

The Lifetable method is used for this paper to estimate the survivor function. The hypothesis is tested to determine whether the survivor function, $R_1(t)= R_2(t)=\ldots=R_K(t)$ for all t, are the same for all paste materials. The graph shown in Figure 20 is converted into Lifetable survival curve for analysis to test the difference in survivor function as shown in Figure 21. The time to failures are grouped into intervals of 100 cycles to obtain the survival estimates.

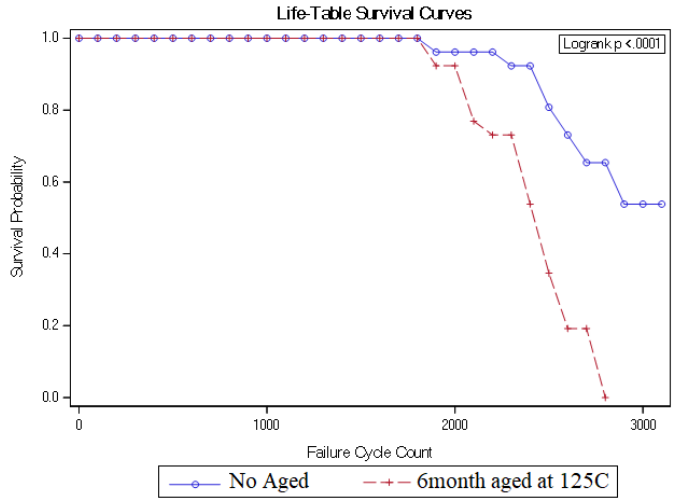

Fig. 21 Lifetable survival curve for 15mm BGA built using SAC305 paste with SAC305 solder alloy

The survival estimate is calculated based on the conditional probability of failure in a following method. For interval i, let t_i be start time and p_i be the estimated conditional probability of failure. The probability of surviving to t_i or beyond is

$$\hat{S}(t) = \prod_{j=1}^{i-1}(1 - p_i) \tag{12}$$

The log-rank test is used to compare the survivor function between groups. It is well known and widely used to test the difference in survivor function [23]. For the two group comparison, the log-rank test is capable of comparing survivor function of the form

$$S_1(t) = [S_2(t)]^{\gamma} \tag{13}$$

Where γ is a positive number other than 1. In this paper, the lifetable survival curves are compared to test the hypothesis that there is a difference in survival function among each solder pastes using log-rank test. It is important to compare the performance of both no aged and aged SAC305 solder materials vs. various solder pastes. The semiparametric estimation is shown in the Table 7 to compare each solder pastes after aging with its no aged. The nonparametric approach which is Lifetable method is followed to compare the performance between SAC305 and other solder pastes. The test of significance for difference in reliability function is also performed simultaneously.

Figure 21 shows the comparison for 15mm BGA package with SAC305 solder paste and Sn-0.92Cu-2.46Bi paste. After the assembly, SAC305 solder paste is superior compared with Sn-

0.92Cu-2.46Bi solder alloy. The same trend is shown for aged samples as well. The reliability function for atleast one of solder paste is different where p-value is less than 0.0001. The analysis of reliability function is shown for Sn-3.8Ag-0.8Cu-3Bi-x1-x2 with SAC305 and Matched solder alloy in Figure 22. It is seen that under pre-aging condition Sn-3.8Ag-0.8Cu-3Bi-x1-x2 with SAC305 is far superior compared to its matched solder alloy. After 6months of aging for the both the materials, there is a crossover between two materials until 1500 cycles where SAC305 solder alloy did better than the matched solder alloy.

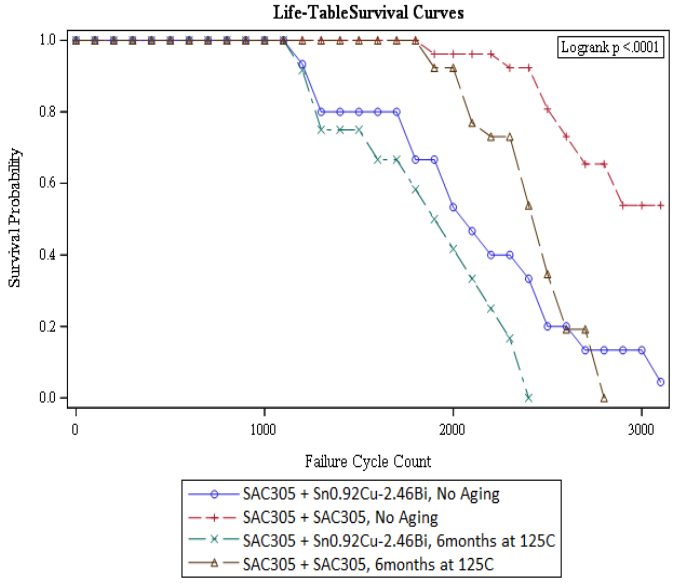

Fig. 21 Lifetable survival curve comparison for 15mm BGA package built with Sn-0.92Cu-2.46Bi compared with SAC305 paste

Later, trend is reversed. With p-value<0.0001, hypothesis testing indicates there is a difference in reliability function among at least one of the solder pastes.

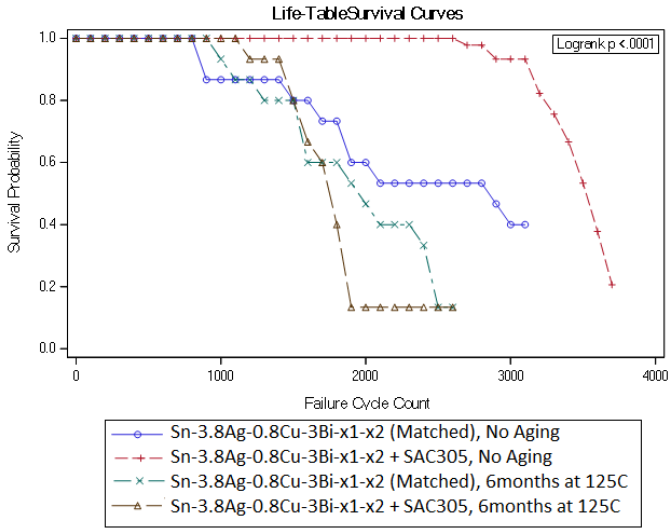

Fig. 22 Lifetable survival curve comparison for 15mm BGA package built with Sn-3.8Ag-0.8Cu-3Bi-x1-x2 paste

The reliability comparison for 15mm BGA package using Sn-2.5Ag-0.5Cu-2In solder paste with SAC305 solder alloy versus matched is shown in Figure 25. After the assembly, the median lifetime for the matched solder alloy is higher than Sn-2.5Ag-0.5Cu-2In solder paste with SAC305 solder alloy. After aging, there are crossover at 1000 cycles, 1600 cycles and 2100 cycles but the median lifetime for the Matched solder alloy is still better than SAC305 solder alloy. The reliability function for atleast one of solder paste is different where p-value is less than 0.0001.

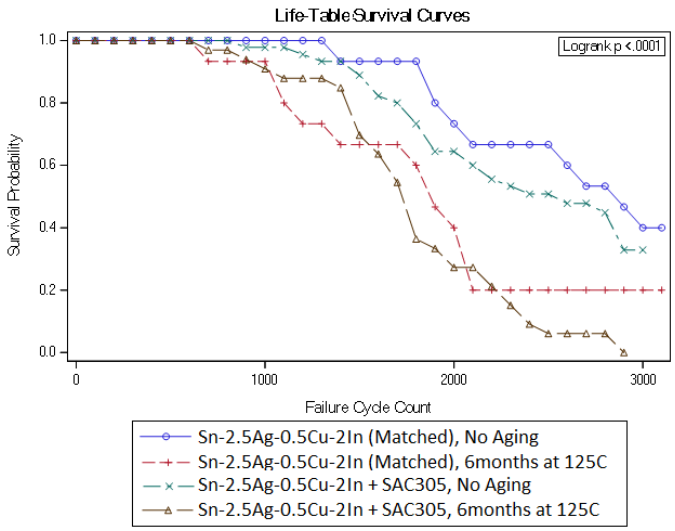

Fig. 25 Lifetable survival curve comparison for 15mm BGA package built with Sn-2.5Ag-0.5Cu-2In

Figure 26 shows the comparison for Sn-3.4Ag-0.7Cu-3.2Bi-3Sb-Ni-x paste with three different solder alloys. After the assembly, Sn-3.4Ag-0.7Cu-3.2Bi-3Sb-Ni-x solder paste with Sn-2Ag-Cu-Ni alloy did better than same paste with SAC305 alloy and Sn-3Ag-3Bi-0.8Cu-Ni alloy until 3300 cycles and later SAC305 solder alloy did better than the solder alloys. Under post aging conditions, Sn-3.4Ag-0.7Cu-3.2Bi-3Sb-Ni-x solder paste with SAC305 solder alloy has the higher median lifetime than other solder alloys. With p-value<0.0001, hypothesis testing indicates there is a difference in reliability function among at least one of the solder pastes.

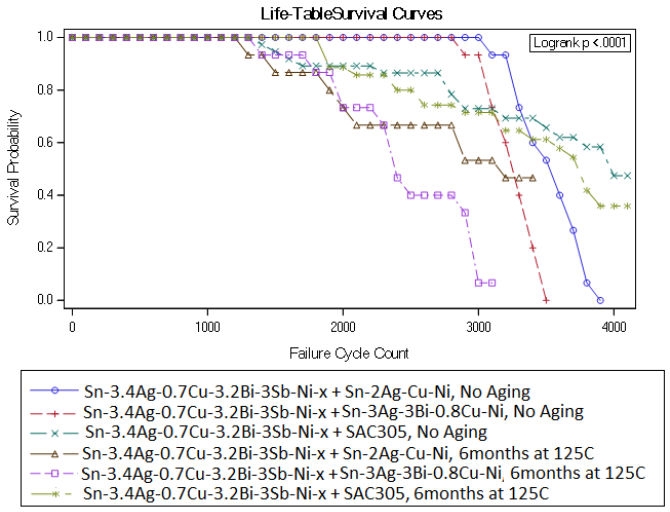

Fig. 26 Lifetable survival curve comparison for 15mm BGA package built with Sn-3.4Ag-0.7Cu-3.2Bi-3Sb-Ni-x paste

The reliability function for SAC solder alloy with Sn-0.5Ag-1Cu-0.03Mn, Sn-3.8Ag-0.7Cu-3Bi-1.5Sb-0.02Ni and SAC Doped Sb solder pastes are shown in Figure 29. Under pre aging condition, the most underperforming solder paste is Sn-0.5Ag-1Cu-0.03Mn, the reliable solder material is SAC doped Sb and Sn-3.8Ag-0.7Cu-3Bi-1.5Sb-0.02Ni appearing to be intermediate. After aging, significant deterioration is seen for Sn-0.5Ag-1Cu-0.03Mn solder paste. There appears to be crossover for Sn-3.8Ag-0.7Cu-3Bi-1.5Sb-0.02Ni and SAC Doped Sb solder pastes making it look like they perform equally better. The log-rank test indicates that with p-value less than 0.0001, there is a difference in reliability function among at least one of the solder pastes.

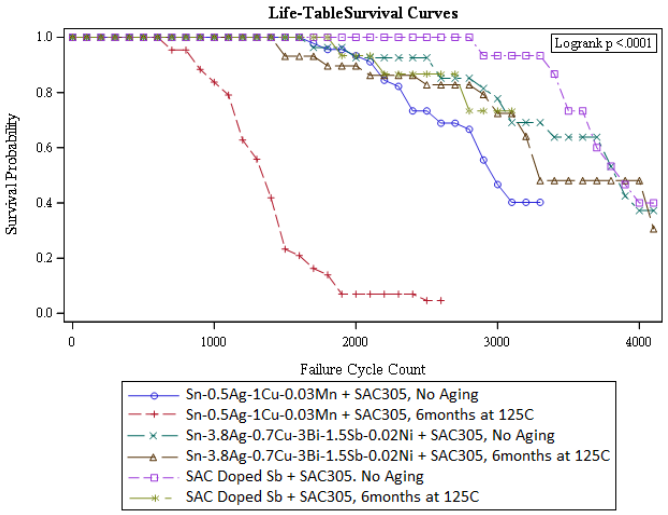

Fig. 29 Lifetable survival curve comparison for 15mm BGA package built with Sn-0.5Ag-1Cu-0.03Mn, Sn-3.8Ag-0.7Cu-3Bi-1.5Sb-0.02Ni and SAC Doped Sb

The given graphs compare between solder pastes. It is important to find the difference in survivor function between SAC305 solder paste and all the other pastes. Also, it is necessary to analyze the significant variation between pastes after assembly and after aging. Pairwise comparison is being done between pastes and p-values are calculated for each comparison. Table 8 shows the p-value for each solder pastes compared with the baseline SAC305 solder paste with SAC305 solder alloy among No aged and 6month aged group as seen in 3rd and 4th column of Table 8. For example, the table shows there is significant difference between thermal shock performance of SAC305 solder paste with SAC305 solder alloy and Sn-0.92Cu-2.46Bi alloy after assembly. For the same paste group, there is no difference in survival curves for 6month aged group. The Sn-2.5Ag-0.5Cu-2In paste with SAC305 showed significant difference and Sn-0.5Ag-1Cu-0.03Mn have shown difference compared with SAC305 solder paste (SAC305 solder alloy) after assembly. Sn-2.5Ag-0.5Cu-2In and SAC405-Dopants mixed with SAC305 solder alloy have shown significant

variation compared with SAC305 solder paste after assembly. [3], [5], [14], [6]–[13]The last column in the above table indicates the significance test for survival curves for each solder paste post-aging compared with its own after assembly. For instance, there is a strong evidence in difference in survival curve between No aged and 6month aged for SAC305 solder paste with SAC305 solder alloy with p-value less than 0.001. Table 7 had shown lower relative risk for SAC405-Dopants, SACX and Sn-3.8Ag-0.7Cu-3Bi-1.5Sb-0.02Ni solder paste. There is no difference in survival function between No aged and aged group for these solder pastes with p-value greater than 0.05.

Table 8. Pairwise comparison of solder pastes compared with SAC305 solder paste (SAC305 solder alloy) and after aging

Solder paste	Solder Alloy	Pairwise comparison with SAC305		Pairwise comparison with aged
		0m	6m	
Sn-3Ag-0.5Cu	Sn-3Ag-0.5Cu	N/A	N/A	<0.0001
	Sn-0.92Cu-2.46Bi	0.0062	0.0944	0.0945
Sn-2.5Ag-0.5Cu-2In	Sn-3Ag-0.5Cu	0.2667	0.0126	<.0001
	Sn-2.5Ag-0.5Cu-2In	0.524	0.1196	0.022
Sn-3.8Ag-0.8Cu-3Bi-1.5Sb-0.10Ni	Sn-3Ag-0.5Cu	0.4059	0.0009	<0.0001
	Sn-3.8Ag-0.8Cu-3Bi-x1-x2	0.4136	0.1525	0.085
Sn-3.8Ag-0.7Cu-3Bi-1.5Sb-0.02Ni	Sn-3Ag-0.5Cu	0.6854	<.0001	0.8677
Sn-3.4Ag-0.7Cu-3.2Bi-3Sb-Ni-x	Sn-3Ag-0.5Cu	0.2882	<.0001	0.4454
	Sn-3Ag-3Bi-0.8Cu-Ni	0.5835	0.8938	<0.0001
	Sn-2Ag-Cu-Ni	0.3657	0.3025	0.0522
Sn-0.5Ag-1Cu-0.03Mn	Sn-3Ag-0.5Cu	0.9055	<0.0001	<0.0001
SAC Doped Sb	Sn-3Ag-0.5Cu	0.2374	0.0007	0.132

The solder pastes mixed with Matched alloys indicated significant difference in curve especially for Sn-2.5Ag-0.5Cu-2In and Sn-3.4Ag-0.7Cu-3.2Bi-3Sb-Ni solder pastes except for Sn-3.8Ag-0.8Cu-3Bi-x1-x2 solder paste. For SAC105 solder alloy mixed with various solder pastes have resulted in significant difference in time to failure between No aged and 6month aged. There is variation in survival function between aged and after assembly for all combinations seen in Sn-2.5Ag-0.5Cu-2In solder paste and Sn-0.5Ag-1Cu-0.03Mn pastes.

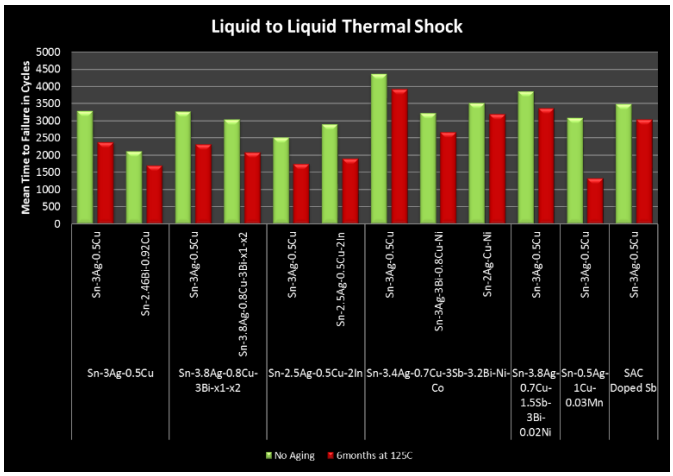

Fig. 30 Characteristic lifetime comparison for 15mm BGA Best profile

The SAC305 solder alloy mixed with Sn-3.4Ag-0.7Cu-3.2Bi-3Sb-Ni solder paste have not shown difference in reliability between after assembly and aged. Figure 30 shows the summary for Characteristic lifetime of 15mm BGA package built using Best profile. Sn-2.5Ag-0.5Cu-2In, Sn-3.8Ag-0.8Cu-3Bi-x1-x2 and Sn-0.5Ag-1Cu-0.03Mn solder paste have significant deterioration compared with SAC305 solder paste. The solder pastes which outperformed SAC305 even after aging are Sn-3.8Ag-0.7Cu-3Bi-1.5Sb-0.02Ni, Sn-3.4Ag-0.7Cu-3.2Bi-3Sb-Ni, SAC405-Dopants and SACX for the Best profile.

The characteristic life of the 15mm BGA with different mix of material compositions are compared. Cox PH model has been developed to determine Hazard rates for each covariates. All the experimental variables showed significant impact on Time to Failure. The survival curve shows that Sn-3.8Ag-0.7Cu-3Sb-3.2Bi-Ni-Co, Sn-3.8Ag-0.7Cu-3Bi-1.5Sb-0.02Ni and SAC doped Sb showed better survival probability. The Failure Analysis and Intermetallic thickness measurement needs to be done in order to investigate crack propagation. Also, the solder material performance after six months of isothermal aging at 125C needs to be compared.

References

[1] O. Source, “Timeline of electrical and electronic engineering,” *Computer Wiki*, 2017. .

[2] A. M. Macdonald, *Chambers twentieth century dictionary*. 1972.

[3] G. Moore, “intel,” *intel*, 1965. [Online]. Available: https://www.intel.com/content/www/us/en/silicon-innovations/moores-law-technology.html.

[4] G. Moore, “Moores Law,” *Wikiipedia*, 2017. [Online]. Available: https://en.wikipedia.org/wiki/Moore%27s_law.

[5] A. Singh, “Global Electronics Industry - What’s Ahead?” [Online]. Available: https://www.linkedin.com/pulse/global-electronics-industry-whats-ahead-anurag-singh.

[6] J. C. Dally, J. W., Lall, P., and Suhling, *Mechanical Design of Electronic Systems*. 2008.

[7] A. Schaller, “System Hierarchy in Printed Electronics,” 2014. [Online]. Available: https://www.linkedin.com/pulse/20140613171816-10763896-system-hierarchy-in-printed-electronics/.

[8] C. (Auburn U. Zhao, “Board Level Reliability of Lead-Free Solder Interconnections with Solder Doping Under Harsh Environment,” Auburn University, 2017.

[9] T. Sanders, “Extreme Environment Reliability of Components for Computing with SAC305 and Alternative High Reliability Solders,” *Dissertation*, 2016.

[10] I. 11357-2:2013, “Plastics -- Differential scanning calorimetry (DSC) -- Part 2: Determination of glass transition temperature and glass transition step height,” *ISO*, 2013. [Online]. Available: https://www.iso.org/standard/57966.html.

[11] Y. Zhu, Q. Liu, B. Liu, and J. Jiang, “Theory of Time-Temperature-Stress Equivalent Principle Based on Schapery Equation and Its Application on Granite,” vol. 20, no. 4, 2014.

[12] G. Kobe, “Material witness,” *Automot. Ind. AI*, vol. 179, no. 6, p. 85, 1999.

[13] R. F. Tylecote, *A History of Metallurgy (2nd Edition)*. CRC Press; 2nd edition, 2002.

[14] N. P. Vijayakumar, “The Effects of Thermal Aging on the Mechanical Behavior of Fine Pitch Electronics Packages,” Auburn, 2012.

[15] X. Ji, R. An, and C. Wang, “Quasi in situ study about growth kinetics of Ag3Sn at the interface of eutectic SnPb / electroplated Ag soder joint in the long-term satellite,” pp. 221–225, 2017.

[16] J. Bath, *Lead-Free soldering standards*. 2007.

[17] “National Institute of Standards and Technology.” [Online]. Available: https://www.metallurgy.nist.gov/phase/solder/solder.html.

[18] E. Kosiba, “Characterization of Low Melting Temperature , Low-Ag , Bi-Containing , Pb-Free Solder Alloys by,” University of Toronto, 2016.

[19] J. G. Lee and K. N. Subramanian, “Effect of Dwell Times on Thermomechanical Fatigue Behavior of Sn-Ag–Based Solder Joints,” *J. Electron. Mater.*, vol. 32, no. 6, pp. 523–530, 2003.

[20] Association Connecting Electronics Industries, “Performance Test Methods and Qualification Requirements for Surface Mount Solder Attachments,” pp. 7–9, 2002.

[21] Reliasoft Corporation, “Accelerated Life Testing Reference,” 2015.

[22] Wikipedia, “Weibull Distribution,” *Wikipedia*, 2017. [Online]. Available: http://reliawiki.org/index.php/The_Weibull_Distribution.

[23] Wikipedia, “Mean,” *Wikiipedia*, 2017. [Online]. Available: https://en.wikipedia.org/wiki/Mean.

[24] Wikipedia, “Median,” *Wikiipedia*, 2017. [Online]. Available: https://en.wikipedia.org/wiki/Median.

[25] Wikipedia, “Mode,” *2Wikiipedia*, 2017. [Online]. Available: https://en.wikipedia.org/wiki/Mode_(statistics).

[26] Wikipedia, “Standard Deviation,” *Wikipedia*, 2017. [Online]. Available: https://en.wikipedia.org/wiki/Standard_deviation.

[27] S. Thirugnanasambandam, T. Sanders, J. L. Evans, M. Bozack, W. Johnson, and J. Suhling, “COMPONENT LEVEL RELIABILITY FOR HIGH TEMPERATURE POWER COMPUTING WITH SAC305 AND ALTERNATIVE HIGH RELIABILITY SOLDERS,” in *Proceedings of SMTA International*, 2014.

[28] DFR Solutions, “Hazard Bath Tub Curve,” *DFR book design for reliability*, 2017. [Online]. Available: https://www.slideshare.net/eraz/dfr-presentation.

[29] S. Thirugnanasambandam *et al.*, “Proportional Hazard Model of doped low creep lead free solder paste under vibration,” in *2016 15th IEEE Intersociety Conference on Thermal and Thermomechanical Phenomena in Electronic Systems (ITherm)*, 2016, pp. 1209–1217.

[30] A. Raj *et al.*, “Proportional Hazard Model of doped low creep lead free solder paste under thermal shock,” in *2016 15th IEEE Intersociety Conference on Thermal and Thermomechanical Phenomena in Electronic Systems (ITherm)*, 2016, pp. 1191–1201.

[31] S. Thirugnanasambandam *et al.*, “The study of vibrational performance on different doped low creep lead free solder paste and solder ball grid array packages,” in *Fourteenth Intersociety Conference on Thermal and Thermomechanical Phenomena in Electronic Systems (ITherm)*, 2014, pp. 920–923.

[32] S. Sridhar, A. Raj, S. Gordon, S. Thirugnanasambandam, J. L. Evans, and W. Johnson, "Drop impact reliability testing of isothermally aged doped low creep lead-free solder paste alloys," in *2016 15th IEEE Intersociety Conference on Thermal and Thermomechanical Phenomena in Electronic Systems (ITherm)*, 2016, pp. 501–506.

[33] S. Thirugnanasambandam *et al.*, "DROP RELIABILITY TEST ON DIFFERENT DIMENSIONAL LEAD-FREE WAFER LEVEL CHIP SCALE PACKAGES," in *SMTA International*, 2012.

[34] S. Thirugnanasambandam *et al.*, "Component level reliability on different dimensions of lead free wafer level chip scale packages subjected to extreme temperatures," in *13th InterSociety Conference on Thermal and Thermomechanical Phenomena in Electronic Systems*, 2012, pp. 612–618.

[35] T. Sanders, S. Thirugnanasambandam, J. L. Evans, M. Bozack, W. Johnson, and J. Suhling, "COMPONENT LEVEL RELIABILITY FOR HIGH TEMPERATURE POWER COMPUTING WITH SAC305 AND ALTERNATIVE HIGH RELIABILITY SOLDERS," in *Proceedings of SMTA International*, 2015, pp. 144–150.

[36] J. Zhang, Z. Hai, S. Thirugnanasambandam, J. L. Evans, M. J. Bozack, and R. Sesek, "Isothermal Aging Effects on the Harsh Environment Performance of Lead-Free Solder Joints," *SMTA Int.*, no. SMTA, pp. 390–397, 2012.

[37] Jiawei Zhang *et al.*, "Thermal Aging Effects on the Thermal Cycling Reliability of Lead-Free Fine Pitch Packages," *IEEE Trans. Components, Packag. Manuf. Technol.*, vol. 3, no. 8, pp. 1348–1357, Aug. 2013.

[38] Y. J. Lee and P. Crosbie, "Reliability of wafer level chip scale packages (WL-CSP) under

dynamic loadings," *... , 2008. ECTC 2008. 58th*, vol. 60060, no. 1, pp. 1782–1786, 2008.

[39] J. Zhang, Z. Hai, J. L. Evans, M. J, J. C, and A. Silver, "CORRELATION Of AgINg EffECTs ON CREEP RATE ANd RELIAbILITy IN LEAd fREE sOLdER JOINTs," *SMTA J.*, vol. 25, no. 3, pp. 19–28, 2012.

[40] J. Zhang, S. Thirugnanasambandam, J. L. Evans, M. J. Bozack, and R. Sesek, "Impact of Isothermal Aging on the Long-Term Reliability of Fine-Pitch Ball Grid Array Packages With Different Sn-Ag-Cu Solder Joints," *IEEE Trans. Components, Packag. Manuf. Technol.*, vol. 2, no. 8, pp. 1317–1328, Aug. 2012.

[41] D. Suraski, "The current status of lead-free solder alloys," *Electron. Packag. Manuf. Trans.*, vol. 24, no. 4, pp. 244–248, 2001.

[42] L. Anand, "Constitutive Equations for the Rate-Dependent Deformation of Metals at Elevated Temperatures," *J. Eng. Mater. Technol.*, vol. 104, no. 1, p. 12, 1982.

[43] V. Vasudevan and X. Fan, "An acceleration model for lead-free (SAC) solder joint reliability under thermal cycling," *Proc. - Electron. Components Technol. Conf.*, vol. 1414, no. 4, pp. 139–145, 2008.

[44] Reliasoft Corporation, "The Weibull Distribution," 2017. [Online]. Available: http://reliawiki.org/index.php/The_Weibull_Distribution.

[45] JEDEC standard, "Temperature Cycling JEDEC JESD22-A104E," *JEDEC Solid State Technology Association 2014*, no. October. pp. 1069–1072, 2009.

[46] T. S. Mukherjee, J. Zilg, M. Tabar, C. Morillo, M. Osterman, and A. Dasgupta, "Effect of Gold and Copper on Microstructural Evolution and Mechanical Properties of Isothermally Aged SAC305 Solder Joints," in *ICEP Proceedings*, 2014, pp. 162–167.

[47] a Mawer, “Plastic Ball Grid Array,” *Area Array Interconnect. Handb.*, pp. 577–613, 2001.

[48] Y. Tian, X. Liu, J. Chow, Y. P. Wu, and S. K. Sitaraman, “Comparison of IMC growth in flip-chip assemblies with 100- and 200-μm-pitch SAC305 solder joints,” *Proc. - Electron. Components Technol. Conf.*, pp. 1005–1009, 2013.

[49] S. Kwon, K. Kim, D. Han, T. Sung, C. Lee, and S. Yoo, “Effect of Interfacial Reaction Layer on the Brittle Fracture of the SAC305 Solder Joint on ENIG and ENEPIG Surface Finish,” in *International Conference on Electronic Materials and Packaging (EMAP)*, 2012, pp. 4–6.

[50] C. Huang *et al.*, “Failure mode of SAC305 lead-free solder joint under thermal stress,” in *International Conference on Electronic Packaging Technology & High Density Packaging*, 2012, pp. 1395–1398.

[51] J. Chen, N. Wan, J. Li, Z. He, and Y. Wu, “Study on thermal fatigue characteristics of lead-free SAC305 solder joint by RPC,” *2016 17th Int. Conf. Electron. Packag. Technol. ICEPT 2016*, pp. 652–655, 2016.

[52] M. Mustafa, “Effects of Aging on the Cyclic Stress Strain and Fatigue Behaviors of Lead-free solders,” Auburn University, 2014.

[53] Y. Leng, *Material Characterizations: Introduction to Microscopic and Spectroscopic Methods*. Wiley, 2013.

[54] S. Ahmed, M. Hasnine, J. C. Suhling, and P. Lall, “Mechanical Characterization of SAC Solder Joints at High Temperature Using Nanoindentation,” *2017 IEEE 67th Electron. Components Technol. Conf.*, pp. 1128–1135, 2017.

[55] P. Lall, A. Shirgaokar, and D. Arunachalam, “Principal component analysis based

development of norris-landzberg acceleration factors and goldmann constants for leadfree electronics," *Proc. - Electron. Components Technol. Conf.*, pp. 251–261, 2009.

[56] S. Hamasha, S. Su, F. Akkara, A. Dawahdeh, P. Borgesen, and A. Qasaimeh, "Solder Joint Reliability in Isothermal Varying Load Cycling," *Intersoc. Conf. Therm. Thermomechanical Phenom. Electron. Syst.*, pp. 4–9, 2017.

[57] P. Wild, T. Grozinger, D. Lorenz, and A. Zimmermann, "Void Formation and Their Effect on Reliability of Lead-Free Solder Joints on MID and PCB Substrates," *IEEE Trans. Reliab.*, vol. 66, no. 4, pp. 1229–1237, 2017.

[58] H. C. Cheng, R. Y. Hong, H. C. Hu, and W. H. Chen, "Role of Plastic Behaviors of Ni₃Sn₄ Intermetallic Compound on Solder Joint Reliability," *IEEE Trans. Device Mater. Reliab.*, vol. 2017, no. c, 2017.

[59] S. Zhang, T. Lin, P. He, N. Zhao, M. Huang, and K. Paik, "A Study on the Bonding Conditions and Nonconductive Filler Contents on Cationic Epoxy-Based Sn-58Bi Solder ACFs Joints for Reliable Flex-on-Board Applications," *IEEE Trans. Components, Packag. Manuf. Technol.*, pp. 1–8, 2017.

[60] J. Chen, N. Wan, and J. Li, "SAC305 solder joint by RPC," *IEEE*, pp. 301–304, 2017.

[61] C. Burke and J. Punch, "A Comparison of the Creep Behaviour of Joint-Scale SACI05 and SAC305 Solder Samples under Shear Conditions," vol. 4, no. 20 Ii, pp. 1–10, 2012.

[62] M. Brânzei, P. Svasta, F. Miculescu, M. Miculescu, and I. Plotog, "Correlation between the thermophysical properties, geometry and microstructure of the SAC305 and SAC-X typical solder joints," *SIITME 2009 - 15th Int. Symp. Des. Technol. Electron. Packag.*, pp. 129–133, 2009.

[63] C. Burke and J. Punch, “A comparison of the creep behavior of joint-scale SAC105 and SAC305 solder alloys,” *IEEE Trans. Components, Packag. Manuf. Technol.*, vol. 4, no. 3, pp. 516–527, 2014.

[64] D. Herkommer, J. Punch, and M. Reid, “Constitutive modeling of joint-scale SAC305 solder shear samples,” *IEEE Trans. Components, Packag. Manuf. Technol.*, vol. 3, no. 2, pp. 275–281, 2013.

[65] C. L. Toh, Y. M. Wong, and L. E. Norum, “Power Electronics Building Block (PEBB) hardware design and reliability prediction,” *PECON 2016 - 2016 IEEE 6th Int. Conf. Power Energy, Conf. Proceeding*, no. c, pp. 166–171, 2017.

[66] K. Li, R. Yi, and Z. Ma, “Reliability analysis of dynamic reliability blocks through conversion into dynamic Bayesian networks,” *IEEE Int. Conf. Ind. Eng. Eng. Manag.*, vol. 2016–Decem, pp. 1330–1334, 2016.

[67] Philip Bates, “PC Operating Temperatures: How Hot Is Too Hot?,” *mud*, 2014. [Online]. Available: http://www.makeuseof.com/tag/pc-operating-temperatures-hot-hot/.

[68] Y. P. Reddy, V. P. Kumar, and P. Sujatha, “Life Data Analysis and Evaluation of the Performance Characteristics of Picker Module,” in *Conference on Power, Control, Communication and Computational Technologies for Sustainable Growth (PCCCTSG)*, 2015, pp. 172–177.

[69] B. Chen *et al.*, “Reduction among Multiple Differential BGA and Via Pairs by Using Design of Experiments (DoE) Method,” pp. 112–117, 2017.

[70] K. G. P. Lall, “Study on the effect of fixtures on deformation and warpage of the double-sided flexible printed circuit board through reflow using DIC.”